Functional Polymers by Post-Polymerization Modification and Electrochemistry

Zur Erlangung des akademischen Grades eines

DOKTORS DER NATURWISSENSCHAFTEN

(Dr. rer. nat.)

von der KIT-Fakultät für Chemie und Biowissenschaften
des Karlsruher Instituts für Technologie (KIT)

genehmigte
DISSERTATION
von

M.Sc. Edgar Molle
aus Heilbronn

1. Referent: Prof. Dr. Patrick Théato
2. Referent: Prof. Dr. Michael Meier

Tag der mündlichen Prüfung: 20.07.2021

meinem Opa gewidmet

Declaration of Authorship

Die vorliegende Arbeit wurde im Zeitraum von Januar 2018 bis Juni 2021 am Institut für Technische Chemie und Polymerchemie (ITCP) und am Institut für Biologische Grenzflächen III (IBG-3) am Karlsruher Institut für Technologie (KIT) unter der wissenschaftlichen Betreuung von Prof. Dr. Patrick Théato angefertigt.

Hiermit versichere ich, dass ich die Arbeit selbstständig angefertigt, nur die angegebenen Quellen und Hilfsmittel benutzt und mich keiner unzulässigen Hilfe Dritter bedient habe. Insbesondere habe ich wörtlich oder sinngemäß aus anderen Werken übernommene Inhalte als solche kenntlich gemacht. Die Satzung des Karlsruher Instituts für Technologie (KIT) zur Sicherung wissenschaftlicher Praxis habe ich beachtet. Des Weiteren erkläre ich, dass ich mich derzeit in keinem laufenden Promotionsverfahren befinde, und auch keine vorausgegangenen Promotionsversuche unternommen habe. Die elektronische Version der Arbeit stimmt mit der schriftlichen Version überein und die Primärdaten sind gemäß Abs. A (6) der Regeln zur Sicherung guter wissenschaftlicher Praxis des KIT beim Institut abgegeben und archiviert.

Karlsruhe, den 08. Juni 2021

_____

Edgar Molle

Abstract

Since Staudinger's postulation on the nature of polymers a little more than 100 years ago, polymers have rapidly advanced into modern everyday life. Until today, numerous polymer classes have been explored and found various application areas. In particular, functional polymers stand out due to extraordinary characteristics and are thus of great academic and industrial interest. Herein, those functional polymers can be obtained by direct polymerization of the respective monomers or, more sophisticated, by post-polymerization modification, which allows the preparation of a great variety of polymers from only one type of polymer. Additionally, synthetic electrochemical methods increasingly attract interest due to several advantages over conventional syntheses and thus currently experience a "renaissance", especially in the field of organic chemistry. Consequently, this highly attractive method could be exploited for the novel preparation and modification of functional polymers in a sophisticated fashion.

The present thesis covers the preparation of functional polymers by electrochemical methods as well as post-polymerization modification. On the one hand, electrochemical means were employed for both the polymerization itself and the modification of polymers, while functional polymers were further functionalized by conventional chemical modification reactions on the other hand.

In a first approach, the polymerization of reactive monomers, i.e. pentafluorophenyl acrylate, 2,6-difluorophenyl acrylate, and glycidyl methacrylate, was initiated by electrochemical reduction of a fluorine-labelled aromatic diazonium salt. As the first two monomers also featured a fluorine label, this system enabled the facile determination of the number-average molar mass of the polymers by ^{19}F NMR spectroscopy in addition to size-exclusion chromatography. Herein, the functional moieties remained intact during the polymerization and the applied electrochemical conditions, as it was proven by NMR and IR spectroscopy. Next to analytical methods, the reactive nature was demonstrated by post-polymerization modification of the resulting polymers with a fluorine-labelled amine, resulting in the respective amides for poly(pentafluorophenyl acrylate) and poly(2,6-difluorophenyl acrylate) and β-amino alcohol for poly(glycidyl methacrylate). The successful functionalization was followed and proven by ^{1}H and ^{19}F NMR spectroscopy, size-exclusion chromatography, as well as IR spectroscopy.

Abstract

In an alternative second approach, the electrochemical polymerization was combined with the electrochemically-mediated functionalization of the resulting polymers based on a catalytic nickel system. Aryl bromides with different substituents and thus varying electron densities were employed for ω-functionalization using styrene and styrene derivatives as well as acrylonitrile as monomers. Additional to organic aryl bromides, a copolymer consisting of 4-methylstyrene and 4-bromostyrene repeating units was employed as ω-group, resulting in a graft copolymer architecture. The characterization by ^{1}H NMR spectroscopy, size-exclusion chromatography, and differential scanning calorimetry suggested a successful incorporation in the case of 4-*tert*-butylstyrene as monomer. Subsequently, acrylonitrile was used for the preparation of a graft copolymer and the outcome was followed by ^{1}H NMR spectroscopy, size-exclusion chromatography, and IR spectroscopy. The comparison of the results demonstrated the enhanced suitability of styrene-derived monomers for this sophisticated method.

The last approach originally based on the electrochemical deprotection of sulfonamides, which would have resulted in the formation of a polymer with primary amine functionalities in the side groups for further modification. However, the electrochemical setup employed in this thesis presumably impeded the successful deprotection under the applied conditions. Nonetheless, the prepared sulfonamide monomers were employed for the synthesis of a novel class of sulfonamide-based polymers derived from 4-vinylaniline and aromatic sulfonyl chlorides with varying electron densities. A qualitative study suggested a stimuli-responsive water solubility depending on the pH in a switchable fashion. The as-prepared sulfonamide polymers were subsequently used in aza-Michael additions with different acrylate-based Michael acceptors (such as butyl acrylate, methyl acrylate, dodecyl acrylate, and pentafluorophenyl acrylate) for the synthesis of novel polymeric protected β-amino acid derivatives. The successful reactions have been followed and proven by NMR and IR spectroscopy as well as size-exclusion chromatography and differential scanning calorimetry.

Zusammenfassung

Seit Staudingers Postulat über die Natur der Polymere vor etwas mehr als 100 Jahren haben Polymere einen rasanten Einzug in den modernen Alltag gefunden. Zahlreiche Polymerklassen sind bis heute erforscht worden und haben vielfältige Anwendungsgebiete gefunden. Hierbei zeichnen sich insbesondere funktionelle Polymere durch außergewöhnliche Eigenschaften aus und sind daher von großem wissenschaftlichen und industriellen Interesse. Diese funktionellen Polymere können entweder durch direkte Polymerisation der jeweiligen Monomere oder, auf ausgefeilte Art und Weise, durch Post-Polymerisationsmodifizierung erhalten werden, was die Herstellung einer großen Vielfalt von Polymeren aus nur einem Polymertyp ermöglicht. Darüber hinaus stoßen synthetische elektrochemische Methoden aufgrund mehrerer Vorteile gegenüber konventionellen Synthesen zunehmend auf Interesse und erleben aktuell eine „Renaissance“, insbesondere im Bereich der organischen Chemie. Konsequenterweise könnte diese hochattraktive Methode für die neuartige Herstellung und Modifizierung von funktionellen Polymeren auf anspruchsvolle Weise genutzt werden.

Die vorliegende Arbeit umfasst die Herstellung funktioneller Polymere durch elektrochemische Methoden sowie Post-Polymerisationsmodifizierung. Einerseits wurden elektrochemische Methoden zur Polymerisation selbst als auch zur Modifizierung von Polymeren genutzt, während funktionelle Polymere andererseits durch konventionelle chemische Modifizierungsreaktionen weitergehend funktionalisiert wurden.

In einem ersten Ansatz wurde die Polymerisation reaktiver Monomere, namentlich Pentafluorphenylacrylat, 2,6-Difluorophenylacrylat und Glycidylmethacrylat, durch elektrochemische Reduktion eines fluorierten aromatischen Diazonium-Salzes initiiert. Da die ersten beiden Monomere ebenfalls mittels Fluoratomen gekennzeichnet waren, erlaubte dieses System die einfache Bestimmung des Zahlenmittels der molaren Masse der Polymere durch ^{19}F-NMR-Spektroskopie zusätzlich zur Analyse durch Größenausschluss-Chromatographie. Hierbei blieben die funktionellen Gruppen während der Polymerisation und den angewandten Bedingungen intakt, wie durch NMR- und IR-Spektroskopie bewiesen wurde. Neben analytischer Methoden wurde die reaktive Natur der resultierenden Polymere durch Post-Polymerisationsmodifizierung mit einem fluorgekennzeichneten Amin gezeigt, was zu den jeweiligen Amiden von Poly(pentafluorphenylacrylat) und Poly(2,6-difluorphenylacrylat) sowie β-Aminoalkohol von Poly(glycidylmethacrylat) führte. Die erfolgreiche

Funktionalisierung wurde mittels ^{1}H- und ^{19}F-NMR-Spektroskopie, Größenausschluss-Chromatographie und IR-Spektroskopie verfolgt und bewiesen.

In einem alternativen zweiten Ansatz wurde die elektrochemische Polymerisation mit der elektrochemisch-vermittelten Funktionalisierung der resultierenden Polymere basierend auf einem katalytischen Nickel-System kombiniert. Für die ω-Funktionalisierung von Polymeren basierend auf Styrol und Styrol-Derivaten sowie Acrylnitril wurden aromatische Bromide mit unterschiedlichen Substituenten und daraus folgend variierenden Elektronendichten eingesetzt. Zusätzlich zu organischen aromatischen Bromiden wurde ein Copolymer bestehend aus 4-Methylstyrol- und 4-Bromstyrolwiederholeinheiten als ω-Gruppe verwendet, was zu einer Pfropfcopolymer-Architektur führte. Die Charakterisierung durch ^{1}H-NMR-Spektroskopie, Größenausschluss-Chromatographie und dynamischer Differenzkalorimetrie legte einen erfolgreichen Einbau im Fall von 4-*tert*-Butylstyrol als Monomer nahe. Anschließend wurde Acrylnitril zur Herstellung eines Pfropfcopolymers verwendet und das Ergebnis mittels ^{1}H-NMR-Spektroskopie, Größenausschluss-Chromatographie und IR-Spektroskopie verfolgt. Der Vergleich der Ergebnisse zeigte die überlegene Eignung von Styrol-abgeleiteten Monomeren für diese anspruchsvolle Methode.

Der letzte im Rahmen dieser Arbeit verfolgte Ansatz basierte ursprünglich auf der elektrochemischen Entschützung von Sulfonamiden, was zur Bildung eines Polymers mit primären Amin-Funktionalitäten in den Seitengruppen geführt hätte. Der elektrochemische Aufbau, der in der vorliegenden Arbeit benutzt wurde, erschwerte vermutlich jedoch die erfolgreiche Entschützung unter den angewandten Bedingungen. Nichtsdestotrotz wurden die hergestellten Sulfonamid-Monomere für die Synthese einer neuartigen Klasse sulfonamid-basierter Polymere abgeleitet von 4-Vinylanilin und aromatischen Sulfonylchloriden mit variierenden Elektrondichten genutzt. Eine qualitative Studie legte eine stimuli-responsive, pH-abhängige Wasserlöslichkeit in einer reversiblen Weise nahe. Die hergestellten Sulfonamid-Polymere wurden anschließend in aza-Michael-Additionen mit unterschiedlichen acrylat-basierten Michael-Akzeptoren (wie Butylacrylat, Methylacrylat, Dodecylacrylat und Pentafluorphenylacrylat) zur Synthese neuartiger polymerer, geschützter *β*-Aminosäure-Derivate eingesetzt. Die erfolgreichen Reaktionen wurden mittels NMR- und IR-Spektroskopie sowie Größenausschluss-Chromatographie und dynamischer Differenzkalorimetrie verfolgt und bewiesen.

Table of Contents

Table of Contents

1 Introduction

Polymers have become almost inevitable in modern everyday life and build a substantial basis for our society. Different polymerization techniques have been explored and found application for the preparation of commodity polymers such as polyethylene and polypropylene for instance, but also for the synthesis of more specialized and tailor-made polymers adapted to the demands for specific applications, e.g. in dentistry[1–4] or professional sports.[5,6] Especially functional polymers are of great interest from both an academic and an industrial viewpoint, as they potentially feature special inherent properties and could thus result in an evolution or even a revolution of distinct application areas or, in a wider perspective, modern everyday life. On the one hand, functional polymers can be obtained by direct polymerization of the respective monomers, however the scope of this strategy is limited due to the incompatibility of specific functional groups with particular polymerization techniques. Thus, polymer chemists have demonstrated the accessibility of a sheer unlimited number of functional polymers by post-polymerization modification (PPM). This allows for a rapid generation of polymer libraries using different substrates by functionalization of a single precursor polymer. In this regard, especially newly established methods in the field of organic chemistry are transferred into both polymer synthesis and modification. Herein, synthetic electrochemistry in particular is lately experiencing a "renaissance"[7,8] due to being considered a sustainable "green"[9] methodology (e.g. sustainable energy production, electrons as inherently clean reactants)[9] and due to the numerous fine-tunable parameters it comes along with, allowing for a high degree of control over the reaction. Thus, various reactions have been reported using synthetic electrochemical methods in the frame of transformations of organic molecules and more are expected to follow. However, the use of non-standardized, partially self-built electrochemical setups including electrode materials with an inherently great variation of quality negatively affects the reproducibility of the vast majority of literature reports and consequently impedes the accessibility of these methods. Nonetheless, the use of electrochemical methods is not limited to the field of academia, several industrial syntheses are based on electrolysis reactions such as the adiponitrile process[10] and the Simons fluorination process.[7] Thus, investigations on the value of electrochemical methods for the field of polymer chemistry are indispensable to benefit from the great opportunities the combination of both fields potentially offers. In fact, electropolymerization[11] of different monomers such as thiophene[12] and pyrrole[13,14] are known for a long time and are used for electrode coating for instance.[15,16] However, other polymerization methods such as electrochemically-mediated atom-transfer radical

polymerizations (eATRP)[17,18] and electrochemically-mediated reversible addition-fragmentation chain-transfer (eRAFT) polymerizations[19–22] have followed only recently and demonstrate that the transfer of electrochemical methods in organic chemistry to the field of polymer chemistry has already started. Still, most reports are focusing on the polymerization itself by electrochemical means, whereas literature concerning electrochemically-driven PPM is rare so far. Therefore, further investigations are urgently required for the establishment of novel electrochemical reactions for both the polymer synthesis and PPM. The numerous literature-precedented reactions in the field of synthetic organic electrochemistry have thus to be evaluated with respect to *inter alia* their conversion to the desired product, their potential applicability to polymer systems, functional group tolerance, and the complexity of the setup. Nevertheless, the combination of both fields, synthetic electrochemistry and polymer chemistry, could result in a synergy leading towards novel polymers and modifications resulting in functional polymers with unprecedented properties and could thus potentially have an impact on modern everyday life.

2 Theoretical Background

The current chapter gives insight into important background information and introduces useful knowledge, both helping to follow the discussion of the research projects mentioned in this work. Therefore, an introduction to polymers and polymer chemistry is given and different polymerization methods, both chain- and step-growth polymerizations, are discussed. Since the present thesis is dealing with chain-growth polymerization techniques, the latter is being discussed in more detail. In the course of this chapter, the field of PPM is introduced. Different efficient reactions have been extensively used to functionalize macromolecules, *inter alia* by the research group of Prof. Théato. Subsequently, the fundamentals of (synthetic) electrochemistry are introduced and the use of electrochemical methods in the field of polymer chemistry is demonstrated by a selection of successfully employed reactions. Eventually, sulfur-nitrogen-based polymeric materials as special class of polymers are addressed.

2.1 Polymer Chemistry

A world as we know it is almost unthinkable without polymers, which have advanced into almost all areas of modern everyday life, ranging from commodity polymers such as affordable packaging materials produced on a multimillion-ton scale[23] to highly specialized materials used in dentistry for instance.[1–4] This diversity of polymers results in a great variety of different properties, novel classes of polymers with unexplored characteristics thus do not only attract scientific interest, but are interesting from an industrial viewpoint as well. However, there are still challenges to overcome in the field of polymer chemistry, e.g. the environmentally friendly recycling,[24–28] important discoveries have nonetheless been made throughout the last decades.

2.1.1 History of Polymer Chemistry

Polymers are ubiquitous in nature and are crucial for the evolution of life on earth. On the one hand for instance, deoxyribonucleic acid (DNA), a biopolymer, is substantial since it carries genetic information of organisms and is composed of a double helical structure of two polynucleotides.[29] On the other hand, natural polymers such as cellulose, natural rubber, silk, or wool have been used long before the term polymer was introduced.[30] The first report on a synthetic thermoset polymer was published by Baekeland in 1907, who used phenol and formaldehyde for the synthesis of so-called "Bakelite".[31] Even before that, modification of natural polymers was employed to obtain useful materials: Parkes developed the first plastic material in 1862[30] followed by Hyatt in 1866,[30] eventually leading to the preparation of celluloid by addition of camphor to nitrocellulose. The preparation of the latter represents one of the first PPM reactions, i.e. the nitration of natural cellulose by Schönbein[32] and Böttger in 1846 independently from each other. Another example for PPM dates back to 1839, when Goodyear and Hancock independently treated natural rubber with sulfur and discovered the vulcanization.[33] Berthelot was one of the first chemists reporting the term polymer in 1866,[34–37] when he called the heating of styrene a "transformation polymérique". Against the beliefs at the time, Staudinger was convinced that polymers are composed of macromolecules that are covalently-linked building blocks[38] and published his article "Über Polymerisation",[39] which translates to "On Polymerization".[40] He received the Nobel Prize in 1953 "for his discoveries in the field of macromolecular chemistry". Other Nobel Prizes went to Ziegler and Natta in 1963 "for their discoveries in the field of the chemistry and technology of high polymers", to Flory in 1974 "for his fundamental work, both theoretical and experimental, in the physical

chemistry of macromolecules", and Heeger, MacDiarmid, and Shirakawa in 2000 for "their discovery and development of conductive polymers". Overall, this impressively demonstrates and stresses the highly diverse nature of polymer chemistry and more Nobel Prizes to polymer chemistry might follow.

2.1.2 General Information about Polymers

Polymers are composed of macromolecules, which are made up from so-called monomers as repeating units. The term monomer is derived from the ancient Greek words *mónos* (one, single) and *méros* (part) and is, according to the IUPAC definition, "a molecule which can undergo polymerization, thereby contributing constitutional units to the essential structure of a macromolecule".[41] There are many different polymerization techniques and thus not one sole crucial structural motif of monomers exists, there are in fact many different natures of monomers. The amount of monomer repeating units incorporated into a macromolecule is described by the degree of polymerization (DP_n), which gives information about the number of monomer units making up a macromolecule.[42] For a homopolymer (i.e. a polymer solely composed of one monomeric species), DP_n is equal to the ratio of the molar mass of the polymer divided by the molar mass of the monomer.

$$DP_n = \frac{M_{polymer}}{M_{monomer}} \quad \text{(I)}$$

Therefore, the molar mass of a polymer plays a crucial role in the field of polymer chemistry. Unlike small organic molecules, synthetic polymers do not feature a single molar mass, but a molar mass distribution caused by the characteristics of the different polymerization processes. The shape of this distribution is highly dependent on the polymerization technique used and among others, two important mathematically-derived molar mass values are of importance: the number-average molar mass (M_n) and weight-average molar mass (M_w).[42] The former is mathematically defined as follows:

$$M_n = \frac{\sum_i N_i M_i}{\sum_i N_i} \quad \text{(II)}$$

where N_i is the number macromolecules featuring molar mass M_i.

The following equation gives the mathematical definition of M_w:

$$M_w = \frac{\sum_i N_i M_i^2}{\sum_i N_i M_i} \quad \text{(III)}$$

Both values are crucial for the calculation of the so-called dispersity $Đ$ used as indication for the width of a molar mass distribution of a polymer. It is defined as the ratio of M_w to M_n and is dependent on the polymerization technique used.[43] Polymer chemists are aiming for low dispersities with nature being their role model featuring many macromolecules with $Đ = 1.00$, while synthetic polymers feature $Đ > 1.00$.

$$Đ = \frac{M_w}{M_n} \quad \text{(IV)}$$

Molar mass distributions of polymers obtained by free radical polymerization (FRP) are usually comparably broad, dispersities are commonly between $1.50 \leq Đ \leq 3.00$ (typically around $Đ \approx 2.0$),[44] while for reversible-deactivation radical polymerization (RDRP) methods, dispersities are usually below $Đ < 1.30$. The dispersity values reached by living anionic polymerization are even lower and close to 1.00.

2.1.3 Macromolecular Architectures

The broad variety of polymerization methods allows for the preparation of tailor-made polymers, featuring different properties and characteristics and thus enabling their use in specific application areas. The simplest class of polymers are so-called homopolymers, which are composed of solely one type of monomer. In contrast to homopolymers, copolymers are composed of at least two different monomers and do not only attract scientific interest, but are also industrially synthesized. Copolymers can be differentiated again in subclasses (**Scheme 1**): there are statistical copolymers (A)), in which the different monomers are randomly arranged, not following any specific incorporation pattern. Alternating copolymers are comprised of monomers in an alternating fashion (C)), while block copolymers consist of multiple block segments made up from the respective monomers (B)). In contrast, graft copolymers are composed of a linear backbone branched with polymer chains from another monomer (D)).

Homopolymers

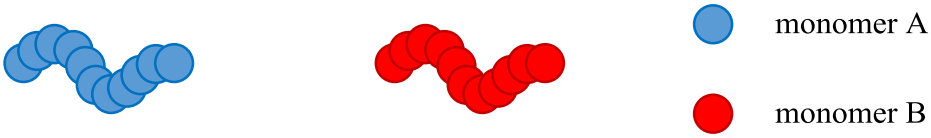

Copolymers

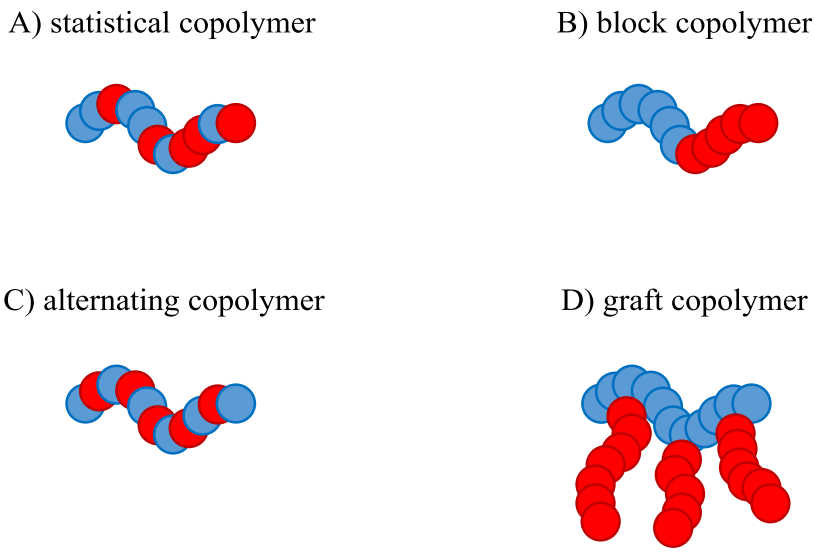

Scheme 1. Structural depiction of homo- and copolymers. Statistical copolymers (A)) are composed of monomer units of at least two different monomers in a random fashion, while they are arranged alternatingly in alternating copolymers (C)). Block copolymers (B)) consist of connected blocks of different monomer units and graft copolymers (D)) are comb-like copolymers, in which polymer chain branches of another monomer are attached to a linear polymer backbone.

2.2 Polymerization Classes

Polymerizations can be classified in two different polymerization classes, i.e. chain-growth polymerization and step-growth polymerization. Prominent examples for the former are radical polymerizations in general and thus FRP and RDRP methods, while polyadditions and polycondensations are commonly known representatives of step-growth polymerization. Both classes are of great scientific interest and play a crucial role in industry and modern everyday life. Polystyrene, a commodity polymer, belongs to the class of chain-growth polymers and is used as packaging[45] and insulation material[46,47] for instance, whereas polyurethanes are commonly synthesized by polyaddition of polyisocyanates and polyols and are used e.g. as foams, coatings, and adhesives.[48–50]

2.2.1 Chain-Growth Polymerization

Different polymerization techniques are classified as chain-growth polymerizations: radical polymerizations, ionic polymerizations,[51,52] coordination polymerizations,[53] and ring-opening polymerizations[54] are well-investigated types of polymerizations and follow the principles and the mechanism of a chain-growth polymerization. This chapter will mainly focus on radical polymerizations since they manifest the basis of the present thesis.

2.2.1.1 Free Radical Polymerization (FRP)

FRP is one of the simplest and most straightforward polymerization methods and allows for the preparation of polymeric material from vinyl monomers in undemanding reaction setups. Nearly half of all industrial polymers are obtained by radical polymerization (40 – 45% in 2012[55]), radical polymerizations thus represent a crucial pillar for industrial polymer chemistry. The polymerization mechanism is divided into following reaction steps, also depicted in **Scheme 2**:

A) Initiation
B) Propagation
C) Termination
D) Chain transfer

A) Initiation

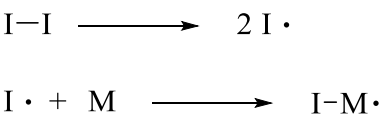

B) Propagation

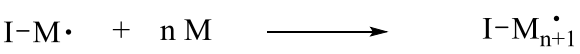

C) Termination

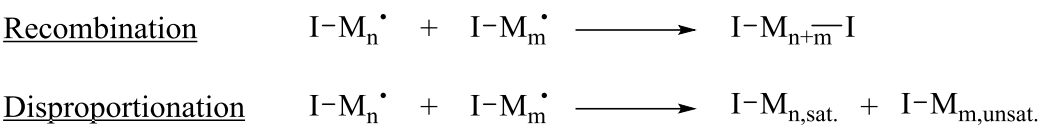

D) Chain Transfer

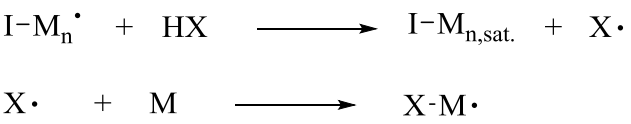

Scheme 2. Mechanism of FRP, including A) initiation, B) propagation, C) termination, and D) chain transfer reactions.

Although autopolymerizations of different monomers (e.g. styrene) have been reported,[56–58] radical initiators are usually added for the initiation (**Scheme 2**, A)). A great variety of initiators has been reported, with thermal and photochemical ones being most commonly used. For the former, 2,2′-azobis(2-methylpropionitrile) (AIBN) is a typical, commercially available radical initiator for thermally-induced polymerizations featuring a 10 hour half-life temperature of 65 °C.[59] Generally, an initiator decomposes upon suitable conditions into a radical species, which is able to initiate a polymerization with vinyl monomers. Upon heating, AIBN decomposes as depicted in **Scheme 3**.[60]

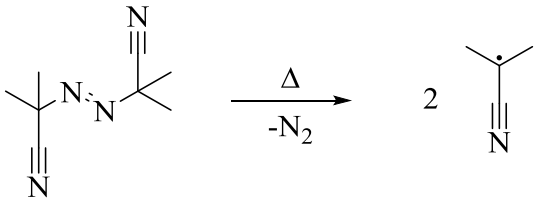

AIBN

Scheme 3. Thermal decomposition of AIBN into two isobutyronitrile radicals under elimination of elemental nitrogen.[60]

The generated radical species are starting the polymerization with present monomers, which is termed propagation (**Scheme 2**, B)). In this step, the polymer chain is constantly growing until termination reactions (**Scheme 2**, C)) or chain transfer reactions (**Scheme 2**, D)) are taking place. Termination reactions can be subdivided into recombination and disproportionation, both cases involving two growing polymer chains.[61] In the former case, two polymer chains recombine to one polymer chain, whereas the latter describes the abstraction of a hydrogen atom from one polymer chain to another, resulting in a saturated polymer chain and another one bearing a vinyl end group. In the chain transfer, the growing polymer chain abstracts for instance a hydrogen atom from another polymer chain or a chain-transfer agent, which leads to branched macromolecules in the first case.[62] Chain-transfer agents are used in industry to lower the molar mass of the obtained polymers.[63] These characteristics of FRP are responsible for the relatively high dispersities (usually $1.50 \leq Đ \leq 3.00$)[44] and the poor control over the molar mass obtained after polymerization. Nonetheless, due to its simplicity, robustness, tolerance, great variety of polymerizable monomers and cost efficiency,[64] it represents an important pillar of industrial polymer chemistry.

Nevertheless, huge efforts have been made to overcome the drawbacks of FRP while staying in the frame of radical polymerizations. The discovered polymerization techniques have been classified under the generic term RDRP.[65]

2.2.1.2 Reversible-Deactivation Radical Polymerization (RDRP)

The idea behind the development of RDRP methods was to combine both the advantages of truly living polymerizations, such as living anionic polymerization,[66] and free radical polymerization, i.e. *inter alia* the astonishingly low dispersities, excellent control over the molar mass (determined by the ratio of monomer to initiator), and the chain-end functionalization in a complete fashion allowing the synthesis of block copolymers in the case of living anionic polymerization,[67] and simple reaction setup as well as its robustness and tolerance resulting in

mild and undemanding reaction conditions in the case of FRP.[64] The most prominent examples are the reversible addition-fragmentation chain-transfer (RAFT) polymerization,[68–70] atom-transfer radical polymerization (ATRP),[71,72] and nitroxide-mediated polymerization (NMP).[73] While RAFT polymerizations rely on the degenerate chain transfer, ATRP and NMP are based on a reversible equilibrium between dormant and active species. Consequently, this equilibrium is actively reducing the amount of present radical species in the system and thus reduces the probability of termination reactions. This however affects the polymerization kinetics drastically, i.e. decreased propagation rates[74] and thus prolonged polymerization times in contrast to FRP can be observed. In the case of RAFT polymerization, the concentration of radical species is kept constant in comparison to FRP, two equilibria[75,76] are implemented to lower the probability of termination reactions. All of these classes allow for the synthesis of complex macromolecular architectures and are not exclusive research topics in scientific research, but also find application in industry.[77]

2.2.1.2.1 Reversible Addition-Fragmentation Chain-Transfer (RAFT) Polymerization

RAFT polymerization was first reported in 1998[68–70] and enables the polymerization of a great variety of monomers in a controlled fashion featuring well-defined molar mass distributions and a high end group fidelity. It is based on a degenerate chain transfer and on the use of a so-called RAFT agent or chain-transfer agent (CTA). The general structure of typical RAFT agents is depicted in **Scheme 4**.

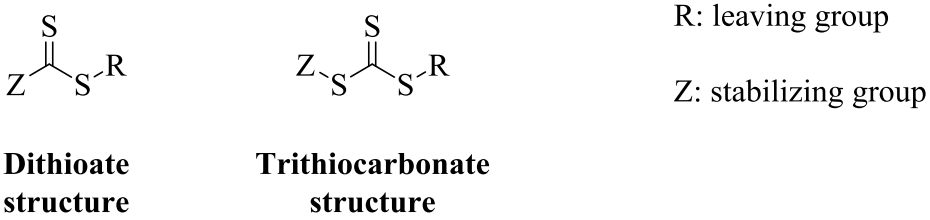

Scheme 4. Typical structure of a RAFT agent, mostly based on dithioate or trithiocarbonate motifs, featuring a leaving group R, which is able to re-initiate polymerization of present monomer units, and a stabilizing group Z, stabilizing the formed intermediate radical.

The mechanism[75,76] of a typical RAFT polymerization is schematically depicted below in **Scheme 5**:

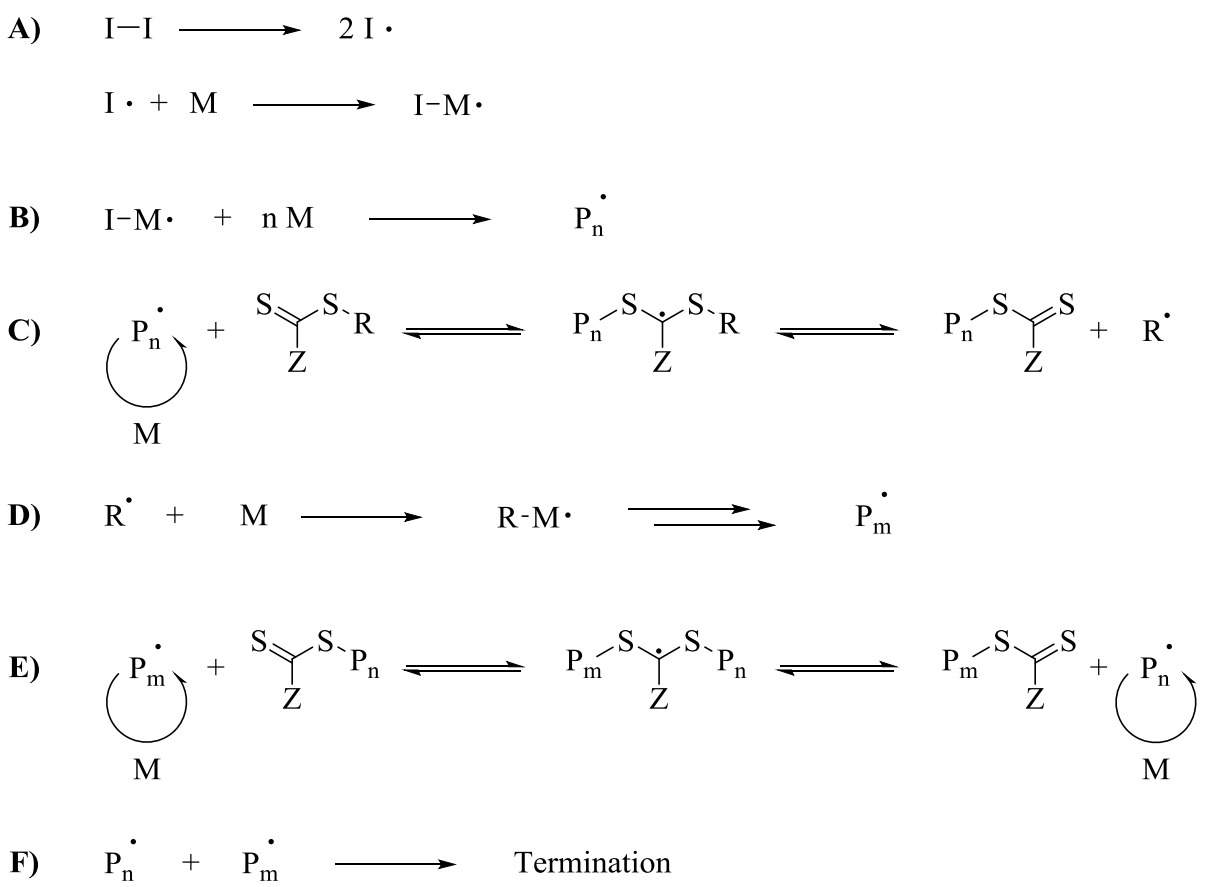

Scheme 5. Mechanism of the typical RAFT process, involving two equilibria (C) and E)) based on the use of a CTA, allowing for the preparation of macromolecules featuring well-defined molar mass distributions and high end group fidelities and enabling the preparation of different (complex) macromolecular architectures.

The initiation (A)) and propagation (B)) are similar to FRP, though different kinds of initiating systems have been reported like photoRAFT polymerization[78,79] and even eRAFT polymerization.[19–22] The crucial equilibria are depicted in **Scheme 5**, namely the so-called pre-equilibrium (C)) and the main equilibrium (E)).[80] In the pre-equilibrium, the propagating chain in its radical form ($P_n^{\bullet}$) attacks the thiocarbonyl functionality of the CTA, resulting in the formation of the intermediate radical species. From hereon, two different pathways exist: on the one hand, the propagating chain can be released again, setting free the initial RAFT agent. On the other hand, the leaving group radical ($R^{\bullet}$) and the polymeric CTA (bearing the propagating chain as leaving group) can be formed, the former being able to re-initiate polymerization of the present monomer units (D)). This propagating chain can then attack the polymeric RAFT agent in a similar fashion, forming the intermediate radical species in the main equilibrium (E)). In this case, either the propagating chain bearing the initiator as end group ($P_n^{\bullet}$) can leave the RAFT agent or the one initiated by the leaving group radical ($P_m^{\bullet}$). Here, the formation of a rapid equilibrium leads to equal propagation chances of both propagating chains,

resulting in similar chain lengths.[81] The RAFT mechanism thus allows for the preparation of polymers featuring narrow molar mass distributions and low dispersities (typically $1.1 \leq Đ \leq 1.3$). One drawback of RAFT polymerization is the necessity to use a suitable CTA for the different classes of monomers.[76] Although some CTAs are commercially available, special monomers may require a tailored design of an appropriate RAFT agent beforehand. Also, for block copolymerizations for instance, not all kinds of monomers can thus be copolymerized in a block copolymerization fashion due to different radical stabilities of the respective monomers. Nonetheless, there have been reports on switchable RAFT agents,[82,83] which are suited for the block copolymerization of different classes of monomers in a pH-dependent fashion. Another disadvantage arising from the use of a CTA is the typical coloration of RAFT polymers due to the structural motifs of the RAFT agent itself, especially when colorless polymers are required. Nonetheless, the presence of the RAFT agent at the end group enables further modification of the resulting polymers. The thiocarbonyl motif allows for hetero-Diels-Alder reactions with dienes[84] for instance, which can be exploited as bioconjugation platform.[85]

2.2.1.2.2 Atom-Transfer Radical Polymerization (ATRP)

ATRP was first reported in 1995, independently from each other, by Sawamoto[71] using ruthenium-based catalysts and Wang and Matyjaszewski,[72] who employed a copper catalyst. The basis of ATRP is a redox equilibrium between dormant and active species, reducing the amount of free radicals present in the system and thus the probability of termination reactions. This equilibrium involves the use of alkyl halides as initiators and a solubilized transition metal (**Scheme 6**). For the latter, copper(I) is the most commonly used catalyst, however, reports have shown the ability of several other transition metals to successfully maintain good control over polymerizations, exemplarily naming iron[86,87] and cobalt.[88]

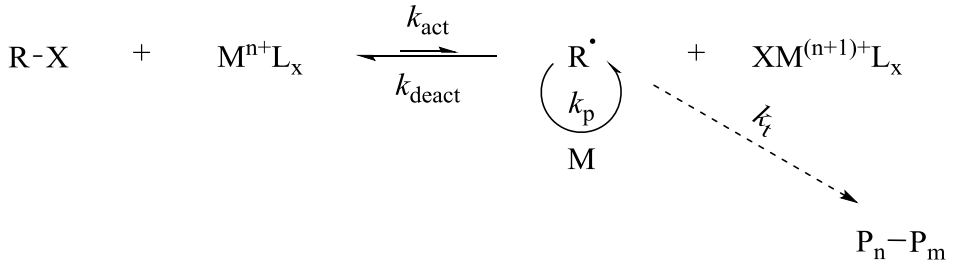

Scheme 6. General mechanism of the ATRP process, involving the use of a metal catalyst (M^{n+}) solubilized by ligands (L_x), which is oxidized while the dormant alkyl halide (R-X) is reduced to the propagating active radical.

According to the depicted mechanism in **Scheme 6**,[89] the transition metal catalyst is oxidized, while the alkyl halide is reduced, resulting in the respective alkyl radical, which is initiating the polymerization. The ratio of k_{act} to k_{deact} is called the ATRP equilibrium constant: K_{ATRP}.[90]

$$K_{ATRP} = \frac{k_{act}}{k_{deact}} \quad \text{(V)}$$

Typically, K_{ATRP} is small, tending to the dormant side of the equilibrium with constants in the regime of $K_{ATRP} \approx 10^{-4} - 10^{-9}$.[91] This equilibrium is affected by many parameters, the ligand solubilizing the transition metal catalyst for instance has a major influence on the activation rate constant k_{act} as shown in literature reports.[90,92] In this case, the authors obtained rate constants for the activation by trapping formed radical species with a large excess of 2,2,6,6-tetramethylpiperidinyl-1-oxy (TEMPO) and an excess of copper(I), assuming pseudo-first-order kinetics under these conditions.[90] Also, the initiator structure influences the activation rate constant drastically.[93] To access the rate constants, the authors performed a systematic study, using consistent reaction conditions (solvent: acetonitrile, T = 35 °C) with gas-chromatographical analysis and evaluation assuming pseudo-first-order kinetics. Different initiators mimicking the respective dormant polymer chains were used for poly(methyl methacrylate) (PMMA), poly(methyl acrylate) (PMA), and polystyrene (PS), using mainly alkyl bromides and alkyl chlorides, but also alkyl iodides and pseudo-halides.

In contrast to RAFT polymerization, polymers obtained by ATRP do not feature a characteristic coloration from the RAFT agent, but they suffer from the use of metal catalysts, which can be tedious to remove from the final polymer and in the case of copper restricts its use in biological applications due to its neurotoxicity.[94,95] Nonetheless, it enables the preparation of polymers with well-defined molar mass distributions, low dispersities as well as high end group fidelities. Analogous to polymers obtained by RAFT polymerization, macromolecules prepared by ATRP have been used in PPM, for instance in the frame of click chemistry.[96–100] The bromide end group can be transformed into the respective azide functionality and thereafter be used in the Huisgen dipolar cycloaddition of azides and alkynes[101] with different alkyne moieties.

2.2.1.2.3 Nitroxide-Mediated Polymerization (NMP)

Researchers at the Commonwealth Scientific and Industrial Research Organisation (CSIRO) in Australia discovered the possibility to use alkoxyamines as initiators for polymerization, the first publication about NMP was a European patent application in 1985.[73,102] Analogous to

ATRP, it is based on an equilibrium between dormant and active species: in this case, an alkoxyamine represents the dormant species being able to reversibly form both an alkyl radical species able to propagate and a nitroxide radical species, which represent the active species. The C-O bond of the alkoxyamine is known to be prone to thermolysis and is homolytically split,[103] resulting in the formation of the active propagating species and the nitroxide moiety, reversibly terminating the propagation by radical trapping (**Scheme 7**).

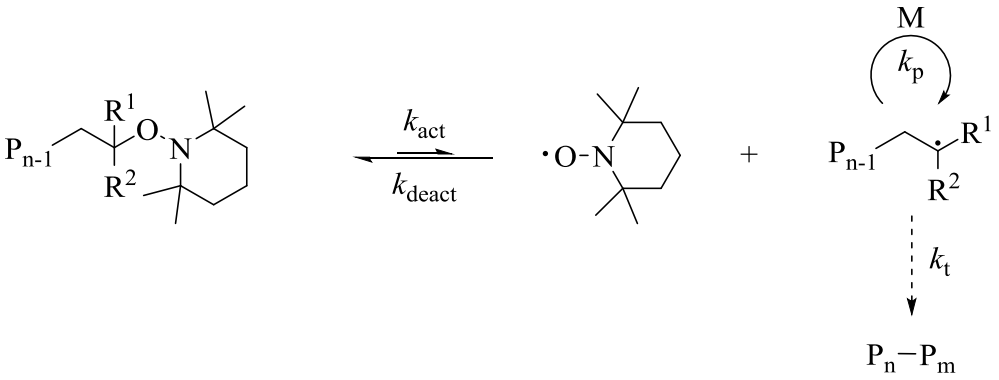

Scheme 7. General mechanism of NMP based on an equilibrium between alkoxyamine (left, dormant species) and a nitroxide radical and the propagating carbon-centered radical species (right, active species).

Originally, a bicomponent pathway using conventional initiation with radical trapping and thus the addition of nitroxide moieties (TEMPO) to the polymerization was employed for NMP.[104] Nonetheless, Rizzardo[73] and Hawker[105,106] developed unimolecular initiators, acting both as initiating species as well as radical trap.

Similar to RAFT polymerization and ATRP, NMP fulfils the criteria of RDRP techniques, resulting in narrow molar mass distributions and a good control over the polymerization, however high temperatures in comparison to the former are required. In contrast to the other two contenders, the transformation or removal of the end groups has not been explored in the same excessive manner.[107] Rizzardo showed the reduction of the TEMPO end group to the respective hydroxy end group in a patent from 1986.[73] Hawker reported a radical approach on the insertion of a non-self-polymerizable monomer involving maleic anhydride and maleimide.[108] Additionally, the alkoxyamine end group could be successfully transformed into the respective bromide and azide end group functionality.[107]

2.2.1.3 Living Anionic Polymerization

With the first report in 1956, Szwarc and coworkers pioneered in the field of living anionic polymerization[66] and back then already demonstrated its potential by preparation of block copolymers.[109] So far, living anionic polymerization enables the synthesis of polymeric materials with the lowest dispersities of the known polymerization methods and allows for the preparation of a broad range of different architectures due to the complete chain end functionalization.[67] In contrast to RDRP techniques, this method formally does not feature termination reactions under suitable conditions and thus represents the class of actual "living" polymerizations. However, the anionic character of the polymerization requires conditions that are more demanding and limits the use of reagents.

2.2.2 Step-Growth Polymerization

Not only chain-growth polymerizations are of scientific and industrial interest, step-growth polymerization represents an interesting and important class of polymerizations and the respective polymers are well-known and find application in different areas of everyday life. In contrast to chain-growth polymerization, the molar mass of the polymer is building up slowly, with only one reaction mechanism for the polymerization contrary to chain-growth polymerizations featuring initiation, propagation, and termination reactions.[110] Important subclasses are polyaddition and polycondensation reactions, based on different kinds of bi- or multifunctional monomers. Polycondensation is accompanied by the evolution of low molar mass compounds in addition to the polymer formation, whereas this is not the case for polyadditions (**Scheme 8**).

Polyaddition

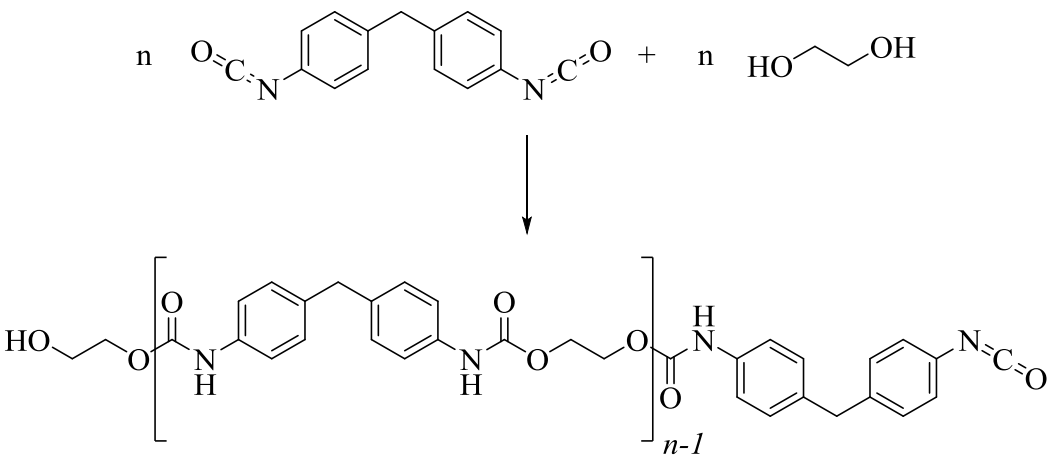

Polycondensation

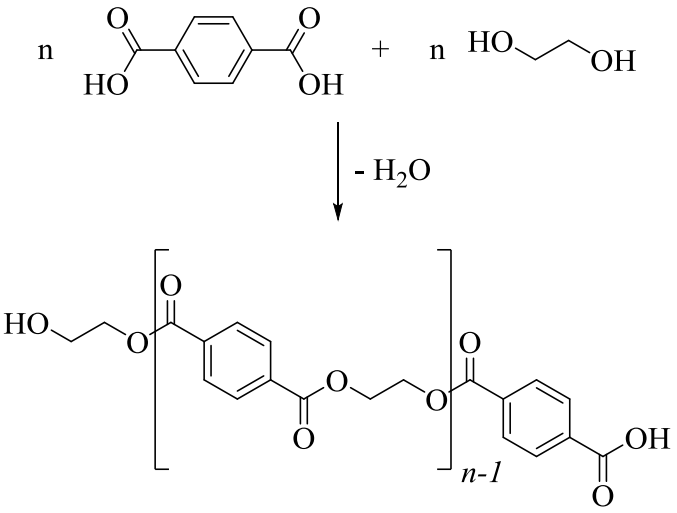

Scheme 8. Comparison of polyaddition (top) and polycondensation (bottom), the latter involving the evolution of a low molar mass compound additional to the actual polymerization.

To obtain high molar masses in a step-growth polymerization fashion, a stoichiometric balance of the two reactants is required.[110] Alternatively, a single monomer featuring two different functionalities in the case of a linear polymer or a 1:1 salt of the respective monomers can be employed to guarantee the balance of functional groups.[110] Carothers and Flory described the theory behind step-growth polymerization in the first half of the last century.[111–113] The Carothers equation describes the correlation of the number-average degree of polymerization with the extent of the reaction *p* (*p* ranging from 0 to 1) for linear step-growth polymerization of an equimolar mixture of two monomers or a single monomer featuring two different functionalities:[114]

$$\overline{DP_n} = \frac{1}{1-p} \quad \text{(VI)}$$

The Carothers equation shows that high degrees of polymerizations and consequently high molar masses can only be obtained at high extents of the reaction, i.e. conversion. Potential step-growth polymerization reactions should thus feature excellent conversions.[110] Various step-growth polymers are part of modern everyday life such as polyesters,[115,116] polyamides,[117] and polyurethanes[48–50] for instance.

2.3 Post-Polymerization Modification (PPM)

PPM is a growing field of polymer chemistry and enables the functionalization of macromolecules after polymerization.[118] It allows to access a great variety of different materials from numerous precursor polymers, which are, in some cases, not accessible by direct polymerization of the respective monomers.[119] First examples of PPM can be traced back to the 1840s, when nitrocellulose was obtained by nitration of cellulose in 1846, independently from each other, by Schönbein[32] and Böttger. Already in 1839, Goodyear and Hancock independently discovered the vulcanization by treatment of natural rubbers with sulfur.[33] Up to now, numerous reports have been published and more are expected to follow. However, not every reaction qualifies for a potential PPM candidate, the reactions should be efficient and ideally feature quantitative conversion without the formation of side products. For small organic molecules, quantitative conversions might not be as important as in the field of PPM, since small organic molecules are comparably easy to be separated from each other, while separation on the polymer level is extremely difficult and in most cases impossible. Throughout the history of PPM, different reaction classes proved themselves as valuable and straightforward candidates. The copper-catalyzed alkyne-azide cycloaddition (CuAAC)[120,121] and thiol-ene reaction[122] have been commonly used to modify polymers.[123,124] In addition, transesterifications and amidations of active ester moieties[125,126] as well as nucleophilic ring-opening reactions, for instance of poly(glycidyl methacrylate) (PGMA),[127] have been employed in an exhaustive fashion to functionalize macromolecules.

One of the most commonly used type of cycloaddition in the field of polymer chemistry is CuAAC.[124] First reports related to polymer synthesis covered the synthesis of dendrimers[128] and the preparation of adhesives by step-growth polymerization of bi- and multifunctional azide and alkyne monomers.[129] In contrast to the thermal alkyne-azide [3+2] cycloaddition, the copper-catalyzed one is regioselective to the 1,4-isomer (**Scheme 9**):[130]

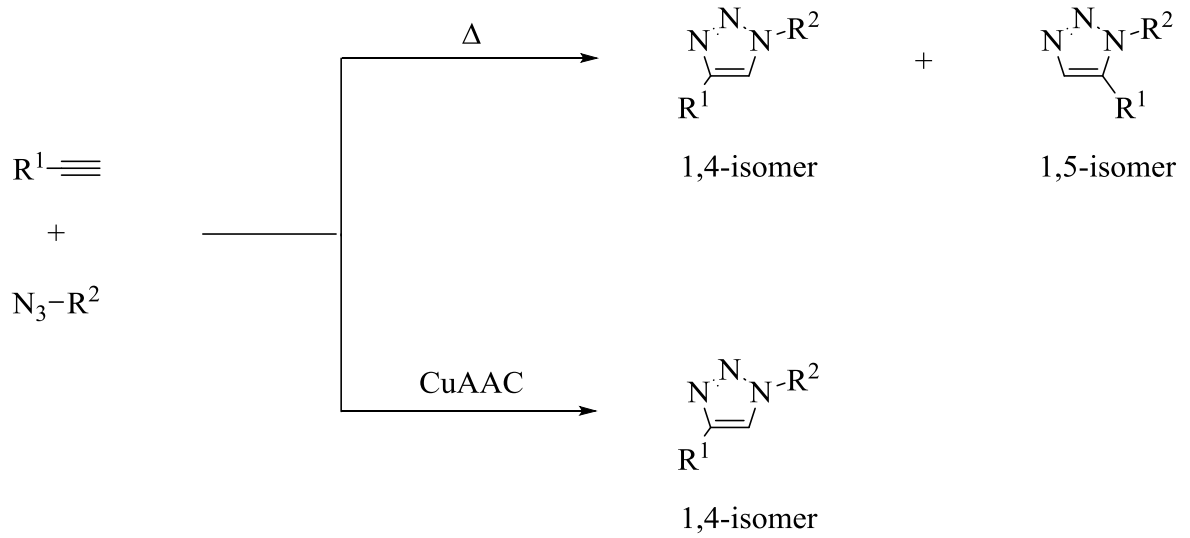

Scheme 9. Regioselectivity of the CuAAC in comparison to the thermal alkyne-azide cycloaddition.

Among others, the group of Prof. Théato could successfully employ CuAAC for PPM, in this case for the preparation of cage-shaped polymers from star polymers.[131] A four-arm star polymer prepared by ring-opening polymerization (ROP) was functionalized with an end group bearing both an azide and an alkyne moiety. The cage formation upon closing by CuAAC forming a triazolophane macrocycle motif was followed and proven by NMR, ultraviolet-visible (UV/Vis) and IR spectroscopy as well as differential scanning calorimetry (DSC), electrospray ionization mass spectrometry (ESI-MS), dynamic light scattering (DLS), and size-exclusion chromatography (SEC).[131] Another recent publication from the research group of Prof. Théato dealt with the synthesis of poly(vinyl ether)s from vinyl ethers *inter alia* bearing an alkyne functionality.[132] The prepared monomers were polymerized by cationic polymerization with pentakis(methoxycarbonyl)cyclopentadiene (PMCCP), which was shown to allow for a controlled cationic polymerization of vinyl ethers.[133] Benzyl azide was used for the PPM after cationic polymerization in a quantitative CuAAC (**Scheme 10**).

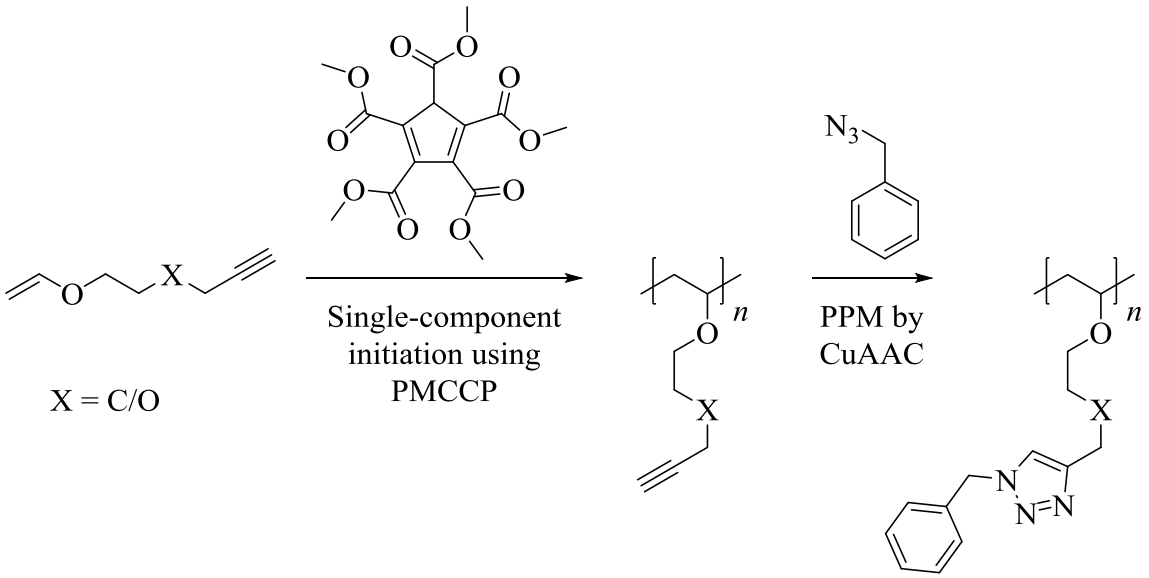

Scheme 10. PPM of alkyne-functionalized poly(vinyl ether)s *via* CuAAC.

Active esters represent a valuable class of compounds for straightforward functionalization, not only in organic chemistry, but also in the field of polymer chemistry. Pioneering works in the preparation and PPM of polymers bearing active ester moieties were published in the 1970s by Ferruti and Ringsdorf.[134,135] Different kinds of active esters have been reported in PPM of polymers obtained by various polymerization techniques.[118] Prominent examples are *N*-hydroxysuccinimide (NHS) esters and pentafluorophenyl esters such as pentafluorophenyl acrylate (PFPA). The latter has been explored as monomer in PPM reactions *inter alia* in the group of Prof. Théato, demonstrating their great potential. Transesterification reactions[126] as well as amidations[125] have been carried out in an almost exhaustive fashion (**Scheme 11**).

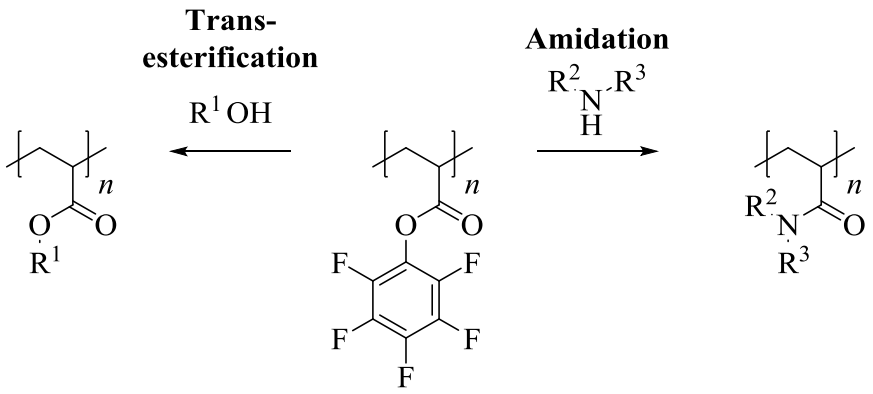

Scheme 11. PPM of poly(pentafluorophenyl acrylate) (PPFPA) *via* transesterification (left) and amidation (right) reactions.

In comparison to NHS esters, pentafluorophenyl esters are less prone to hydrolysis and feature a good solubility in different solvents.[125,136] The latter have been reported among others in single-chain nanoparticle (SCNP) systems[137–139] and for bioconjugation.[118] Additionally, polymer brushes made from PFPA grafted on silica particles were used for protein separation after immobilization with antibody.[140]

Moreover, nucleophilic ring-opening reactions have also been used in the field of PPM. Glycidyl methacrylate (GMA) is a commercially available monomer bearing an epoxide functionality and is thus attractive for the straightforward synthesis of PGMA and its functionalization. Different kinds of nucleophiles have been reported in ring-opening reactions with PGMA, resulting in a broad variety of further functionalization possibilities (**Scheme 12**).[127] Additional to the incorporated new functionalities, the hydroxy groups formed after ring-opening can be addressed by further functionalization.

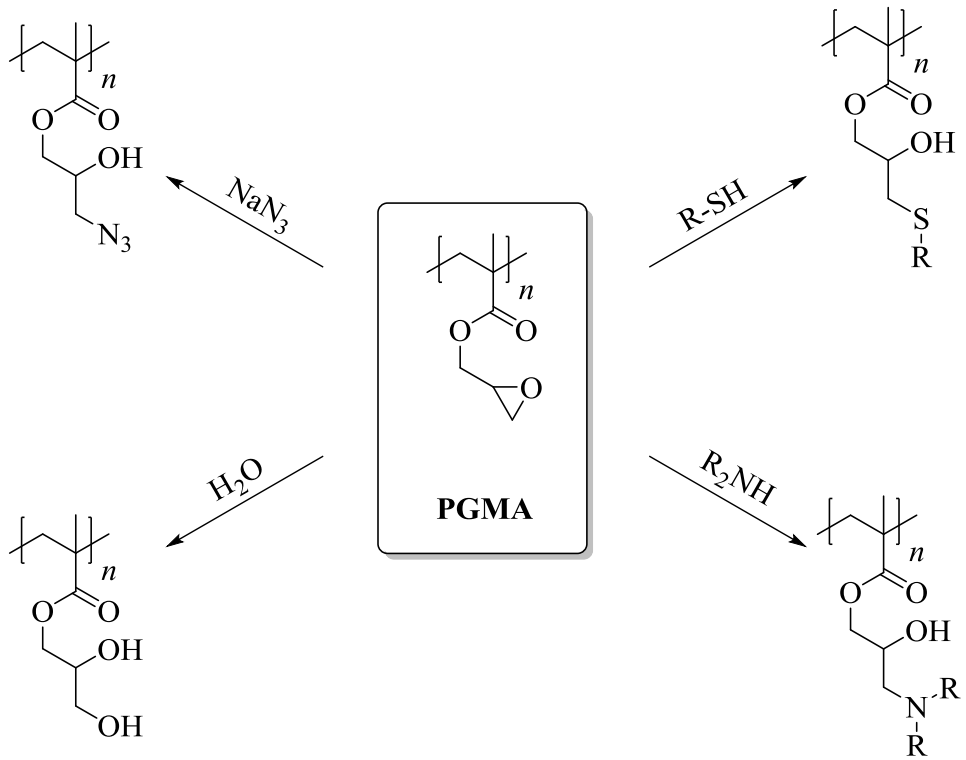

Scheme 12. Schematic extract of possible ring-opening reactions starting from PGMA as PPM precursor towards a broad range of novel functional materials.[127]

For instance, Matyjaszewski and coworkers demonstrated the preparation of graft copolymers by functionalization of a copolymer consisting of GMA and methyl methacrylate (MMA) repeating units with sodium azide in the presence of ammonium chloride as proton source to quench anionic ring-opening polymerization reactions.[141] The authors used ATRP for the

copolymerization and alkyne-functionalized poly(ethylene oxide) (PEO) chains for the CuAAC after ring-opening with sodium azide (**Scheme 13**).[141]

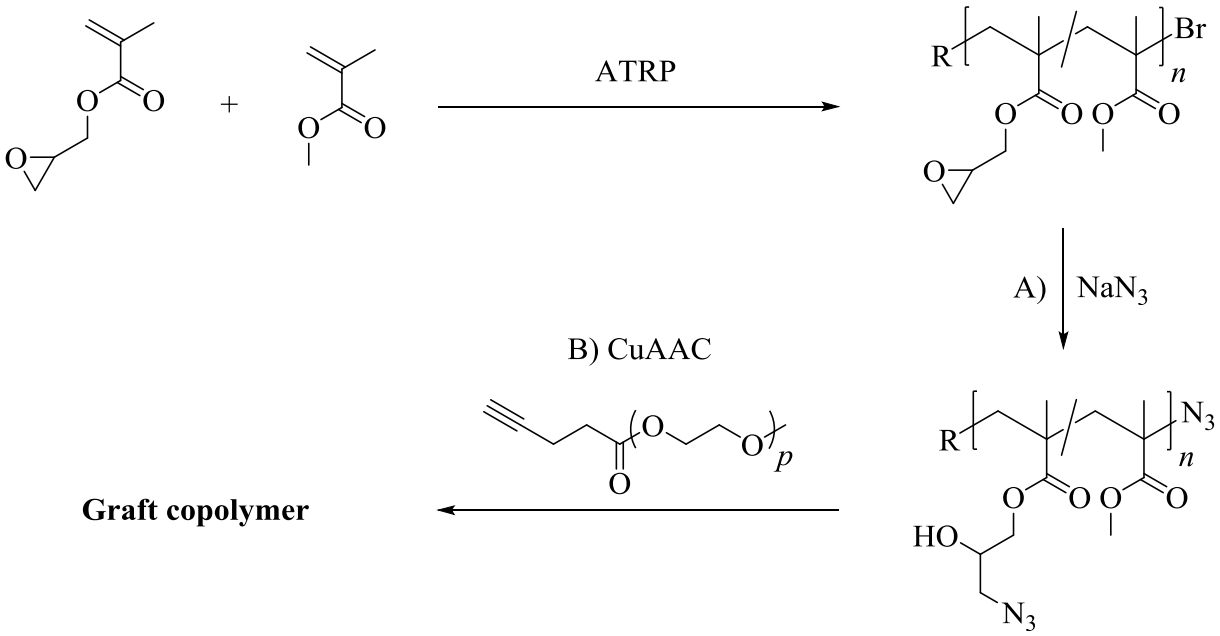

Scheme 13. Two consecutive PPM reactions starting from a PGMA copolymer *via* A) ring-opening of the epoxide with sodium azide and B) CuAAC with alkyne-functionalized PEO chains.[141]

2.4 Synthetic Electrochemistry

Synthetic (organic) electrochemistry represents a powerful toolbox for both the preparation of new substrates and the optimization of already reported synthesis pathways. Currently, it is a hot topic in scientific research and experiences a "renaissance"[7,8] with numerous different groups around the world exploring and discovering new findings every day. However, the use of electrochemistry is not restricted to scientific research laboratories, on the contrary, it plays a major role among others in the production of chlorine gas[142,143] and sodium hydroxide[142] for instance, but also of aluminum and organic substrates.[142] The use of synthetic electrochemistry is considered a sustainable alternative[9] to common synthesis procedures due to replacing oxidizing or reducing agents by electrons, thus gaining importance especially in times of raw material shortage. Additionally, the energy used to power a potentiostat (see later in this chapter) can be won in a climate-neutral fashion, enhancing the "green" character[9] of this methodology. It might surprise that only recently research groups are more and more focusing on implementing synthetic organic electrochemical methods into synthesis procedures, while first reports were already published almost 200 years ago. The so-called Kolbe electrolysis was one of the first reports[8,9] on synthetic electrochemistry published by Faraday in 1834[144] and further explored by Kolbe in 1849[145] and is still subject of scientific reports, including the elucidation of its mechanism.[146]

In general, an electrochemical setup consists of the following parts (**Figure 1**):[147] first, a power source, mostly a potentiostat, to deliver electricity and thereby powering the electrochemical reaction is required. There are several models from various suppliers with different characteristics to choose from. Under potentiostatic conditions (i.e. constant potentials), the potential, also called voltage (indication for the driving force behind the occurring redox processes),[148] can be fine-tuned, while under galvanostatic conditions (i.e. constant currents), the current (defined as charge per time and describing the rate of electron movement and inherently correlated with the potential)[148] can be adjusted by the potentiostat. Herein, the power source is connected to the electrodes, which are divided into cathode and anode. Reduction is taking place at the cathode, whereas the oxidation is occurring at the anode. The electrodes are typically made from metals or carbon-based materials and are in many cases self-made. Optionally, a reference electrode is used to monitor the actual voltage under potentiostatic conditions. Moreover, the electrodes can also be divided between "working electrode" and "counter electrode", the former is involved in the desired reaction and the latter is responsible to keep the electric circuit complete.

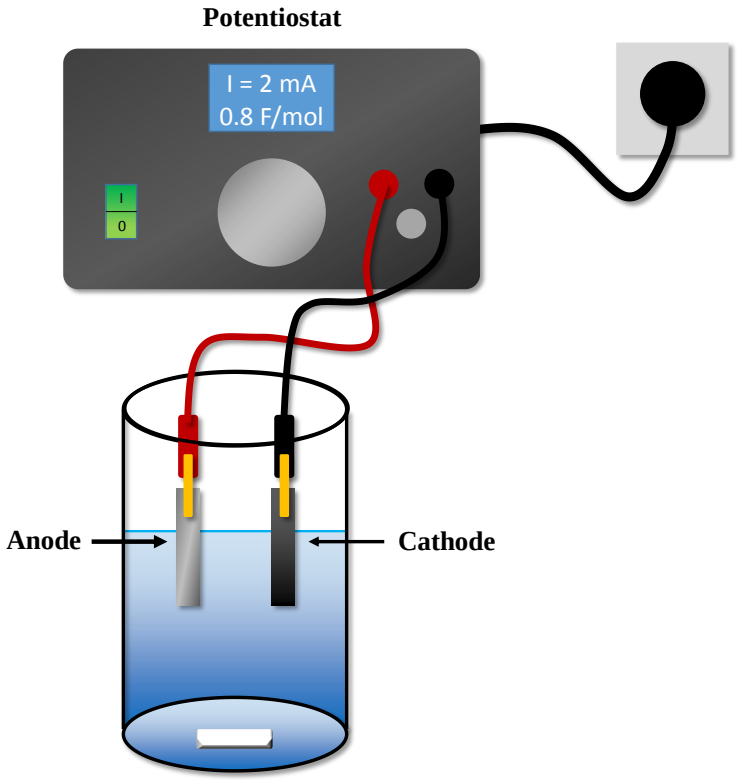

Figure 1. Depiction of a simple undivided cell setup: the potentiostat powers the reaction by delivering currents into the reaction mixture.

Two different kinds of setups need to be differentiated: the undivided cell is the simpler one and thus more appealing to industrial applications, while the divided cell setup allows for the separation of oxidation and reduction processes, using a frit or a permeable membrane (**Figure 2**).[148] Both oxidative and reductive processes are occurring in the same compartment in the undivided cell setup, it is thus necessary to consider the desired electrochemical transformation of the starting material as well as the electrochemical processes at the counter electrode.[148,149] In the case of a planned anodic oxidation reaction, proton donors are commonly employed, which will be reduced to gaseous hydrogen as "non-productive" side reaction.[148,149] For desired cathodic reductions, so-called sacrificial metal anodes (such as zinc or magnesium for instance) can be employed, which themselves are consumed during the electrolysis by oxidation to the respective metal ions.[148,150] In the case of a divided cell setup however, two "productive" reactions can be performed at the same time in two different cell compartments, if they require opposite redox manipulations.[148] Divided cell setups are indispensable when a species involved in the electrolysis requires protection from the counter electrode. The use of a frit or a membrane allows for the separation of the anodic and cathodic compartments, but increases the resistance as well as the complexity of the setup.[148] The undivided cell setup is the setup of choice if an industrial application is envisaged. Additionally, several reports have been

published on electrochemical flow setups, enhancing large scale electrochemical reactions by improved mass transfer for instance.[151,152]

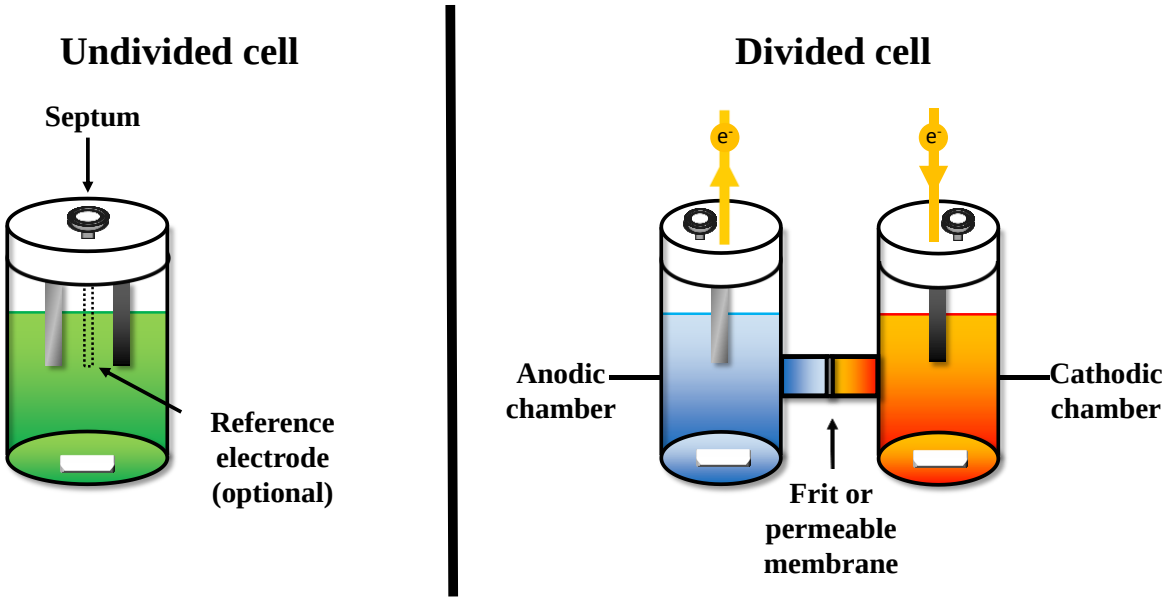

Figure 2. Schematic comparison of the undivided cell setup (left) and the divided one (right), the latter featuring separation of the anodic and cathodic chamber by a frit or a permeable membrane.[148]

In the simplest case, the electrolysis compartment contains the starting material dissolved in a suitable solvent and electrolyte. The latter is required due to the non-conductive nature of organic solvents.[149] Usually, soluble organic salts, such as tetrabutylammonium tetrafluoroborate (Bu_4NBF_4), are used to reduce the cell resistance in comparison to pure solvent, but also ionic liquids can be used for instance.[149] Furthermore, redox catalysts can be added to the solution if problems arise from the heterogeneous electron transfer in a direct electrolysis. These mediators must feature stability in both oxidation states, triarylamines,[153] quinones,[154] arylimidazoles,[155] nitroxyl radicals,[156] and transition metal ions[7,149] are common examples. The mediators are oxidized or reduced by heterogeneous electron transfer reactions and then oxidize or reduce the substrate in a homogeneous fashion (**Scheme 14**).

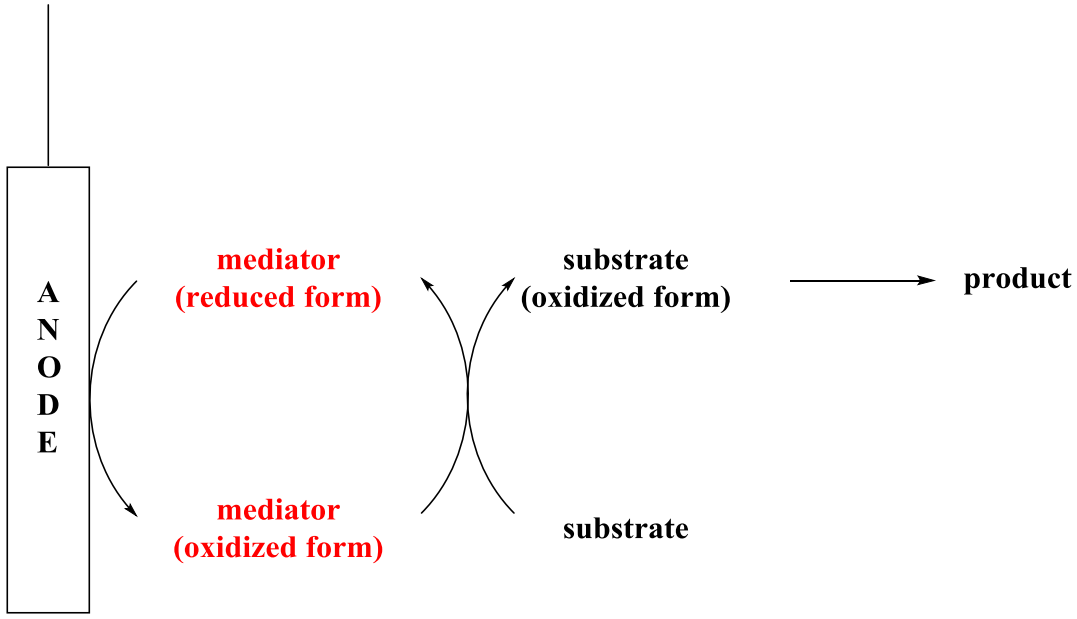

Scheme 14. Exemplary depiction of a mediated process, in which the mediator is electrochemically oxidized at the anode and subsequently oxidizes the substrate upon reduction to the initial mediator, resulting in the irreversible formation of the desired product.

Highly interesting and impactful electrochemical reactions have been reported in the field of synthetic organic chemistry, such as the metal- and reagent-free selective cross-coupling of phenols,[157] the electrochemically enabled, nickel-catalyzed amination,[158] and the "e-Birch" reduction.[158] Additionally, many literature reports regarding organic chemistry deal with electrochemically-mediated coupling reactions based on a nickel redox system:[159–163] different kinds of reactions have been reported and the scope of each of them was carefully evaluated by exhaustive screenings. Specifically, the work of Jiao *et al.* for instance focused on the cross-coupling of alkyl halides to aryl halides using a catalytic nickel system involving the application of electrochemical reduction reactions.[163] The authors postulated following mechanism for their cross-coupling reactions (**Scheme 15**):

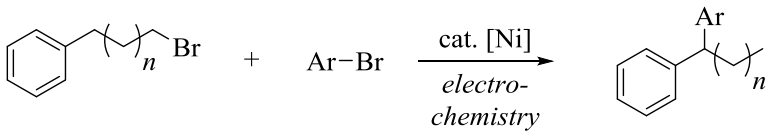

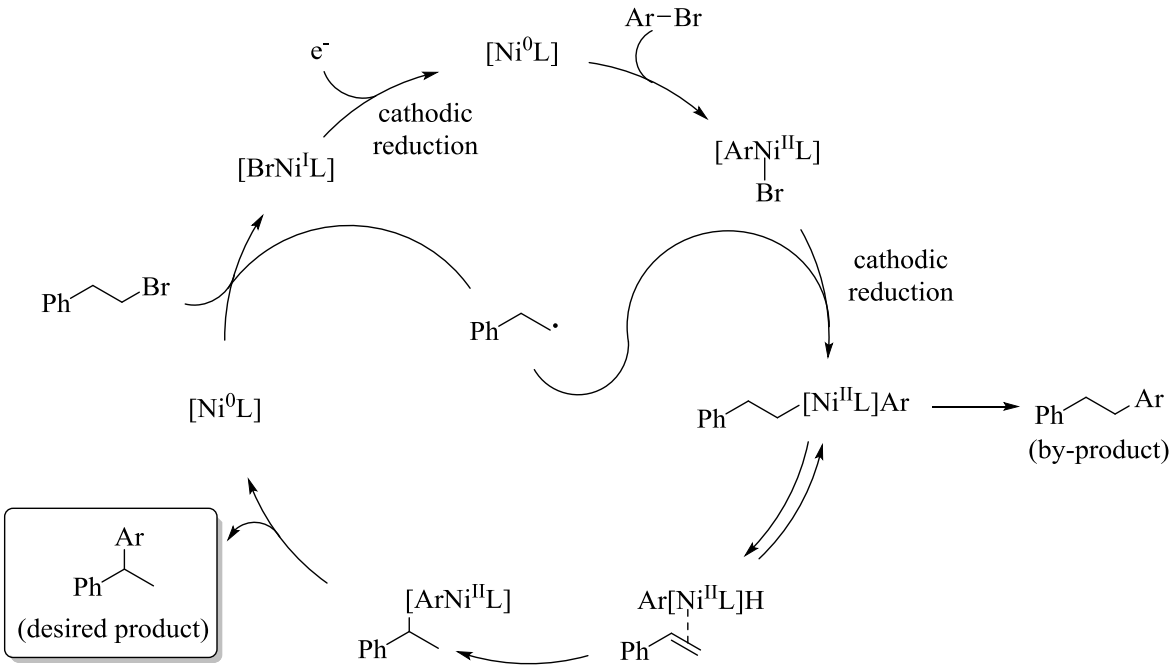

Scheme 15. Depiction of the nickel-catalyzed electrochemical reductive relay cross-coupling of alkyl halides to aryl halides with a plausible catalytic cycle.[163]

The catalytic cycle involves the use of a Ni^0 species after cathodic reduction of the Ni^{II} catalyst. Subsequently, the aryl bromide can undergo oxidative addition to the Ni^0 species and, after cathodic reduction, react with an alkyl radical species. This mechanism explains the formation of the linear by-product by direct reductive elimination. However, following the catalytic cycle, a more thermodynamically stable benzylic species is formed by β-hydride elimination/reinsertion steps.[163] Subsequently, reductive elimination yields the desired product and the resulting Ni^0 species can form alkyl radicals of the starting material. The nickel catalyst is then regenerated by electrochemical reduction.

In the field of polymer chemistry however, the use of synthetic electrochemistry is still lagging behind, however, electrochemical methods have been employed in different fields. Electropolymerization is a well-known field and involves the anodic oxidation of monomers like thiophene[164] and pyrrole,[165] but also electropolymerizations of acrylonitrile[166] and styrene[167] have been reported. In the case of pyrrole and thiophene[12] as monomers, the electropolymerization[11] leads to the formation of a conductive film covering the electrodes

and was first reported for pyrrole.[14] In these cases, anodic oxidation is leading to radical cation species, however, several postulated mechanisms exist for the electropolymerization of pyrrole.[13] Nonetheless, this phenomenon is used for electrode coating for instance,[15,16] in battery applications,[11] and in the field of information storage.[11]

However, reports involving both polymers and synthetic electrochemistry are not limited to electropolymerizations: eATRP[17,18] for instance allows for the synthesis of well-defined polymers by electrochemical fine-tuning of the equilibrium between Cu^{I} and Cu^{II} species. A first report on an electrochemically-induced initiation of RDRP was published in 2009, based on the electrochemical reduction of a Fe^{III}Salen complex.[168] The electrochemical control over an ATRP employing Cu^{I} and Cu^{II} was reported in 2011 by the group of Prof. Matyjaszewski.[169] The mechanism of eATRP is depicted below (**Scheme 16**):

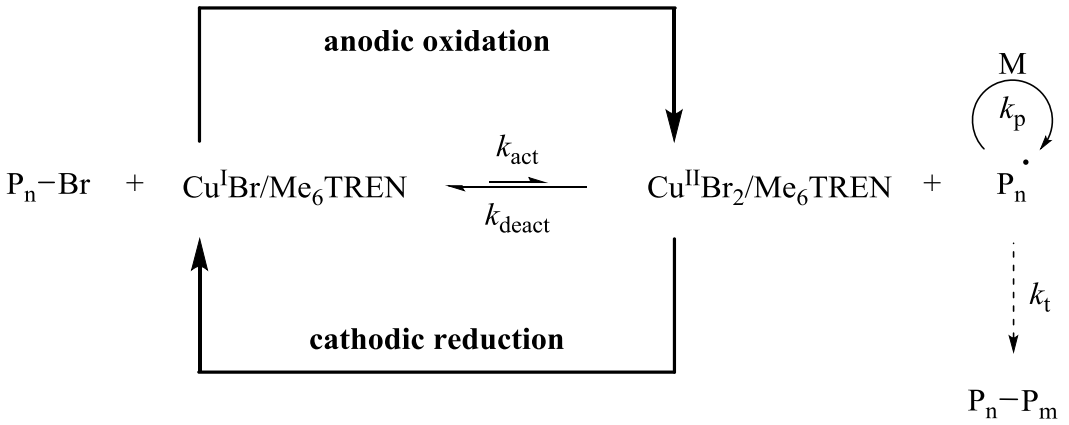

Scheme 16. Mechanism of eATRP using cathodic currents to (re)generate $Cu^{I}Br$/tris[2-(dimethylamino)ethyl]amine with optional anodic currents to transform it back into $Cu^{II}Br_2$/tris[2-(dimethylamino)ethyl]amine, enabling a well-controlled ATRP in a switchable fashion.[169]

The use of synthetic electrochemistry inherently offers the possibility to fine-tune numerous parameters in the course of the reaction. This unique feature was exploited to switch the polymerization on and off in a reversible fashion by varying the applied potential to induce oxidation and reduction of the catalyst.[169] A divided cell setup was used for this publication, thus circumventing potential side reactions at the counter electrode, but suffering from its more complex setup in comparison to an undivided cell.

In a more simplified approach, the group of Prof. Matyjaszewski reported the so-called simplified eATRP (seATRP), in which the necessity for a divided cell setup and potentiostatic conditions could be overcome by using sacrificial anode materials in a simple two-electrode cell setup.[170] Usually, platinum mesh electrodes separated from the reaction solution were

employed as anode, however, the authors could simplify the reaction setup by employing an aluminum wire, which is not interfering with the electrochemical redox manipulation of the copper catalyst.

Synthetic electrochemical means were intended to be implemented in the field of RAFT polymerization in an analogous fashion to eATRP. Ideally, the RAFT agent itself could be electrochemically transformed into a dithioate or trithiocarbonate anion and the respective radical of the leaving group by one-electron reduction, the latter being able to initiate polymerization. However, according to cyclic voltammetry (CV) and electrolysis experiments, the weak C-S bond is irreversibly cleaved in a two-electron reduction fashion, resulting in the dithioate or trithiocarbonate anion and the reduced form of the R group of the CTA.[19] This process is depicted in **Scheme 17** for 4-cyano-4-(phenylcarbonothioylthio)-2-methylpropionic acid (CPAD).

Irreversible two-electron reduction of CPAD

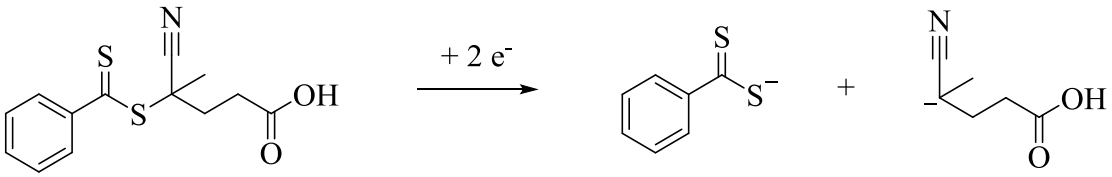

Scheme 17. Electrochemical two-electron reduction of CPAD as exemplary CTA, involving the irreversible formation of the dithioate anion in this case and the anion of the leaving group.

This finding is in accordance with another report, in which a direct electroreduction of the CTA resulted in the irreversible consumption of the latter accompanied by uncontrolled polymerizations.[21] Thus, a mediated approach is in most cases the basis for eRAFT polymerizations. The group of Prof. Matyjaszewski reported the use of a commercially available diazonium salt as source of radical species upon electrochemical reduction (**Scheme 18**).[19] The reduction takes place at mild conditions, leaving the CTA unaffected. The polymerizations were conducted *inter alia* using potentiostatic conditions with an applied potential of E_{app} = -0.1 V against a saturated calomel electrode (SCE).[19] The reactions were carried out in a divided cell setup, using a platinum wire counter electrode (anode) separated from the polymerization solution under both potentiostatic and galvanostatic conditions.

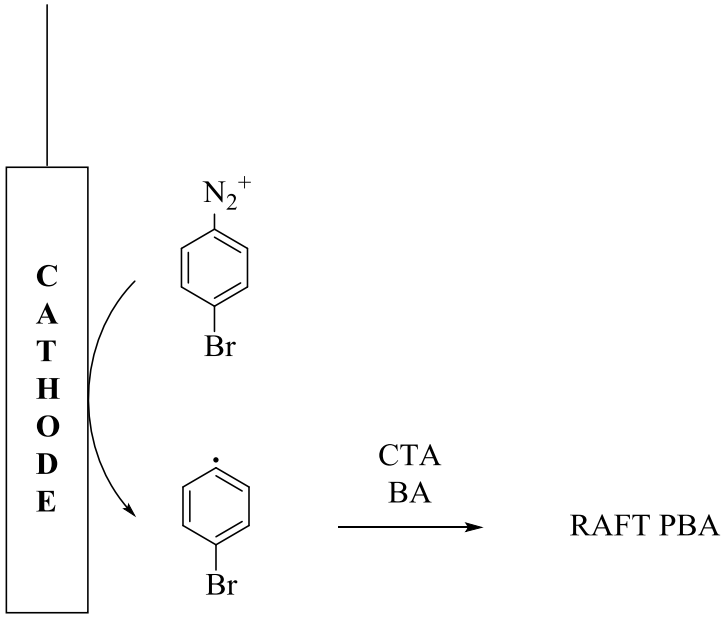

Scheme 18. Schematic depiction of the eRAFT polymerization of butyl acrylate (BA) based on the initiation *via* electrochemical cathodic reduction of an aromatic diazonium salt, resulting in poly(butyl acrylate) (PBA).

This publication laid the foundation for the first project (**Chapter 4.1**), which grounded on a fluorine-labelled aromatic diazonium salt for electrochemical initiation of the polymerization of reactive monomers (PFPA, 2,6-difluorophenyl acrylate (DFPA), and GMA), which are partially fluorine-labelled (PFPA and DFPA) and thus enabled straightforward analysis and determination of the number-average molar mass by ^{19}F NMR spectroscopy. These reactive polymers were subsequently used in PPM reactions to transform the active ester moieties to the respective amides and the epoxide functionality in PGMA to β-amino alcohols.

2.5 Sulfur-Nitrogen Polymers

A great variety of different polymers has been prepared and analyzed and many of them find application in various fields. Chemists were able to incorporate a broad range of functionalities into polymeric materials, resulting in unreported and highly interesting properties, not only from a scientific point of view, but also from an industrial one. However, macromolecules bearing sulfur-nitrogen motifs are still an underestimated class of polymers, even outperforming their conventional analogues in many disciplines,[171] with sulfur as the second chalcogene after oxygen being abundantly available in nature and accumulating in a multi-million ton scale as side product of oil and natural gas refining.[172]

Poly(thiazyl) or poly(sulfur nitride) is a polymer only consisting of S-N bonds and its structure is abbreviated with $(SN)_x$. It was discovered in 1910 when tetrasulfur tetranitride was subjected to heat in vacuum over silver gauze.[173] This inorganic polymer features many typical characteristics of metals. Scanning electron micrographs revealed that the obtained $(SN)_x$ crystals are composed of parallel fibers featuring an electric conductivity in the range of metals with a temperature dependence typical for metals.[174] However, the focus of this chapter lies on organic polymers featuring different sulfur-nitrogen (S-N) bond motifs. Various kinds of S-N functionalities either incorporated in the main chain or in the side group of polymers have been reported. The first main-chain poly(sulfenamide)s were reported in 2011 and 2012 by Bowden and coworkers in the frame of two PhD theses.[175,176] Both approaches were based on transamination of diamines with activated dithiol moieties (**Scheme 19**).

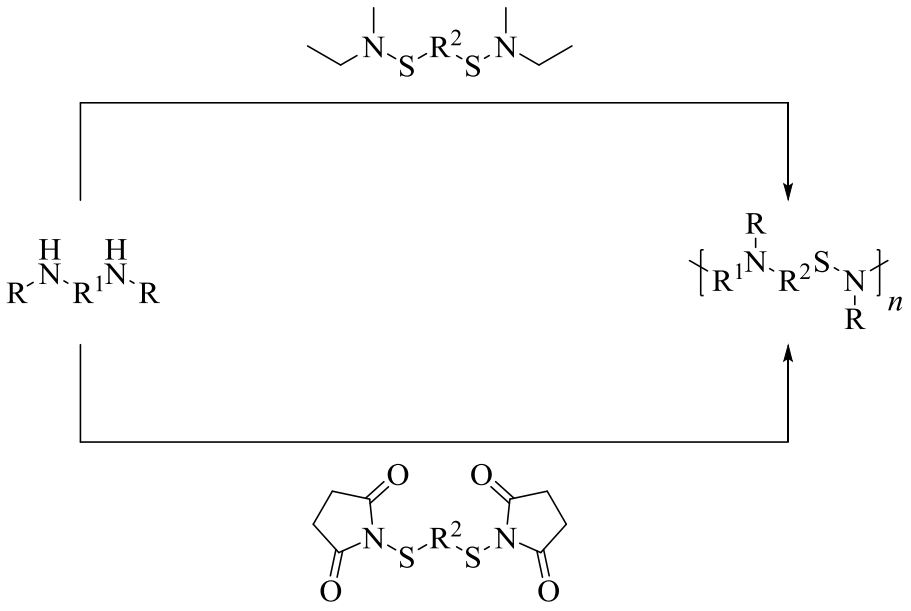

Scheme 19. Two different, but related routes towards poly(sulfenamide)s, based on transamination reactions.

Additionally, a report involved *inter alia* sulfenamide side groups in commercially available polymers for an evaluation of their structural properties and of their role as potential flame retardants.[177] The authors were able to show that sulfenamide derivatives can aid to self-extinguish different polymer films upon exposure to an ignition source. Among others, the authors employed following polymer structure for their study (**Scheme 20**):

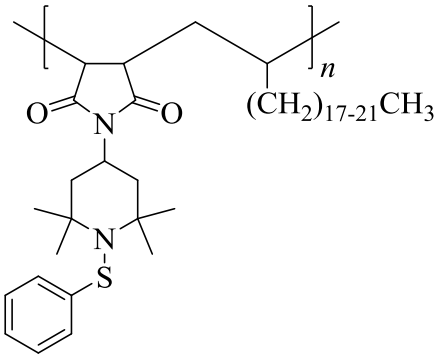

Scheme 20. Tentative structure of sulfenamide-functionalized Uvinul® 5050 H.

Replacement of the substitution on the sulfur atom by a second amine results in the formation of so-called diaminosulfides. The group of Bowden was another time pioneering in this field and reported main-chain poly(diaminosulfide)s based on the following synthetic strategy (**Scheme 21**):[178]

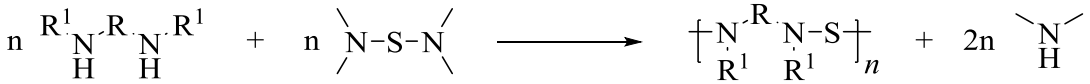

Scheme 21. Preparation of poly(diaminosulfides) by polymerization of diamines using a sulfur transfer agent.

Attempts with different sulfur transfer agents were conducted, however, some of them featured a poor solubility in organic solvents, limiting the applicability in polymerization reactions. The depicted diaminosulfide was *inter alia* used for the polymerization of diamines in either benzene or chloroform under reflux conditions, respectively. Polymers with different main-chain motifs could be obtained as depicted in **Scheme 22**.

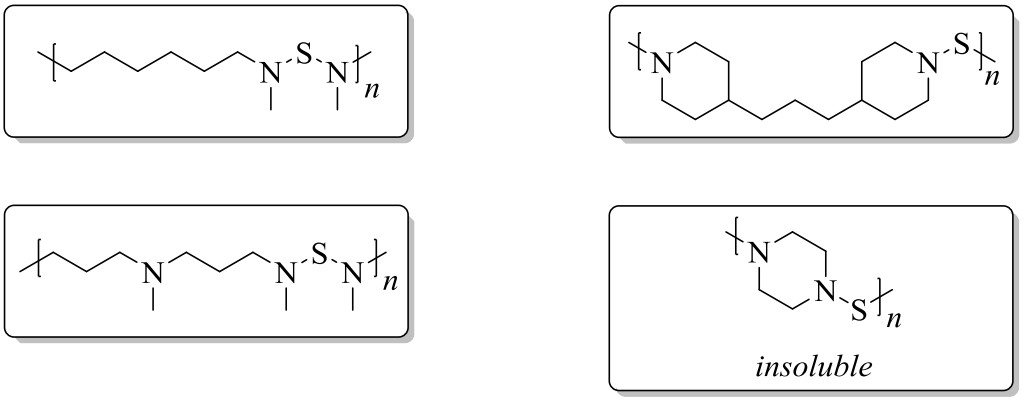

Scheme 22. Poly(diaminosulfide)s prepared from diamines and a sulfur transfer agent in different solvents (benzene and chloroform) at reflux conditions.

Already in the early 1970s, the synthesis and characteristics of poly(aminodisulfide)s have been reported, using aromatic amines (aniline in the case of **Scheme 23**) and sulfur monochloride.[179] The authors reported to have conducted the polymerization at 30 °C ≤ *T* ≤ 50 °C.[179] Additionally, almost 40 years thereafter, Bowden and coworkers demonstrated that, in case of using a base such as triethylamine at *T* = -78 °C, the previously reported polymerization of aniline and sulfur monochloride results in reaction pathway B) in **Scheme 23**.[180] This polymer can also be interpreted as representative of a poly(diaminodisulfide), as the repeating unit consists of a S-S-N backbone. This however implies the presence of a N-S-S-N structural motif, thus classifying them both as poly(aminodisulfide)s and poly(diaminodisulfide)s, the latter being used by the authors of the respective publication.[180]

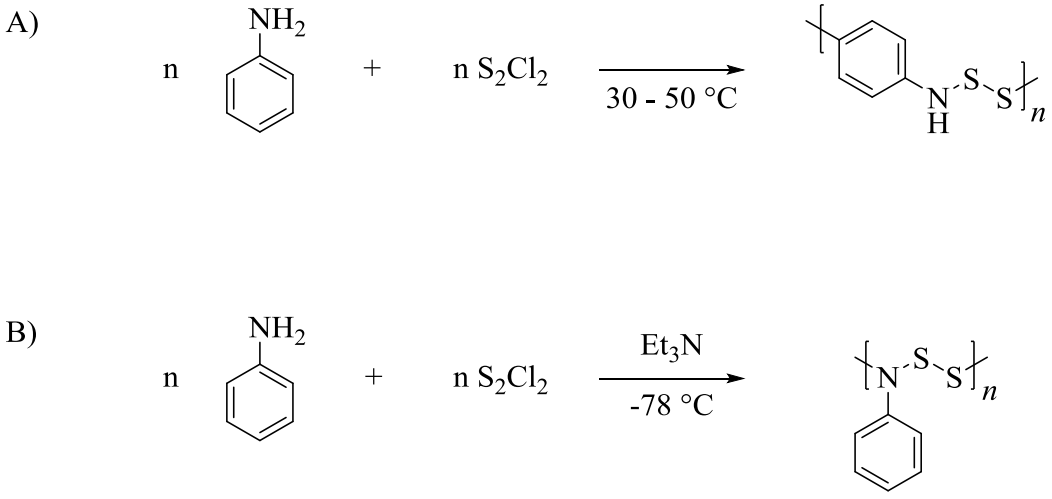

Scheme 23. Influence of the reaction conditions on the synthesis of poly(aminodisulfide)s from aniline and sulfur monochloride, resulting in the incorporation of the aromatic moiety either in the backbone (A)) or as a side group (B)).

In this report, the authors also published the synthesis of other poly(diaminodisulfide)s based on disulfide monomers (**Scheme 24**). Different disulfide monomers were attempted to be synthesized, but their purification and solubility was rather poor and thus limiting their use in polymerizations.[180]

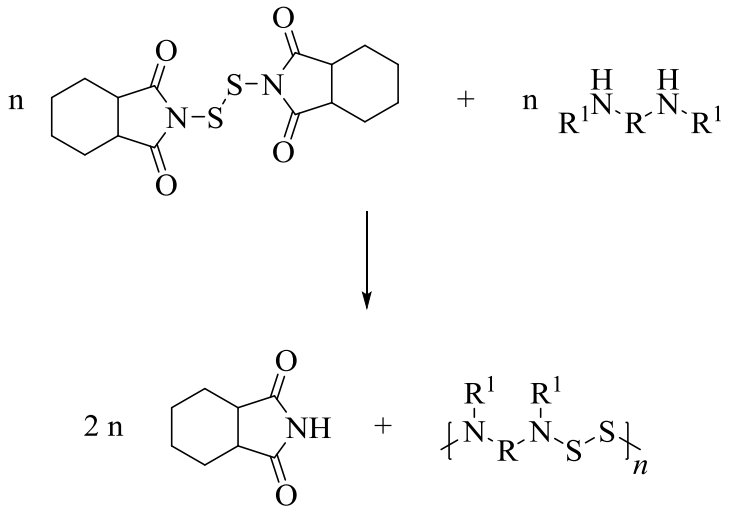

Scheme 24. Preparation of different poly(diaminodisulfide)s by polymerization of various diamines with dithiobiscyclohexanedicarboximide as disulfide monomer.

The different examples are not only interesting from a scientific viewpoint, but also with regards to potential applications. The polymers feature attractive properties making them *inter alia* suitable in the fields of energy storage, metal-ion detection, and in biomedicine.[171]
Specifically of interest for the present thesis, sulfonamide-based polymers represent another attractive class of sulfur-nitrogen polymers. Already in 1959, Sundet, Murphey, and Speck reported on the preparation of poly(sulfonamide)s by polycondensation of diamines and disulfonyl chlorides.[181] Both aliphatic and aromatic diamines were used, however high molar mass poly(sulfonamide)s were limited to the aliphatic ones. Furthermore, Imai and Okunoyama reported the preparation of "polyamide-sulfonamides" and their properties in 1972 based on polycondensation of *m*- and *p*-chlorosulfonylbenzoyl chlorides and diamines.[182] The general polymerization concept is depicted in **Scheme 25**.

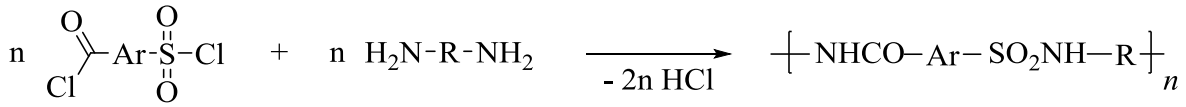

Scheme 25. Preparation of "polyamide-sulfonamides" by polycondensation of *m*- and *p*-chlorosulfonylbenzoyl chlorides and diamines.

However, particularly for the synthesis of sulfonamide-based polymers *via* radical polymerization, different works *inter alia* focused on the synthesis of methacrylamide-derived sulfonamide monomers as depicted in **Scheme 26**. These monomers were thereafter used in radical polymerization procedures (FRP and RAFT) for the synthesis of the respective sulfonamide polymers and copolymers.[183–186]

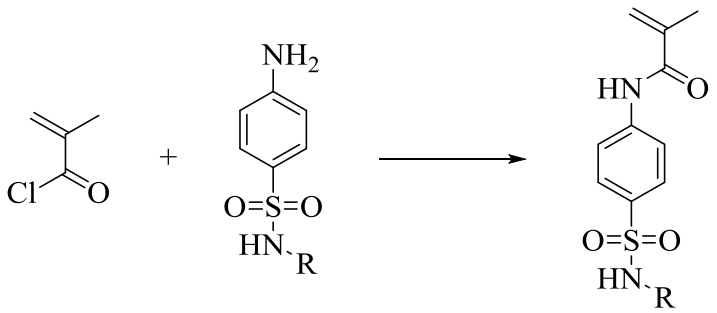

Scheme 26. Synthesis of methacrylamide-derived sulfonamide monomers.[185]

Interestingly, the obtained polymers featured a pH-dependent water solubility. They dissolved in water when pH > pK_a, but readily precipitated when pH < pK_a (**Scheme 27**). This feature was exploited to demonstrate the CO_2-dependent water solubility: the polymer was dissolved in an aqueous NaOH solution and the mixture was alternatingly purged with CO_2 and N_2. The dissolution of CO_2 in water results in the formation of carbonic acid, which can protonate present anionic sulfonamide polymers and thus led to the precipitation of the sulfonamide polymers in water.[183] However, the polymers started to dissolve again when the mixture was purged with N_2. The authors repeated this procedure to demonstrate the reversible water solubility of the sulfonamide polymers.[183]

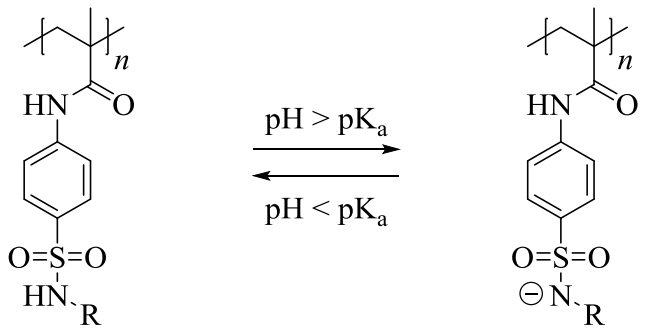

water-insoluble *water-soluble*

Scheme 27. Switchable, pH-dependent water solubility of methacrylamide-derived sulfonamide polymers.

Furthermore, the influence of different substituents on the water solubility behavior was studied by Abel *et al.*, exhibiting a drastic effect of the choice of substituent on the pK_a and consequently on the pH required to fully dissolve the polymer.[183]

In addition, Kakuchi and Théato followed another approach towards sulfonamide polymers, i.e. by PPM.[187] The authors prepared poly(pentafluorophenyl 4-vinylbenzenesulfonate) and exploited its reactive nature attributed to the pentafluorophenyl motif towards amines for the synthesis of the respective sulfonamide polymer. Subsequently, the resulting sulfonamide moiety was further functionalized by Mitsunobu reaction under suitable conditions, enabling a sequential PPM of poly(pentafluorophenyl 4-vinylbenzenesulfonate) (**Scheme 28**).

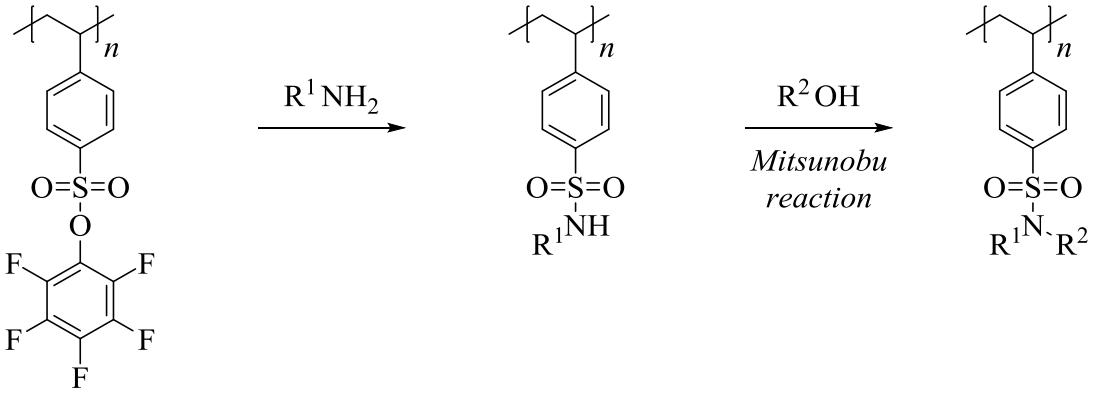

Scheme 28. Synthesis of aromatic sulfonamide polymers by PPM with subsequent Mitsunobu reaction for sequential PPM.[187]

Nonetheless, this chapter does not aim to list every class of sulfur-nitrogen polymers, but is rather meant to raise awareness of this class of innovative and attractive polymers, thus showing that pioneering works have been done and numerous reports are expected to be published in the future.

3 Motivation and Goal

In this thesis, a fully commercially available electrochemical setup, ranging from the potentiostat coming in a set with a suitable vial and electrodes, shall be employed for the electrochemical transformations to enhance reproducibility of the herein reported electrochemical reactions.

On the one hand, the electrochemically-initiated polymerization of reactive monomers based on a literature report employing an aromatic diazonium salt for electrochemically-mediated RAFT polymerization[19] is envisaged in the first project. In contrast to the as-mentioned publication, the polymerization should be performed on a simple undivided cell setup using galvanostatic conditions, allowing a straightforward, unprecedented, and easily accessible electrochemically-initiated polymerization of reactive monomers for the production of different functional polymers. Therefore, a fluorine-labelled diazonium salt is intended to be used as initiator in combination with fluorinated monomers among others in order to follow the polymerization itself by ^{19}F NMR spectroscopy and to determine the M_n of the resulting polymers in an analogous fashion. Additionally, the reactive nature of the resulting polymers should be demonstrated and consequently exploited by subsequent PPMs with another fluorine-labelled reactive moiety. This project thus aims for the demonstration of the compatibility of electrochemical methods with polymer chemistry in general and useful, but reactive monomers, such as PFPA, in particular.

On the other hand, a more complex *in-situ* ω-functionalization of electrochemically-polymerized macromolecules based on a catalytic nickel system and aryl bromides is envisaged for the one-step synthesis of defined polymers. This approach would represent a sophisticated and innovative one-batch pathway towards polymers with precise ω-functionalities from different monomers and a broad range of commercially available aryl bromides. In addition to small organic aryl bromides, polymeric aryl bromide moieties should be prepared and their suitability for this approach should be evaluated. Consequently, the one-pot preparation of graft copolymers would be enabled by synthetic electrochemistry in a straightforward fashion.

Lastly, the potential of electrochemical reactions as means for PPM should be explored and evaluated. In particular, the electrochemical deprotection of sulfonamide-tethered polymers should be examined, as an electrochemical deprotection would result in the release of reactive groups at “the push of a button” and consequently open further functionalization possibilities. This approach would thus allow a straightforward control over the temporal release of different functionalities, which might be of interest for different kinds of applications.

Consequently, this thesis is dealing with novel preparation and functionalization methods of functional polymers by electrochemistry and PPM, accordingly the respective results are described in **Chapter 4 (Results and Discussion)** within the specific subchapters.

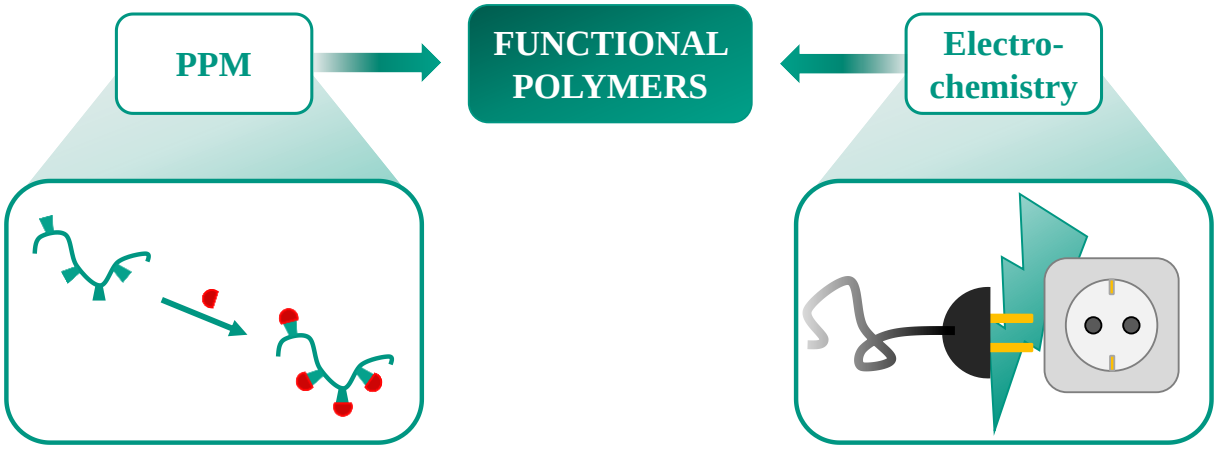

4 Results and Discussion

In the first part, different reactive monomers were polymerized by electrochemical means and subsequently modified by amidation of active ester moieties and ring-opening of epoxide functionalities, respectively. A fluorine-labelled initiator (i.e. 4-fluorobenzenediazonium tetrafluoroborate) was used allowing for the straightforward analysis and determination of the number-average molar mass in the case of fluorine-labelled monomers.

The second chapter deals with the nickel-catalyzed electrochemical ω-functionalization of macromolecules obtained by electrochemical polymerization, involving different aryl bromides as quenching agents for the polymerization.

In the last chapter, the aza-Michael functionalization of a novel class of aromatic poly(*N*-(4-vinylphenyl)sulfonamide)s with different electron-deficient alkenes is shown. Originally, the monomers and polymers synthesized in this project were intended to be used in electrochemical deprotections resulting in the respective free amine functionalities, which could be addressed by subsequent PPM reactions.

4.1 Electrochemically-Initiated Polymerization of Reactive Monomers *via* 4-Fluorobenzenediazonium Salts

This subchapter deals with the electrochemically-initiated polymerization of reactive monomers using a fluorine-labelled initiator, which allowed the straightforward analysis and determination of the M_n values of the obtained fluorine-labelled polymers by fluorine NMR spectroscopy. Specifically, 4-fluorobenzenediazonium tetrafluoroborate was used as initiator and DFPA, PFPA, and GMA as monomers. The development of such electrochemical polymerization techniques allowed for a straightforward polymerization of reactive monomers at "the push of a button" in a controlled and very mild fashion. The obtained polymers were then subjected to PPM with another fluorine-labelled molecule, i.e. 2,2,2-trifluoroethylamine. This enabled to follow the reaction and characterize the resulting products by ^{19}F NMR spectroscopy. The successful PPMs proved the reactive nature of the polymers, which remained intact under the electrochemical conditions, and ultimately demonstrated the compatibility of synthetic electrochemical methods with the field of polymer chemistry.

Parts of this chapter and the associated parts in the experimental section were adapted from a publication draft written by the author (Edgar Molle), which was submitted to Polymer Chemistry and is currently under revision.

Model monomer *N*-(2,2,2-trifluoroethyl)acrylamide was synthesized by Tilman Grüger in the frame of his Bachelor Thesis under the co-supervision of the author (Edgar Molle), which is also marked with a footnote in the respective experimental section.

4.1.1 General Concept

The concept (**Scheme 29**) behind this project based on three different reactive monomers, i.e. PFPA, DFPA, and GMA, which were employed in the electrochemically-initiated polymerization followed by PPM of the resulting polymers. A simple undivided cell setup in combination with commercially available electrodes was used to ensure accessibility and reproducibility of the polymerization. An aromatic, fluorine-labelled diazonium salt (4-fluorobenzenediazonium tetrafluoroborate) was envisaged as radical initiator upon cathodic reduction, allowing to prove the incorporation of the 4-fluorophenyl motif into the polymers by ^{19}F NMR spectroscopy. As discussed in **Chapter 2.4** (see **Scheme 18**), a similar electrochemical initiation system, i.e. its commercially available bromine derivative, was employed for the electrochemically-mediated RAFT polymerization of BA and MMA.[19] In contrast, the fluorine label allowed to follow the polymerization and to characterize the resulting polymers by fluorine NMR spectroscopy in a straightforward fashion. Also, for PFPA and DFPA as monomers, it enabled the determination of the M_n values of the polymers without being dependent on a SEC system. The reactive nature of the obtained polymers was proven by NMR and IR spectroscopy and furthermore exploited by PPMs, resulting in the amides for PPFPA and poly(2,6-difluorophenyl acrylate) (PDFPA) along the β-amino alcohol for PGMA, respectively. Therefore, another fluorine-labelled, reactive molecule, namely 2,2,2-trifluoroethylamine, was employed to repeatedly benefit from ^{19}F NMR spectroscopy as analytical method.

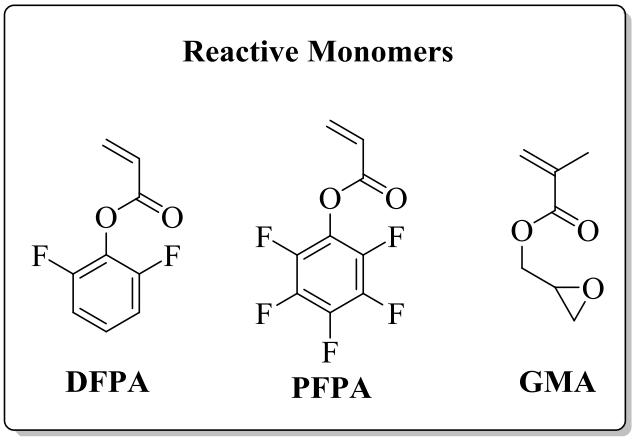

Electrochemically-initiated polymerization of reactive monomers with subsequent PPM

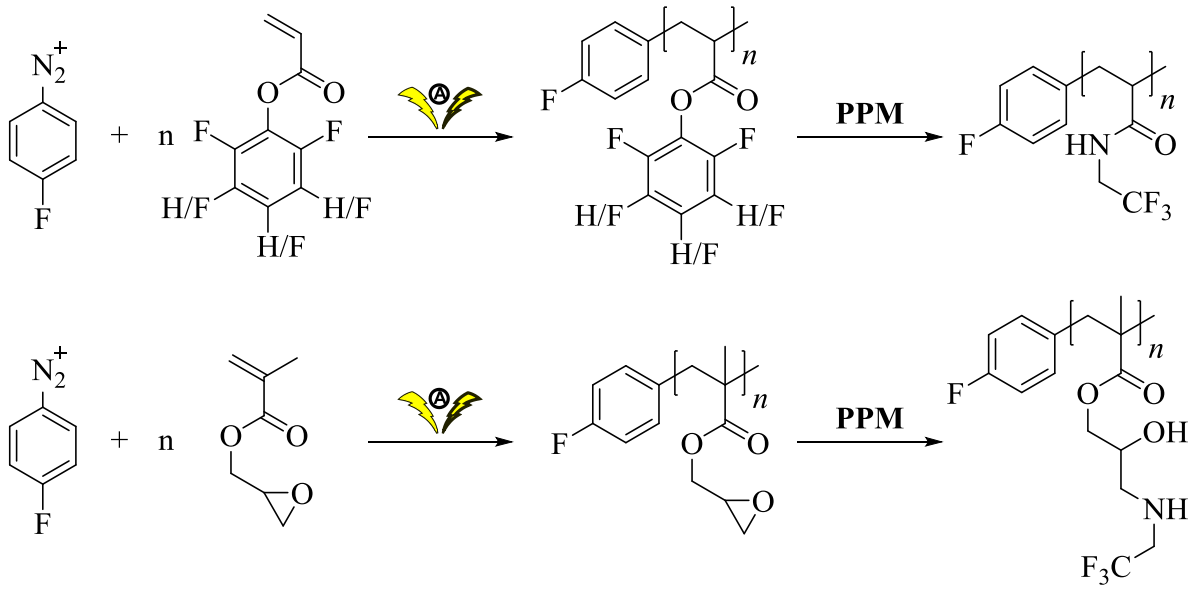

Scheme 29. Depiction of the general concept of electrochemically-initiated polymerizations of reactive monomers (PFPA, DFPA, and GMA), using a fluorine-labelled aromatic diazonium salt as initiator with subsequent functionalization of the obtained polymers.

4.1.2 Initiator and Monomer Synthesis

The fluorine-labelled aromatic diazonium salt, i.e. 4-fluorobenzenediazonium tetrafluoroborate, was used as the crucial compound in this project. It was able to generate radical species upon electrochemical cathodic reduction, which could subsequently initiate the polymerization process. Prior to experiments with 4-fluorobenzenediazonium tetrafluoroborate, polymerizations with its commercially available bromine derivative were successfully carried out using an undivided cell setup with galvanostatic conditions. Subsequently, 4-fluorobenzenediazonium tetrafluoroborate was synthesized (**Scheme 30**) according to standard diazotation procedures in literature.[188,189] The synthesis was carried out on small batches (≤0.5 g) due to the potential inherent explosion hazards of diazonium salts.[190]

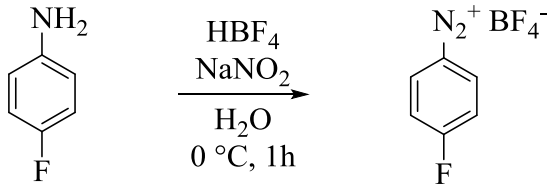

Scheme 30. Synthesis of 4-fluorobenzendiazonium tetrafluoroborate from 4-fluoroaniline using aqueous tetrafluoroboric acid (HBF_4) and sodium nitrite ($NaNO_2$).

The desired product was obtained by filtration and precipitation steps in a yield of 39% and was stored at T = -20 °C protected from light sources to circumvent potential decomposition reactions.

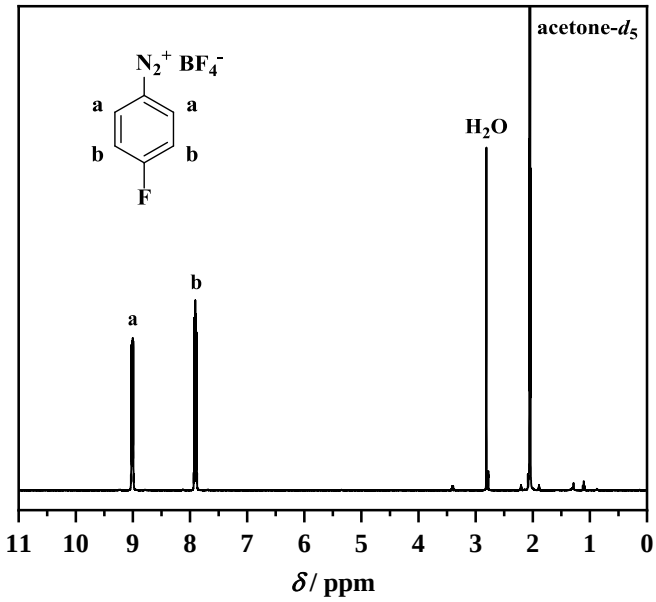

Figure 3. ^{1}H NMR spectrum of the isolated 4-fluorobenzenediazonium tetrafluoroborate; solvent: acetone-d_6.

In **Figure 3**, the ^{1}H NMR spectrum of 4-fluorobenzenediazonium tetrafluoroborate is depicted. It showed two signals at chemical shifts of δ = 8.98 – 9.04 ppm and δ = 7.87 – 7.94 ppm with an integration ratio of 1:1. Additionally, the ^{19}F NMR spectrum in **Figure 4** exhibited two signals at δ = -86.66 ppm and at δ = -151.09 ppm, arising from the fluorine atom in *para* position and the tetrafluoroboric anion.

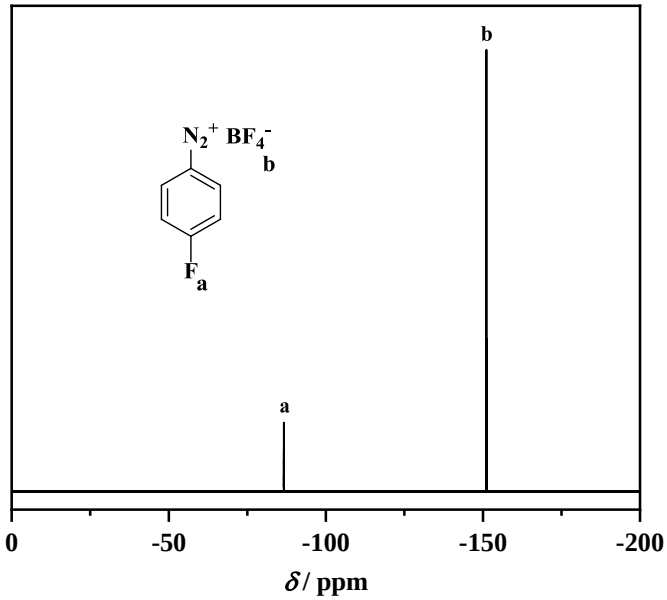

Figure 4. ^{19}F NMR spectrum of the isolated 4-fluorobenzenediazonium tetrafluoroborate; solvent: acetone-d_6.

PFPA as first active ester monomer was synthesized from pentafluorophenol and acryloyl chloride as depicted in **Scheme 31** and was obtained in a yield of 67% after purification by column chromatography.

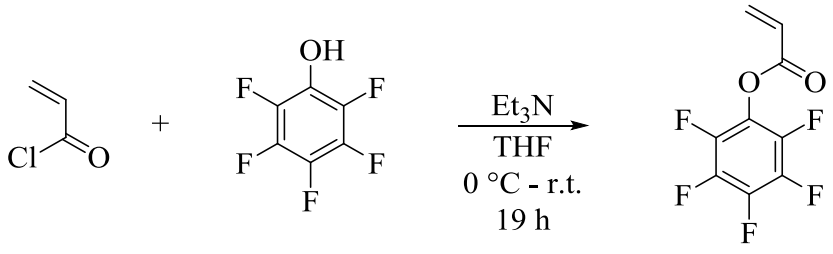

Scheme 31. Synthesis of PFPA from acryloyl chloride and pentafluorophenol.

PFPA as monomer is literature-known and has been excessively employed as monomer for the synthesis and PPM of active ester polymers.[125,126,137–140]

DFPA was prepared in a similar fashion (**Scheme 32**) and was obtained as a yellow liquid in good yield (77%) after aqueous workup and purification by column chromatography.

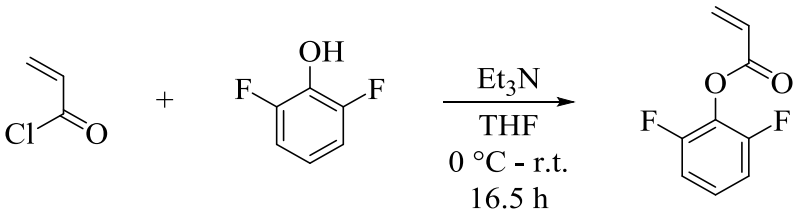

Scheme 32. Synthesis of DFPA starting from acryloyl chloride and 2,6-difluorophenol.

The obtained product was analyzed by ^{1}H and ^{19}F NMR spectroscopy: the proton NMR spectrum is depicted in **Figure 5** and showed signals arising from the aromatic protons in *para* and *meta* position at chemical shifts of δ = 7.34 – 7.43 ppm and δ = 7.15 – 7.23 ppm as well as from the vinylic protons at δ = 6.68 ppm, δ = 6.48 ppm, and δ = 6.24 ppm.

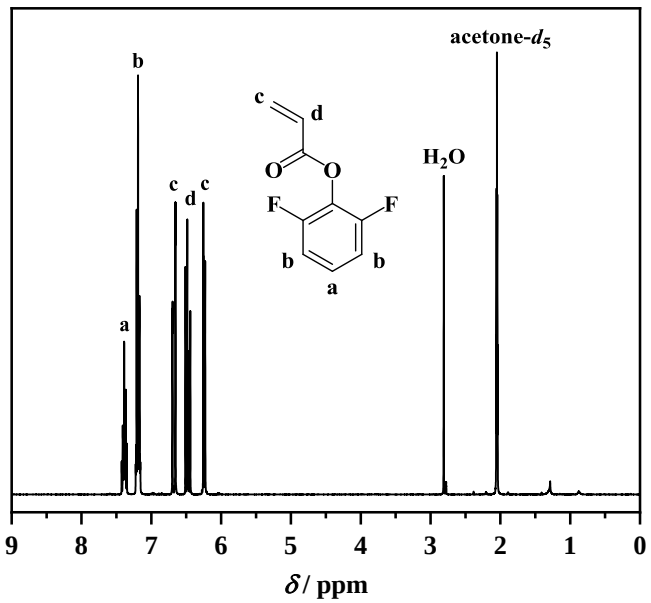

Figure 5. ^{1}H NMR spectrum of DFPA obtained after reaction of acryloyl chloride and 2,6-difluorophenol; solvent: acetone-d_6.

The ^{19}F NMR spectrum (**Figure 6**) also confirmed the successful synthesis of DFPA, solely exhibiting one signal arising from the two fluorine atoms in *ortho* position in DFPA at a chemical shift of δ = -128.34 – -128.47 ppm.

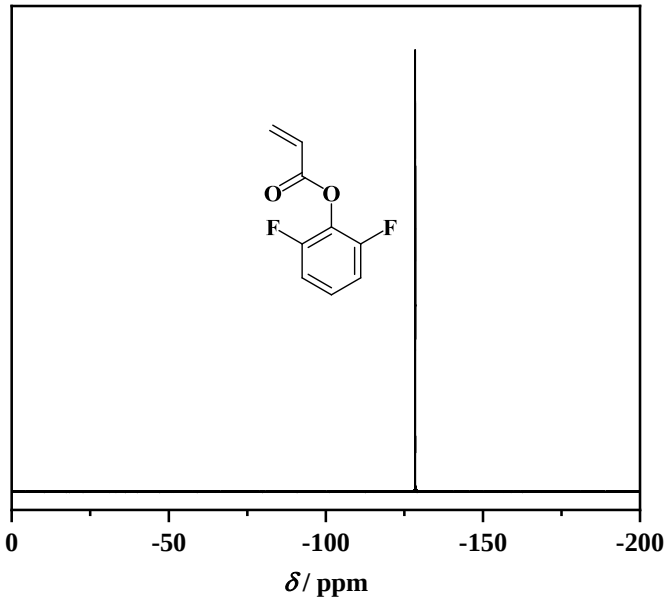

Figure 6. ^{19}F NMR spectrum of DFPA; solvent: acetone-d_6.

In contrast to PFPA and DFPA as monomers, GMA was obtained from a commercial supplier.

4.1.3 Polymerization and PPM of PFPA and PPFPA

Two different fluorine-labelled reactive monomers, namely PFPA and DFPA, were employed as reactive monomers for the electrochemically-initiated polymerization. On the one hand, PFPA and DFPA feature fluorine atoms allowing for the straightforward calculation of the M_n values of the resulting polymers by ^{19}F NMR spectroscopy and on the other hand, their structure allows for modifications of the ester moiety due to its electron-deficient nature. The electron deficiency is however more pronounced in the case of PFPA, milder reaction conditions are thus applicable for the functionalization of PPFPA in contrast to PDFPA.

The as-prepared monomer PFPA was used along with the initiator 4-fluorobenzenediazonium tetrafluoroborate in an electrochemically-initiated polymerization in a solution of Bu_4NBF_4 as electrolyte in *N*,*N*-dimethylformamide (DMF) (**Scheme 33**).

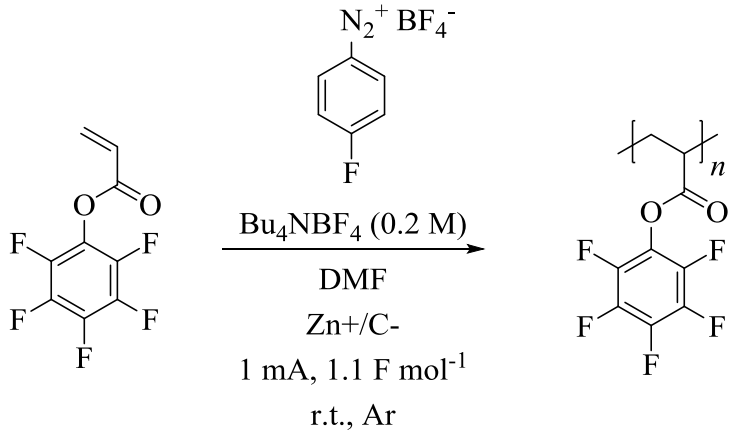

Scheme 33. Electrochemically-initiated polymerization of PFPA using 4-fluorobenzenediazonium tetrafluoroborate as radical initiator upon electrochemical cathodic reduction.

Instead of a divided cell setup as used in the electrochemically-mediated RAFT polymerization with high-cost platinum electrodes,[19] a simple undivided cell setup was employed. Therefore, in a first polymerization approach, galvanostatic conditions (constant current of 4 mA for a duration of 4 F mol^{-1}, the use of a reference electrode could consequently be avoided) were applied. Herein, a sacrificial zinc anode was employed to suppress undesired oxidation reactions at the anode, since the polymerization is solely based on the reduction of the diazonium salt. A reticulated vitreous carbon (RVC) cathode was used as affordable material featuring a high ratio of surface area to volume due to its porous structure.[191] This attempt yielded polymeric material and the project was further pursued in the frame of a Bachelor Thesis.[192] It was *inter alia* demonstrated that graphite as simple cathodic electrode material

can be used for the polymerization, facilitating the cleaning process of the electrode materials. Also, different other fluorine-labelled monomers such as 4-fluorostyrene and pentafluorostyrene were tested: for 4-fluorostyrene as monomer, no polymer was obtained, and an insoluble gel at the cathode was formed in the case of pentafluorostyrene, transforming into hairy fibers upon drying.[192] This phenomenon of a gel formation for pentafluorostyrene as monomer could be reproduced, even when the electrolysis was carried out in the absence of an initiating moiety, indicating a direct electrochemical polymerization. Hence, the focus was set on PFPA as fluorine-labelled monomer and the conditions were adapted: for purification, the obtained polymers were precipitated twice in cold methanol to remove residual monomers and Bu_4NBF_4 used as electrolyte. After the first precipitation, the solids were dissolved and filtered by a syringe filter to remove insoluble graphite from the cathode. In the cases of a polymerization duration of 4 F mol^{-1}, constant currents of 4 mA and 2 mA appeared to result in degradations visible in the respective fluorine NMR spectra. Only at a constant current of 1 mA, the decomposition could be circumvented, revealing the electrochemically-sensitive nature of PFPA and its polymer (**Figure 7**).

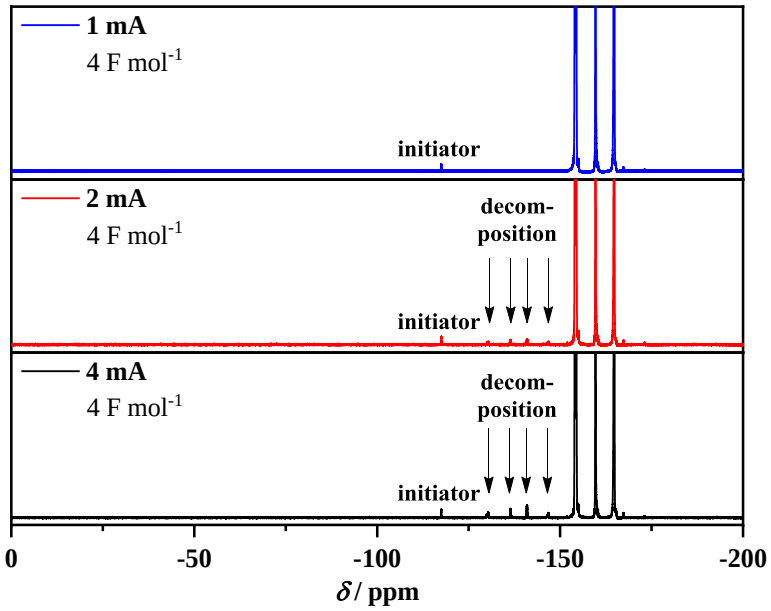

Figure 7. Comparison of ^{19}F NMR spectra of the electrochemically-initiated polymerization of PFPA (10.00 eq. with respect to the initiator) using constant currents of 4 mA (bottom, black line), 2 mA (middle, red line), and 1 mA (top, blue line) for 4 F mol^{-1}, exhibiting signals of potential decomposition for the first two currents and thus revealing the electrochemically-sensitive nature of PFPA and its polymer; solvent: acetone-d_6.

With these results in mind, future electrochemically-initiated polymerizations of PFPA were carried out at constant currents of 1 mA. However, the duration was reduced to 1.1 F mol^{-1} with

respect to 4-fluorobenzenediazonium tetrafluoroborate as initiator, equaling to 1.1 electrons absorbed by the system. The polymerization time was reduced to ensure a polymerization initiated by the 4-fluorobenzene radical and exclude the possibility of a direct electrochemical polymerization of the monomer. The latter was tested in an experiment with identical conditions (constant current of 1 mA and a duration of 4 F mol^{-1}) to the actual polymerization, however, in the absence of the initiator. The reaction led to negligible amounts of hardly soluble material. Furthermore, the chain lengths of the resulting PPFPA polymers were tuned by variation of the ratio of monomer to initiator, whilst the amount of the latter (0.12 mmol) was kept constant throughout all experiments. A monomer to initiator ratio of 20 and above resulted in a hardly soluble gel formed between the electrodes, suggesting that the monomer concentration was exceeding the limitations under these conditions. Nonetheless, the results of the polymerizations of PFPA with different reaction conditions are included in **Table 1**. M_n values determined by ^{19}F NMR spectroscopy were obtained by integration of the signals arising from PPFPA (δ = -153.68 – -154.71 ppm, δ = -159.40 – -159.88 ppm, and δ = -164.30 – -165.04 ppm) and the fluorine signal of the initiator (δ = -117.42 – -117.60 ppm), allowing to calculate the number of repeating units and consequently the M_n values. The respective values obtained from ^1H NMR spectroscopy were calculated in a similar fashion, the integrals of the aromatic protons arising from the initiator (δ = 7.28 – 7.39 ppm and δ = 7.02 – 7.12 ppm) were compared to the backbone signals of PPFPA (δ = 3.11 – 3.41 ppm and δ = 2.10 – 2.68 ppm). Additionally, the M_n and dispersity values were determined by SEC using both tetrahydrofuran (THF) and *N*,*N*-dimethylacetamide (DMAc) as eluents, referring to calibrations with linear narrow PMMA and PS standards.

Table 1. Details and results of the electrochemically-initiated polymerization of PFPA (1 mA, 1.1 F mol^{-1}) as reactive monomer.

Entry	Eq.	M_n[a] g mol^{-1}	M_n[b] g mol^{-1}	M_n[c] g mol^{-1}	$Đ$[c]	M_n[d] g mol^{-1}	$Đ$[d]
1[g]	40.00	33240	40180	41800[e]	2.30[e]	30300[e]	2.48[e]
				37000[f]	2.28[f]	34300[f]	2.29[f]
2	10.00	22630	35030	19200[e]	1.83[e]	13900[e]	2.03[e]
				17400[f]	1.76[f]	16500[f]	1.83[f]
3	5.00	14170	24480	13600[e]	1.61[e]	9900[e]	1.82[e]
				12500[f]	1.53[f]	12000[f]	1.65[f]
4[h]	5.00	14290	22500	13200[e]	1.59[e]	9500[e]	1.72[e]
				12100[f]	1.52[f]	11500[f]	1.57[f]

[a] Determined by ^{1}H NMR spectroscopy; [b] determined by ^{19}F NMR spectroscopy; [c] determined by SEC using THF as eluent; [d] determined by SEC using DMAc as eluent; [e] PMMA calibration; [f] PS calibration; [g] monomer concentration presumably exceeded polymerization limitations, resulting in a viscous mixture and the formation of hardly soluble material between the electrodes; [h] 2 mA instead of 1 mA.

The results obtained by fluorine NMR spectroscopy were in most cases overestimating the chain lengths of the PPFPA macromolecules. The relatively low intensity signal of the fluorine atom from the initiating motif in comparison to the PPFPA signals (**Figure 8**) complicated a proper integration and consequently the determination of M_n values. The values (**Table 1**) obtained by proton NMR spectroscopy (**Figure 9**) were mostly in accordance with the SEC results (THF as eluent and PPMA calibration) (**Figure 10**). The obtained results indicated a clear trend: the chain length increased with increasing ratio of monomer to initiator. Additionally, in the case of using 10.00 equivalents with respect to the initiator, the obtained polymer featured, according to NMR spectroscopy, approximately 95 repeating units (^{1}H NMR) or 147 repeating units (^{19}F NMR) on average. Nonetheless, NMR spectroscopy showed that the structural motifs of the polymers, and thus the reactive character of the polymers, were not affected by the polymerization.

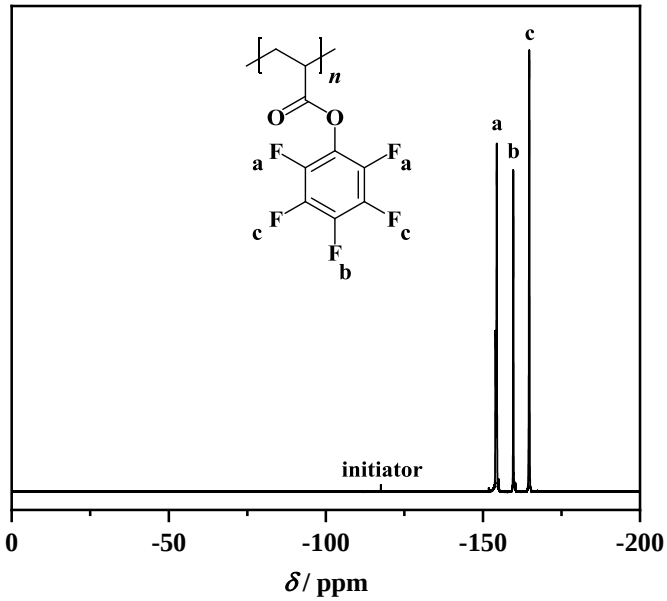

Figure 8. Exemplary ^{19}F NMR spectrum of PPFPA obtained by electrochemically-initiated polymerization of PFPA (in this case: 5.00 equivalents with respect to the initiator, **Table 1**, Entry 3); solvent: acetone-d_6.

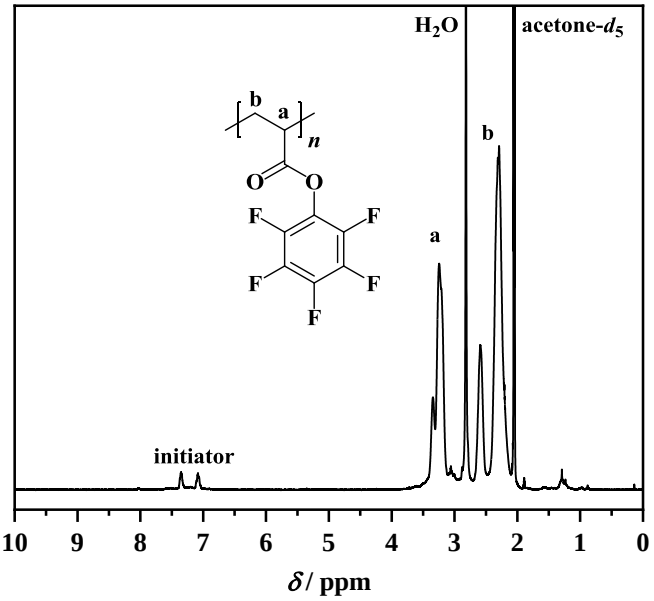

Figure 9. Exemplary ^{1}H NMR spectrum of PPFPA obtained by electrochemically-initiated polymerization of PFPA (in this case: 5.00 equivalents with respect to the initiator, **Table 1**, Entry 3); solvent: acetone-d_6.

The resulting polymers were analyzed by SEC with THF as eluent as depicted in **Figure 10**. Additionally, the polymers were also characterized by SEC with DMAc as eluent (see **Chapter 6.4.2.2**, **Figure 67**) due to its more pronounced suitability for the analysis of the resulting polyamides obtained upon PPM.

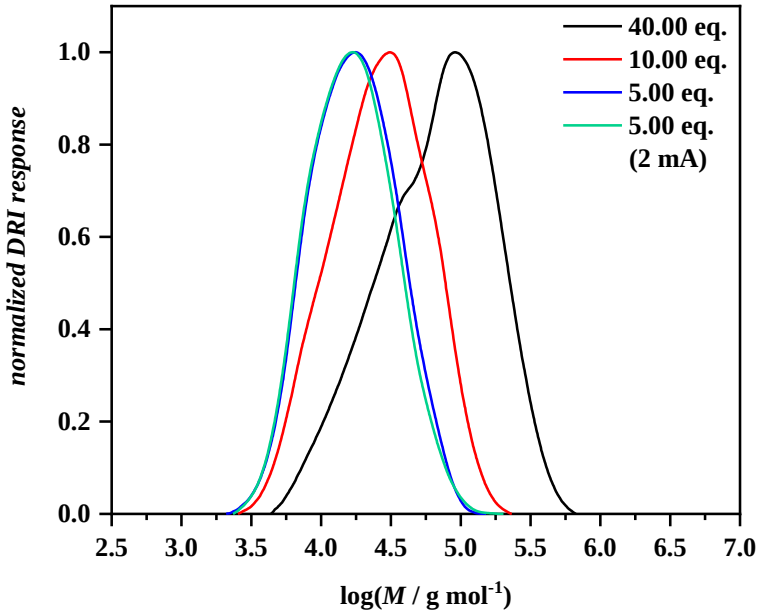

Figure 10. Comparison of SEC traces using THF as eluent (PMMA calibration) of the polymers obtained by the electrochemically-initiated polymerization of PFPA with different equivalents of PFPA with respect to 4-fluorobenzenediazonium tetrafluoroborate as initiator (black line: 40.00 equivalents; red line: 10.00 equivalents; blue line: 5.00 equivalents; green line: 5.00 equivalents, 2 mA).

The SEC traces showed relatively narrow distributions except in the case of the electrochemically-initiated polymerization of 40.00 equivalents with respect to the initiator. In this case, a hardly soluble gel was formed between the electrodes, which indicated that the monomer concentration was exceeding the limitations of this polymerization method, hence resulting in a broadened molar mass distribution.

To stress the reactive character of the polymers prepared by electrochemical means, the active ester polymer obtained after polymerization (10.00 equivalents PFPA with respect to the initiator) was subjected to PPM reaction using a fluorine-labelled amine, i.e. 2,2,2-trifluoroethylamine (**Scheme 34**).

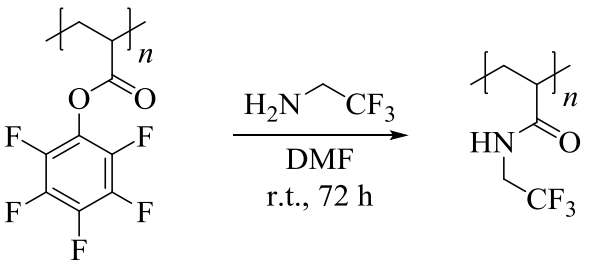

Scheme 34. PPM of PPFPA using 2,2,2-trifluoroethylamine for the synthesis of the respective polyamide.

PPFPA has been excessively explored in PPMs due to its electron-deficient nature of the active ester moiety.[119,125,193–197] Before using the conditions depicted in **Scheme 34**, triethylamine was employed as auxiliary base at room temperature. An excess of amine (3.00 equivalents with respect to a PFPA repeating unit) was used and the polymer was purified by precipitation in petroleum ether (PE).

^{19}F NMR spectroscopy (**Figure 11**, bottom) revealed the complete removal of signals arising from PPFPA (δ = -153.80 – -154.64 ppm, δ = -159.42 – -159.82 ppm, and δ = -164.35 – -164.95) and two new signals arising at δ = -72.00 – -73.20 ppm and δ = -69.24 – -70.45 ppm. However, the desired polyacrylamide should only exhibit one main signal arising from the CF_3 functionality in fluorine NMR spectroscopy at δ = -72.00 – -73.20 ppm. The second signal at δ = -69.24 – -70.45 ppm could indicate the formation of the respective imide instead of the amide: the use of an auxiliary base, such as triethylamine, appeared to favor the imide formation. This result was considered in the following PPM, which was performed in the absence of an auxiliary base. Additionally, the excess of amine (25.00 equivalents with respect to PFPA repeating units) was increased to suppress the imide formation. The polymer was purified in a similar fashion, but this time giving mainly one signal in the fluorine NMR spectrum at δ = -72.30 – -72.98 ppm (**Figure 11**, top).

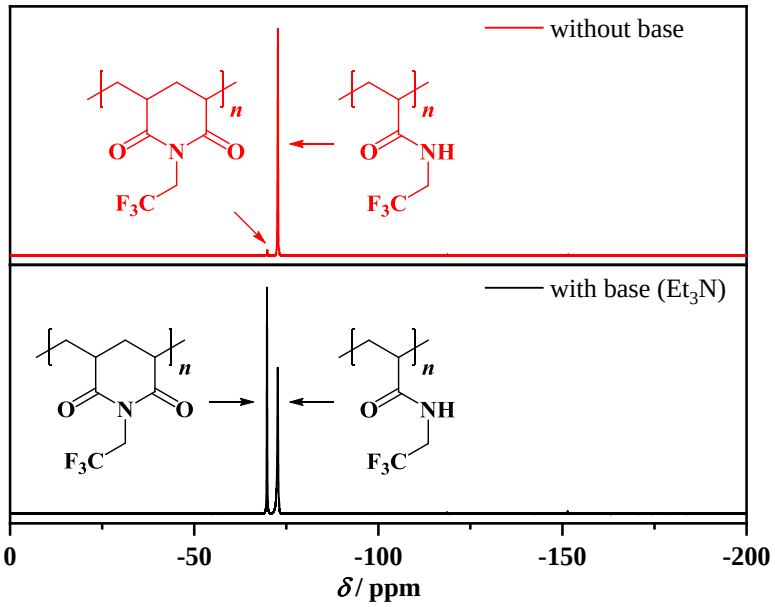

Figure 11. Comparison of ^{19}F NMR spectra obtained after PPM using 2,2,2-trifluoroethylamine with (bottom, black line) and without (top, red line) the presence of a base; solvent: acetone-d_6.

To confirm the chemical shifts in ^{19}F NMR spectroscopy, the respective monomer *N*-(2,2,2-trifluoroethyl)acrylamide was synthesized (see **Chapter 6.4.5.1**) and subsequently polymerized *via* FRP (**Scheme 35**). This approach resulted solely in the formation of the respective polyamide, circumventing the formation of imide functionalities.

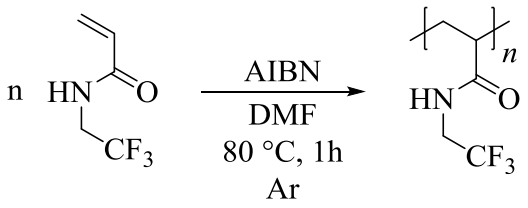

Scheme 35. Polymerization of *N*-(2,2,2-trifluoroethyl)acrylamide *via* FRP to confirm the chemical shift of the CF_3 functionality in fluorine NMR spectroscopy.

Subsequently, the resulting polymer was characterized by NMR and IR spectroscopy as well as SEC (see **Chapter 6.4.5.2**). The fluorine NMR spectrum is depicted below in comparison with the spectrum obtained after PPM (**Figure 12**). It exhibited solely one signal at δ = -72.36 – -72.98 ppm, as expected (**Figure 12**, top, red line). This consequently proved the assumption that the desired polyacrylamide was obtained only under the optimized reaction conditions without the use of a base, such as triethylamine.

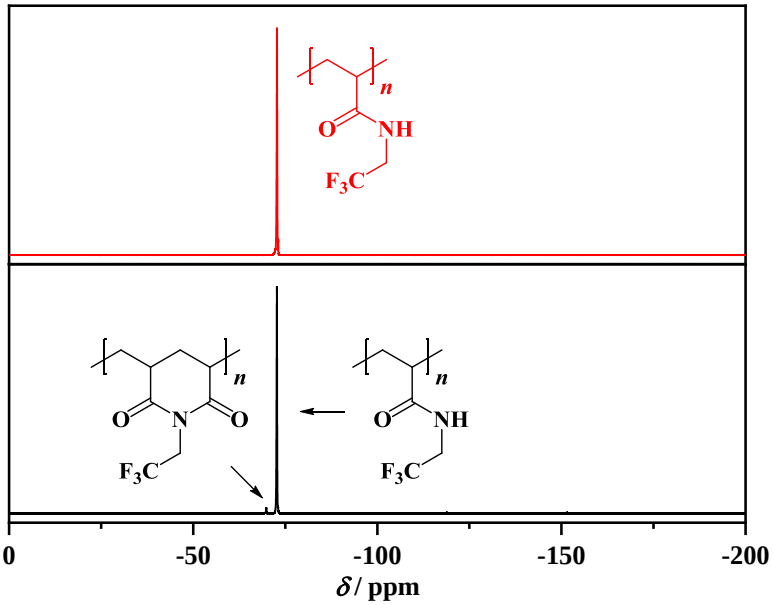

Figure 12. Comparison of ^{19}F NMR spectra of poly(*N*-(2,2,2-trifluoroethyl)acrylamide) obtained by either PPM of PPFPA in absence of a base (bottom, black line) or direct polymerization of its respective monomer (top, red line); solvent: acetone-d_6.

Subsequently, the characterization results before and after PPM were compared and analyzed. First, the SEC trace using DMAc as eluent was shifted towards higher molar masses (from M_n = 13900 g mol^{-1} before PPM to M_n = 16100 g mol^{-1} after PPM with a slightly increased dispersity $Đ$ (before PPM: $Đ$ = 2.03, after PPM: $Đ$ = 2.18) after the reaction (**Figure 13**).

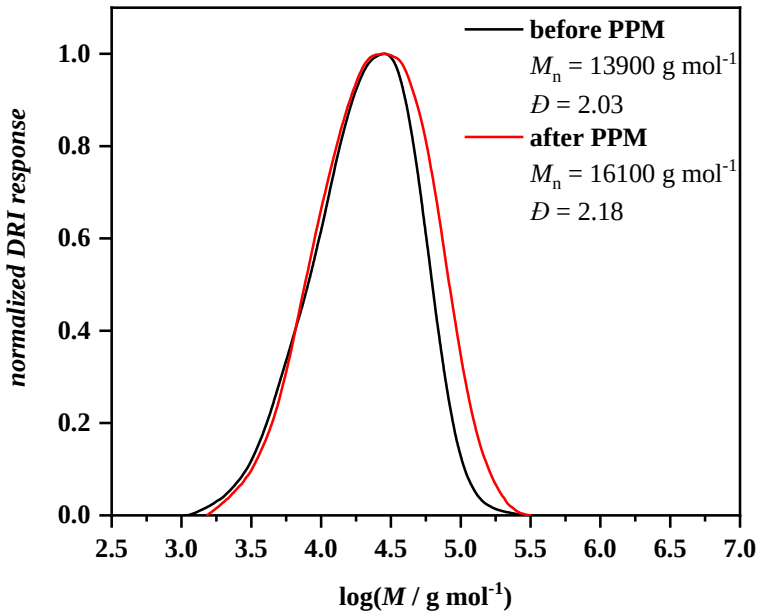

Figure 13. Comparison of SEC traces using DMAc as eluent (PMMA calibration) after PPM (red line) in comparison to PPFPA as starting polymer before PPM (black line) with a slight increase of M_n and dispersity.

The comparison of ^{1}H NMR spectra depicted in **Figure 14** revealed new signals arising from the amide formation: the amide proton appeared at δ = 7.53 – 8.06 ppm, while the CH_2 motif from the incorporated 2,2,2-trifluoroethylamine motif could be observed at δ = 3.67 – 4.26 ppm. The resonances resulting from the protons of the backbone were shifted to chemical shifts of δ = 2.15 – 2.66 ppm and δ = 1.37 – 1.98 ppm, respectively.

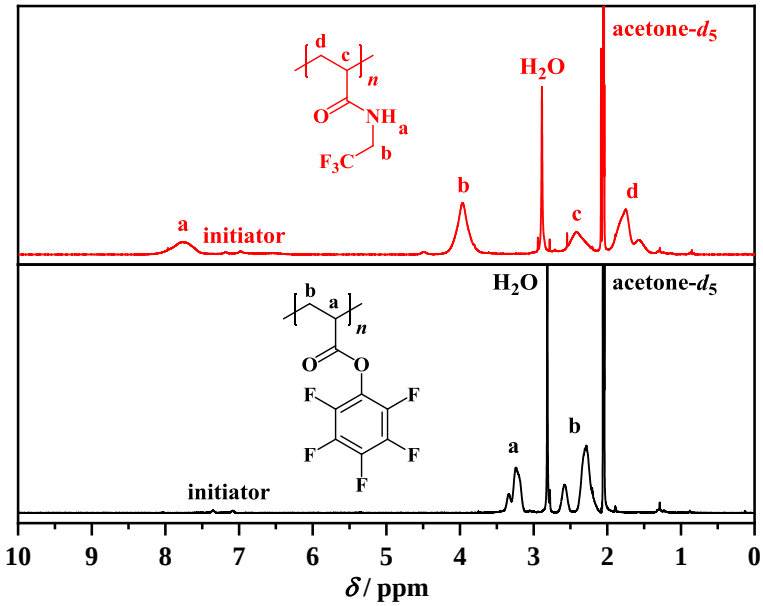

Figure 14. Comparison of the ^{1}H NMR spectra before (bottom, black line) and after (top, red line) PPM of PPFPA with 2,2,2-trifluoroethylamine; solvent: acetone-d_6.

The comparison of the ^{19}F NMR spectra (**Figure 15**) was one of the most straightforward techniques to demonstrate the successful functionalization of PPFPA. In this case, the signals arising from the latter (δ = -153.80 – -154.64 ppm, δ = -159.42 – -159.82 ppm, and δ = -164.35 – -164.95 ppm) completely disappeared after PPM and a new main signal arose (δ = -72.30 – -72.98 ppm) assigned to the formation of poly(*N*-(2,2,2-trifluoroethyl)acrylamide). The chemical shift was identical to the polyacrylamide obtained by direct polymerization of its monomer (**Figure 12**). Nonetheless, almost negligible amounts of imide (2%) were formed according to ^{19}F NMR spectroscopical analysis.

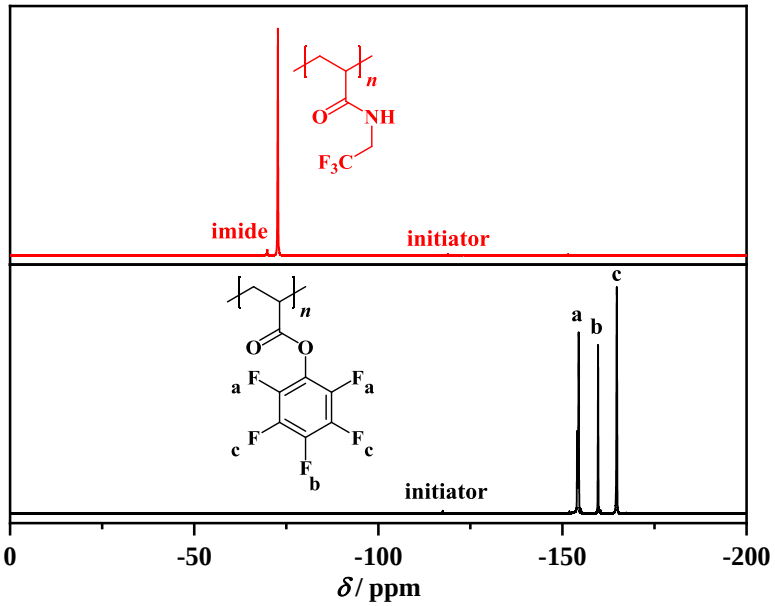

Figure 15. Comparison of ^{19}F NMR spectra before (bottom, black line) and after (top, red line) PPM with 2,2,2-trifluoroethylamine, exhibiting the complete removal of PPFPA signals resulting in the formation of poly(*N*-(2,2,2-trifluoroethyl)acrylamide) as main product; solvent: acetone-d_6.

Additionally, the comparison of IR spectra showed the removal of the carbonyl vibration of the ester at a wavenumber of $\tilde{\nu}$ = 1782 cm^{-1}, accompanied by a new carbonyl vibration of the formed amide at a wavenumber of $\tilde{\nu}$ = 1662 cm^{-1} (**Figure 16**). Also, the N-H vibration at a wavenumber of $\tilde{\nu}$ = 3200 – 3500 cm^{-1} was arising after PPM. Importantly, the spectrum after PPM was almost identical to the one of poly(*N*-(2,2,2-trifluoroethyl)acrylamide) obtained by direct polymerization of its respective monomer (see **Chapter 6.4.5.2**, **Figure 105**).

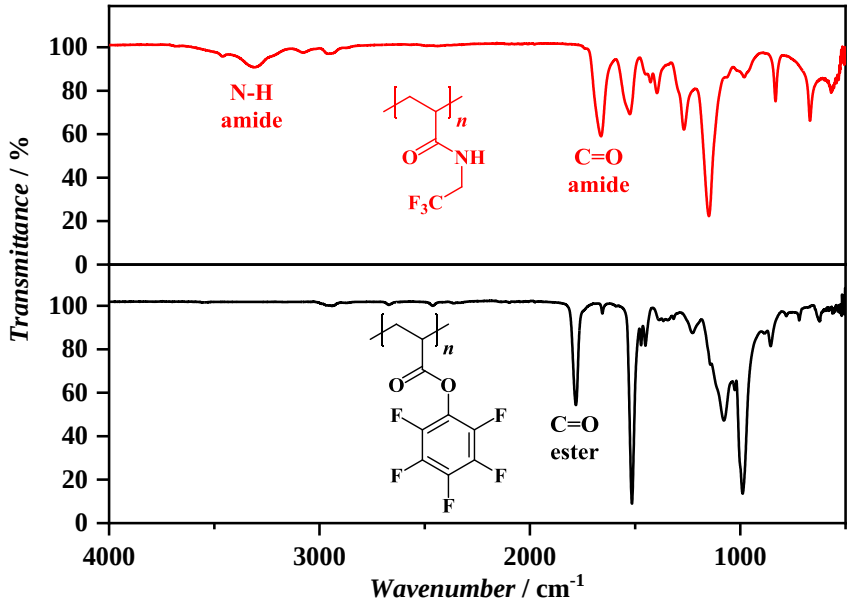

Figure 16. Comparison of ATR-FT-IR spectra before (bottom, black line) and after (top, red line) PPM of PPFPA with 2,2,2-trifluoroethylamine, showing the complete removal of the carbonyl vibration of the active ester of PPFPA, while a new carbonyl vibration of the amide arose.

4.1.4 Polymerization and PPM of DFPA and PDFPA

To further elucidate the compatibility of this polymerization method with other fluorine-labelled monomers, DFPA was alternatively used in the electrochemically-initiated polymerization. In contrast to PFPA as monomer, DFPA and its respective polymer only feature one signal in ^{19}F NMR spectroscopy, arising from the fluorine atoms in *ortho* position.

After successful synthesis (see **Chapter 4.1.2**), the monomer DFPA was directly employed in electrochemically-initiated polymerization reactions using 4-fluorobenzenediazonium tetrafluoroborate as radical source upon electrochemical cathodic reduction (**Scheme 36**).

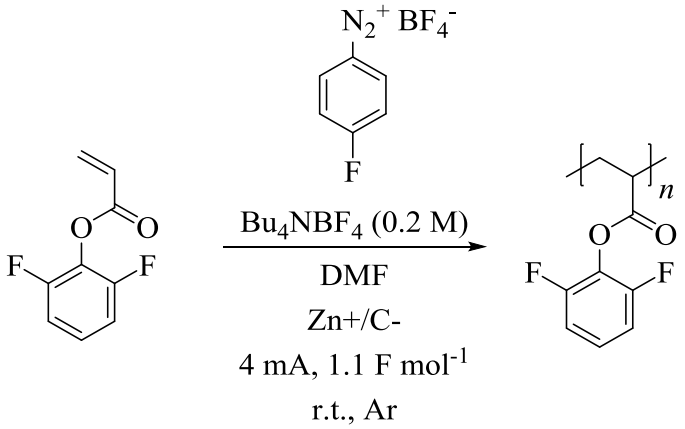

Scheme 36. Electrochemically-initiated polymerization of DFPA using 4-fluorobenzenediazonium tetrafluoroborate as initiator upon electrochemical cathodic reduction.

In contrast to PFPA as fluorine-labelled reactive monomer, DFPA and its polymer did not seem to be as sensitive towards electrochemical currents. A constant current of 4 mA could thus be used in the polymerization procedure. Since the polymerization of 20.00 equivalents of PFPA with respect to the initiator led to the formation of a hardly soluble gel between the electrodes, two polymerizations were carried out with 5.00 and 10.00 equivalents, respectively, resulting in two polymers with different chain lengths (**Table 2**). Analogous to the polymerizations of PFPA and in accordance with the expectation, the chain lengths were increasing with increasing monomer to initiator ratios. Whereas the conditions were adapted from the electrochemically-initiated polymerization of PFPA (see **Chapter 4.1.3**), a constant current of 4 mA was applied. After 1.1 F mol^{-1} passed through the system, the polymers were isolated and purified in an analogous fashion to PPFPA (see **Chapter 4.1.3**).

Table 2. Details and results of the electrochemically-initiated polymerization of DFPA (4 mA, 1.1 F mol^{-1}) as reactive monomer.

Entry	Eq.	M_n[a] g mol^{-1}	M_n[b] g mol^{-1}	$Đ$[b]	M_n[c] g mol^{-1}	$Đ$[c]
1	10.00	35250	16800[d]	1.83[d]	14600[d]	2.49[d]
			15300[e]	1.75[e]	17300[e]	2.23[e]
2	5.00	21330	11300[d]	1.58[d]	8900[d]	2.13[d]
			10500[e]	1.50[e]	11000[e]	1.89[e]

[a] Determined by ^{19}F NMR spectroscopy; [b] determined by SEC using THF as eluent; [c] determined by SEC using DMAc as eluent; [d] PMMA calibration; [e] PS calibration.

Subsequently, the polymers were analyzed by NMR and IR spectroscopy as well as SEC. The fluorine NMR spectra (**Figure 17**) exhibited two signals, one arising from the fluorine atom attached to the initiating moiety at δ = -117.66 – -117.86 ppm and the other one assigned to the fluorine atoms from the DFPA repeating units at δ = -126.55 – -127.38 ppm.

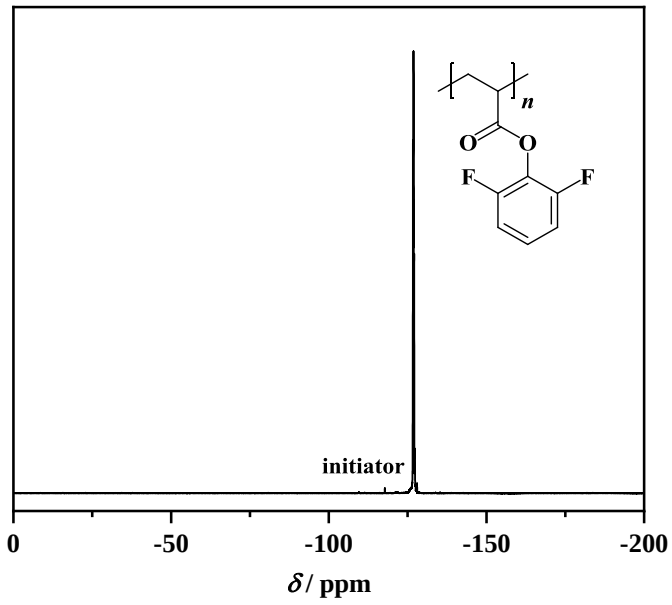

Figure 17. Exemplary ^{19}F NMR spectrum of PDFPA obtained by electrochemically-initiated polymerization of DFPA (in this case: 10.00 equivalents with respect to the initiator, **Table 2**, Entry 1); solvent: acetone-d_6.

The values obtained by fluorine NMR spectroscopy were, analogous to the case of PFPA as monomer, overestimating the M_n in comparison to SEC. In this case however, M_n values could not be determined by proton NMR spectroscopy, since the resonances of the aromatic protons in *meta* and *para* position of the DFPA repeating units were overlapping with the signals of the

initiator, as can be seen in **Figure 18**. The ^{1}H NMR spectrum exhibited signals at chemical shifts of δ = 7.15 – 7.38 ppm (aromatic proton in *para* position), δ = 6.87 – 7.13 ppm (aromatic protons in *meta* position), and at δ = 3.22 – 3.42 ppm and δ = 2.16 – 2.65 ppm arising from the backbone protons. The respective signals arising from PDFPA could be observed both in ^{1}H and ^{19}F NMR spectroscopy. They thus proved that the reactive character of the polymers was not affected by the electrochemically-initiated polymerization using an aromatic diazonium salt as initiating species upon cathodic reduction.

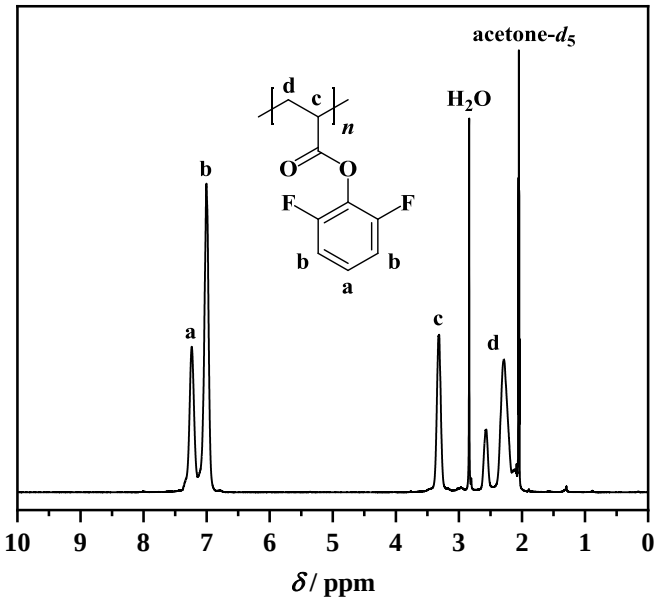

Figure 18. Exemplary ^{1}H NMR spectrum of PDFPA obtained by electrochemically-initiated polymerization of DFPA (in this case: 10.00 equivalents with respect to the initiator, **Table 2**, Entry 1); solvent: acetone-d_6.

SEC analysis with THF as eluent (**Figure 19**) proved the trend of increasing chain lengths with increasing monomer to initiator ratio with dispersity values typical for FRP ($1.58 \leq Đ \leq 1.83$). The polymerization of 10.00 equivalents of DFPA with respect to 4-fluorobenzenediazonium tetrafluoroborate yielded a molar mass distribution with a slight shoulder towards higher molar masses. However, this phenomenon was not observed when only 5.00 equivalents of DFPA were used in the polymerization.

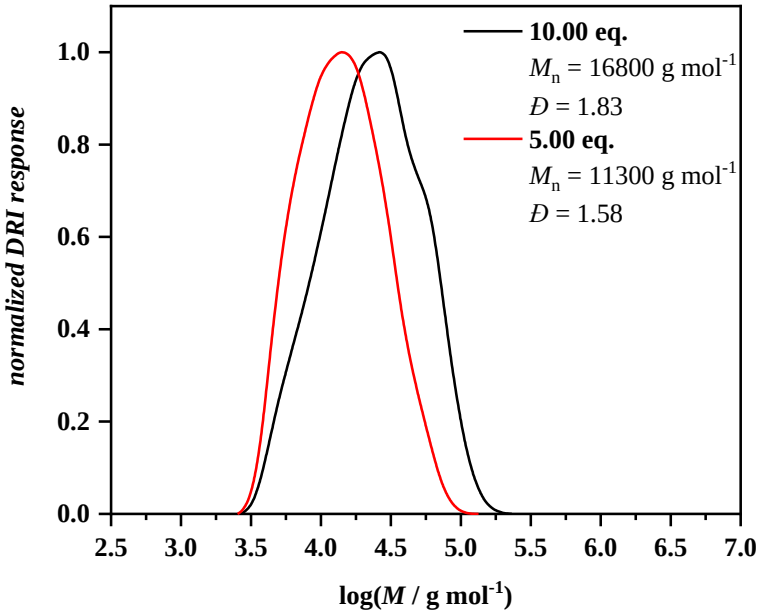

Figure 19. Comparison of SEC traces using THF as eluent (PMMA calibration) of the polymers obtained by the electrochemically-initiated polymerization of DFPA with different equivalents of DFPA with respect to 4-fluorobenzenediazonium tetrafluoroborate as initiator (black line: 10.00 equivalents; red line: 5.00 equivalents).

The SEC results using DMAc as eluent (see **Chapter 6.4.3.2**, **Figure 81**) did not exhibit any shoulder for both samples, but in comparison to the results obtained with THF as eluent, the dispersity values were higher ($2.13 \leq Đ \leq 2.49$) and the molar masses were lower. SEC analysis only allowed for a rough estimation of the M_n values, especially a comparison of results obtained from different SEC setups is difficult. Nonetheless, the respective results are listed in **Table 2**.

Subsequently, the resulting PDFPA was used as starting material in a PPM reaction with 2,2,2-trifluoroethylamine. Due to its less pronounced active ester character in comparison to PFPA, a successful and complete amidation required harsher reaction conditions (**Scheme 37**).

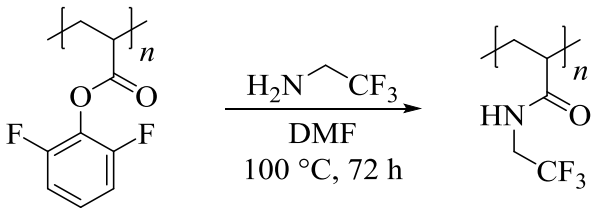

Scheme 37. PPM of PDFPA using 2,2,2-trifluoroethylamine for the synthesis of the respective polyamide.

In other words, a large excess of 2,2,2-trifluoroethylamine (25.00 equivalents per repeating unit) was used with respect to PDFPA (polymerization of 10.00 equivalents with respect to

4-fluorobenzenediazonium tetrafluoroborate as initiator) at elevated temperatures (100 °C) without the addition of a base. The resulting polymer was isolated in analogy to **Chapter 4.1.3**. Subsequently, the obtained polymers were analyzed by SEC as well as NMR and IR spectroscopy. SEC using DMAc as eluent showed a slight decrease of the molar mass from M_n = 14600 g mol^{-1} before PPM to M_n = 13100 g mol^{-1} after the reaction with similar dispersity (**Figure 20**).

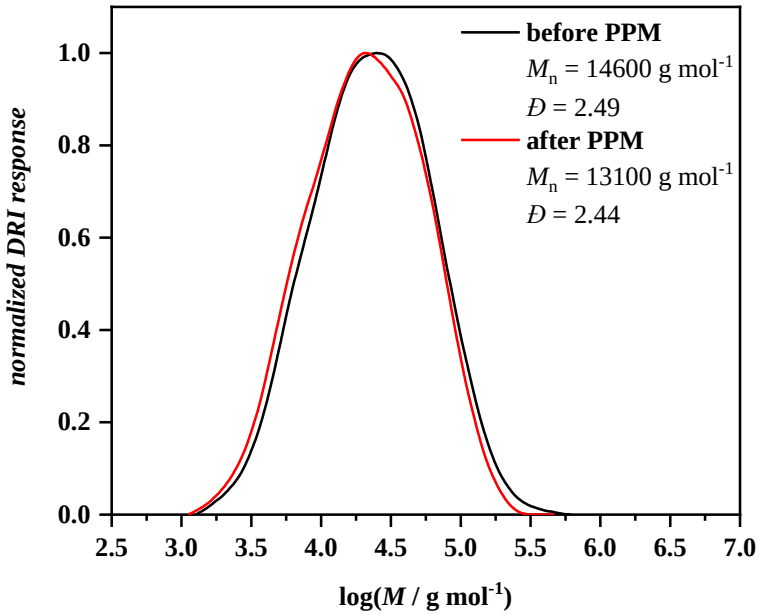

Figure 20. Comparison of SEC traces using DMAc as eluent (PMMA calibration), exhibiting a shift towards lower molar masses after PPM (red line) in comparison to PDFPA as starting polymer before PPM (black line) with a slight decrease of dispersity.

In contrast to the PPM of PPFPA, the ^{1}H NMR spectrum after PPM of PDFPA did not show the exclusive formation of the respective amide (**Figure 21**). The spectrum exhibited signals at chemical shifts of δ = 6.80 – 7.70 ppm, δ = 4.29 – 4.60 ppm, δ = 3.83 – 4.17 ppm, δ = 2.50 – 3.35 ppm, and δ = 1.25 – 1.90 ppm. It seemed that the formation of the respective imide was taking place in addition to the amide formation, promoted by the harsher reaction conditions. The concurrent imide formation was thus hard to be avoided.

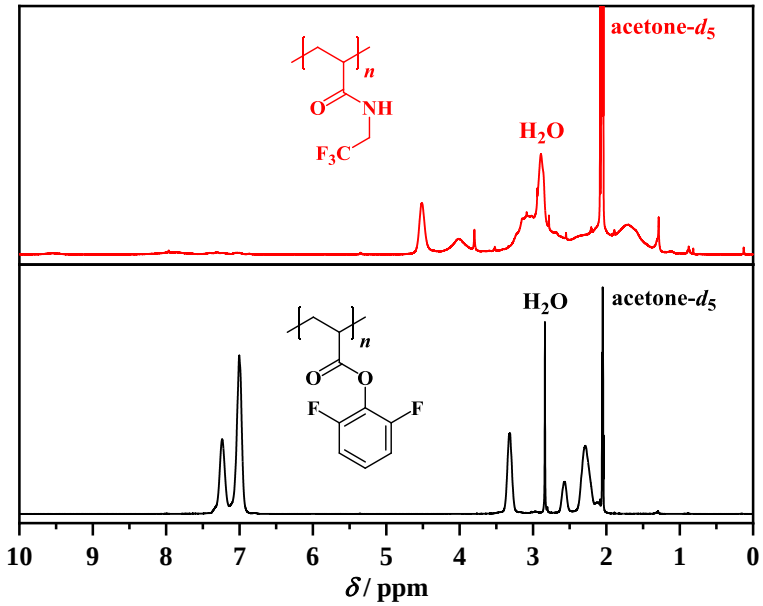

Figure 21. Comparison of the ^{1}H NMR spectra before (bottom, black line) and after (top, red line) PPM of PDFPA with 2,2,2-trifluoroethylamine, the signals in the spectrum after PPM presumably arising from more than one species; solvent: acetone-d_6.

The ^{19}F NMR spectrum was in accordance with the assumption that more than one structural motif was formed by PPM. Two main signals (δ = -71.80 – -73.16 ppm and δ = -68.75 – -70.40 ppm) were observed after PPM accompanied by a complete removal of the signal arising from PDFPA (δ = -126.55 – -127.38 ppm) (**Figure 22**). The signal at δ = -68.75 – -70.40 ppm indicated the formation of imide functionalities, while the signal at δ = -71.80 – -73.16 ppm was matching the chemical shift of poly(*N*-(2,2,2-trifluoroethyl)acrylamide) obtained by direct polymerization of its monomer.

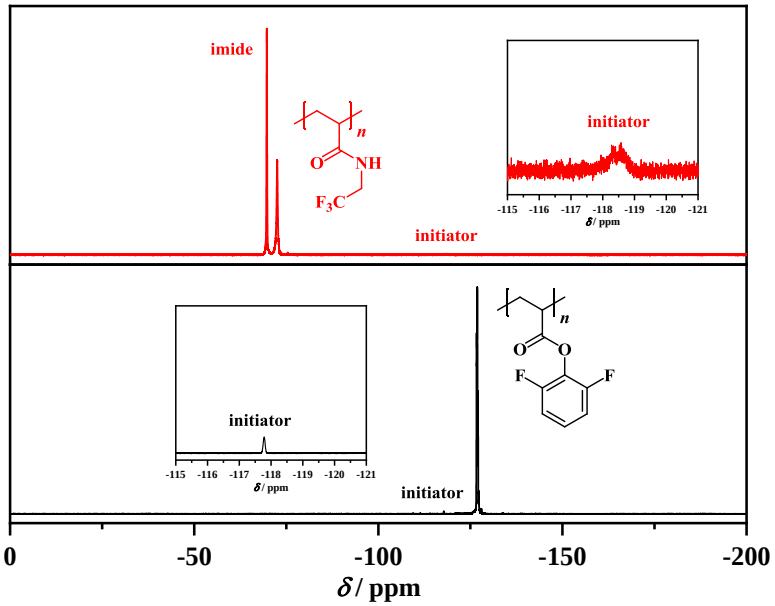

Figure 22. Comparison of the ^{19}F NMR spectra before (bottom, black line) and after (top, red line) PPM of PDFPA with 2,2,2-trifluoroethylamine, the signals in the spectrum after PPM presumably arising from more than one species; solvent: acetone-d_6.

Eventually, an ATR-FT-IR spectrum of the polymer obtained after PPM was recorded and compared to the starting material PDFPA (**Figure 23**). The carbonyl vibration arising from the ester bond of PDFPA at a wavenumber of $\tilde{\nu}$ = 1770 cm^{-1} disappeared completely, however, new carbonyl vibrations at wavenumbers of $\tilde{\nu}$ = 1689 cm^{-1} and $\tilde{\nu}$ = 1626 cm^{-1} arose. The spectrum demonstrated that more than one carbonyl-based species was present after PPM.

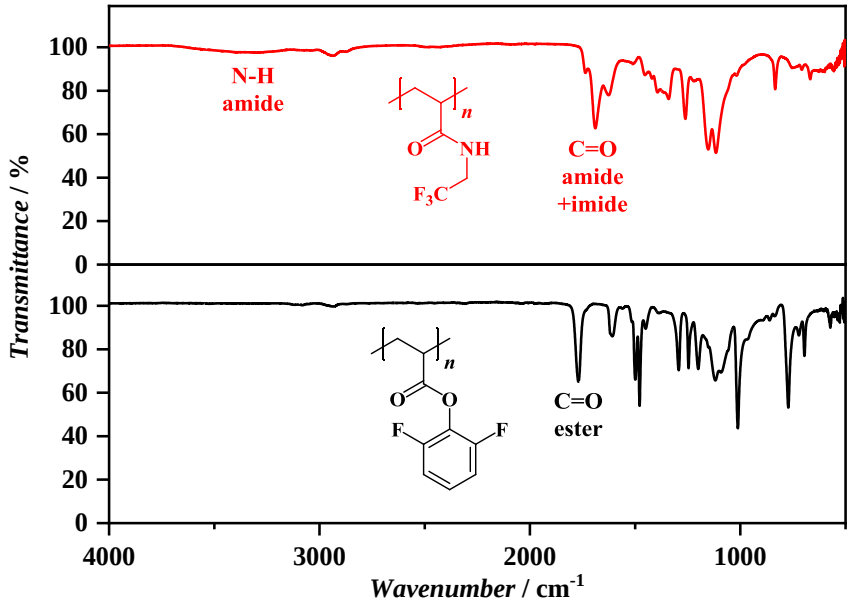

Figure 23. Comparison of ATR-FT-IR spectra before (bottom, black line) and after (top, red line) PPM of PDFPA with 2,2,2-trifluoroethylamine, showing the complete removal of the carbonyl vibration of the PDFPA ester, while new carbonyl vibrations of the amide and imide arose.

4.1.5 Polymerization and PPM of GMA and PGMA

Furthermore, GMA was used as reactive monomer for the electrochemically-initiated polymerization. In contrast to PFPA and DFPA, GMA features an epoxide functionality instead of an electron-deficient ester moiety. Additionally, GMA is commercially available at a reasonable price.

In a first attempt, GMA was employed as monomer using a constant current of 4 mA until 4 F mol^{-1} passed through the system (**Scheme 38**). The polymerization was performed in a similar fashion to PFPA and DFPA as reactive monomers and led to the formation of PGMA. However, the polymerization time was reduced to 2 F mol^{-1} (in contrast to PFPA and DFPA: 1.1 F mol^{-1}) since GMA and PGMA appeared to feature a high stability towards the electrochemical currents.

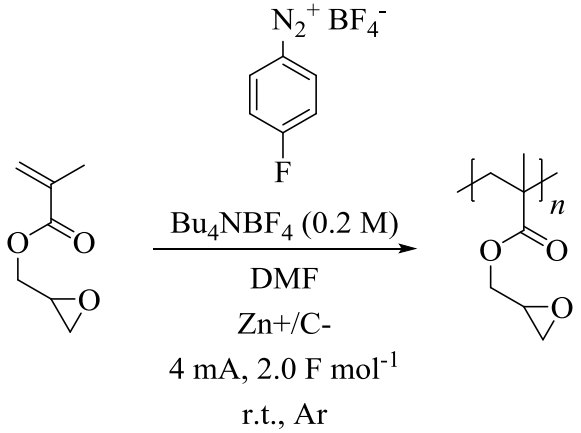

Scheme 38. Electrochemically-initiated polymerization of GMA using 4-fluorobenzenediazonium tetrafluoroborate as initiator upon electrochemical cathodic reduction.

Analogous to the electrochemically-initiated polymerizations of PFPA and DFPA, the monomer to initiator ratios were varied to obtain macromolecules featuring different chain lengths (**Table 3**). The resulting polymers were purified similarly to PPFPA and PDFPA (see **Chapters 4.1.3** and **4.1.4**, respectively). Subsequently, the obtained polymers were analyzed by SEC as well as NMR and IR spectroscopy.

Table 3. Details and results of the electrochemically-initiated polymerization of GMA (4 mA, 2.0 F mol^{-1}) as reactive monomer.

Entry	Eq.	M_n[a] g mol^{-1}	M_n[b] g mol^{-1}	$Đ$[b]	M_n[c] g mol^{-1}	$Đ$[c]
1	40.00	14500	15700[d]	2.40[d]	12600[d]	3.10[d]
			14700[e]	2.24[e]	15400[e]	2.68[e]
2	20.00	10350	8200[d]	1.85[d]	6200[d]	2.40[d]
			7900[e]	1.71[e]	8000[e]	2.06[e]
3	10.00	6970	6800[d]	1.60[d]	5200[d]	2.00[d]
			6500[e]	1.50[e]	6700[e]	1.76[e]

[a] Determined by ^{1}H NMR spectroscopy; [b] determined by SEC using THF as eluent; [c] determined by SEC using DMAc as eluent; [d] PMMA calibration; [e] PS calibration.

The M_n values obtained by proton NMR spectroscopy were in accordance with the values obtained by SEC using both THF and DMAc as eluents. Remarkably, the polymerization of GMA led to smaller chain lengths as in comparison to the polymerization of PFPA and DFPA, probably caused by the higher reactivity of acrylate monomers in comparison to methacrylate ones, resulting in higher polymerization rates for the former.[198] The proton NMR spectra exhibited the typical signals arising from PGMA reported in literature with integrals in a matching fashion. Additionally, the spectra showed signals arising from the aromatic protons of the initiator, allowing for the calculation of the M_n values depicted in **Table 3**. An exemplary ^{1}H NMR spectrum recorded in deuterated dichloromethane (DCM) is depicted below in **Figure 24**. Signals from the initiator appeared at a chemical shift of δ = 6.90 – 7.36 ppm, while the signals of the actual PGMA could be observed at δ = 4.22 – 4.40 ppm and δ = 3.69 – 3.85 ppm (CH_2 motif attached to the ester), δ = 3.17 – 3.26 ppm (CH group tethered to the oxygen atom of the epoxide functionality), δ = 2.75 – 2.87 ppm and δ = 2.58 – 2.67 ppm (CH_2 moiety adjacent to the oxygen atom of the epoxide group), and at δ = 1.63 – 2.10 ppm and δ = 0.62 – 1.26 ppm (backbone CH_2 and CH_3 group, respectively).

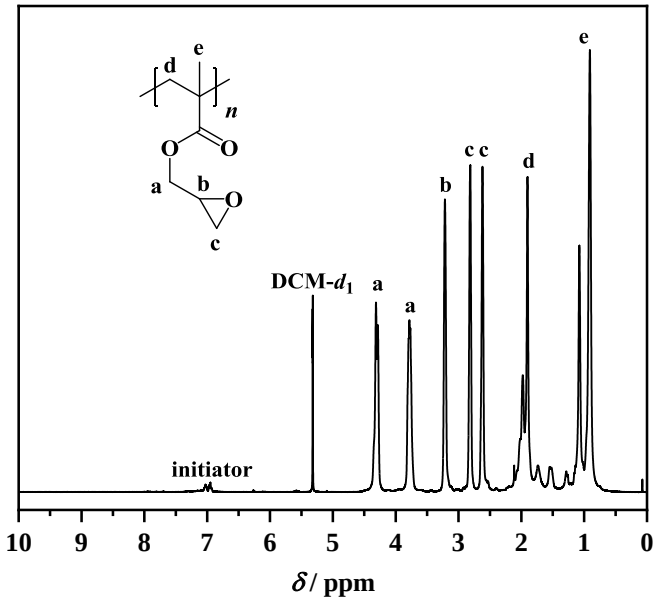

Figure 24. Exemplary ^{1}H NMR spectrum of PGMA obtained by electrochemically-initiated polymerization of DFPA (in this case: 20.00 equivalents with respect to the initiator, **Table 3**, Entry 2); solvent: DCM-d_2.

The SEC traces for the polymerizations of 20.00 and 40.00 equivalents did not feature defined molar mass distributions, both using THF (**Figure 25**) and DMAc (see **Chapter 6.4.4.1**, **Figure 90**) as eluents. Presumably, the monomer concentration might have been too high to ensure a sufficient conductivity, impeding polymerizations resulting in unimodal molar mass distributions. This was in accordance with the results of the electrochemically-initiated polymerization of PFPA, however, a gel formation in the case of GMA was not observed. The polymerization of 10.00 equivalents with respect to the initiator resulted in PGMA with a more defined molar mass distribution and a dispersity of $Đ$ = 1.60 according to SEC using THF as eluent and $Đ$ = 2.00 according to SEC with DMAc as eluent.

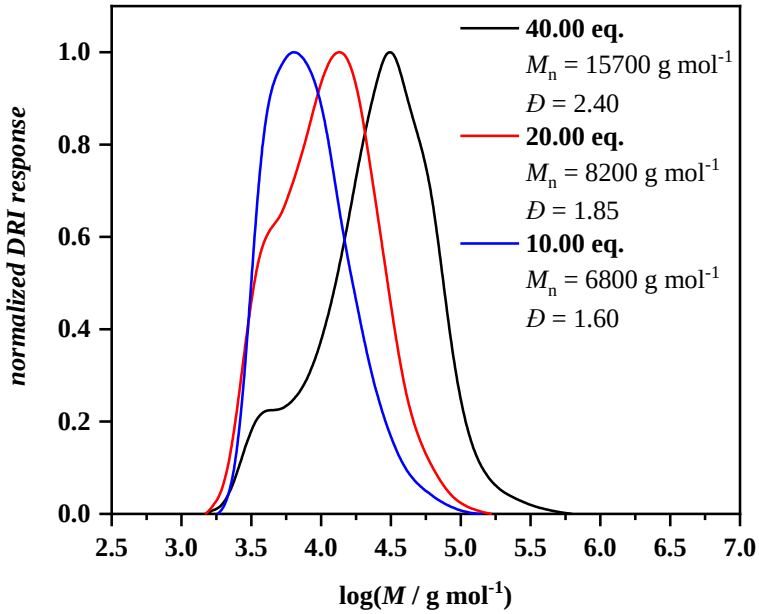

Figure 25. Comparison of SEC traces using THF as eluent (PMMA calibration) of the polymers obtained by the electrochemically-initiated polymerization of GMA with different equivalents of GMA with respect to 4-fluorobenzenediazonium tetrafluoroborate as initiator (black line: 40.00 equivalents; red line: 20.00 equivalents; blue line: 10.00 equivalents). The polymerization of more than 10.00 equivalents with respect to 4-fluorobenzenediazonium tetrafluoroborate seemed to result in PGMA with less defined molar mass distributions.

Additionally, an ATR-FT-IR spectrum of PGMA obtained by the electrochemically-initiated polymerization of GMA (20.00 equivalents with respect to the initiator) was recorded (see **Chapter 6.4.4.1**, **Figure 93**). The spectrum clearly showed the epoxide vibration of PGMA at a wavenumber of $\tilde{\nu}$ = 906 cm^{-1} as reported in literature.[199] In combination with the ^{1}H NMR spectra, the IR spectrum demonstrated that the reactive character of the obtained PGMA remained intact under the electrochemically-initiated polymerization conditions.

Subsequently, the as-prepared PGMA was also used in functionalization reactions. 2,2,2-Trifluoroethylamine was employed in a similar fashion to PPFPA and PDFPA, however, the reactive site of PGMA was its epoxide functionality in the repeating unit. The nucleophilic ring-opening of the latter allowed for the synthesis of β-amino alcohols (**Scheme 39**).

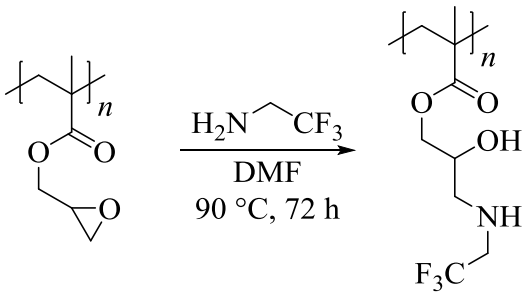

Scheme 39. PPM of PGMA using 2,2,2-trifluoroethylamine for the synthesis of the respective poly(*β*-amino alcohol).

A first attempt of the ring-opening of the epoxide functionality of PGMA using a slight excess of 2,2,2-trifluoroethylamine (4.00 equivalents per GMA repeating unit) in the presence of triethylamine as base at 60 °C for 72 hours resulted in insoluble material after precipitation, probably due to cross-linking reactions.[200] Specifically, unreacted epoxide functionalities can undergo ring-opening reactions in the presence of secondary amine moieties from already formed *β*-amino alcohols, resulting in intra- and intermolecular chain linkages.[201] This phenomenon can however be circumvented by using larger excesses of the respective amine.[202] Thus, the functionalization was carried out in the absence of a base with a large excess of the amine (25.00 equivalents per repeating unit) at elevated temperature (T = 90 °C) (**Scheme 39**). After 72 hours, the reaction mixture was precipitated in cold diethyl ether to remove unreacted amine moieties.

SEC analysis (DMAc as eluent, PMMA calibration) of the resulting polymer showed a clear shift towards higher molar masses, from M_n = 6200 g mol^{-1} before the reaction to M_n = 20300 g mol^{-1} (**Figure 26**).

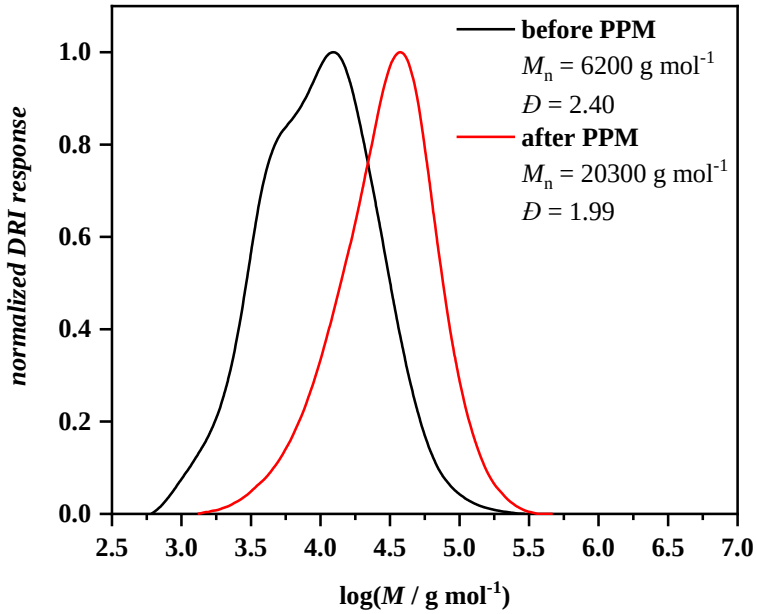

Figure 26. Comparison of SEC traces using DMAc as eluent (PMMA calibration), exhibiting a significant shift towards higher molar masses after PPM (red line) in comparison to PGMA as starting polymer before PPM (black line).

NMR spectroscopy proved the successful functionalization of PGMA obtained by the electrochemically-initiated polymerization with 2,2,2-trifluoroethylamine. Indeed, the ^{1}H NMR spectra before and after the functionalization differed significantly from each other: the comparison (**Figure 27**) showed the disappearance of the signals arising from PGMA after reaction accompanied by the appearance of new signals at δ = 4.25 – 4.55 ppm (proton of the CH group adjacent to the OH group), δ = 3.86 – 4.12 ppm (CH_2 motif attached to the ester), δ = 3.17 – 3.47 ppm (CH_2 group of the incorporated 2,2,2-trifluoroethylamine motif), and δ = 2.70 – 2.98 ppm (CH_2 moiety tethered to the nitrogen atom) (**Figure 27**, top, red line). These signals were attributed to the formation of the poly(β-amino alcohol) upon ring-opening of the epoxide moiety with the employed fluorine-labelled amine.

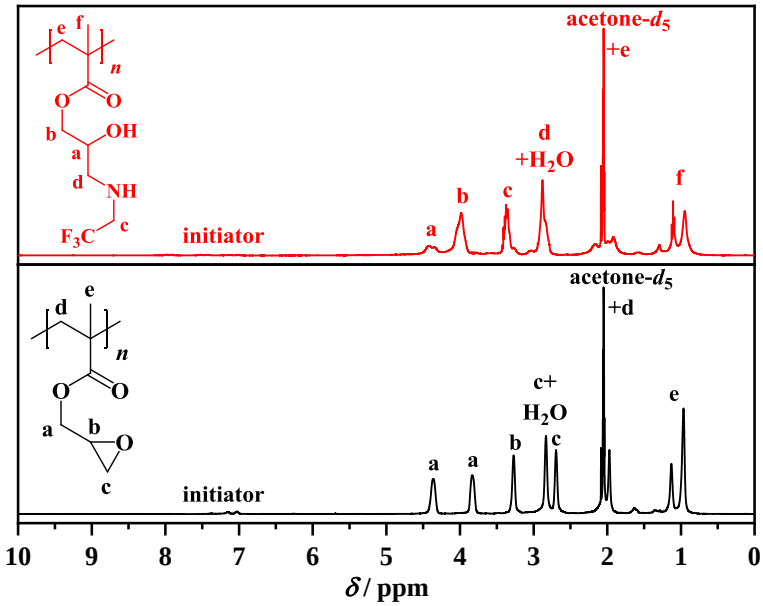

Figure 27. Comparison of the ^{1}H NMR spectra before (bottom, black line) and after (top, red line) PPM of PGMA with 2,2,2-trifluoroethylamine; solvent: acetone-d_6.

Additionally, ^{19}F NMR spectroscopy revealed the incorporation of other fluorine species in addition to the fluorine-labelled initiator (**Figure 28**). The main signal at δ = -72.35 ppm arose from the incorporation of 2,2,2-trifluoroethylamine by ring-opening of the epoxide. However, it was accompanied by a signal of lower intensity at δ = -71.59 ppm, the latter potentially arising from either the ring-opening of one epoxide moiety by an already incorporated secondary amine functionality adjacent to the former, from the formation of the other regioisomer, or from amide formation.

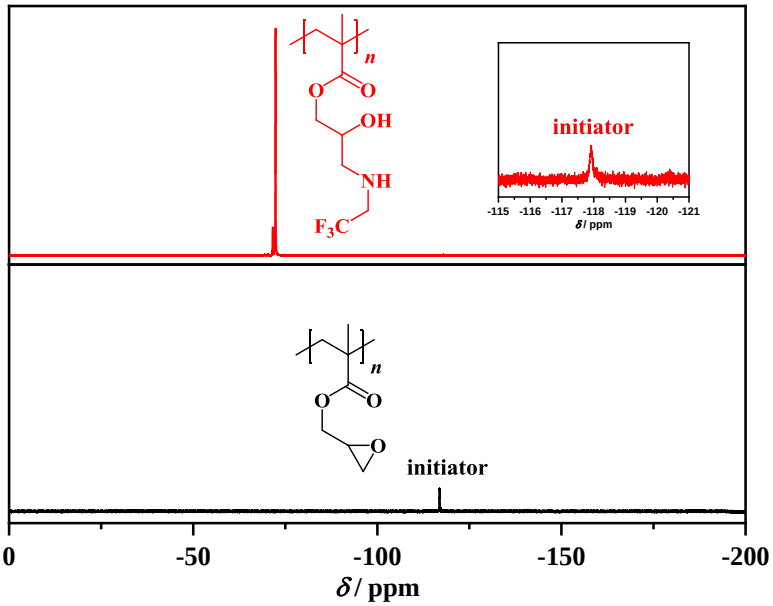

Figure 28. Comparison of the ^{19}F NMR spectra before (bottom, black line; solvent: DCM-d_2) and after (top, red line; solvent: acetone-d_6) PPM of PGMA with 2,2,2-trifluoroethylamine.

Furthermore, the polymer obtained after PPM of PGMA was analyzed by IR spectroscopy. The comparison of the IR spectra before and after PPM (**Figure 29**) exhibited the disappearance of the epoxide vibration of PGMA at a wavenumber of $\tilde{\nu}$ = 906 cm^{-1} accompanied by new vibrations in the range of wavenumbers of $\tilde{\nu}$ = 3200 – 3600 cm^{-1}, assigned to the formation of the β-amino alcohol moieties.

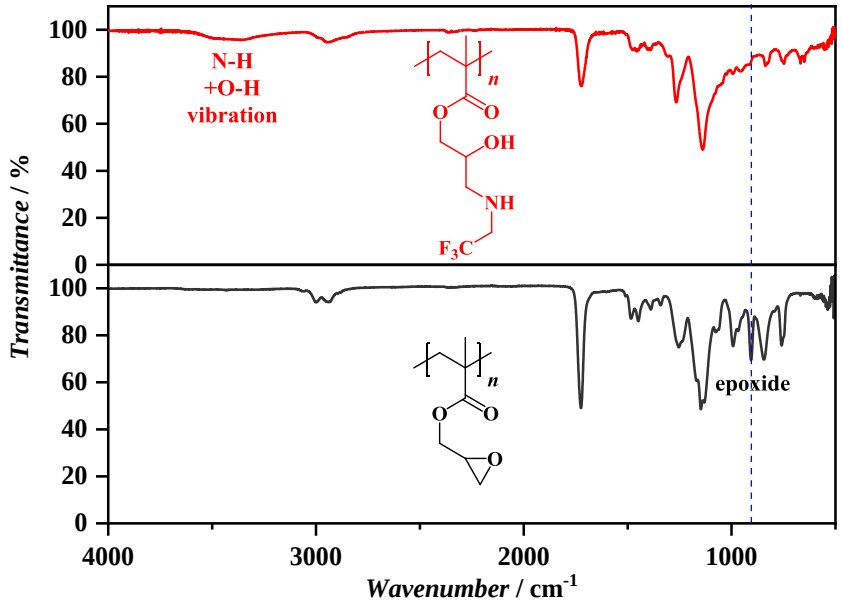

Figure 29. Comparison of ATR-FT-IR spectra before (bottom, black line) and after (top, red line) PPM of PGMA with 2,2,2-trifluoroethylamine, showing the disappearance of the epoxide vibrations accompanied by the appearance of N-H and O-H vibrations.

4.1.6 Conclusion and Outlook

In conclusion, the electrochemically-initiated polymerization of reactive monomers, i.e. PFPA, DFPA, and GMA, was realized. To do so, a simple, easily accessible, and reproducible electrochemical method for polymerization initiation by cathodic reduction of a fluorine-labelled aromatic diazonium salt, i.e. 4-fluorobenzenediazonium tetrafluoroborate, was used. The fluorine labels on both initiator and PFPA as well as DFPA enabled the straightforward determination of the M_n values of the obtained polymers by ^{19}F NMR spectroscopy. In addition, the polymers were analyzed by SEC as well as NMR and IR spectroscopy, proving that the structural motifs and thus the reactive character remained intact during the electrochemically-initiated polymerization. In the case of PFPA as reactive monomer, the electrochemical parameters were fine-tuned towards milder reaction conditions as the fluorine NMR spectra exhibited signals presumably arising from decomposition. Furthermore, for all three reactive polymers PPFPA, PDFPA, and PGMA, PPM reactions were carried out using a fluorine-labelled amine to demonstrate the successful reaction and consequently the intact reactive nature of the polymers by ^{19}F NMR spectroscopy. In the case of PPFPA, first reaction attempts resulted in a copolymer of the respective amide and probably the imide, formed by a nucleophilic attack of an amide functionality on an adjacent PFPA repeating unit. Herein, the imide formation could be circumvented by the use of a large excess of amine and the absence of an additional base. However, in the case of PDFPA, copolymers were obtained in all cases since the ester does not feature an electronegativity as pronounced as for PPFPA. Thus, harsher reaction conditions were required, which seemed to favor the formation of a copolymer instead of the homopolymer of the respective acrylamide. Moreover, PGMA was successfully functionalized to the respective poly(β-amino alcohol) after adaptation of the reaction conditions to avoid the formation of insoluble products, presumably due to cross-linking reactions. The comparison of the NMR and IR spectra as well as the size-exclusion chromatograms proved the successful PPM, based on the mild electrochemically-initiated radical polymerization of reactive monomers. In conclusion, the approach presented in this subchapter enabled the novel straightforward polymerization of reactive monomers by “the push of a button” in a controlled and very mild fashion, as the electrochemical polymerization parameters could be fine-tuned to the individual needs, even for the polymerization of electrochemically-sensitive monomers. In an analogous fashion, the synthesis of a variety of diazonium salts could be envisaged in the future to introduce different kinds of α-groups into reactive macromolecular structures, which would allow for an orthogonal functionalization of both the reactive side groups of the polymers and their α-group.

4.2 Electrochemically-Mediated Nickel-Catalyzed ω-Functionalization

This subchapter deals with the electrochemically-mediated nickel-catalyzed ω-functionalization of polymers obtained by electrochemical polymerization. The present approach was intended to be employed for the *in-situ* ω-functionalization of different electrochemically-polymerized macromolecules by the use of both non-polymeric and polymeric aryl bromides. Herein, this system would allow for the straightforward chain end manipulation during the polymerization process and, when polymeric aryl bromides are used, for the facile one-pot synthesis of graft copolymers. Therefore, the feasibility and limitations with regards to potential monomers and aryl bromides were evaluated, as this approach would combine the electrochemical polymerization with the electrochemically-mediated functionalization of growing macromolecules in an elegant fashion. Additionally, the results suggested a straightforward one-step graft copolymer synthesis in a sophisticated manner.

4.2.1 General Concept

This project was based on electrochemically-mediated nickel-catalyzed coupling reactions, in particular on the work of Jiao *et al.*[163] with the depicted postulated mechanism in **Chapter 2.4**, **Scheme 15**. According to this mechanism, aryl bromide species undergo oxidative addition to a Ni^0 catalyst and can subsequently react with present radical species. This reaction was intended to be exploited for the *in-situ* ω-functionalization of electrochemically-polymerized macromolecules (**Scheme 40**). Styrene[167] and acrylonitrile[166] for instance have been reported to undergo electropolymerization upon cathodic reduction.

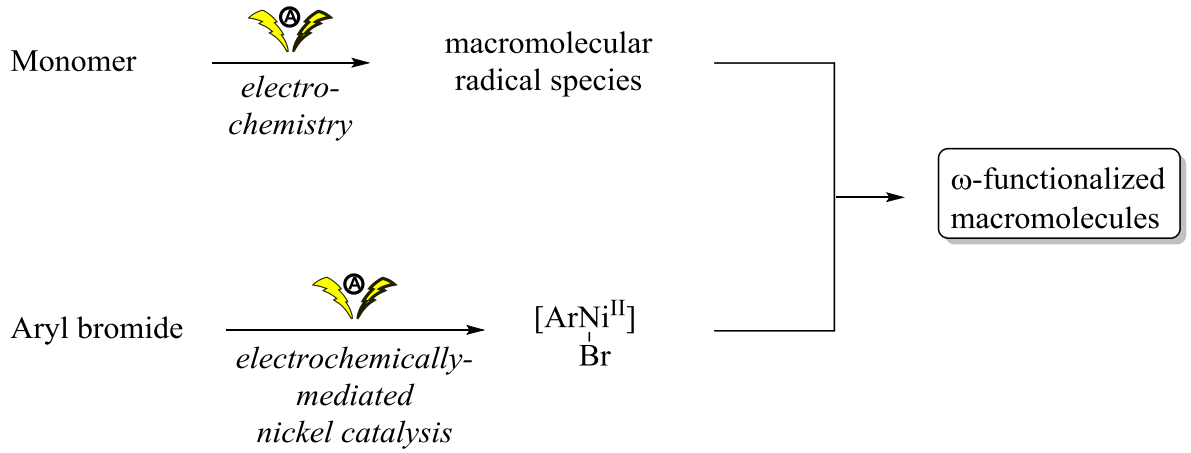

Scheme 40. Depiction of the general concept behind this project: macromolecular radical species generated by electrochemical means from the respective monomers should be ω-functionalized by an electrochemically-mediated nickel catalysis system using aryl bromides.

Thus, styrene-derived monomers as well as acrylonitrile were envisaged to be used in combination with commercially available aryl bromides such as bromobenzene and derivatives with varying electron-densities. Additionally, the suitability of polymeric aryl bromides for the ω-functionalization should be evaluated, as this approach would allow for a sophisticated one-step graft copolymer synthesis.

4.2.2 Non-Polymeric Aryl Bromides for the Electrochemically-Mediated Nickel-Catalyzed ω-Functionalization

The project described in this subchapter was based on an electrochemical nickel catalytic cycle, in which aryl bromides were used to terminate propagating polymer chains, which were initiated by the electrochemical formation of the radical anions of the monomer species, and thus served as end groups of the formed macromolecules (**Scheme 41**).

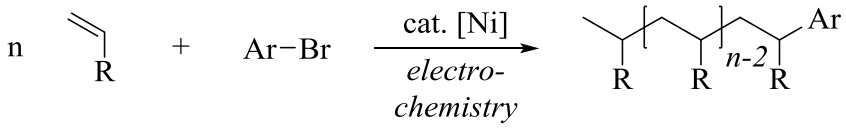

Scheme 41. General simplified concept behind the electrochemically-mediated nickel-catalyzed ω-functionalization.

For this project, the identical electrochemical setup as described in **Chapter 4.1** was employed, guaranteeing the reproducibility of a straightforward and affordable, commercially available potentiostat including its equipment. The setup comprised an undivided cell, reducing the complexity in comparison to a divided cell setup. Nickel(II) bromide ethylene glycol dimethyl ether complex ($NiBr_2$·dme) was used as nickel catalyst together with 4,4′-di-*tert*-butyl-2,2′-dipyridyl (bbbpy) as ligand in a 0.1 M solution of Bu_4NBF_4 in DMF. Galvanostatic conditions were employed to ensure a simple and industrially-friendly setup. As depicted in the mechanism of the electrochemical nickel catalysis system in **Chapter 2.4**, **Scheme 15**, solely the cathodic reduction was of importance for this kind of reaction. To avoid interference of potentially arising oxidation reactions with the desired product formation, a sacrificial zinc anode was used, which was oxidized itself throughout the course of the reaction. A simple graphite electrode was employed as cathode.

At first, different kinds of monomers were examined for the polymerization and ω-functionalization with bromobenzene as the simplest aryl bromide. Styrene as widely available and commonly employed monomer was chosen as starting point (**Scheme 42**) due to its electrochemical stability, and the absence of any functional groups that could potentially interfere with the electrochemical reduction reactions.

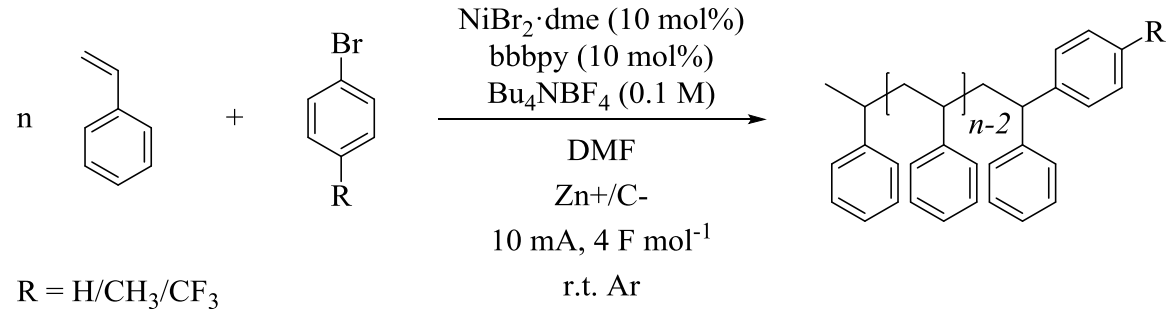

Scheme 42. Electrochemically-mediated nickel-catalyzed ω-functionalization of polystyrene obtained by electrochemical polymerization of styrene.

Herein, the focus laid on the successful polymerization, which could be achieved in the first attempts. However, only polymers of low molar masses were obtained. Therefore, the monomer concentration and its equivalents with respect to the aryl bromide were increased. Additionally, the loading of the nickel catalyst and the ligand were decreased from 25 mol% with respect to the aryl bromide to 10 mol%. The obtained molar masses were still comparably low (M_n = 4800 g mol^{-1}, determined by SEC using THF as eluent, PS calibration) with a relatively low dispersity ($Đ$ = 1.37), using bromobenzene as aryl bromide. Interestingly, the chain lengths and dispersities obtained were varying drastically depending on the aryl bromide used as ω-functionalization agent (**Figure 30**). The values for the molar masses (determined by SEC using THF as eluent, PS calibration) were lowest for bromobenzene (M_n = 4800 g mol^{-1}, $Đ$ = 1.37). However, the electron-deficient nature of the trifluoromethyl group on 4-bromobenzotrifluoride resulted in the formation of significantly longer macromolecules with a significantly higher M_n (M_n = 10300 g mol^{-1}, $Đ$ = 1.66) accompanied by a second, low molar mass distribution (M_n = 700 g mol^{-1}; $Đ$ = 1.21). According to the SEC results (THF as eluent, PS calibration), 4-bromotoluene behaved similarly to bromobenzene as ω-functionalizing agent with a M_n value of the obtained polymers of M_n = 5800 g mol^{-1} and a dispersity of $Đ$ = 1.49. In general, substituents seemed to result in longer chain lengths and higher dispersities. Remarkably, in contrast to bromobenzene and 4-bromotoluene as aryl bromides for the electrochemically-mediated nickel-catalyzed ω-functionalization, 4-bromobenzotrifluoride stood out in terms of the reached molar masses of the obtained polymers. Also, the isolated yields in this case were significantly lower than with bromobenzene and 4-bromotoluene.

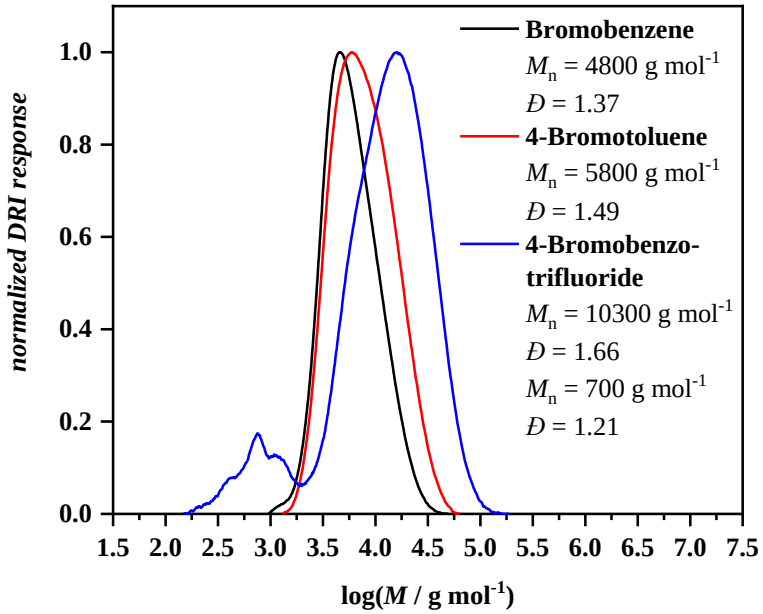

Figure 30. Comparison of SEC traces using THF as eluent (PS calibration) of the electrochemically-mediated nickel-catalyzed ω-functionalization of polystyrene, employing bromobenzene (black line), 4-bromotoluene (red line), and 4-bromobenzotrifluoride (blue line) as aryl bromides.

Moreover, the comparison of the proton NMR spectra using bromobenzene and 4-bromotoluene as aryl bromide showed a signal at a chemical shift of δ = 2.20 – 2.28 ppm in the case of the latter, presumably arising from the methyl group caused by the incorporation of the 4-bromotoluene motif into the polymer structure (**Figure 31**). The ^{19}F NMR spectrum (see **Chapter 6.5.1.1**, **Figure 110**) of the product obtained after electrochemically-mediated nickel-catalyzed ω-functionalization of polystyrene using 4-bromobenzotrifluoride exhibited a fluorine signal at a chemical shift of δ = -62.48 – -62.70 ppm, which could be attributed to the CF_3 motif of incorporated 4-bromobenzotrifluoride moieties.

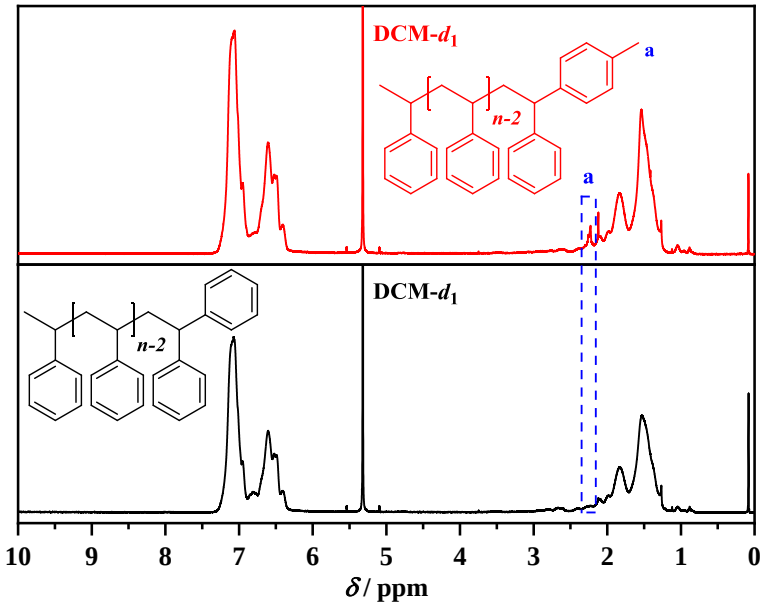

Figure 31. Comparison of ^{1}H NMR spectra of the electrochemically-mediated nickel-catalyzed ω-functionalization of polystyrene, employing bromobenzene (bottom, black line) and 4-bromotoluene (top, red line) as aryl bromides; solvent: DCM-d_2.

Additionally, the influence of different reaction times, in this case measured using the amount of transmitted electrons per amount of substance (F mol^{-1}) was evaluated for the ω-functionalization of polystyrene with aryl bromide. In the first attempt, the reaction was stopped after 4 F mol^{-1} passed through the system, but the impact of a shorter (2 F mol^{-1}) and longer reaction (8 F mol^{-1}) was examined (**Figure 32**). The size-exclusion chromatograms suggested that shorter reaction times (thus less electrons passing through the system) resulted in a decrease of both reached molar masses of the polymers and dispersities. The comparison of the SEC traces revealed the following results: the shape at the low molar mass fraction was almost identical, while tailing towards higher molar masses was more pronounced with increasing reaction durations and consequently increasing amounts of electrons transferred to the mixture. This might be due to the formation of longer polymer chains until the polymers become ω-functionalized and thus terminated towards more progressed reaction times. The decreasing aryl bromide concentration in the course of the reaction, being already comparably low at the beginning of the reaction with respect to the styrene content in the mixture (75.00 eq. with respect to bromobenzene), might have resulted in a longer propagation time span before ω-functionalization and thus termination of the polymerization. Consequently, longer polymer chains would form with increasing reaction time, which could potentially explain this finding. However, the mechanism of this reaction was not further investigated, which could have delivered hints or even proofs for the assumptions and explanations.

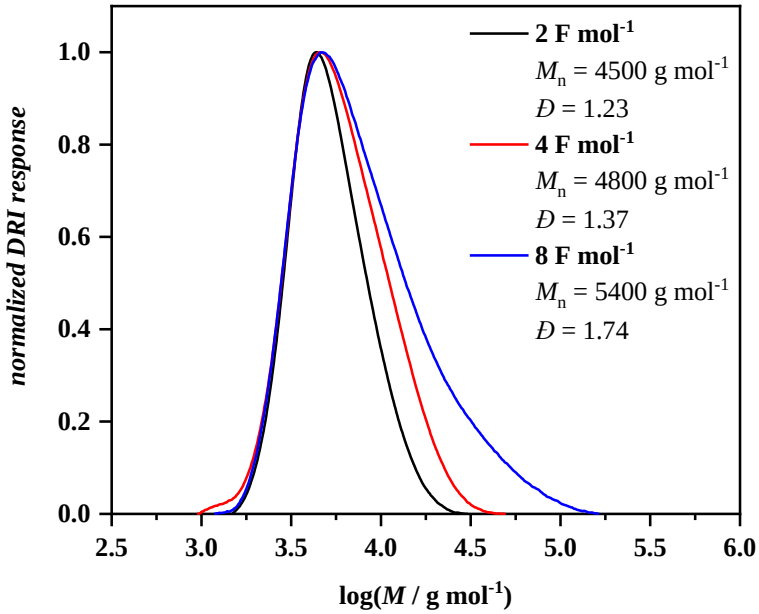

Figure 32. Comparison of SEC traces using THF as eluent (PS calibration) of the electrochemically-mediated nickel-catalyzed ω-functionalization of polystyrene, employing bromobenzene as aryl bromide with different reaction times of 2 F mol^{-1} (black line), 4 F mol^{-1} (red line), and 8 F mol^{-1} (blue line).

Moreover, a control experiment was carried out in the absence of bromobenzene as aryl bromide in addition to the actual experiment with aryl bromide. Styrene was used as monomer and in contrast to the experiments mentioned above, 50.00 equivalents of styrene were used with respect to bromobenzene. The control experiment was conducted in an analogous fashion, but without the addition of bromobenzene. Interestingly, both reactions featured increasing voltages throughout the reaction and the results thus presumably differed from the results described above. However, the comparison of the size-exclusion chromatograms is depicted below (**Figure 33**). The use of bromobenzene as aryl bromide for the ω-functionalization seemed to suppress the formation of smaller polystyrene chains, resulting in a decreased dispersity ($Đ$ = 2.05 with bromobenzene versus $Đ$ = 2.54 in the absence of the latter). This clearly showed the impact of the presence of an aryl bromide species on the outcome of the reaction.

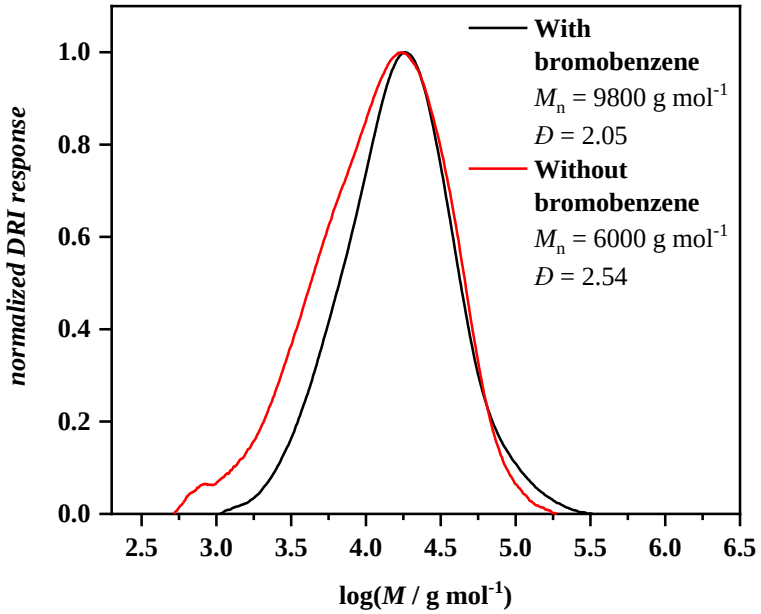

Figure 33. Comparison of the size-exclusion chromatograms (THF as eluent, PS calibration) of the electrochemically-mediated nickel-catalyzed ω-functionalization using styrene in the presence of bromobenzene (black line) and in absence of the latter (red line) as control experiment.

To demonstrate the scope of this ω-functionalization, different monomers were tested. First, MMA and BA as methacrylate and acrylate representatives were chosen due to their commercial availability and simple structural motifs involving an ester functionality. However, the reactions yielded hardly soluble material, leading to the assumption that cross-linking reactions took place with BA and MMA as potential monomers. Sticking with the styrene structural motif, pentafluorostyrene was employed as its polymer would offer the ability to perform PPM, for instance by *para*-fluoro-thiol reactions (PFTR).[203] However, the polymerization attempt resulted in the formation of a hardly soluble gel-like structure at the cathode, drastically reducing the amount of monomer units present to undergo polymerization and significantly decreasing the yield. This phenomenon was reproducible in a control reaction without the presence of any additives apart from the actual monomer, solvent, and electrolyte in the electrochemical cell setup. Nonetheless, it turned out that this system allowed for the polymerization of 4-fluorostyrene as mono-fluorinated monomer and of acrylonitrile, in the case of acrylonitrile as monomer resulting in polymers featuring increased dispersities ($Đ$ = 2.74, determined by SEC using DMAc as eluent with PS calibration). The corresponding size-exclusion chromatograms for the polymerization and the respective ω-functionalization of 4-fluorostyrene and acrylonitrile (both 50.00 equivalents of monomer with respect to bromobenzene) are depicted in **Figure 34**. Noteworthy, the SEC trace of the former was

obtained using THF as eluent, whereas for the latter, DMAc was employed as eluent, since poly(acrylonitrile) was not soluble in THF.

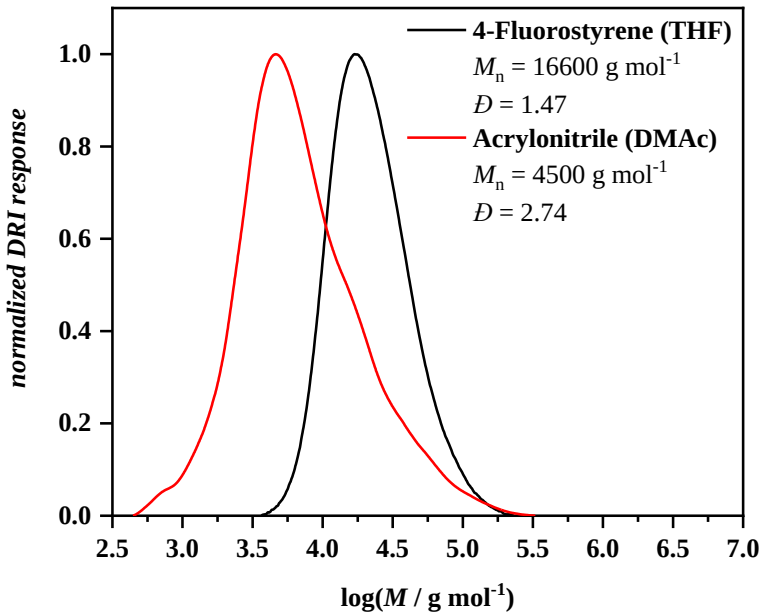

Figure 34. SEC traces of the polymerization and ω-functionalization of 4-fluorostyrene (black line, THF as eluent and PS calibration) and acrylonitrile (red line, DMAc as eluent and PS calibration) as monomers (both 50.00 equivalents with respect to bromobenzene as aryl bromide).

In the case of 4-fluorostyrene as monomer, another reaction was carried out with 4-bromobenzotrifluoride as aryl bromide for the ω-functionalization. Analogous to the reaction using 4-bromobenzotrifluoride as aryl bromide with styrene as monomer, the yield of the reaction was low. Nonetheless, the incorporation of the trifluoromethyl motif could be proven by ^{19}F NMR spectroscopy. Herein, it allowed for the calculation of the M_n value by comparison of the integrals of the signals arising from the CF_3 moiety (δ = -64.87 – -64.96 ppm) and from the fluorine atom in *para* position in poly(4-fluorostyrene) (δ = -119.80 – -120.47 ppm) in the fluorine NMR spectrum (**Figure 35**). The integration of the respective signals exhibited a M_n value of M_n = 31100 g mol^{-1} with approximately 253 repeating units per chain on average.

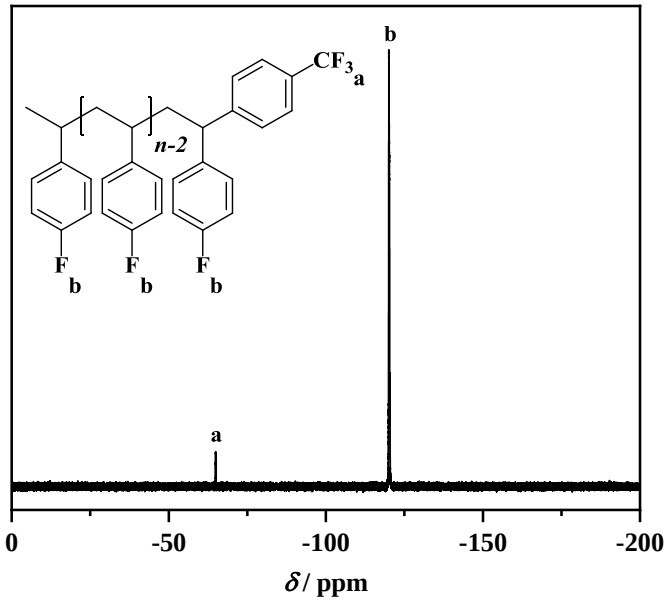

Figure 35. ^{19}F NMR spectrum of the electrochemically-mediated nickel-catalyzed ω-functionalization using 4-fluorostyrene as monomer and 4-bromobenzotrifluoride as aryl bromide; solvent: THF-d_8.

In comparison to the determination of the M_n value by fluorine NMR spectroscopy, SEC using THF as eluent with PS calibration exhibited a significantly lower M_n value of M_n = 18000 g mol^{-1} and a dispersity of $Đ$ = 1.31 (**Figure 36**). On the one hand, this could be due to a non-quantitative ω-functionalization. In other words, not every polymer chain was carrying the trifluoromethylphenyl motif as ω-group, but the macromolecules without ω-capping featured the same chain lengths, especially considering the low dispersity. Additionally, there was a second signal in SEC at the low limit with a M_n = 500 g mol^{-1}. Interestingly, the results suggested that this phenomenon was characteristic and also exclusive for 4-bromobenzotrifluoride as aryl bromide, as similar results were obtained when it was used in combination with styrene as monomer. This signal could possibly be arising from oligomers of 4-fluorostyrene, which were not tethered to 4-bromobenzotrifluoride. On the other hand, the integration in ^{19}F NMR spectroscopy of low intensity signals and thus the obtained M_n highly depended on the set boundaries as well as the applied post-processing, which might explain the overestimation of the chain lengths. Additionally, SEC was not an absolute method for the determination of molar masses of poly(4-fluorostyrene) and the values obtained were in this case reported against linear PS standards. This could also explain the difference of the results obtained from ^{19}F NMR spectroscopy and SEC using THF as eluent.

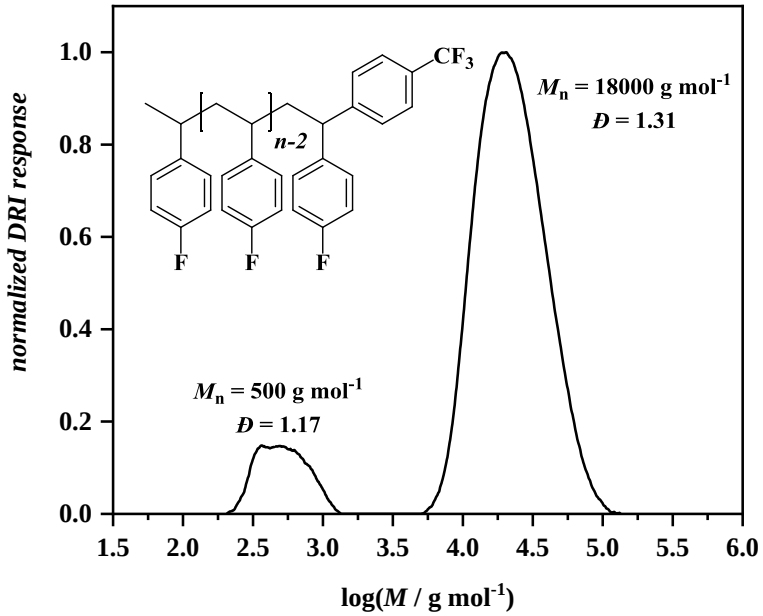

Figure 36. Size-exclusion chromatogram (THF as eluent, PS calibration) of the polymer obtained by electrochemically-mediated nickel-catalyzed ω-functionalization using 4-fluorostyrene as monomer and 4-bromobenzotrifluoride as aryl bromide.

4.2.3 Polymeric Aryl Bromides for the Electrochemically-Mediated Nickel-Catalyzed ω-Functionalization

In addition to derivatives of bromobenzene used for the ω-group functionalization of different polymers, polymers bearing aryl bromide functionalities in the side group were evaluated for the preparation of graft copolymers. At first, a homopolymer of 4-bromostyrene was synthesized by FRP using AIBN as thermal initiator. Subsequently, poly(4-bromostyrene) was used in an analogous fashion to the aryl bromides reported in **Chapter 4.2.2**, however, the reactions in most cases yielded hardly soluble material only. The density of aryl bromide functionalities tethered to polymers was presumably too high, potentially leading to a coupling of multiple poly(4-bromostyrene) chains and consequently insoluble cross-linked products *via* nickel-catalyzed biaryl cross-coupling reactions. This phenomenon was also mentioned as potential side reaction for the nickel-catalyzed electrochemical reductive relay cross-coupling of alkyl halides to aryl halides.[163] Among others, copolymers of 4-bromostyrene and 4-methylstyrene were thus prepared by FRP. The latter was chosen as comonomer (**Scheme 43**) instead of styrene in order to quantify the content of incorporated 4-bromostyrene units in the copolymer in an efficient manner.

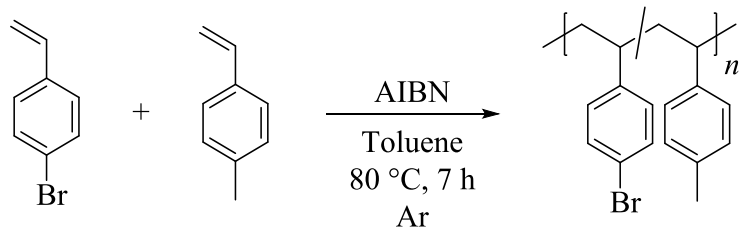

Scheme 43. Synthesis of poly(4-bromostyrene-*ran*-4-methylstyrene) by FRP of 4-bromostyrene and 4-methylstyrene for the electrochemically-mediated nickel-catalyzed ω-functionalization as polymeric aryl bromide moiety.

AIBN was used as thermal initiator and the polymerization was carried out for 7 hours in toluene (**Scheme 43**). The polymer was isolated by precipitation in cold methanol and featured a M_n value of M_n = 3000 g mol^{-1} with a dispersity of $Đ$ = 1.26 (determined by SEC with THF as eluent, PS calibration) (**Figure 37**). Generally, the focus here was set on the synthesis of short polymer chains of poly(4-bromostyrene-*ran*-4-methylstyrene) to mimic the chemistry of small organic aryl bromides to some extent.

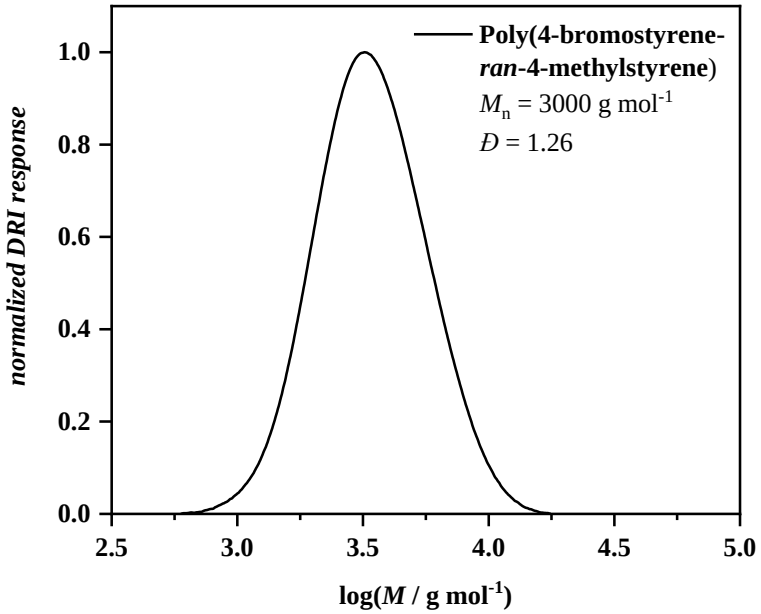

Figure 37. Size-exclusion chromatogram with THF as eluent (PS calibration) of poly(4-bromostyrene-*ran*-4-methylstyrene) obtained by copolymerization of 4-bromostyrene and 4-methylstyrene.

According to ^{1}H NMR spectroscopy (**Figure 38**), the copolymer consisted of 21 mol% of 4-bromostyrene repeating units, which was determined by comparison of the integrals of the signals arising from the methyl group of 4-methylstyrene (δ = 2.13 – 2.47 ppm) and the signals arising from aromatic protons (δ = 6.17 – 7.59 ppm). Therefore, the number of aromatic protons arising from 4-methylstyrene repeating units was deducted from the total amount of aromatic protons. The content of 4-bromostyrene was in accordance with the feed ratio of 4-bromostyrene to 4-methylstyrene employed in the copolymerization (1:3 ratio of 4-bromostyrene to 4-methylstyrene). This comparably low ratio was targeted to lower the content of aryl bromide moieties in the copolymer in order to suppress cross-linking reactions.

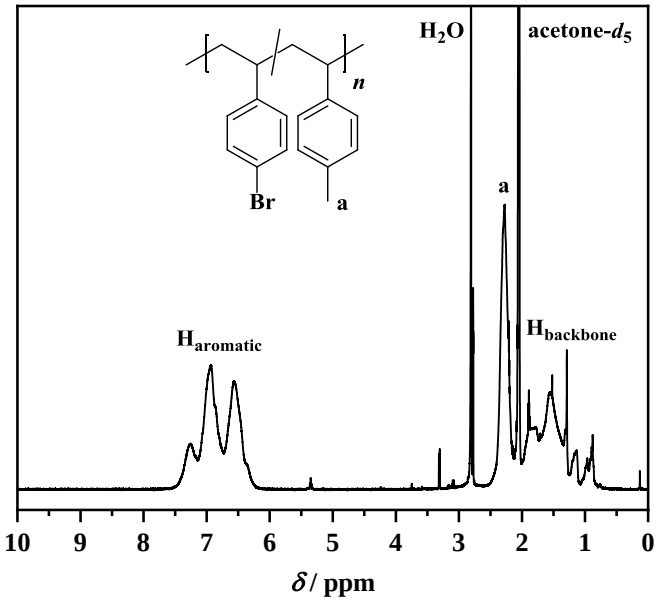

Figure 38. ^{1}H NMR spectrum of poly(4-bromostyrene-*ran*-4-methylstyrene) obtained by copolymerization of 4-bromostyrene and 4-methylstyrene; solvent: acetone-d_6.

Furthermore, the DSC data of the obtained polymer (see **Chapter 6.5.2.1**, **Figure 124**) showed a single glass transition temperature (T_g) at T_g = 104 °C, which was in the range of the reported one of polystyrene with a T_g of approximately $T_g \approx 100$ °C.[204,205]

Afterwards, the prepared copolymer poly(4-bromostyrene-*ran*-4-methylstyrene) was employed in an electrochemically-mediated nickel-catalyzed ω-functionalization with 4-*tert*-butylstyrene analogous to the reactions carried out with bromobenzene and its derivatives (**Scheme 44**). 4-*tert*-Butylstyrene was chosen due to its simple structural bonding motifs and its *tert*-butyl group in *para* position. The distinct shift of the *tert*-butyl group in ^{1}H NMR spectroscopy allowed to distinguish the signals arising from the monomer and the copolymer ω-group. Analogous to the reactions mentioned in **Chapter 4.2.2**, the reactions were performed under similar conditions when non-polymeric aryl bromides were used.

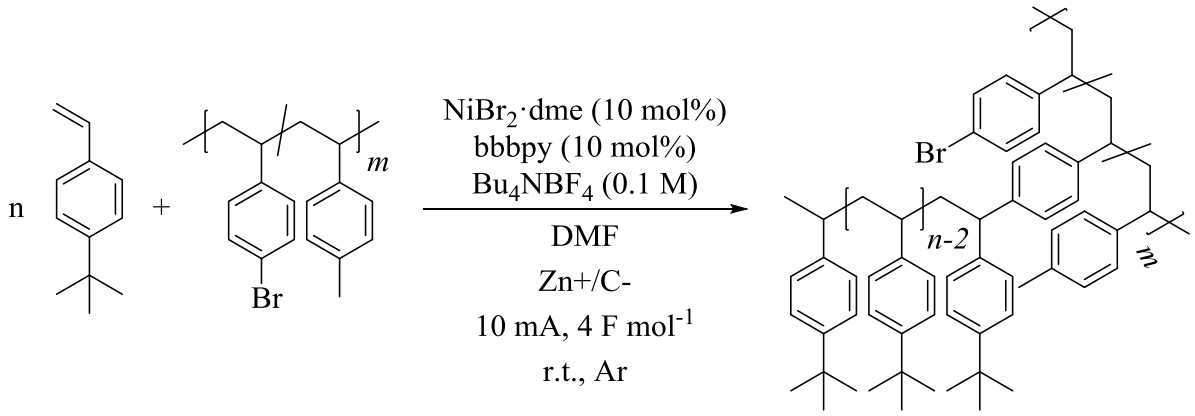

Scheme 44. Poly(4-bromostyrene-*ran*-4-methylstyrene) as polymeric aryl bromide for the electrochemically-mediated nickel-catalyzed ω-functionalization using 4-*tert*-butylstyrene as monomer.

The resulting product was purified by precipitation in cold methanol for catalyst, ligand, electrolyte, and residual monomer removal and analyzed by ^{1}H NMR spectroscopy, SEC, and DSC. The comparison of the proton NMR spectra before and after the reaction revealed the appearance of new signals featuring a chemical shift of δ = 1.1 – 1.5 ppm in addition to the signals of the copolymer used as aryl bromide, especially the signals of the methyl group arising from the copolymer consisting of 4-methylstyrene repeating units at shifts of δ = 2.1 – 2.5 ppm were clearly visible (**Figure 39**).

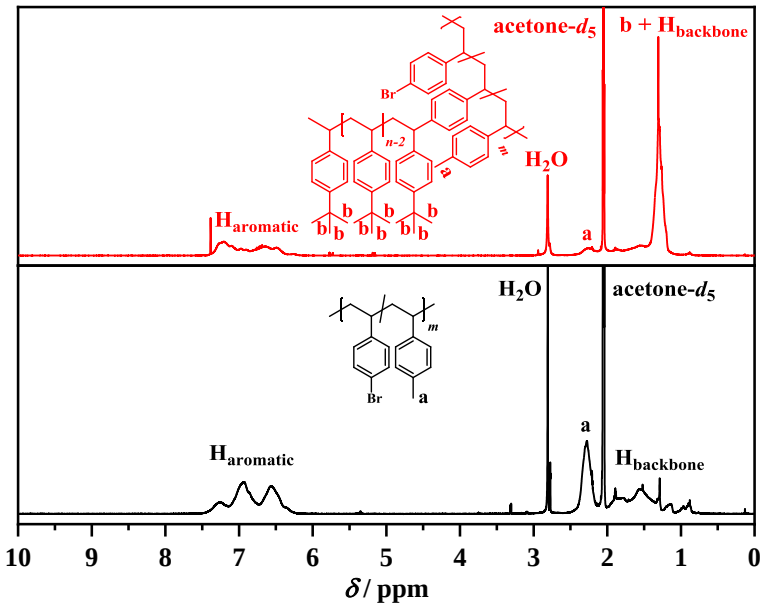

Figure 39. Comparison of the ^{1}H NMR spectra of poly(4-bromostyrene-*ran*-4-methylstyrene) before (bottom, black line) and after (top, red line) the electrochemically-mediated nickel-catalyzed ω-functionalization using 4-*tert*-butylstyrene as monomer; solvent: acetone-d_6.

The proton NMR spectrum after the reaction exhibited signals from both polymeric 4-*tert*-butylstyrene as well as poly(4-bromostyrene-*ran*-4-methylstyrene) used for the ω-functionalization. However, this did not ultimately prove the formation of a graft copolymer: if the copolymer bearing aryl bromide functionalities was not attached to poly(4-*tert*-butylstyrene) and remained intact under the electrochemical conditions, purification by precipitation would result in the isolation of a combination of two distinct polymers, i.e. poly(4-*tert*-butylstyrene) and poly(4-bromostyrene-*ran*-4-methylstyrene). Consequently, the ^{1}H NMR spectrum would feature signals arising from both polymeric species. The obtained product was thus analyzed by SEC using THF as eluent (PS calibration), exhibiting solely one unimodal molar mass distribution, which was, in comparison to the SEC trace of poly(4-bromostyrene-*ran*-4-methylstyrene), shifted towards higher molar masses (from M_n = 3000 g mol^{-1} to M_n = 4500 g mol^{-1} after the reaction) (**Figure 40**). This result indicated the formation of a single polymeric species after the reaction. The shape of the chromatogram after the reaction remained almost unaffected, while the dispersity increased from $Đ$ = 1.26 for polymeric aryl bromide to $Đ$ = 1.55, presumably due to different chain lengths of poly(4-*tert*-butylstyrene) and different grafting densities on the copolymer.

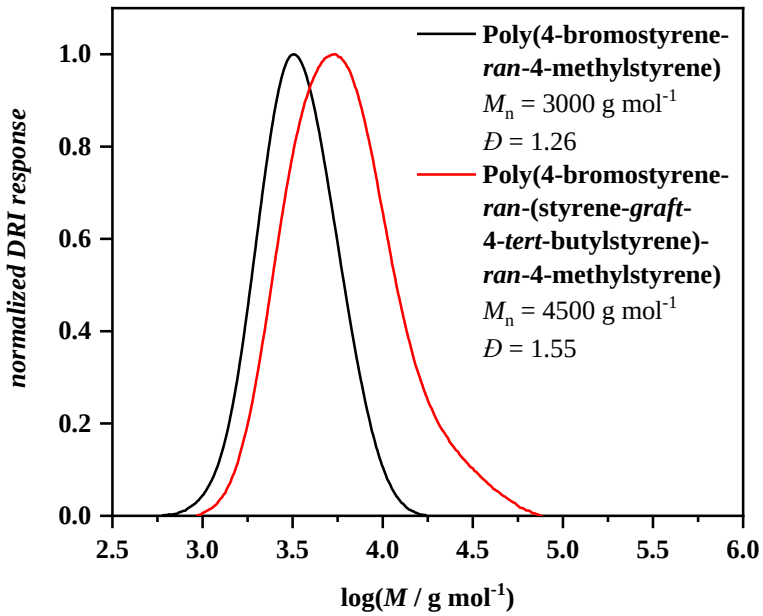

Figure 40. Comparison of the size-exclusion chromatograms (THF as eluent, PS calibration) of poly(4-bromostyrene-*ran*-4-methylstyrene) before (black line) and after (red line) the electrochemically-mediated nickel-catalyzed ω-functionalization using 4-*tert*-butylstyrene as monomer.

In addition, a DSC measurement of the obtained product was performed. It showed two distinct glass transitions at T_g = 103 °C and T_g = 126 °C in comparison to the polymeric aryl bromide,

which featured only one glass transition at T_g = 104 °C (**Figure 41**). The second glass transition observed after the electrochemically-mediated nickel-catalyzed polymer ω-functionalization with 4-*tert*-butylstyrene as monomer matched the value of poly(4-*tert*-butylstyrene) in literature.[206]

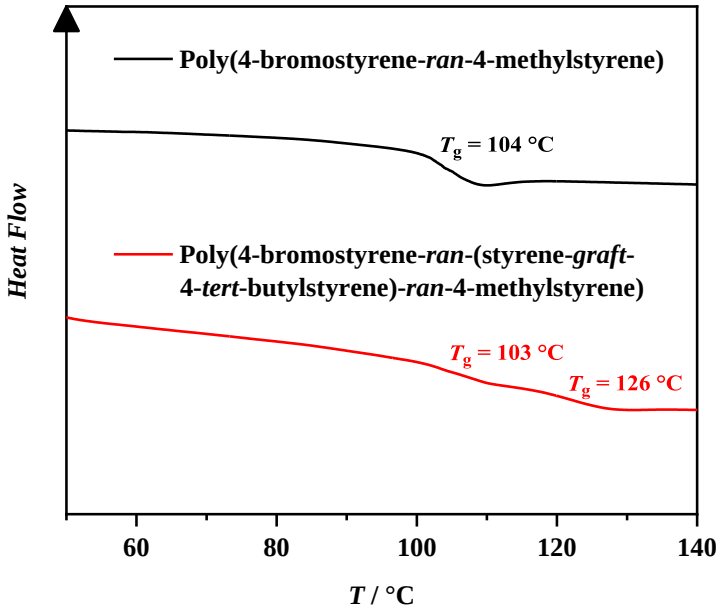

Figure 41. Comparison of the DSC results of poly(4-bromostyrene-*ran*-4-methylstyrene) (black line) employed in the electrochemically-mediated nickel-catalyzed ω-functionalization using 4-*tert*-butylstyrene as monomer (red line).

Moreover, a control reaction was performed in a similar fashion to the reaction described above (**Scheme 44**), but in the absence of 4-*tert*-butylstyrene as monomer (**Scheme 45**).

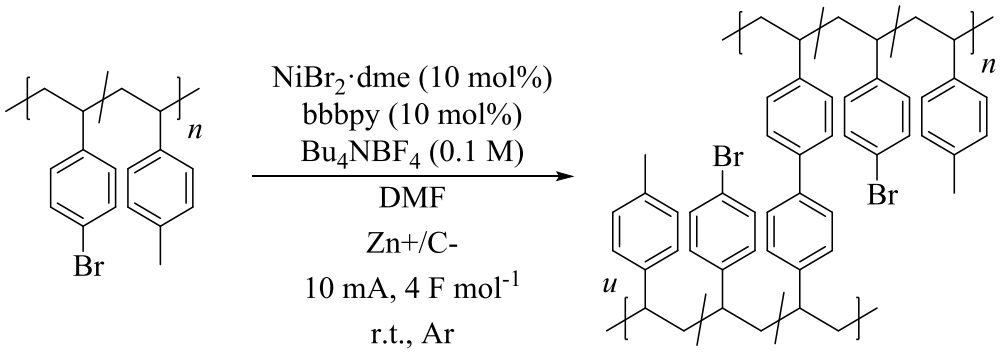

Scheme 45. Electrochemically-mediated nickel-catalyzed biaryl coupling of poly(4-bromostyrene-*ran*-4-methylstyrene) as control experiment in absence of 4-*tert*-butylstyrene as monomer.

Theoretically, the copolymer composed of mainly 4-methylstyrene and 4-bromostyrene units should undergo biaryl coupling reactions of the 4-bromostyrene repeating units, either in an intramolecular fashion or intermolecularly. As non-diluted reaction conditions were employed in this reaction, the intermolecular biaryl coupling should consequently be preferred. The obtained product was hardly soluble in common organic solvents, meeting the expected outcome of an intermolecular C-C bond formation resulting in cross-linking of the copolymer. Thus, only the soluble fraction of the resulting product could be analyzed by ^{1}H NMR spectroscopy and SEC using THF as eluent. The former exhibited the presence of signals arising from aromatic protons, the backbone, and the methyl group of the 4-methylstyrene repeating units and was in accordance with the expectation. The spectrum was almost identical to the one of the starting material, however, a change in the appearance of the signals arising from the aromatic protons could be observed (see **Chapter 6.5.2.2**, **Figure 129**). This could be due to the consumption of the bromide atoms tethered to the aromatic moieties. The comparison of the size-exclusion chromatograms using THF as eluent (PS calibration) of the polymeric aryl bromide, i.e. poly(4-bromostyrene-*ran*-4-methylstyrene), the ω-capping of poly(4-*tert*-butylstyrene) with the polymeric aryl bromide, and the control reaction in absence of a monomer clearly differed from each other (**Figure 42**): the control reaction mainly yielded insoluble products, the soluble fraction however featured an increased M_n value of M_n = 3900 g mol^{-1}, while its counterpart in presence of 4-*tert*-butylstyrene as monomer resulted in polymers with M_n = 4500 g mol^{-1}. More interestingly though, in contrast to the actual ω-capping of poly(4-*tert*-butylstyrene) with poly(4-bromostyrene-*ran*-4-methylstyrene) as polymeric aryl bromide ($Đ$ = 1.55), the dispersity of the polymers obtained by the control experiment, in other words the cross-linking of the polymeric aryl bromide, drastically decreased from $Đ$ = 1.26 to $Đ$ = 1.19. On the one hand, this could be caused by the insolubility of a large fraction of the obtained polymeric material, which potentially featured a higher dispersity and was removed by filtration prior to the measurement. On the other hand, the dispersity usually decreases upon cross-linking of one polymer species, since smaller macromolecules can react with longer polymer chains and vice versa.

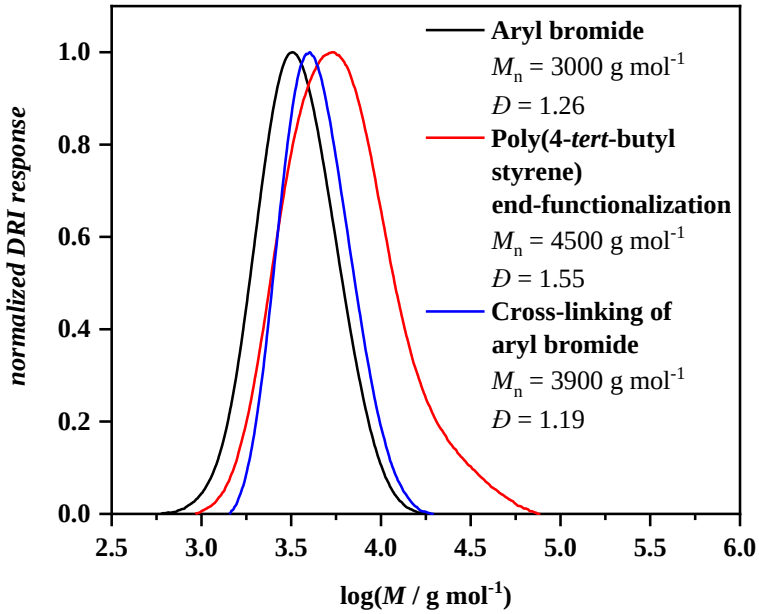

Figure 42. Comparison of the SEC traces (THF as eluent, PS calibration) of the polymeric aryl bromide (black line), the ω-functionalization of poly(4-*tert*-butylstyrene) using the latter (red line), and the control experiment in absence of a monomer (blue line).

These results suggested the successful ω-functionalization of poly(4-*tert*-butylstyrene) with a polymeric aryl bromide, i.e. poly(4-bromostyrene-*ran*-4-methylstyrene), resulting in graft copolymers based on polystyrene structural motifs. Since acrylonitrile as a non-styrene-derived monomer successfully yielded polymeric material in the case of bromobenzene as aryl bromide for the ω-functionalization, it was employed as monomer in a similar fashion as 4-*tert*-butylstyrene with the same copolymer structure as polymeric aryl bromide (**Scheme 46**).

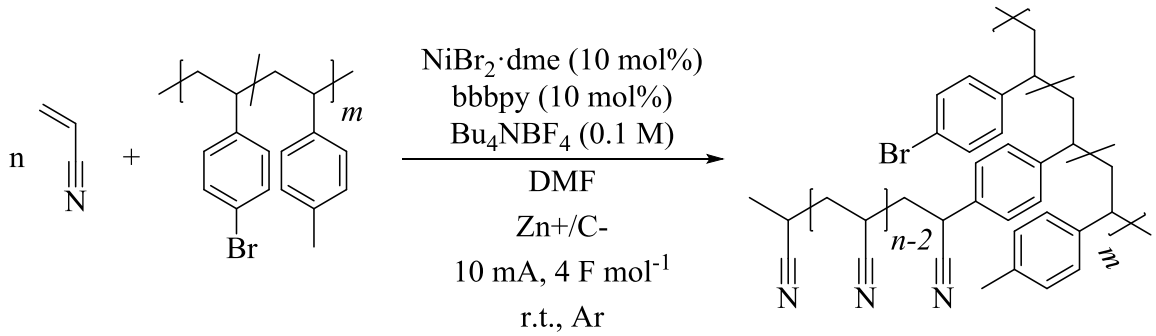

Scheme 46. Poly(4-bromostyrene-*ran*-4-methylstyrene) as polymeric aryl bromide for the electrochemically-mediated nickel-catalyzed ω-functionalization using acrylonitrile as monomer.

The reaction was carried out in a similar fashion to the ω-functionalization of poly(4-*tert*-butylstyrene) with poly(4-bromostyrene-*ran*-4-methylstyrene). The resulting

polymers featured only poor solubility in THF and acetone, but dissolved readily in DMF and DMAc, which is already an indication for the successful formation of polymeric species based on poly(acrylonitrile). The polymer obtained after precipitation in cold methanol was analyzed by ^{1}H NMR spectroscopy, SEC, and IR spectroscopy. Deuterated dimethyl sulfoxide (DMSO) was employed as solvent for the ^{1}H NMR spectrum since the resulting polymer featured reasonable solubility in the latter (**Figure 43**, bottom). However, the product obtained after the reaction did not exhibit full solubility in DMSO and the respective spectrum did not show signals arising from aromatic protons. Another proton NMR spectrum was thus recorded in deuterated acetone as solvent (**Figure 43**, top): the product was not well soluble and only with magnification, signals arising from the product became visible. Signals arising from aromatic protons could be observed, but the intensities of the signals arising from the resulting product were fairly low, limiting the informative value of this measurement.

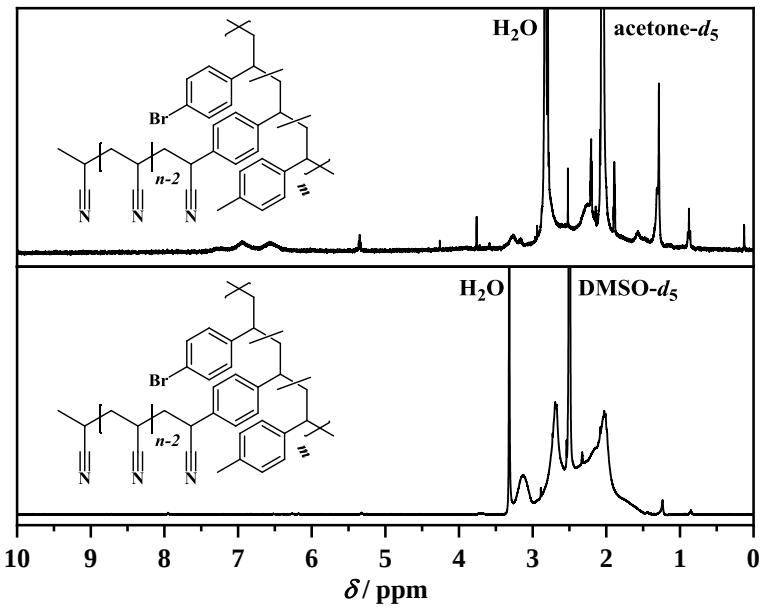

Figure 43. Comparison of the ^{1}H NMR spectra of the polymer obtained after the electrochemically-mediated nickel-catalyzed ω-functionalization using acrylonitrile as monomer and poly(4-bromostyrene-*ran*-4-methylstyrene); solvents: DMSO-d_6 (bottom); acetone-d_6 (top).

SEC using DMAc as eluent (PS calibration) exhibited a clear shift towards higher molar masses as expected with a significant increase of dispersity (from $Đ$ = 1.31 to $Đ$ = 2.66) after the reaction (**Figure 44**). SEC analysis of the homopolymer obtained above in **Chapter 4.2.2** for acrylonitrile as monomer with bromobenzene as aryl bromide already showed a relatively high dispersity ($Đ$ = 2.74). The chromatogram did not exhibit the initial trace of the copolymer used as aryl bromide, but this could be due to an unsuccessful ω-functionalization of the

poly(acrylonitrile) prepared by electrochemical means with an excessive ratio of unfunctionalized poly(acrylonitrile) to still intact poly(4-bromostyrene-*ran*-4-methylstyrene) in the obtained product and the signal of the initial polymeric aryl bromide thus not being pronounced in SEC as well as proton NMR spectroscopy.

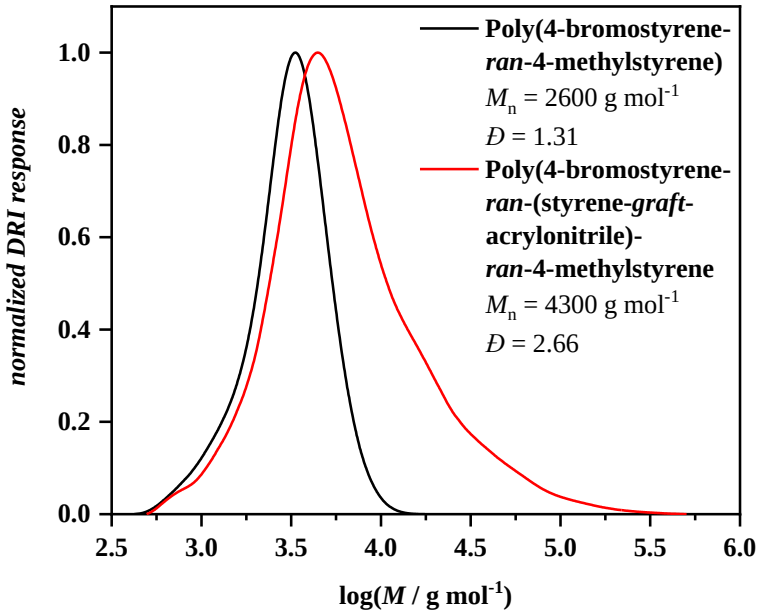

Figure 44. Comparison of the size-exclusion chromatograms (DMAc as eluent, PS calibration) of poly(4-bromostyrene-*ran*-4-methylstyrene) (black line) employed in the electrochemically-mediated nickel-catalyzed ω-functionalization using acrylonitrile as monomer.

In this case, IR spectroscopy was employed for further characterization due to the distinct vibration of the nitrile functionality in acrylonitrile and thus in the ω-functionalization of poly(acrylonitrile) with poly(4-bromostyrene-*ran*-4-methylstyrene). The comparison of the IR spectra (**Figure 45**) showed the appearance of a new vibration at a wavenumber of $\tilde{\nu}$ = 2244 cm^{-1}, which was characteristic for the presence of a nitrile functionality. The intensity of the signal however was rather low. The prominent signal at a wavenumber of $\tilde{\nu}$ = 1661 cm^{-1} arose from DMF, which was still present and rather hard to remove, as the polymer was dissolved in DMF to be precipitated into cold methanol.

The results suggested an enhanced suitability of styrene-derived monomers in comparison to acrylonitrile for the sophisticated electrochemically-mediated nickel-catalyzed preparation of graft copolymers. Further investigations on the impact of the monomer type on the efficiency of the graft copolymer synthesis are thus necessary in order to improve the synthesis of poly(acrylonitrile)-based graft copolymers by the present approach.

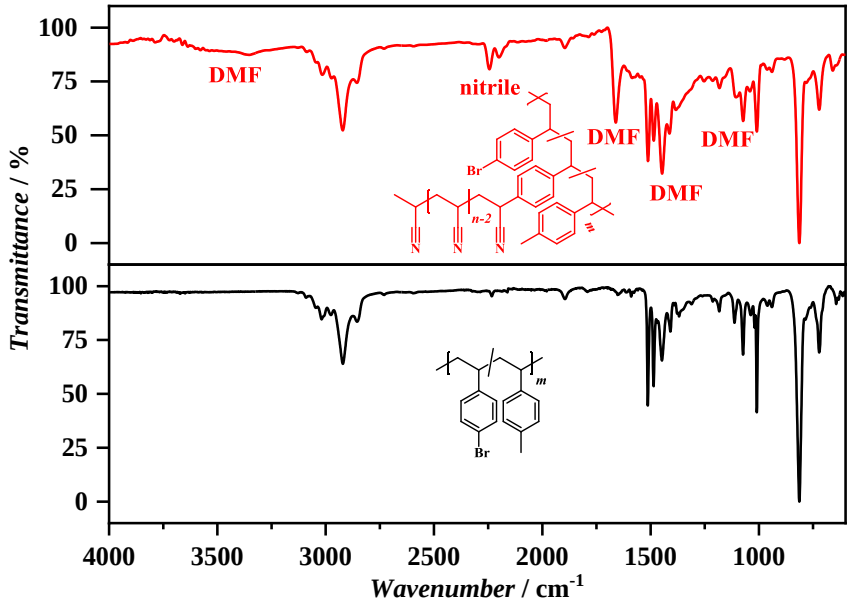

Figure 45. Comparison of the IR spectra of poly(4-bromostyrene-*ran*-4-methylstyrene) (bottom, black line) employed in the electrochemically-mediated nickel-catalyzed ω-functionalization using acrylonitrile as monomer (top, red line).

4.2.4 Conclusion and Outlook

This chapter described the electrochemically-mediated nickel-catalyzed ω-functionalization with polymeric and non-polymeric aryl bromides. Different monomers were employed in electrochemical polymerizations using bromobenzene and derivatives: styrene-based monomers with their simple structures in absence of functionalities were suited the most for this kind of ω-functionalization of propagating chains. Also, acrylonitrile could be polymerized in this fashion, but resulted in the formation of polymeric material featuring a comparatively high dispersity. The influence of the choice of aryl bromide as well as different polymerization times were investigated for styrene as monomer. A control experiment without the use of any aryl bromide moiety showed an increased dispersity and the size-exclusion chromatogram exhibited the formation of a larger fraction of small macromolecules in comparison to the reaction in presence of bromobenzene as aryl bromide. Subsequently, polymeric aryl bromides were employed as ω-functionality precursors. To avoid the formation of insoluble material presumably due to cross-linking reactions when a homopolymer comprising aryl bromide moieties, i.e. poly(4-bromostyrene), was employed as polymeric aryl bromide, a copolymer was synthesized composed of 4-bromostyrene and 4-methylstyrene repeating units. The latter was employed as comonomer due the methyl group in *para* position, featuring a distinct signal in ^{1}H NMR spectroscopy and thus allowing for the determination of the aryl bromide content in the copolymer. This copolymer was thereafter employed in an electrochemically-mediated nickel-catalyzed ω-functionalization using 4-*tert*-butylstyrene as monomer. 4-*tert*-Butylstyrene was chosen to a similar reason to the one of 4-methylstyrene: the *tert*-butyl motif featured a distinct shift in proton NMR spectroscopy and allowed to trace the reaction and prove the formation of a poly(4-*tert*-butylstyrene) scaffold. The reaction outcome was analyzed by ^{1}H NMR spectroscopy, SEC, and DSC. ^{1}H NMR spectroscopical analysis showed signals arising from both the aryl bromide copolymer and poly(4-*tert*-butylstyrene). DSC analysis revealed two glass transitions of the obtained polymer, one matching the one of the aryl bromide copolymer and the other one arising from poly(4-*tert*-butylstyrene). The comparison of the SEC traces of the aryl bromide copolymer on the one hand and the resulting polymer after the electrochemically-mediated nickel-catalyzed ω-functionalization on the other hand showed a single unimodal molar mass distribution, shifted towards higher molar masses in comparison to poly(4-bromostyrene-*ran*-4-methylstyrene) employed as polymeric aryl bromide with an increasing dispersity. A control experiment without the addition of 4-*tert*-butylstyrene as monomer was performed, resulting in hardly soluble material, which suggested the cross-linking by intermolecular biaryl cross-coupling reactions of the aryl bromide moieties.

Acrylonitrile was moreover employed as monomer in a similar fashion, poly(4-bromostyrene-*ran*-4-methylstyrene) was used as polymeric aryl bromide analogous to the reaction with 4-*tert*-butylstyrene. The obtained polymers featured an altered solubility behavior. SEC analysis showed a shift towards higher molar masses with increasing dispersity and the IR spectrum showed the appearance of a signal of low intensity vibrations arising from a nitrile functionality. However, the reaction has to be further explored, especially with regard to the degree of ω-functionalization. A full functionalization of the formed propagating macromolecular chains would be desirable and would allow for the straightforward introduction of ω-groups to polymers due to the vast diversity of different aryl bromides and their commercial availability. In this regard, mass spectrometry could potentially help to identify the end groups of the prepared macromolecules, as two or even more distributions could potentially be observed featuring different end groups. Nonetheless, the successful ω-functionalization was shown for different monomers using different aryl bromides, both of polymeric and non-polymeric nature. Consequently, the results suggested a straightforward one-pot preparation of graft copolymers enabled by electrochemical means based on a catalytic nickel system. The great availability of different aryl bromides would allow for the incorporation of a broad range of functionalities into styrene-derived macromolecules as ω-functionalities at "the push of a button", representing a sophisticated way to *in-situ* modify growing macromolecular chains.

4.3 Synthesis and Post-Polymerization Modification of Poly(*N*-(4-vinylphenyl)sulfonamide)s

In this subchapter, the straightforward synthesis of a novel class of aromatic poly(*N*-(4-vinylphenyl)sulfonamide)s from the respective monomers with varying electron densities is demonstrated. Subsequently, the prepared polymers were carefully characterized. Interestingly, a qualitative study revealed smart materials behavior, specifically a pH-dependent water solubility in a switchable fashion. Moreover, the aromatic sulfonamide-based polymers were employed in aza-Michael additions with different electron-deficient alkenes as Michael acceptors for the sophisticated preparation of unprecedented polymeric protected β-amino acid derivatives, resulting in a drastic alteration of the polymers' properties.

Parts of this chapter and the associated parts in the experimental section were adapted with permission from a publication written by the author (Edgar Molle).[207]

4.3.1 General Concept

Originally, the idea behind this project was to use amine-comprising monomers, which should be employed in their protected form as aromatic sulfonamides (**Scheme 47**). These monomers should then be polymerized and subsequently deprotected by electrochemical means, resulting in free amine functionalities as handle for different modification reactions. Herein, ideally RAFT polymerization should be employed as polymerization method of choice: after electrochemical deprotection, polymers with narrow molar mass distributions featuring primary amine moieties would be obtained. A direct RAFT polymerization from the unprotected amine monomers would be challenging due to the proneness of CTAs to undergo aminolysis reactions, which have been employed as end group modification methods.[208–211]

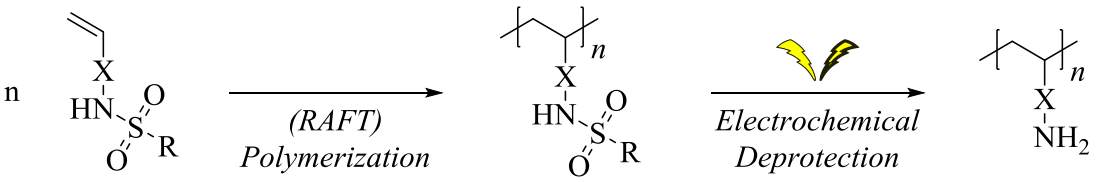

Scheme 47. Initial project idea using monomers featuring protected amine functionalities for the electrochemical deprotection after polymerization, resulting in a primary amine handle for PPM.

Horner and Neumann were the first to report on the electrochemical deprotection of sulfonamides[212] using a mercury cathode and also pioneered in the electrochemical cleavage of sulfones.[213] Since then, several reactions have been published based on this kind of chemistry, mainly relying on the use of a mercury cathode and a divided cell setup.[214–216] Nonetheless, the influence of different non-mercury cathodic materials was explored on *N*-tosyl-L-serine, exhibiting the best yields of detosylation using lead as cathode material.[217] Additionally, several groups have reported the use of a vitreous carbon disc electrode as working electrode in a divided cell setup for the cleavage of the S-N bond.[215,218,219]

The electrochemical setup used in this thesis however was rather simple featuring an undivided cell and limited the choice of electrode materials to the ones accessible from the supplier or material that is adapted to the connections of the vial cap. A mercury electrode was not available for the electrochemical setup employed in the present thesis and its use should, if possible, be avoided due to the toxicity of mercury.[220] However, the other reports based on a carbon-based cathode materials suggested the feasibility of the electrochemical deprotection using the setup described in this thesis, at least with regard to the electrodes. Consequently, first monomers

were synthesized and characterized. Styrene-based monomers (M1-M4) and methacrylate-derived ones (M5) (**Scheme 48**) have been prepared.

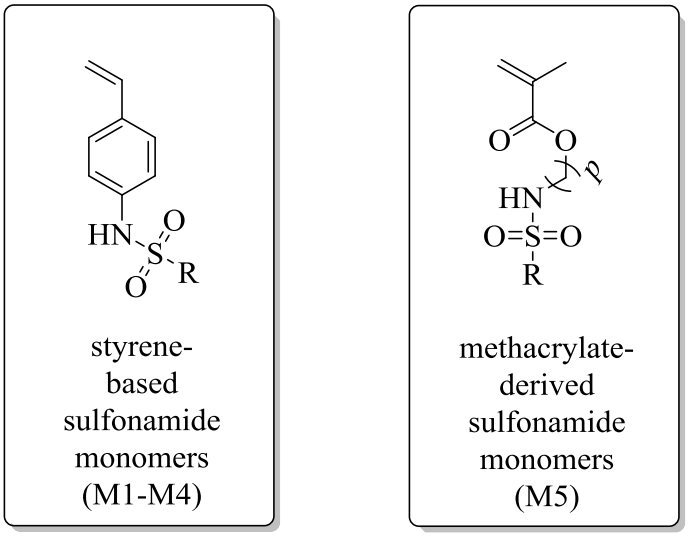

Scheme 48. Two different classes of sulfonamide monomers, based on either styrene (left) or a methacrylate structure (right).

4-Methyl-*N*-(4-vinylphenyl)benzenesulfonamide (M2) as representative of the styrene-based monomers is literature-known[221] and was synthesized in a one-step reaction from commercially available 4-vinylaniline and 4-toluenesulfonyl chloride (see **Chapter 4.3.2**, **Scheme 52**).

Moreover, the synthesis of 3-((4-methylphenyl)sulfonamido)propyl methacrylate (M5) as representative of methacrylate-derived sulfonamide monomers is described in **Scheme 49**. The methacrylate-derived sulfonamide monomer was obtained in a two-step reaction depicted below, starting from 3-aminopropanol and 4-methylbenzenesulfonyl chloride. After aqueous workup, the compound was purified by column chromatography and obtained in a mediocre yield of 44%. Subsequently, *N*-(3-hydroxypropyl)-4-methylbenzenesulfonamide was used with methacryloyl chloride together with triethylamine as auxiliary base to eventually obtain 3-((4-methylphenyl)sulfonamido)propyl methacrylate (M5) in a good yield of 75%.

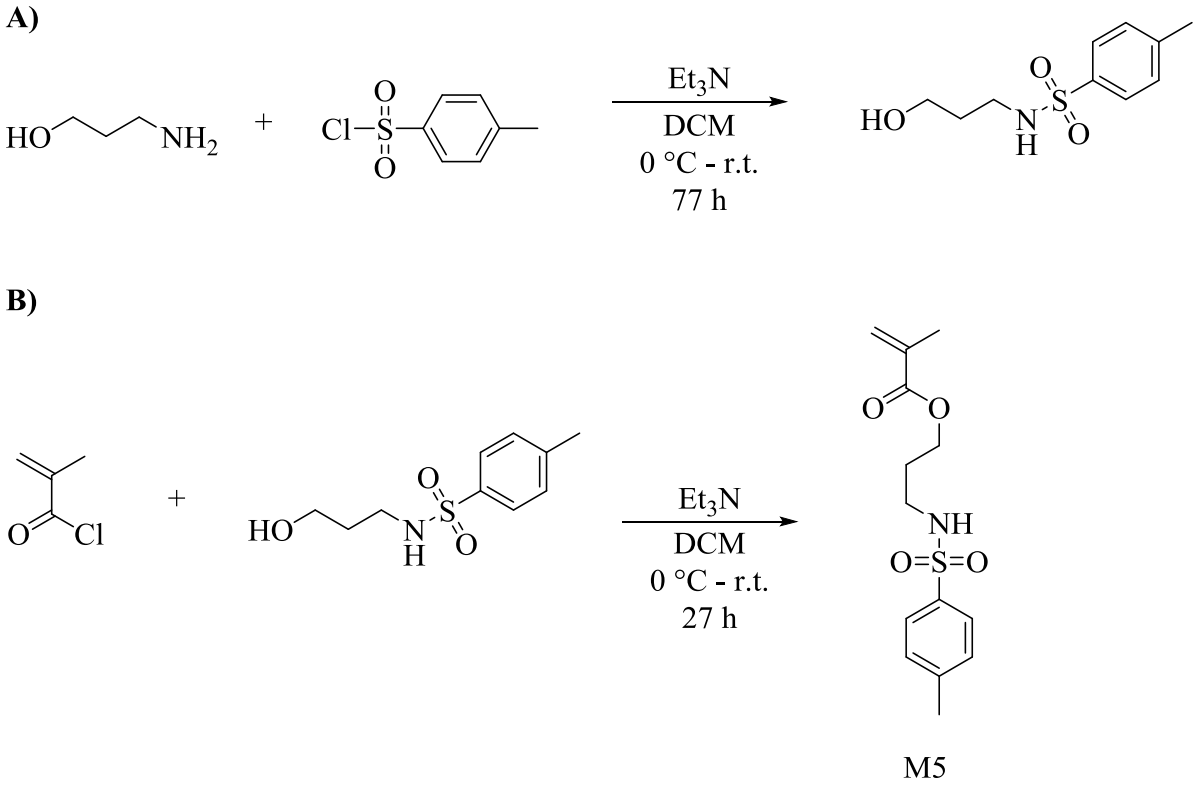

Scheme 49. Two-step synthesis route A) and B), respectively, towards 3-((4-methylphenyl)sulfonamide)propyl methacrylate (M5).

Subsequently, the respective electrochemical behavior of the monomers was evaluated by CV: the respective data exhibited in both cases an irreversible reduction at voltages of -2.3 V < voltage < -2.0 V against an Ag/AgCl reference electrode in acetonitrile (**Figure 46**). This was in accordance with the electrochemical properties of sulfonamides reported in literature.[215,219] Thus, these findings pointed towards an irreversible reductive cleavage of the S-N bond by electrochemical means.

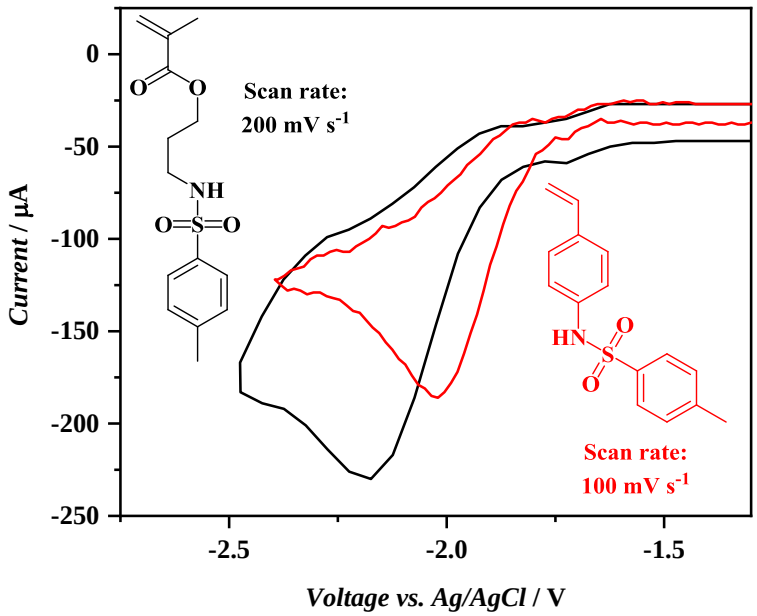

Figure 46. Irreversible reduction of both the methacrylate-derived and styrene-based sulfonamide monomer shown by cyclic voltammetry in acetonitrile.

However, electrolysis experiments (see **Chapter 6.6.6.1**) on the monomer level under different conditions did not yield the desired detosylated product. Initially, Bu_4NBF_4 was used as electrolyte in DMF under potentiostatic conditions with a glassy carbon cathode and a graphite anode. Alternatively, tetrabutylammonium hydrogensulfate (Bu_4NHSO_4) as both electrolyte and proton source was employed. However, according to thin-layer chromatography (TLC), the monomers mostly remained intact throughout the electrolysis experiments. In addition, an electrolysis attempt of the respective polymer in the case of the styrene-based sulfonamide was carried out, using a solution of poly(4-methyl-*N*-(4-vinylphenyl)sulfonamide) (P2) in acetonitrile with Bu_4NHSO_4 as electrolyte under potentiostatic conditions, but the structural motif of the polymer did not change according to SEC and NMR spectroscopy (see **Chapter 6.6.6.2.2**). Interestingly, another literature report demonstrated that the mercury cathode can be avoided when naphthalene was used as mediator in an undivided cell setup.[222] The authors claimed high yields (70 – 97%) for the electrochemical detosylation of different substrates using a platinum cathode and a magnesium rod as anode. The setup used in this thesis did not comprise both kinds of electrode materials at this point, a graphite anode and a platinum plated cathode were thus employed in the reaction. According to TLC and also proven by proton NMR spectroscopy, the reaction mixture after the electrochemical detosylation attempt using naphthalene as mediator contained numerous species of different nature (see **Chapter 6.6.6.1.3**). Consequently, this finding impeded the use of the as-mentioned approach for the detosylation on the macromolecular level, since it is almost impossible to remove or separate

macromolecular side products from the desired polymer. Therefore, this project targeting the electrochemical deprotection of sulfonamide polymers had to be discarded.

Nonetheless, polymers derived from sulfonamide monomers (however in an inversed bond sequence from a backbone perspective and based on a methacrylamide motif) showed interesting smart materials behavior (see **Chapter 2.5**).[183–186] Thus, a set of different styrene-based sulfonamide monomers featuring a secondary amine functionality as handle for functionalization *via* aza-Michael addition with electron-deficient alkenes as Michael acceptors was synthesized and polymerized, and subsequently employed in PPM reactions (**Scheme 50**).

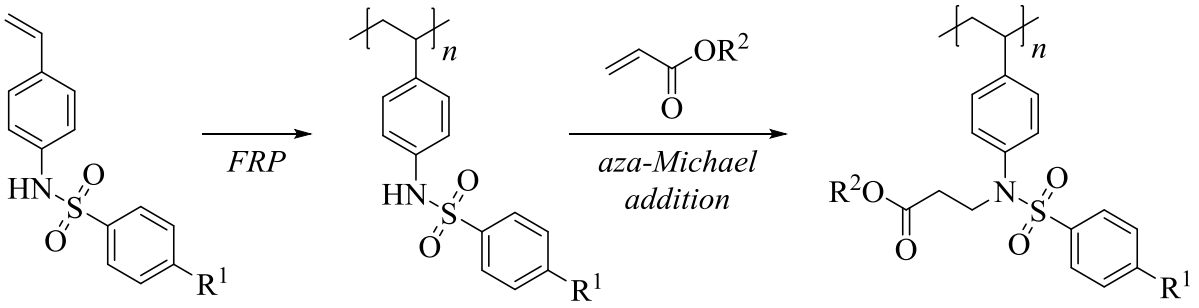

Scheme 50. Novel class of aromatic poly(*N*-(4-vinylphenyl)sulfonamide)s used in PPM reactions *via* aza-Michael addition with electron-deficient alkenes.

4.3.2 Synthesis of Aromatic Sulfonamide Monomers M1-M4

Analogous to the synthesis of 4-methyl-*N*-(4-vinylphenyl)benzenesulfonamide (M2), a set of different *N*-*(*4-vinylphenyl)sulfonamides was synthesized starting from 4-vinylaniline and benzenesulfonyl chloride and derivatives of the latter. Thus, sulfonyl chlorides with different substituents in *para* position were used, resulting in styrene-based sulfonamide monomers with varying electron densities. In comparison to unsubstituted *N*-(4-vinylphenyl)benzenesulfonamide (M1), an electron-donating methyl group (M2) as well as a fluorine atom (M3) and a nitro group (M4) as electron-withdrawing substituents were installed (**Scheme 51**). All these monomers featured a sulfonamide functionality, but in contrast to reported monomers bearing the sulfonamide bond motif,[183–186] it was inverted for monomers M1-M4. From a backbone perspective of the respective polymers, instead of a SO_2-NH group, monomers M1-M4 were based on a NH-SO_2 motif, thus allowing for the preparation of a broad range of different amine-based polymers. On the one hand, the removal of the sulfonamide moiety after polymerization by deprotection under suitable conditions would result in a polystyrene with amine functionalities in *para* position, allowing for the straightforward functionalization of the amine groups. On the other hand, a deprotection after aza-Michael addition would lead to the formation of another secondary amine functionality, which could be addressed by PPM. On top of that, most reported sulfonamide-based monomers are derived from methacrylamide,[183–186] whilst the sulfonamides herein were based on styrene. Styrene-derived sulfonamide polymers are however only scarcely represented in literature: Kakuchi and Théato reported on sequential PPM reactions of poly(pentafluorophenyl 4-vinylbenzenesulfonate), resulting in styrene-derived sulfonamide polymers.[187] However, the bond sequence of the sulfonamide from a backbone perspective is still inverted to the monomers and polymers reported herein.

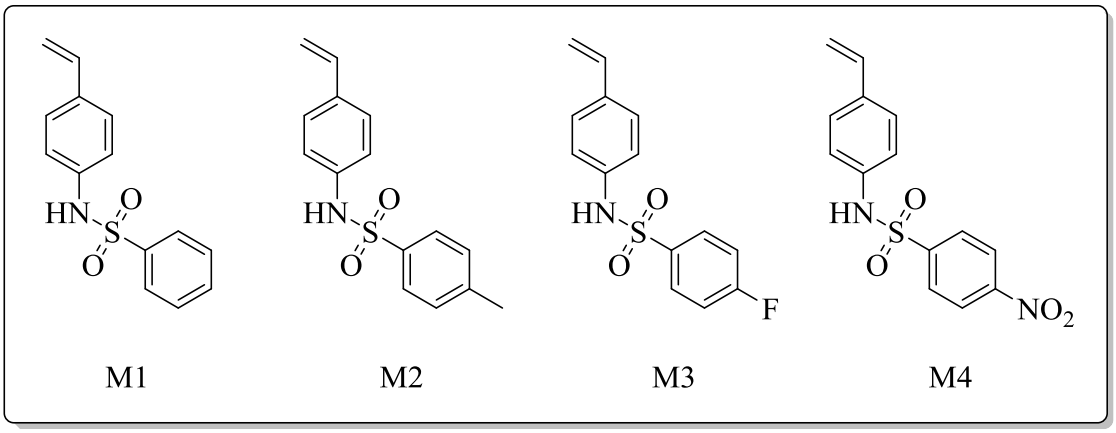

Scheme 51. Aromatic sulfonamide monomers M1-M4 featuring varying electron densities based on 4-vinylaniline.

The monomers M1-M4 were obtained in the following fashion (**Scheme 52**), with R being the respective substituent for each monomer. Details on the synthesis of the sulfonamide monomers M1-M4 are listed in **Table 4**.

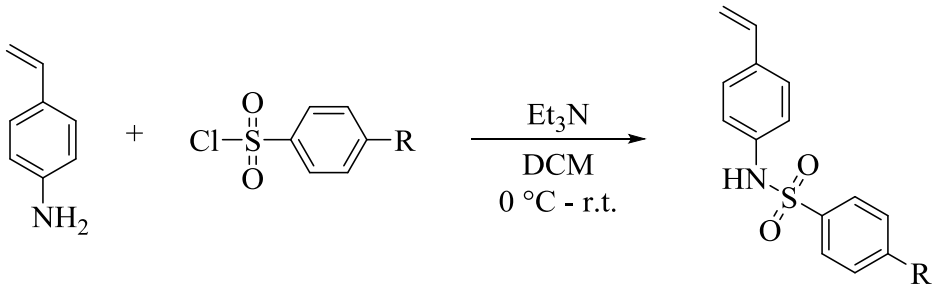

Scheme 52. One-step synthesis of monomers M1-M4 using 4-vinylaniline and different commercially available aromatic sulfonyl chlorides.

Table 4. Details on the synthesis of monomers M1-M4.

Entry	Monomer	R	Reaction time	Isolated yield
1	M1	-H	16 h	73%
2	M2	$-CH_3$	23.5 h	68%
3	M3	-F	17 h	67%
4	M4	$-NO_2$	13 h	28%

The monomers could be isolated in a successful fashion proven by NMR and IR spectroscopy as well as ESI-MS. However, in contrast to the other monomers, monomer M4 featuring a nitro substituent in *para* position could only be obtained in a moderate yield, i.e. 28% (**Table 4**).

4.3.3 Free Radical Polymerization of Aromatic Sulfonamide Monomers M1-M4

The successfully synthesized sulfonamide monomers M1-M4 were polymerized by FRP to yield sulfonamide-based polymers P1-P4, respectively, which should be subsequently used in functionalization reactions by aza-Michael addition with electron-deficient alkenes as Michael acceptors. Low molar masses were targeted to mimic the chemistry of small organic sulfonamide molecules, allowing for a straightforward analysis. The different electron densities of each monomer required the adaptation and fine-tuning of the polymerization conditions individually. In addition, the radical polymerization of M4 turned out to be challenging presumably due to the nitro group, as nitro compounds have been reported to have an inhibition effect on the radical polymerization of styrene.[223] The polymerizations were in all cases performed with AIBN as thermal radical initiator at elevated temperature (T = 80 °C) in DMF as solvent (**Scheme 53**). Details on the polymerization of the sulfonamide monomers M1-M4 are listed in **Table 5**.

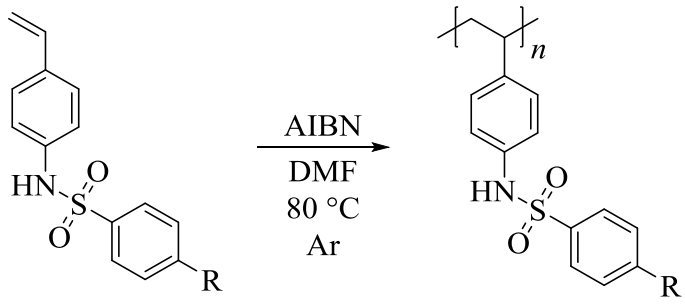

Scheme 53. Preparation of polymers P1-P4 by polymerization of the respective sulfonamide monomers M1-M4.

Table 5. Details on the polymerizations of monomers **M1**-**M4**.

Entry	Monomer	R	Ratio M:AIBN	Polymerization time
1	M1	-H	5:1	6 h
2	M2	$-CH_3$	5:1	4.5 h
3	M3	-F	10:1	9 h
4	M4[a]	$-NO_2$	20:1 to 20:10	33 h

[a] After heating for 24.5 hours with a ratio of M:AIBN of 20:1, 0.50 eq. of AIBN were added and the polymerization was conducted for another 8.5 hours.

The required polymerization times necessary to give similar yields after purification differed significantly among the monomers: electron-donating groups seemed to increase

polymerization rates, whereas electron-withdrawing groups appeared to have a decelerating effect on the polymerization kinetics. However, these observations have not been further investigated by a kinetic study to eventually prove the assumption due to a different focus of this project. Additionally, the polymerization of M4 featuring a nitro group in *para* position led to poor yields only, even after an optimized polymerization procedure, and did not allow a full characterization, not to mention potential functionalization reactions on it. The substrate scope was thus limited to P1-P3 and further optimizations of the synthesis of P4 were discarded. P1-P3 were characterized by NMR and IR spectroscopy, SEC, DSC and TGA. An exemplary ^{1}H NMR spectrum is depicted for P1 (**Figure 47**) to prove the intact nature of the sulfonamide moiety after polymerization, which was in accordance with the TGA measurements (see **Chapter 6.6.3**), exhibiting a high thermal stability up to $T \approx 400$ °C. Prominent signals in the proton NMR spectrum attributed to the intact sulfonamide polymer P1 could be observed at chemical shifts of $\delta = 8.63 - 9.05$ ppm (arising from the N-H functionality) as well as $\delta = 7.62 - 7.88$ ppm, $\delta = 7.17 - 7.61$ ppm, $\delta = 6.74 - 7.15$ ppm, and $\delta = 6.03 - 6.72$ ppm, arising from the aromatic protons with matching integrals. The signals arising from the backbone protons appeared at $\delta = 0.70 - 1.81$ ppm.

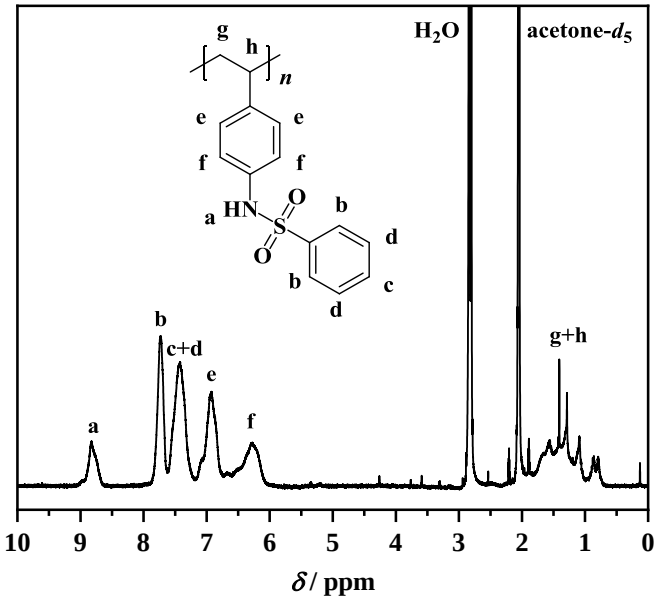

Figure 47. Exemplary ^{1}H NMR spectrum of poly(*N*-(4-vinylphenyl)benzenesulfonamide) (P1); solvent: acetone-d_6.

SEC analysis using THF as eluent (PS calibration) exhibited low molar masses as intended and low dispersities (**Figure 48**). The latter were surprisingly low for polymers obtained by FRP, on the one hand, low molar mass fractions of the polymer could potentially not have precipitated

to a similar extent as the high molar mass fractions. On the other hand, THF as eluent for SEC and potentially also the SEC setup itself might not have been the optimal choice for the characterization of this type of polymers, although the sulfonamide polymers featured full solubility in THF. Thus, SEC analysis using DMAc as eluent of another batch of P1 was performed exhibiting a dispersity value of $Đ$ = 1.61 in comparison to $Đ$ = 1.19 with THF as eluent (**Figure 49**). The dispersity value obtained by SEC with DMAc as eluent matched the character of FRP in contrast to the one resulting from the SEC measurement in THF.

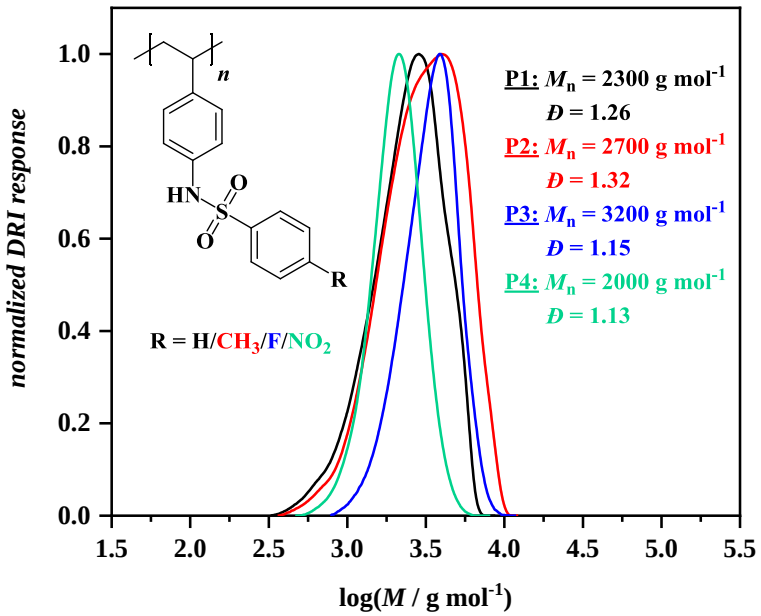

Figure 48. Comparison of size-exclusion chromatograms of P1-P4 using THF as eluent (PS calibration) (black line: P1; red line: P2; blue line: P3; green line: P4).

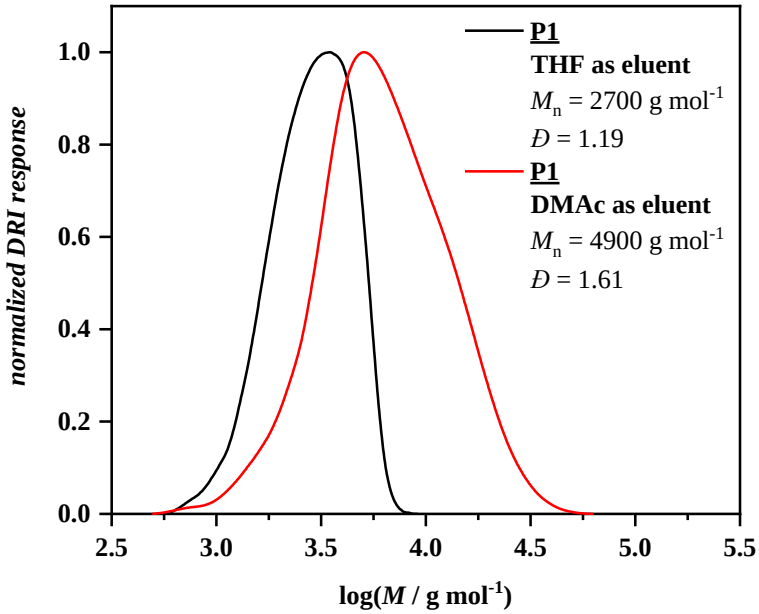

Figure 49. Comparison of SEC results of P1 using THF (black line) and DMAc (red line) as eluent (PS calibration).

The resulting polymers with exception of P4 (which could not be fully characterized due to the low yields after polymerization) exhibited glass transitions in a temperature range of 120 °C ≤ T_g ≤ 125 °C, which was higher than the reported glass transition at T_g ≈ 100 °C for pure polystyrene.[204,205] This observation was presumably caused by the limited free movement of the polymer chains by intermolecular interactions of the secondary amine functionalities and additional π-π stacking of the aromatic sulfonamide protecting groups, both increasing the T_g. Additionally, substituents seemed to increase the glass transition temperature as it is shown in **Table 6**, although the differences were not very pronounced.

Table 6. SEC and DSC results for sulfonamide polymers P1-P4.

Entry	Polymer	R	M_n[a] / g mol^{-1}	$Đ$[a]	T_g[b] / °C
1	P1	-H	2300	1.26	120
2	P2	-CH_3	2700	1.32	125
3	P3	-F	3200	1.15	123
4	P4	-NO_2	2000	1.13	-[c]

[a] Determined by SEC using THF as eluent (PS calibration); [b] determined by DSC; [c] no analysis possible due to low yield.

In addition to the characterization described and depicted above, the pH-responsive switchable water solubility was explored for P1. The sulfonamide monomers based on methacrylamide

featuring the inverted NH-SO_2 bond motif were reported to be water-soluble when pH > pK_a and to become water-insoluble upon acidification to pH < pK_a.[183–186] Thus, a vial was charged with P1 and distilled water. The sulfonamide polymer did not dissolve, but upon addition of aqueous 1 M NaOH solution, it readily dissolved (**Figure 50**). The nature of the sulfonamide moiety allowed for a switchable pH-dependent water solubility as illustrated below (**Scheme 54**).

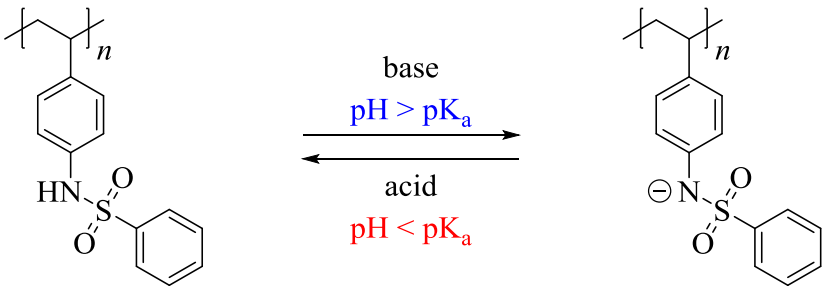

water-insoluble *water-soluble*

Scheme 54. Switchable and reversible pH-dependent water solubility of poly(*N*-(4-vinylphenyl)benzenesulfonamide) (P1).

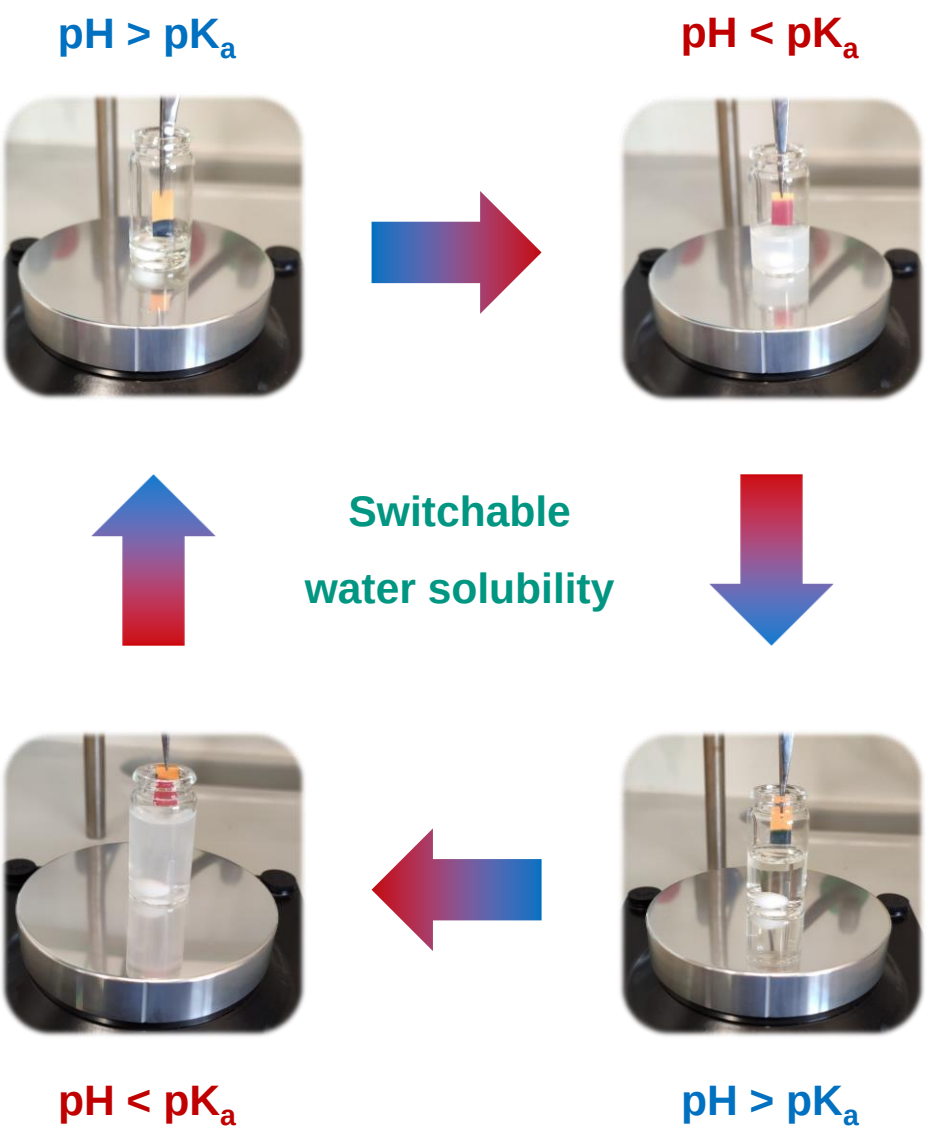

Figure 50. Switchable pH-dependent water solubility of P1, readily dissolving in aqueous medium if pH > pK_a, while being insoluble, when pH < pK_a.

4.3.4 Post-Polymerization Modification of Aromatic Sulfonamide Polymers P1-P3

The secondary amine functionality of the as-prepared polymers P1-P3 was used as handle for PPM by aza-Michael addition[224–226] with electron-deficient alkenes (i.e. acrylate derivatives) as Michael acceptors, resulting in the formation of unprecedented polymeric protected β-amino acid derivatives (**Scheme 55**).

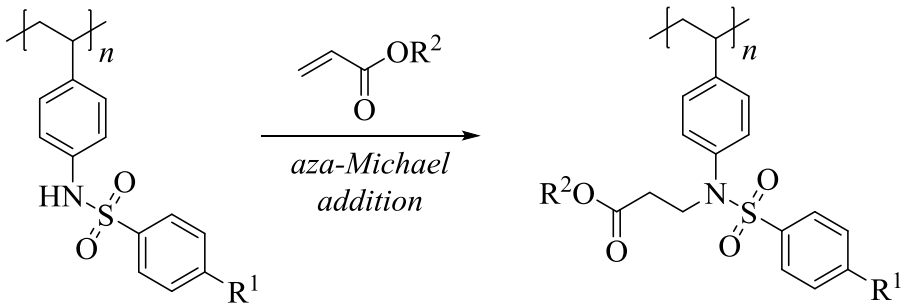

Scheme 55. Straightforward preparation of polymeric protected β-amino acid derivatives by aza-Michael addition of P1-P3 with acrylate derivatives as electron-deficient alkenes.

Acrylate derivatives were chosen as Michael acceptors on the one hand due to their great availability and as the successful aza-Michael addition would result in novel polymeric protected β-amino acid derivatives on the other hand. Interestingly, β-amino acid derivatives attract increasing scientific interest and could potentially lead to new applications when incorporated into synthetic polymers, since they feature antibacterial and antifungal activities among others[227] and are used in the synthesis of β-peptides exhibiting proteolytic stability both *in vitro* and *in vivo*.[228] Butyl acrylate, methyl acrylate, dodecyl acrylate, and PFPA were used as Michael acceptors for the functionalization together with 1,5,7-triazabicyclo[4.4.0]dec-5-ene (TBD) as organic superbase catalyst for the aza-Michael additions.[229] The aza-Michael additions were carried out for four days under an inert argon atmosphere at elevated temperatures (T = 80 °C) in DMF as solvent (**Scheme 56**).

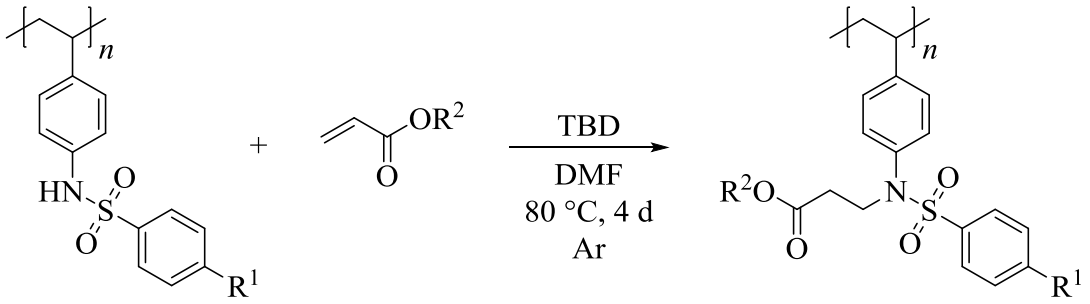

Scheme 56. Aza-Michael addition of the sulfonamide polymers P1-P3 with different acrylate-based Michael acceptors using TBD as catalyst.

The resulting polymers were purified by precipitation steps and subsequent aqueous workup. Diethyl ether was used as precipitation medium in the cases of butyl acrylate, methyl acrylate, and pentafluorophenyl acrylate as electron-deficient alkenes. However, the use of dodecyl acrylate seemed to alter the solubility behavior of the resulting polymer drastically and methanol instead of diethyl ether was thus used for the precipitation. The reaction outcome was judged by NMR and IR spectroscopy as well as SEC and DSC measurements (**Table 7**).

Table 7. Details on the aza-Michael additions of P1-P3 with different acrylates, including the respective SEC and DSC results before and after PPM.

Entry	Polymer used in PPM	Michael acceptor	***before PPM***			***after PPM***		
			M_n[a] / g mol^{-1}	$Đ$[a]	T_g[b] / °C	M_n[a] / g mol^{-1}	$Đ$[a]	T_g[b] / °C
1	P1	Butyl acrylate	2300	1.26	120	3900	1.39	48
2	P1	Dodecycl acrylate	2300	1.47	120	7700	1.34[c]	56
4	P1	PFPA	2700	1.19	120	1600	2.06	-
5	P2	Butyl acrylate	2700	1.32	125	4300	1.42	72
6	P2	Methyl acrylate	2700	1.32	125	3600	1.40	56
7	P3	Butyl acrylate	3200	1.15	123	6400	2.12[d]	86 193

[a] Determined by SEC using THF as eluent (PS calibration); [b] determined by DSC; [c] decrease of dispersity could be explained by altered solubility behavior after reaction, causing problems of purification by precipitation; [d] the functionalization of P3 led to tailing in the size-exclusion chromatogram, which was not observed for the other samples. The obtained product presumably interacted with the SEC setup used for analysis.

SEC analysis exhibited a shift towards higher molar masses in all cases except for the PPM using PFPA as Michael acceptor. In this case, the functionalization results were unclear and presumably decomposition or other side reactions (such as *para* fluoro substitution or nucleophilic attack on the active ester for instance) were taking place. Moreover, the functionalization of P3 led to a drastic increase of the dispersity after the reaction: a tailing in the size-exclusion chromatogram could be observed and the reaction was repeated to exclude operational errors, leading to a similar outcome. The only difference in this case was the fluorine atom as substituent in comparison to P1 and P2. The resulting polymer could have potentially interacted with the SEC setup used for characterization, thus leading to the observed tailing. The comparison of the size-exclusion chromatograms (THF as eluent, PS calibration) before and after PPM is exemplarily depicted for the reaction of P1 with butyl acrylate (**Figure 51**), exhibiting a clear shift of the molar mass distribution with increasing M_n values from M_n = 2300 g mol^{-1} before PPM to a value of M_n = 3700 g mol^{-1} after PPM. The dispersity slightly increased from $Đ$ = 1.26 to $Đ$ = 1.43.

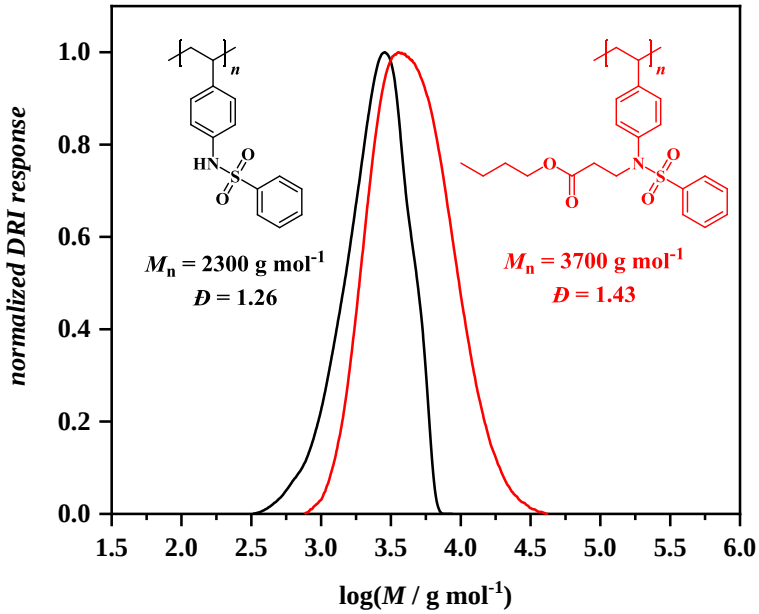

Figure 51. Comparison of size-exclusion chromatograms using THF as eluent (PS calibration) before (black line) and after (red line) PPM by aza-Michael addition of P1 with butyl acrylate.

Furthermore, the glass transition temperatures were dramatically decreased in comparison to the sulfonamide polymers before PPM. The bulky, but flexible substituent tethered to the nitrogen atom after PPM presumably decreased the amount of π-π stacking between the polymer chains and thus resulted in a free movement of the polymer chains at lower temperatures in comparison to the unfunctionalized sulfonamide polymers. In fact, DSC analysis revealed a significant decrease of the T_g = 120 °C before PPM to T_g = 48 °C after aza-Michael addition of P1 with butyl acrylate (**Figure 52**). The reaction of P1 with dodecyl acrylate resulted in a decrease of the T_g as well, but not in the same or even more pronounced extent to the outcome with butyl acrylate as Michael acceptor. Typically, the opposite should be observed: the incorporation of dodecyl acrylate should have decreased the T_g more drastically in comparison to butyl acrylate due to the longer alkyl chain as side group. In this case however, the functionalization only proceeded partially with approximately half of the secondary sulfonamide moieties bearing the dodecyl acrylate motif after PPM as determined by ^{1}H NMR spectroscopy, which could explain this observation.

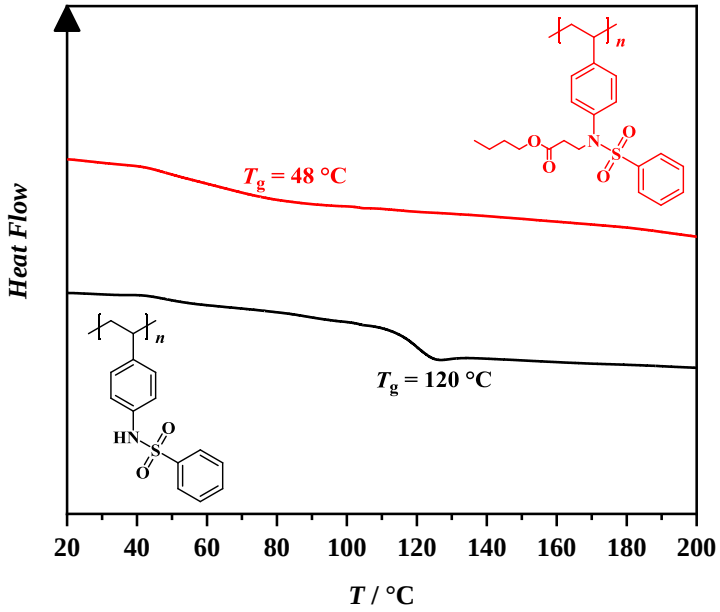

Figure 52. Comparison of DSC results before (black line) and after (red line) PPM by aza-Michael addition of P1 with butyl acrylate.

The comparison of ^{1}H NMR spectra before and after PPM clearly showed the appearance of new signals arising from the incorporation of the ester moieties, depicted in **Figure 53** for the aza-Michael addition of P1 with butyl acrylate. Especially the signals attributed to the attached butyl acrylate moiety, i.e. the CH_2O motif tethered to the carbonyl of the ester (δ = 3.94 – 4.10 ppm), the CH_2 group next to the nitrogen atom (δ = 3.48 – 3.90 ppm), and the CH_2 moiety adjacent to it (δ = 2.36 – 2.48 ppm), were clearly proving the successful aza-Michael addition. The integration of the signals confirmed the quantitative (>99%) formation of the polymeric protected β-amino acid derivative in this case. This was also the case for the aza-Michael addition of P3 with butyl acrylate, however the reaction using P2 as sulfonamide polymer with its methyl substituent in *para* position did not proceed quantitatively (82%) with butyl acrylate. Even using a less bulky acrylate (methyl acrylate) did not result in a full functionalization (66%). This phenomenon might be attributed to the methyl group of P2, being the only difference between the different sulfonamide polymers.

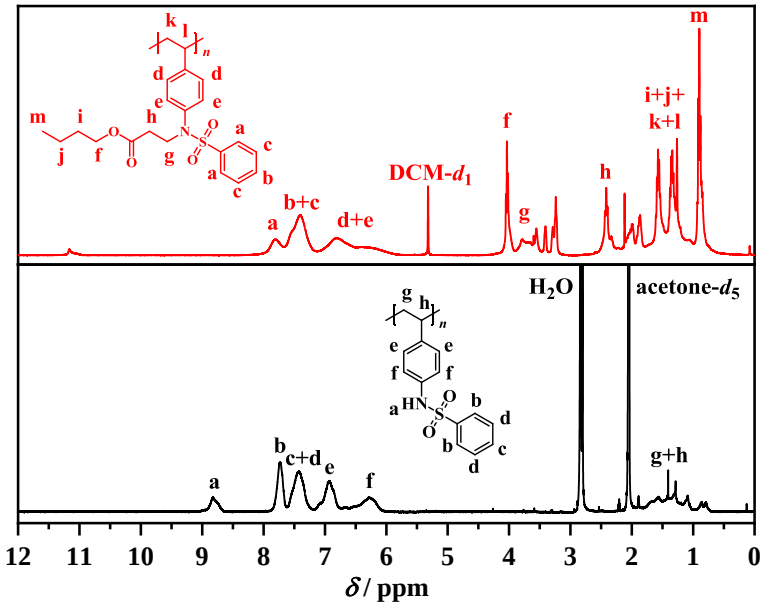

Figure 53. Comparison of ^{1}H NMR spectra before (bottom, black line; solvent: acetone-d_6) and after (top, red line; solvent: DCM-d_2) PPM by aza-Michael addition of P1 with butyl acrylate.

To prove the chemical shifts of the aza-Michael adducts in ^{1}H NMR spectroscopy, a small organic molecule sulfonamide, i.e. *N*-phenylbenzenesulfonamide, was prepared and used in an aza-Michael addition with butyl acrylate in a similar fashion to the polymers P1-P3 (**Scheme 57**).

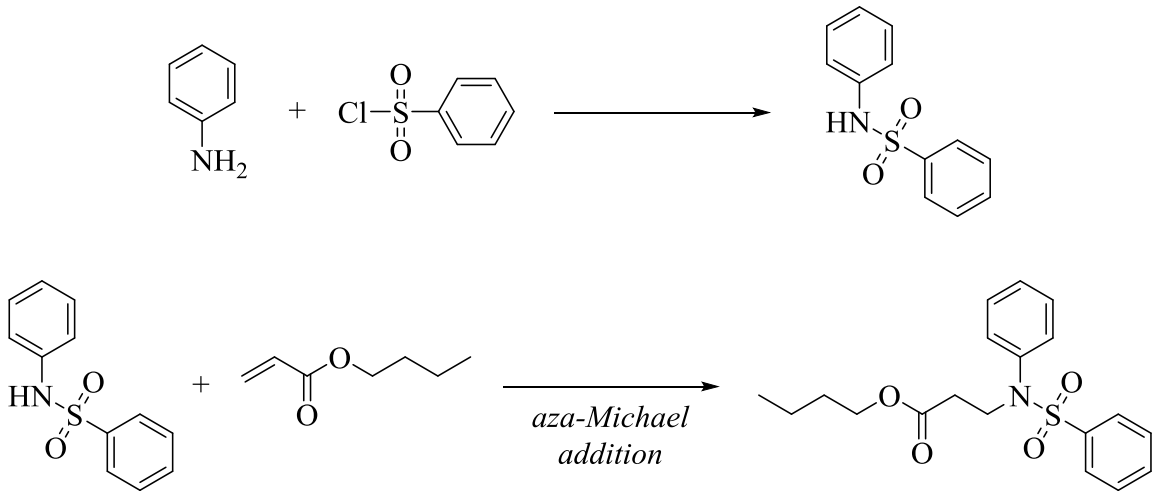

Scheme 57. Synthesis of *N*-phenylbenzenesulfonamide starting from aniline with subsequent aza-Michael addition using butyl acrylate as Michael acceptor.

Eventually, the ^{1}H NMR spectrum of the isolated product confirmed the assignment of the newly arising signals after aza-Michael addition of P1 with butyl acrylate. It showed prominent resonances of the aza-Michael adduct butyl 3-(*N*-phenylphenylsulfonamido)propanoate

(**Figure 54**), i.e. at chemical shifts of δ = 3.98 ppm (CH_2O motif adjacent to the carbonyl of the ester), δ = 3.84 ppm (CH_2 motif tethered to the nitrogen atom), δ = 2.51 ppm (CH_2 motif next to the carbonyl group), and at δ = 1.49 – 1.58 ppm, δ = 1.29 – 1.38 ppm, and δ = 0.91 ppm (remaining protons of the incorporated alkyl chain).

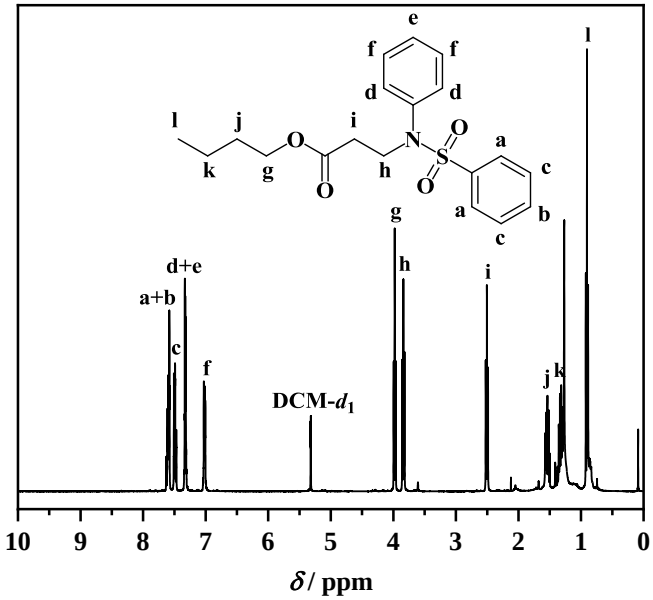

Figure 54. ^{1}H NMR spectrum of the model compound, i.e. butyl 3-(*N*-phenylphenylsulfonamido)propanoate obtained after aza-Michael addition of *N*-phenylbenzenesulfonamide with butyl acrylate; solvent: DCM-d_2.

Additionally, the comparison of the IR spectra (**Figure 55**) before and after aza-Michael addition of *N*-phenylbenzenesulfonamide with butyl acrylate as model compound exhibited the disappearance of the N-H vibration at a wavenumber of $\tilde{\nu}$ = 3203 cm^{-1}, while the appearance of the carbonyl vibration at $\tilde{\nu}$ = 1731 cm^{-1} after aza-Michael addition was observed.

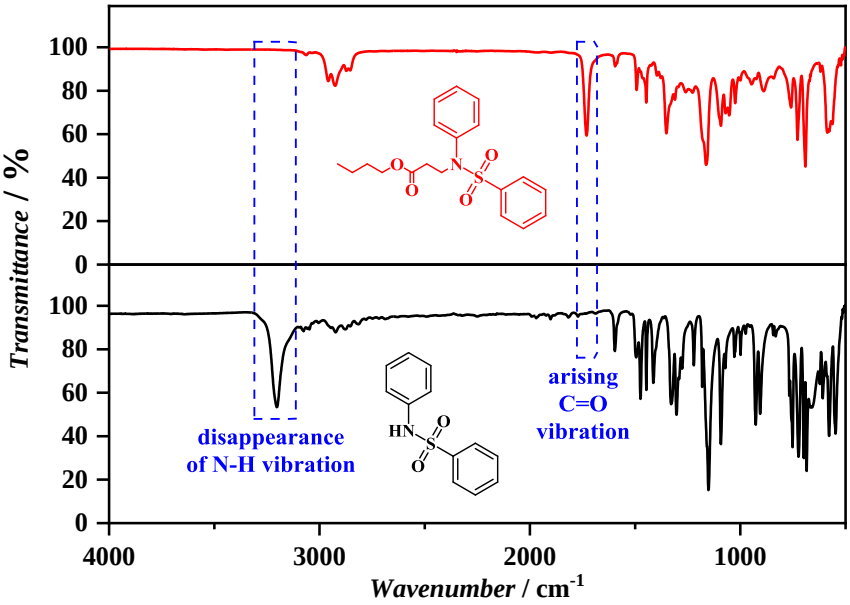

Figure 55. Comparison of the ATR-FT-IR spectra before (bottom, black line) and after (top, red line) the aza-Michael addition of *N*-phenylbenzenesulfonamide with butyl acrylate.

Based on these results, the comparison of the IR spectra before and after aza-Michael addition of sulfonamide polymers P1-P3 showed the appearance of a new carbonyl vibration accompanied by the decrease of the N-H vibrations from the precursor sulfonamide polymer. In the case of the exemplarily depicted comparison of the IR spectra before and after the reaction of P1 with butyl acrylate (**Figure 56**), the N-H vibration at a wavenumber of $\tilde{\nu}$ = 3256 cm^{-1} disappeared almost completely after PPM. Additionally, as expected, a new signal appeared after PPM at a wavenumber of $\tilde{\nu}$ = 1728 cm^{-1}, which was characteristic for the presence of a carbonyl motif in an ester and could thus be attributed to the successful reaction of P1 with butyl acrylate.

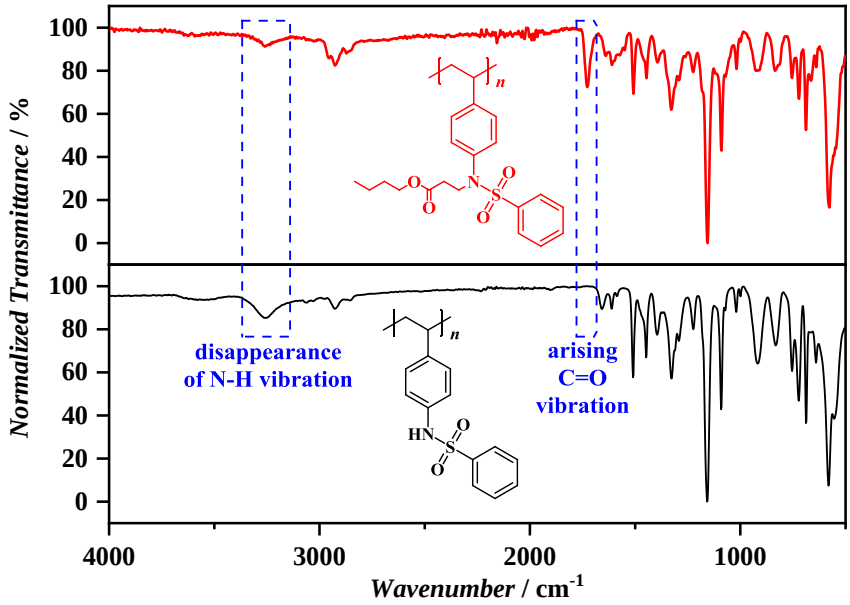

Figure 56. Comparison of ATR-FT-IR spectra before (bottom, black line) and after (top, red line) PPM by aza-Michael addition of P1 with butyl acrylate.

4.3.5 Conclusion and Outlook

In this chapter, the synthesis of a novel class of styrene-derived sulfonamide-based polymers from their respective monomers and its application in PPM by aza-Michael addition with different acrylates as Michael acceptors was described. A set of aromatic sulfonamide monomers with varying electron densities was synthesized in a one-step reaction from commercially available 4-vinylaniline and the respective aromatic sulfonyl chlorides. The different electron densities seemed to influence the polymerization kinetics of the FRP in DMF using AIBN as thermal radical initiator. At this point, the nitro-derivative of the monomers was rather challenging to be polymerized and was thus excluded from the subsequent PPM by aza-Michael addition. Butyl acrylate was used as Michael acceptor for the three different sulfonamide polymers P1-P3 and resulted in a clear shift in the size-exclusion chromatograms towards higher molar masses in all cases. The respective signals from the formation of polymeric protected β-amino acid derivatives appeared in the proton NMR spectra and the successful reactions were also proven by IR spectroscopy. The former showed a quantitative conversion for P1 (substituent: -H) and P3 (substituent: -F), while the functionalization of P2 (substituent: $-CH_3$) did not proceed quantitatively. IR spectroscopy exhibited the decrease of N-H vibrations and the appearance of a C=O vibration arising from the incorporation of the acrylate moiety. In all cases, the T_g could be drastically decreased from values around $T_g = 120 - 125$ °C for the unfunctionalized sulfonamide polymers P1-P3, caused by the incorporation of a bulky, but flexible moiety in the side group, which presumably reduced the amount of π-π stacking. Additionally, other acrylate compounds were employed, i.e. methyl acrylate in the case of P2 to promote higher degrees of functionalization, but the decreased steric hindrance of the acrylate moiety still did not result in a quantitative conversion. Furthermore, dodecyl acrylate as well as pentafluorophenyl acrylate were employed, PFPA however was presumably too reactive or fragile for the conditions employed and did thus not qualify as suitable Michael acceptor, while the functionalization of P1 with dodecyl acrylate did not proceed in a quantitative fashion. Nonetheless, these results demonstrated a straightforward preparation of unknown polymeric protected β-amino acid derivatives. Furthermore, it was shown that the novel class of sulfonamide-based polymers exhibited pH-responsive behavior with regards to the water solubility, which can be switched from a water-soluble polymer ($pH > pK_a$) to a water-insoluble one when $pH < pK_a$. Although the original idea of an electrochemical deprotection and release of functional groups at “the push of a button” could not be realized, a novel and interesting class of new sulfonamide polymers featuring smart materials behavior was successfully prepared in a straightforward fashion and

subsequently employed in aza-Michael additions towards unprecedented polymeric protected β-amino acid derivatives with a broad substrate range.

5 Conclusion and Outlook

The use of synthetic electrochemistry is a trending topic nowadays, not only due to times of raw material shortage and a growing focus on environmentally friendly alternatives to conventional synthesis methods, but also with regard to its unique features and the numerous parameters, such as operation mode (galvanostatic versus potentiostatic), choice of current/potential and electrode materials as well as duration of the electrolysis, that can be fine-tuned, thus allowing for an immense degree of control over the reaction. Indeed, especially the field of organic chemistry is experiencing a revival or "renaissance"[7,8] of synthetic electrochemical techniques. Consequently, synthetic electrochemical means should be rapidly implemented in the field of polymer chemistry to benefit from their advantages and to have a substantial impact on both scientific and industrial applications. This thesis aimed to combine both research areas in a pioneering fashion, as respective examples have only been scarcely precedented in literature.

The electrochemical cathodic reduction of an aromatic, commercially available diazonium salt was used as radical initiator in a RAFT polymerization and was published only recently (2017).[19] Based hereon, a fluorine-labelled derivative of the diazonium salt was synthesized and employed as radical initiator upon electrochemical reduction for the polymerization of reactive and *inter alia* fluorine-labelled monomers. Noteworthy, this polymerization was performed with a simple undivided cell setup using standard and abundant electrode materials (sacrificial zinc anode and graphite cathode). PFPA, DFPA, and GMA were employed as monomers and the electrochemically-initiated polymerizations allowed for the straightforward synthesis of the respective polymers. The reactive nature was on the one hand proven by NMR as well as IR spectroscopy. On the other hand, PPMs were carried out with a fluorine-labelled amine, successfully resulting in the respective amides and *β*-amino alcohol. Consequently, the intact reactive character after polymerization using electrochemical means as well as the compatibility of the latter with even electrochemically-sensitive monomers could be demonstrated.

Moreover, polymerization and polymer modification by electrochemical means were intended to be combined in an electrochemically-mediated nickel-catalyzed approach for ω-functionalization using aryl bromides. Different monomers were employed and tested, accordingly styrene-derived monomers as well as acrylonitrile turned out to be suitable for this approach. However, acrylate- and methacrylate-based monomers resulted in hardly soluble material. Different aryl bromides were used with varying electron densities, which affected the

polymerization drastically. Additionally, a copolymer consisting of 4-bromostyrene and 4-methylstyrene repeating units was synthesized comprising polymeric aryl bromides as potential ω-group, the latter was used as comonomer to quantify the 4-bromostyrene content by ^{1}H NMR spectroscopy. 4-*tert*-Butylstyrene was employed first as monomer due to the characteristic shift of the *tert*-butyl group in ^{1}H NMR spectroscopy. The respective spectrum showed the formation of poly(4-*tert*-butylstyrene) as well as signals arising from the aryl bromide copolymer and SEC analysis revealed a unimodal distribution, which was clearly shifted towards higher molar masses in comparison to the SEC trace of the original aryl bromide copolymer. DSC analysis exhibited two distinct glass transitions, one from poly(4-*tert*-butylstyrene) and one arising from the aryl bromide copolymer motif. Additionally, acrylonitrile was tested as monomer using the same aryl bromide copolymer: in this case, however, the proton NMR spectroscopy hardly showed any aromatic signals after the reaction, but the SEC trace was again shifted towards higher molar masses. The comparison of IR spectra showed arising vibrations from the nitrile group, but not in a very pronounced fashion. Further research is thus necessary to fully understand the reaction and especially the determination of the degree of functionalization requires additional investigations, but the results suggested a straightforward and sophisticated one-pot polymerization with an *in-situ* modification of the growing styrene-derived macromolecular chains, enabling even the electrochemical synthesis of graft copolymers.

Lastly, the electrochemical PPM, i.e. the electrochemical deprotection reaction of sulfonamides, was investigated. In literature, mostly more complex electrochemical setups as well as mercury electrodes were employed for this kind of reactions and it turned out that the simple setup used in this work did not meet the demands for a successful reaction. The synthesized monomers varying in electron densities were thus used in polymerizations to deliver a novel class of sulfonamide polymers exhibiting smart materials behavior, i.e. a stimuli-responsive, switchable water solubility. The obtained polymers were subsequently used in aza-Michael additions with different acrylates as Michael acceptors, resulting in the successful preparation of unprecedented polymeric protected β-amino acid derivatives, paving the way for the preparation of novel and interesting materials in a straightforward fashion.

In conclusion, the implementation of electrochemical means to the field of polymer chemistry remains a challenging topic, which requires further investigations. The possibility to electrochemically-initiate polymerizations of rather electrochemically-sensitive monomers could be shown without affecting their reactive nature, but for PPM, quantitative electrochemical reactions are required due to the lacking possibility of separation of unreacted

functional groups from reacted ones in a single macromolecule. Nonetheless, the almost invaluable impact of both PPM and synthetic electrochemistry on the field of polymer chemistry could be demonstrated, especially with regards to the preparation of functional polymers. This implementation of electrochemical methods in the field of polymer chemistry could have a drastic impact on both polymer synthesis and functionalization and could become a trending topic in the near future, analogous to the "renaissance" of synthetic electrochemical methods in organic chemistry. Thus, the projects presented and discussed herein could be classified as pioneering works, which aim for an approximation of the fields of (synthetic) electrochemistry and polymer chemistry for fruitful collaborations and a vivid exchange of knowledge and skills to mutually tackle both todays as well as future challenges.

6 Experimental Section

This chapter gives in-depth details about the instrumentation used for characterization, the materials employed in the frame of the present thesis, as well as experimental procedures and analytical results.

6.1 Instrumentation

6.1.1 NMR spectroscopy

^{1}H NMR, ^{13}C NMR, and ^{19}F NMR spectra were recorded on a Bruker Ascend III 400 MHz spectrometer at a frequency of ν = 400 MHz, ν = 101 MHz, and ν = 377 MHz, respectively. All samples were dissolved in deuterated solvents, chemical shifts are reported relative to the residual solvent signals.

6.1.2 Size-Exclusion Chromatography

6.1.2.1 Size-Exclusion Chromatography (SEC) using THF as Eluent - I

SEC measurements with THF as eluent were performed on an Agilent 1200 Series System, comprising an autosampler, a differential Refractive Index (RI) detector, three PLgel 5 µm Mixed C columns (300 × 7.5 mm) and a PLgel 3 µm Mixed E column (300 × 7.5 mm). The measurements were performed at a temperature of T = 35 °C and a flow rate of 1.0 mL min^{-1}. Samples were measured at a concentration of 2 mg mL^{-1} and filtered prior to measurement. All number-average molar mass M_n and dispersity $Đ$ values were extrapolated from a range of linear poly(methyl methacrylate) standards between 800 and 2.2 × 10^{6} g mol^{-1} and linear polystyrene standards between 370 and 2.52 × 10^{6} g mol^{-1}.

6.1.2.2 Size-Exclusion Chromatography (SEC) using THF as Eluent - II

SEC measurements with THF as eluent were performed on a PL-SEC 50 Plus Integrated System, comprising an autosampler, a differential Refractive Index (RI) detector, three PLgel 5 µm Mixed C columns (300 × 7.5 mm) and a PLgel 3 µm Mixed E column (300 × 7.5 mm). The measurements were performed at a temperature of T = 35 °C and a flow rate of 1.0 mL min^{-1}. Samples were measured at a concentration of 2 mg mL^{-1} and filtered prior to

measurement. All number-average molar mass M_n and dispersity $Đ$ values were extrapolated from a range of linear polystyrene standards between 474 and 2.52 × 10^6 g mol^{-1}.

6.1.2.3 Size-Exclusion Chromatography (SEC) using DMAc as Eluent

SEC measurements with DMAc as eluent were performed on an Agilent 1200 Series System, comprising an autosampler, a differential Refractive Index (RI) detector and two PLgel 5 µm Mixed C columns (300 × 7.5 mm). The measurements were performed at a temperature of T = 50 °C and a flow rate of 0.5 mL min^{-1}. Samples were measured at a concentration of 2 mg mL^{-1} and filtered prior to measurement. All number-average molar mass M_n and dispersity $Đ$ values were extrapolated from a range of linear poly(methyl methacrylate) standards between 800 and 2.2 × 10^6 g mol^{-1} and linear polystyrene standards between 474 and 2.52 × 10^6 g mol^{-1}.

6.1.3 Attenuated Total Reflection (ATR) Fourier-Transform (FT) Infrared (IR) Spectroscopy (ATR-FT-IR)

ATR-FT-IR spectra were recorded on a Bruker Vertex 80 from 500 - 4000 cm^{-1} at 25 °C and on a Bruker Alpha II ATR-IR from 500-4000 cm^{-1} at 25 °C.

6.1.4 Differential Scanning Calorimetry (DSC)

Differential scanning calorimetry measurements were conducted on a DSC Q200 (TA Instruments) in a range from -60 °C or 0 °C to 250 °C with a scan rate of 10 K min^{-1} for all measurements.

6.1.5 Thermogravimetric Analysis (TGA)

Thermogravimetic analysis measurements were performed on a TA Instruments TGA 5500 with a heating rate of 10 °C min^{-1} in a temperature range from room temperature to 1000 °C.

6.1.6 Electrospray Ionization Mass Spectrometry (ESI-MS)

Electrospray ionization mass spectra were recorded on a Thermo Fisher Q-Exactive Orbitrap mass spectrometer. Analytes were dissolved in a 3:2 mixture of THF/MeOH (0.03 mg mL^{-1}) enriched with 100 μmol sodium trifluoroacetate and filtered prior to injection.

6.2 Electrochemical Setup and Equipment

6.2.1 Cyclic Voltammetry (CV)

Cyclic voltammograms were recorded on an IKA ElectraSyn 2.0 potentiostat comprising a glassy carbon disk working electrode, a platinum plated counter electrode, and an Ag/AgCl (3 M $KCl_{aq.}$) reference electrode. The sulfonamide samples (5 mM) were dissolved in a solution of tetrabutylammonium hexafluorophosphate (Bu_4NPF_6) (0.1 M) solution of acetonitrile and the solutions were deoxygenated by argon purging prior to measurement.

6.2.2 Electrochemical Reactions

A commercially available potentiostat, i.e. IKA ElectraSyn 2.0, was used in combination with the respective IKA vials (5 mL + 10 mL) equipped with a septum on the outlet and an argon-filled balloon on top (**Figure 57**). Commercially available electrodes designed for the use with the IKA ElectraSyn 2.0 were purchased from IKA, a sacrificial zinc anode and a graphite cathode were used as electrode materials. After completion of the reaction, the electrodes were detached from the vial cap, rinsed with THF and acetone, and wiped with an acetone-soaked wipe. Thereafter, the surfaces of the electrodes were carefully scratched off with an APOLLO Ever-Sharp Blade and eventually wiped with an acetone-soaked wipe again. When necessary, the graphite electrode was placed in vial filled with acetone and placed in an ultrasonic bath. The solvent was changed three times and the electrode was again wiped with an acetone-soaked wipe.

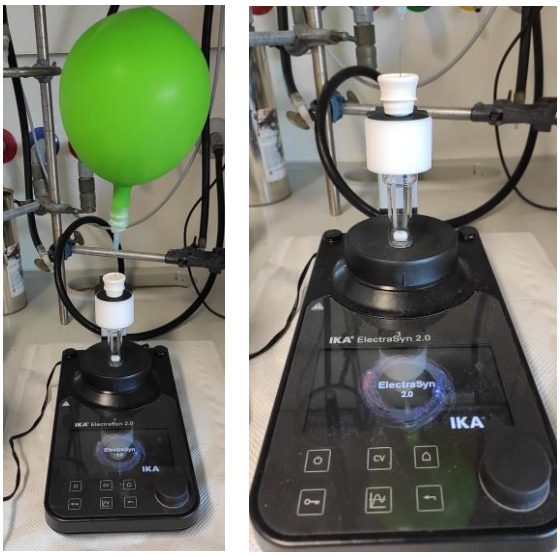

Figure 57. Electrochemical setup employed in the frame of the present thesis: IKA ElectraSyn 2.0 potentiostat with IKA vials (5 mL + 10 mL, in this picture: 5 mL vial) equipped with working and counter electrode, a septum on the outlet and an argon-filled balloon on top.

6.3 Materials

Acrylonitrile (Sigma Aldrich, ≥99%), 4-bromostyrene (TCI, >95%), butyl acrylate (TCI, >99%), dodecyl acrylate (Sigma Aldrich, 90%), 4-fluorostyrene (Acros Organics, 97%), glycidyl methacrylate (Sigma Aldrich, 97%), methyl acrylate (TCI, >99%), 4-methylstyrene (TCI, >96%), pentafluorostyrene (Alfa Aesar, 98%), styrene (Alfa Aesar, 99%), and 4-*tert*-butylstyrene (Alfa Aesar, 94%) were passed through basic aluminum oxide prior to use. Acetone (AnalaR NORMAPUR), acetonitrile (Acros Organics, 99.9%, anhydrous), acryloyl chloride (Alfa Aesar, 96%), 3-aminopropanol (Alfa Aesar, 99%), aniline (Sigma Aldrich, ≥99%), 2,2′-azobis(2-methylpropionitrile) (AIBN) (Sigma Aldrich, 98%), benzenesulfonyl chloride (Sigma Aldrich, 99%), bromobenzene (Sigma Aldrich, ≥99.5%), 4-bromobenzotrifluoride (TCI, >98%), 4-bromotoluene (abcr, 98%), cyclohexane (CH) (AnalaR NORMAPUR), dichloromethane (DCM) (VWR, AnalaR NORMAPUR), dichloromethane (DCM) (Acros Organics, 99.8%, anhydrous), diethyl ether (Fisher, ≥99%), 2,6-difluorophenol (Sigma Aldrich, 98%), *N*,*N*-dimethylformamide (DMF) (Acros Organics, 99.8%, anhydrous), 4,4′-di-*tert*-butyl-2,2′-dipyridyl (bbbpy) (Sigma Aldrich, 98%), ethyl acetate (EA) (AnalaR NORMAPUR), 4-fluoroaniline (Sigma Aldrich, 99%), 4-fluorobenzenesulfonyl chloride (Acros Organics, 98%), hydrochloric acid (Roth, 37%), magnesium sulfate (Roth, ≥99%), methacryloyl chloride (Acros Organics, 95%), methanol (AnalaR NORMAPUR), 4-methylbenzenesulfonyl chloride (Sigma Aldrich, ≥98%), naphthalene (Alfa Aesar, 99+%), nickel(II) bromide ethylene glycol dimethyl ether complex ($NiBr_2$·dme) (abcr, 97%), 4-nitrobenzenesulfonyl chloride (Sigma Aldrich, 97%), pentafluorophenol (abcr, 99%), petroleum ether (PE) (AnalaR NORMAPUR), sodium hydroxide (Merck, ≥99%), sodium nitrite (Honeywell, ≥99%), sodium thiosulfate (Roth, ≥99%), tetrabutylammonium hexafluorophosphate (Bu_4NPF_6) (Sigma Aldrich, 98%), tetrabutylammonium hydrogensulfate (Bu_4NHSO_4) (Sigma Aldrich, 97%), tetrabutylammonium tetrafluoroborate (Bu_4NBF_4) (Sigma Aldrich, 99%), tetraethylammonium bromide (Et_4NBr) (Acros Organics, 98%), tetrafluoroboric acid (Sigma Aldrich, 48 wt%), tetrahydrofuran (THF) (Acros Organics, 99.5%, anhydrous), tetrahydrofuran (THF) (AnalaR NORMAPUR), toluene (Acros Organics, 99.85%, anhydrous), 1,5,7-triazabicyclo[4.4.0]dec-5-ene (TBD) (Sigma Aldrich, 98%), triethylamine (Acros Organics, 99%), 2,2,2-trifluoroethylamine (TCI, >97%), and 4-vinylaniline (TCI, >95%) were used as received.

6.4 Procedures for the Electrochemically-Initiated Polymerization of Reactive Monomers *via* 4-Fluorobenzenediazonium Salts

6.4.1 Synthesis of 4-Fluorobenzenediazonium Tetrafluoroborate

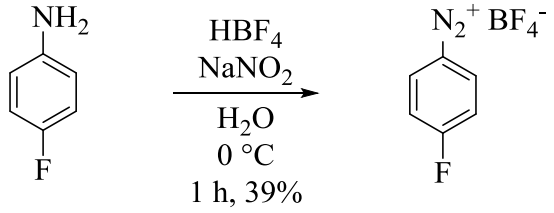

4-Fluoroaniline (566 mg, 5.00 mmol, 1.00 eq.) was dissolved in distilled water (2.5 mL) and 48 wt% solution of tetrafluoroboric acid (HBF_4) in water (1.7 mL). Afterwards, the solution was cooled to 0 °C and sodium nitrite (345 mg, 5.00 mmol, 1.00 eq.) in distilled water (1.0 mL) was added dropwise. The reaction was stirred at 0 °C for 1 hour and the mixture was filtered. The solid obtained thereafter was dissolved in a minimum amount of acetone. Diethyl ether was added until precipitation of the diazonium salt. Subsequently, the precipitate was washed thoroughly with diethyl ether and dried under vacuum giving a colorless solid (0.41 g, 0.19 mmol, 39%).

^{1}H NMR (acetone-d_6): δ / ppm = 8.98 – 9.04 (m, 2H, H_a), 7.87 – 7.94 (m, 2H, H_b).

^{13}C NMR (acetone-d_6): δ / ppm = 170.43, 138.06, 120.59, 112.21.

^{19}F NMR (acetone-d_6): δ / ppm = -86.66 (tq, J = 8.3, 4.2 Hz, 1F, F_a), -151.09 (d, J = 20.3 Hz, 4F, F_b).

ATR-FT-IR: $\tilde{\nu}$ / cm^{-1} = 3116, 2360, 2295 (N≡N), 1579, 1484, 1432, 1330, 1305 (Ar-N), 1260, 1250, 1167, 1118, 1013, 850, 836, 807, 769, 685, 668.

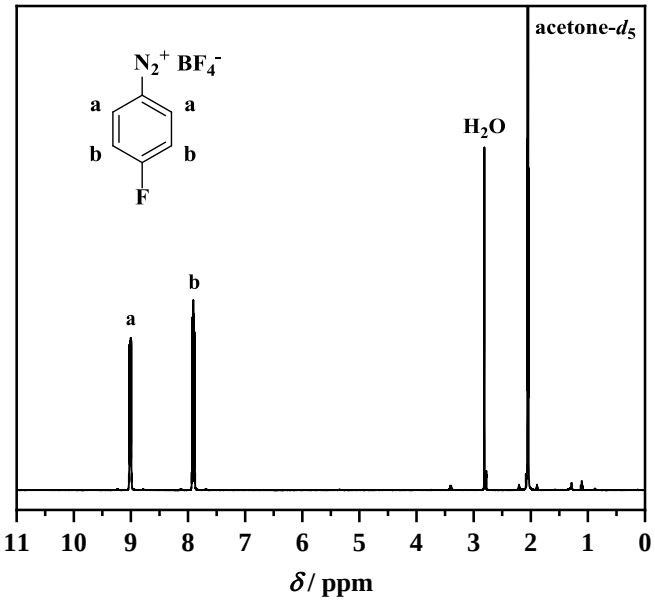

Figure 58. ^{1}H NMR spectrum of 4-fluorobenzenediazonium tetrafluoroborate; solvent: acetone-d_6.

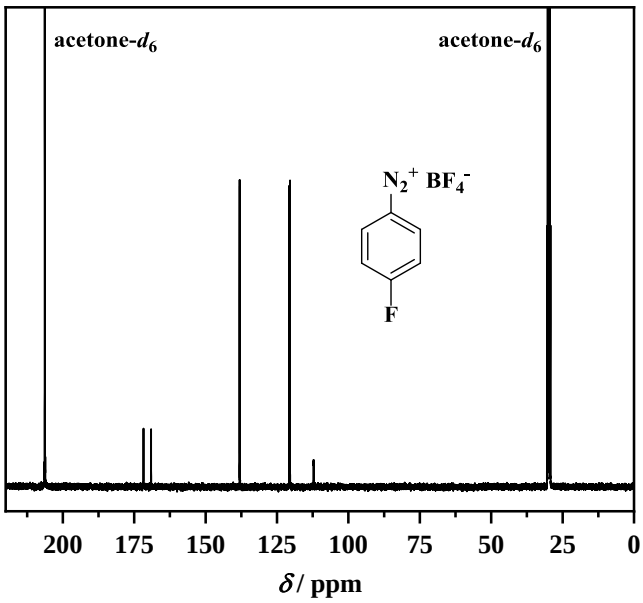

Figure 59. ^{13}C NMR spectrum of 4-fluorobenzenediazonium tetrafluoroborate; solvent: acetone-d_6.

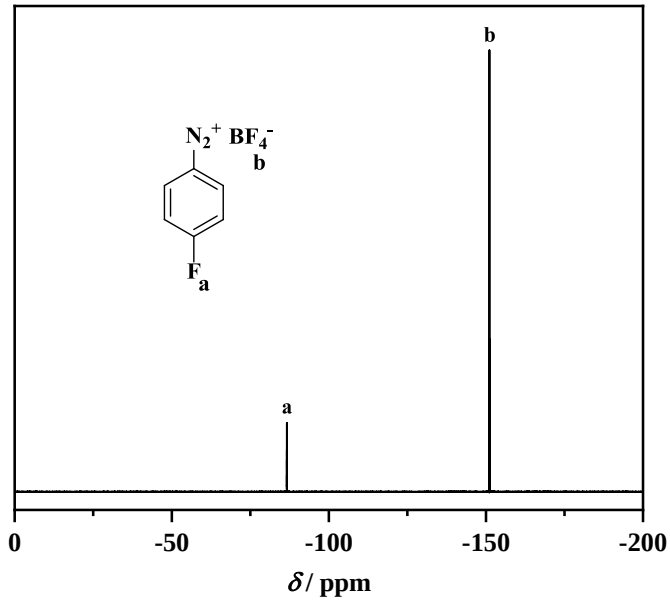

Figure 60. ^{19}F NMR spectrum of 4-fluorobenzenediazonium tetrafluoroborate; solvent: acetone-d_6.

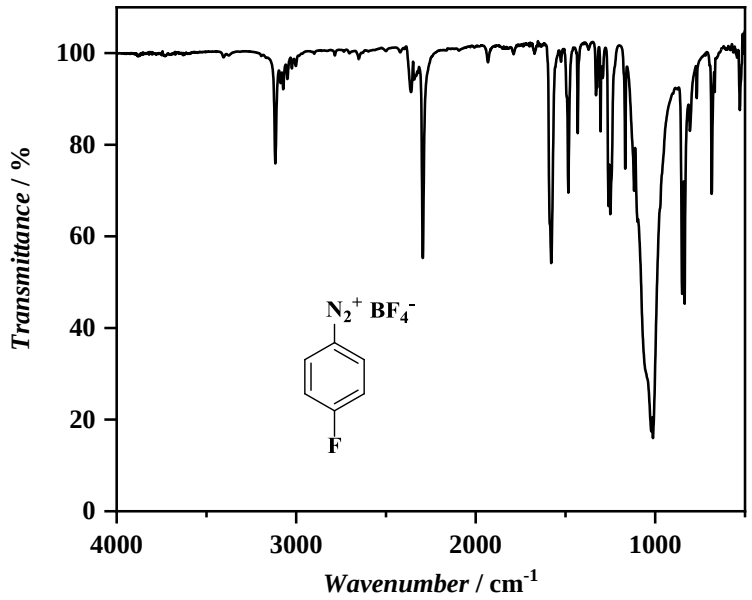

Figure 61. ATR-FT-IR spectrum of 4-fluorobenzenediazonium tetrafluoroborate.

6.4.2 PFPA as Reactive Monomer

6.4.2.1 Synthesis of PFPA

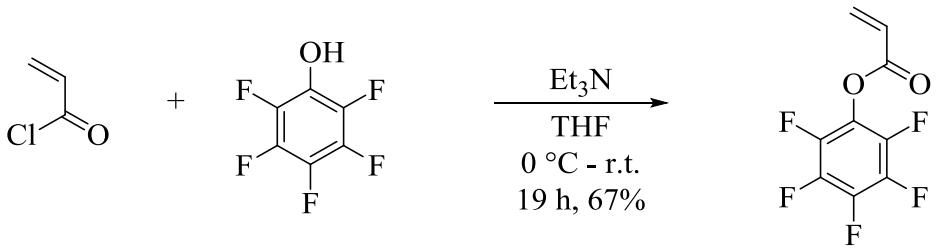

Pentafluorophenol (6.00 g, 32.6 mmol, 1.00 eq.) was dissolved in anhydrous THF (40 mL). The solution was cooled to 0 °C and triethylamine (5.45 mL, 3.96 g, 39.1 mmol, 1.20 eq.) was added. A solution of acryloyl chloride (3.18 mL, 3.54 g, 39.1 mmol, 1.20 eq.) in anhydrous THF (10 mL) was added slowly and the mixture was stirred at 0 °C for one hour and at room temperature for 18 hours. Afterwards, the solvent was removed under reduced pressure and diethyl ether (75 mL) was added. The organic phase was washed with water (3 × 75 mL) and with brine (1 × 75 mL). Subsequently, the organic phase was dried over magnesium sulfate and the solvent was removed under reduced pressure. Finally, the crude product was purified by column chromatography using PE as eluent giving a colorless liquid (5.20 g, 21.9 mmol, 67%).

R_f (PE) = 0.31

^{1}H NMR ($CDCl_3$): δ / ppm = 6.72 (dd, J = 17.3, 0.9 Hz, 1H, H_a), 6.37 (dd, J = 17.3, 10.5 Hz, 1H, H_b), 6.18 (dd, J = 10.5, 1.0 Hz, 1H, H_a).
^{13}C NMR ($CDCl_3$): δ / ppm = 161.83, 142.64, 140.99, 140.14, 139.31, 138.44, 136.81, 135.63, 125.49, 124.94 – 125.38.
^{19}F NMR ($CDCl_3$): δ / ppm = -152.21 – -152.65 (m, 2F, F_a), -157.93 (t, J = 21.8 Hz, 1F, F_b), -162.24 – -162.162.42 (m, 2F, F_c).
ATR-FT-IR: $\tilde{\nu}$ / cm^{-1} = 1771 (C=O), 1634 (C=C), 1516 (C=C), 1472, 1406, 1292, 1218, 1112, 1070, 1030, 994, 870, 796.

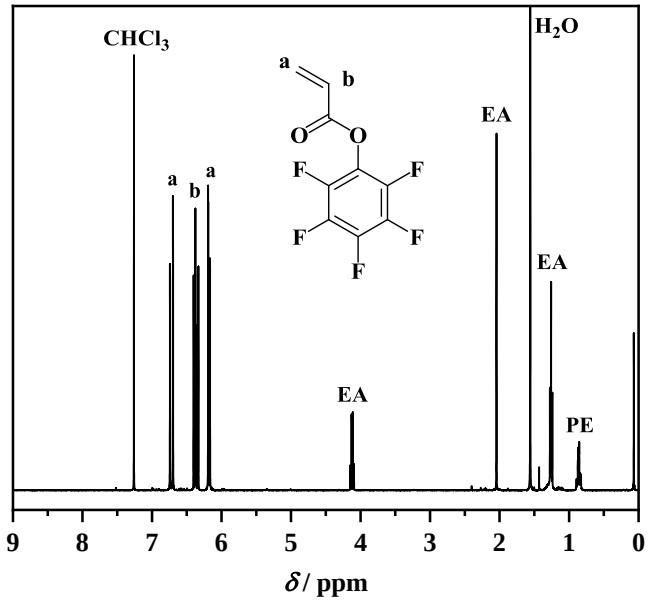

Figure 62. ^{1}H NMR spectrum of PFPA; solvent: $CDCl_3$.

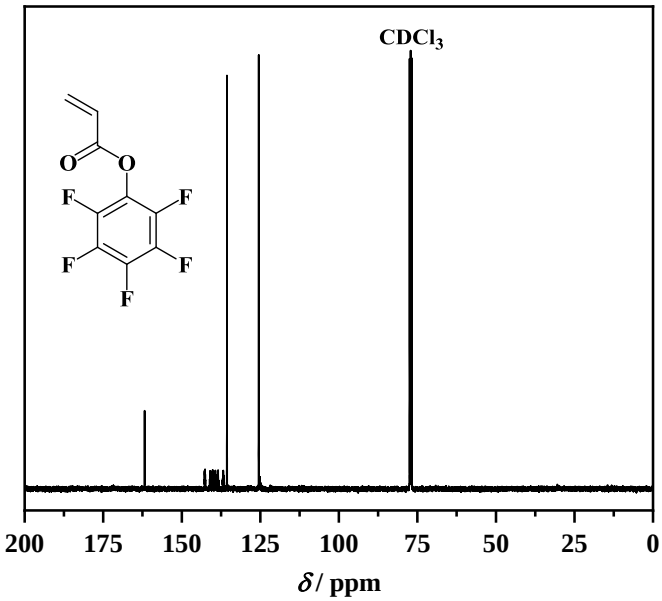

Figure 63. ^{13}C NMR spectrum of PFPA; solvent: $CDCl_3$.

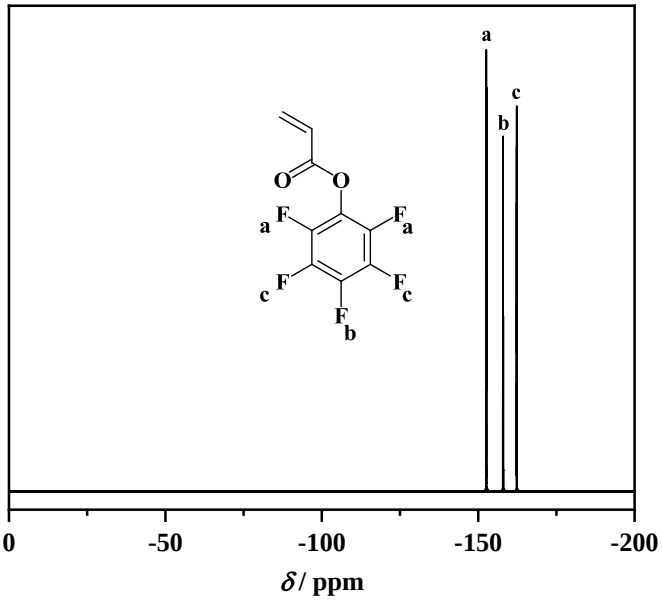

Figure 64. ^{19}F NMR spectrum of PFPA; solvent: $CDCl_3$.

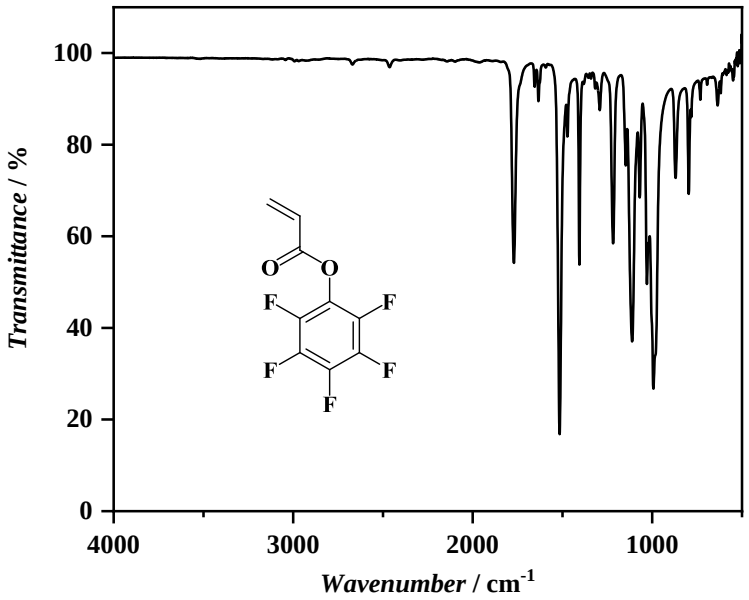

Figure 65. ATR-FT-IR spectrum of PFPA.

6.4.2.2 Electrochemically-Initiated Polymerization of PFPA

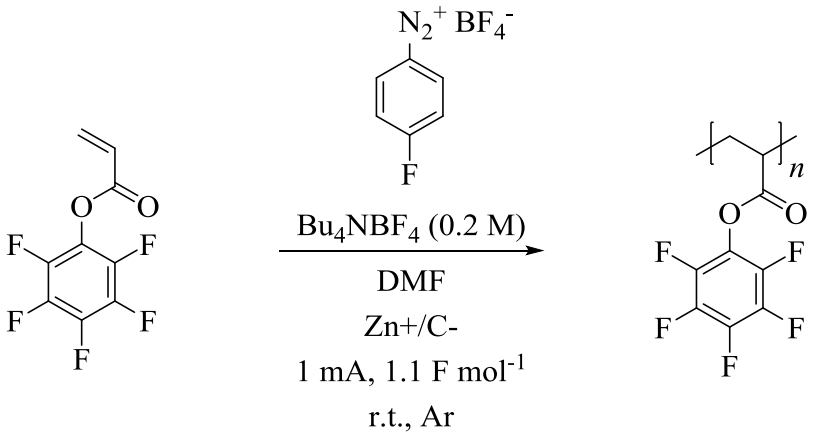

A dry ElectraSyn vial (5 mL) was charged with PFPA (see **Table 8** for equivalents), Bu_4NBF_4 (0.132 g, 0.400 mmol, 0.2 M), 4-fluorobenzenediazonium tetrafluoroborate (0.025 g, 0.120 mmol, 1.00 eq.), and anhydrous DMF (2 mL). The vial was closed with the respective IKA ElectraSyn cap bearing a sacrificial zinc anode and a graphite cathode and the solution was deoxygenated by argon purging for 15 minutes. A constant current of 1 mA was applied until 1.1 F mol^{-1} passed through the system. The electrodes were rinsed with THF and acetone. Afterwards, the mixture was precipitated in cold methanol, the solids obtained by centrifugation were dissolved in acetone and filtered (to remove graphite from the mixture) prior to a second precipitation in cold methanol. Finally, the solids were obtained by centrifugation and dried under vacuum giving a yellowish solid.

^{1}H NMR (acetone-d_6): δ / ppm = 7.28 – 7.39 (2H, $H_{initiator}$), 7.02 – 7.12 (2H, $H_{initiator}$), 3.11 – 3.41 (1H, H_a), 2.10 – 2.68 (2H, H_b).

^{19}F NMR (acetone-d_6): δ / ppm = -117.42 – -117.60 (1F, $F_{initiator}$), -153.68 – -154.71 (2F, F_a), -159.40 – -159.88 (1F, F_b), -164.30 – -165.04 (2F, F_c).

ATR-FT-IR: $\tilde{\nu}$ / cm^{-1} = 1782 (C=O), 1515 (C=C), 1472, 1451, 1227, 1078, 989, 856, 624.

Table 8. Details and results of the electrochemically-initiated polymerization of PFPA (1 mA, 1.1 F mol^{-1}) as reactive monomer.

Entry	Eq.	M_n[a] g mol^{-1}	M_n[b] g mol^{-1}	M_n[c] g mol^{-1}	$Đ$[c]	M_n[d] g mol^{-1}	$Đ$[d]
1[g]	40.00	33240	40180	41800[e]	2.30[e]	30300[e]	2.48[e]
				37000[f]	2.28[f]	34300[f]	2.29[f]
2	10.00	22630	35030	19200[e]	1.83[e]	13900[e]	2.03[e]
				17400[f]	1.76[f]	16500[f]	1.83[f]
3	5.00	14170	24480	13600[e]	1.61[e]	9900[e]	1.82[e]
				12500[f]	1.53[f]	12000[f]	1.65[f]
4[h]	5.00	14290	22500	13200[e]	1.59[e]	9500[e]	1.72[e]
				12100[f]	1.52[f]	11500[f]	1.57[f]

[a] Determined by ^{1}H NMR spectroscopy; [b] determined by ^{19}F NMR spectroscopy; [c] determined by SEC using THF as eluent; [d] determined by SEC using DMAc as eluent; [e] PMMA calibration; [f] PS calibration; [g] monomer concentration too high, resulting in a viscous mixture and the formation of hardly soluble material between the electrodes; [h] 2 mA instead of 1 mA.

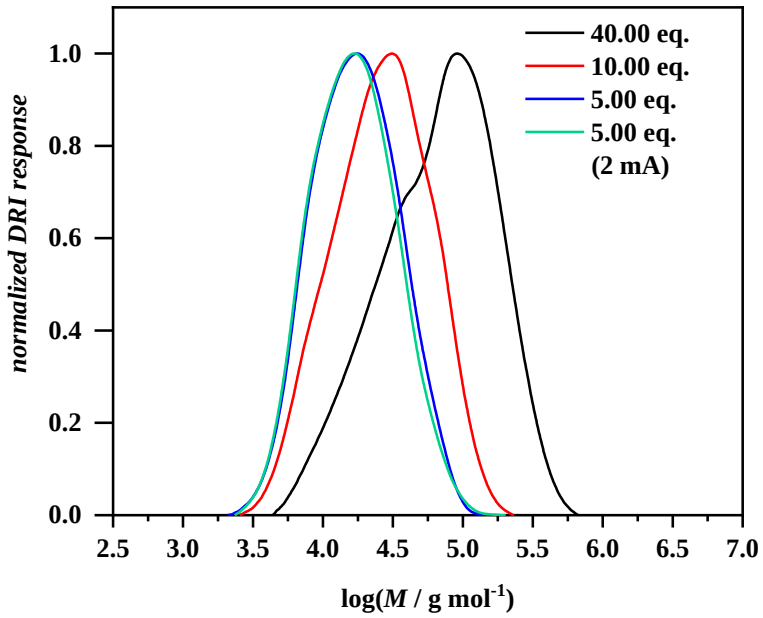

Figure 66. Comparison of SEC traces using THF as eluent (PMMA calibration) of the polymers obtained by the electrochemically-initiated polymerization of PFPA.

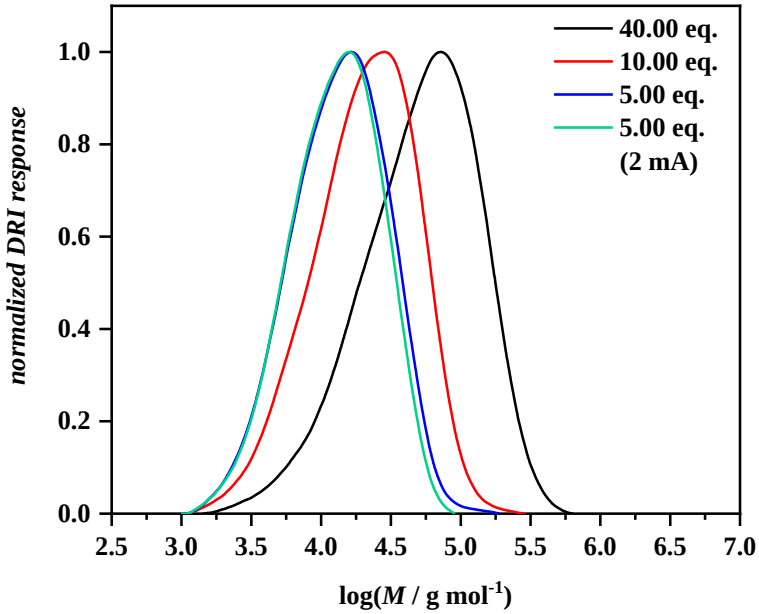

Figure 67. Comparison of SEC traces using DMAc as eluent (PMMA calibration) of the polymers obtained by the electrochemically-initiated polymerization of PFPA.

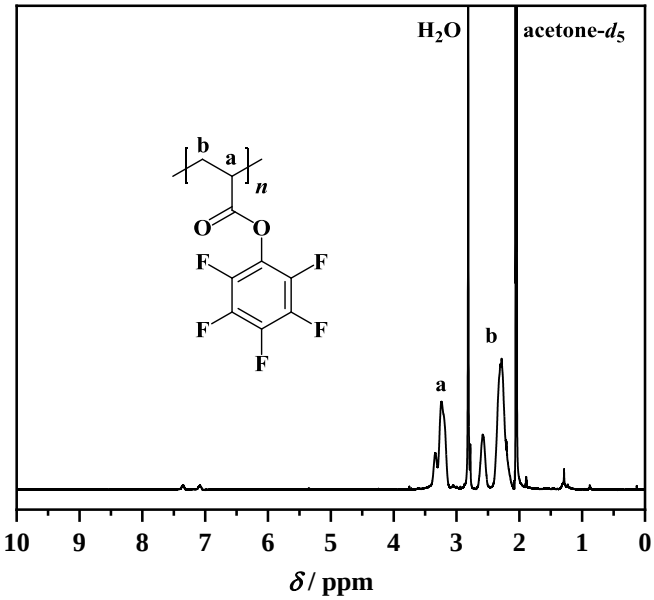

Figure 68. Exemplary ^{1}H NMR spectrum of PPFPA obtained by the electrochemically-initiated polymerization of PFPA (in this case: 10.00 eq. with respect to the initiator); solvent: acetone-d_6.

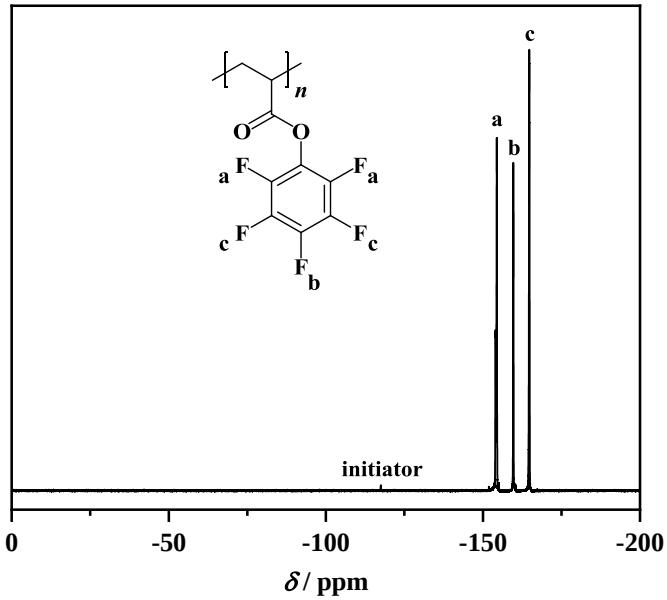

Figure 69. Exemplary ^{19}F NMR spectrum of PPFPA obtained by the electrochemically-initiated polymerization of PFPA (in this case: 10.00 eq. with respect to the initiator); solvent: acetone-d_6.

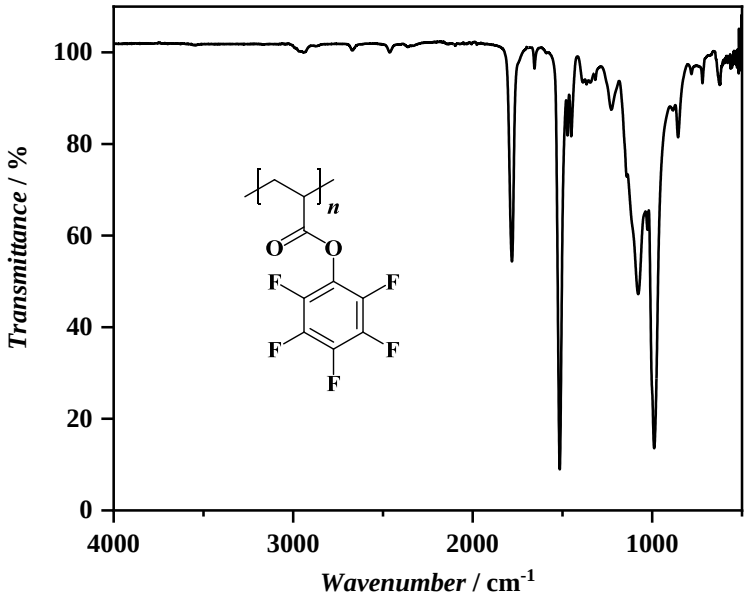

Figure 70. Exemplary ATR-FT-IR spectrum of PPFPA obtained by the electrochemically-initiated polymerization of PFPA (in this case: 10.00 eq. with respect to the initiator).

6.4.2.3 Post-Polymerization Modification (PPM) of PPFPA

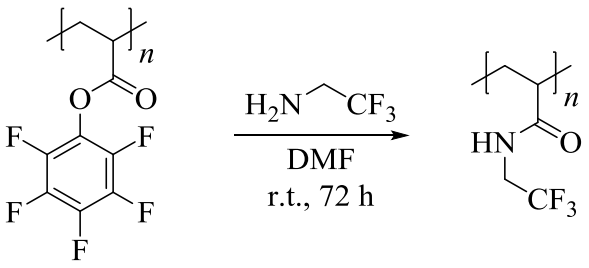

PPFPA (0.040 g, 0.168 mmol of repeating units, 1.00 eq.) was dissolved in anhydrous DMF (1 mL) and 2,2,2-trifluoroethylamine (0.33 mL, 0.416 g, 4.20 mmol, 25.0 eq.) was subsequently added. The solution was stirred at room temperature for 72 hours and the solvent was removed under reduced pressure. Afterwards, the residue was dissolved in acetone and precipitated in PE. The solids obtained by centrifugation were dissolved in acetone and precipitated a second time in PE. Finally, the solids were obtained by centrifugation and dried under vacuum.

^{1}H NMR (acetone-d_6): δ / ppm = 7.53 – 8.06 (1H, H_a), 7.12 – 7.24 (2H, $H_{initiator}$), 6.92 – 7.03 (2H, $H_{initiator}$), 3.67 – 4.26 (2H, H_b), 2.15 – 2.66 (1H, H_c), 1.37 – 1.98 (2H, H_d).
^{19}F NMR (acetone-d_6): δ / ppm = -69.70 – -70.10 (3F, F_{imide}), -72.30 – -72.98 (3F, F_{amide}), -118.63 – -119.00 (1F, $F_{initiator}$).
ATR-FT-IR: $\tilde{\nu}$ / cm^{-1} = 3306 (N-H), 1662 (C=O), 1525, 1396, 1268, 1149, 981, 833, 669.

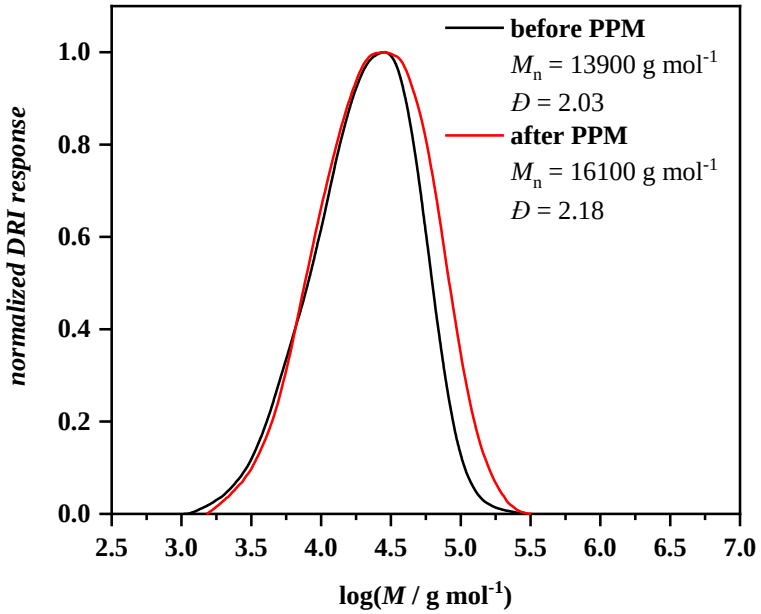

Figure 71. Comparison of SEC traces using DMAc as eluent (PMMA calibration) of PPFPA before (black line) and after PPM (red line).

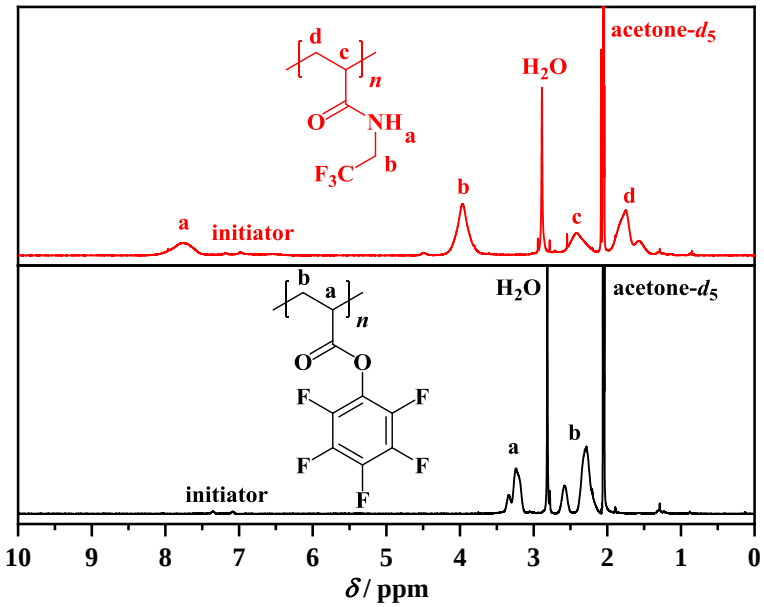

Figure 72. ^{1}H NMR spectroscopical comparison of PPFPA before (bottom, black line) and after PPM (top, red line); solvent: acetone-d_6.

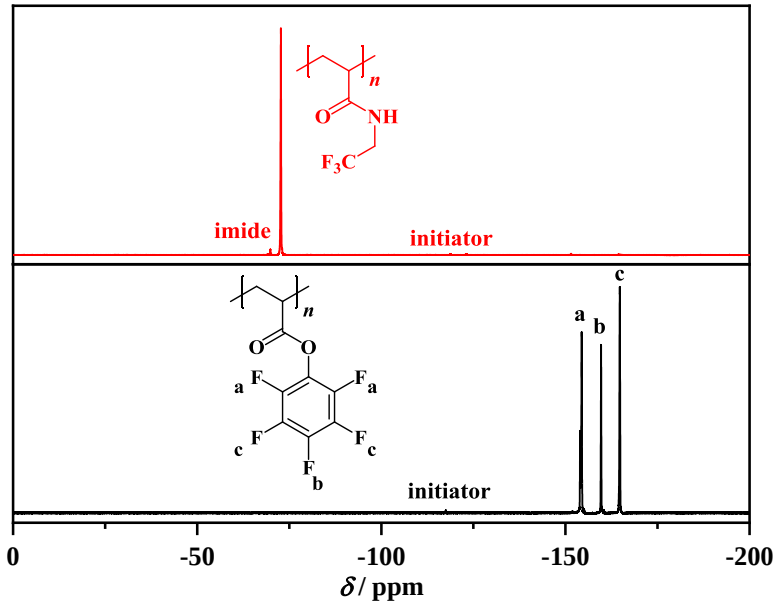

Figure 73. ^{19}F NMR spectroscopical comparison of PPFPA before (bottom, black line) and after PPM (top, red line); solvent: acetone-d_6.

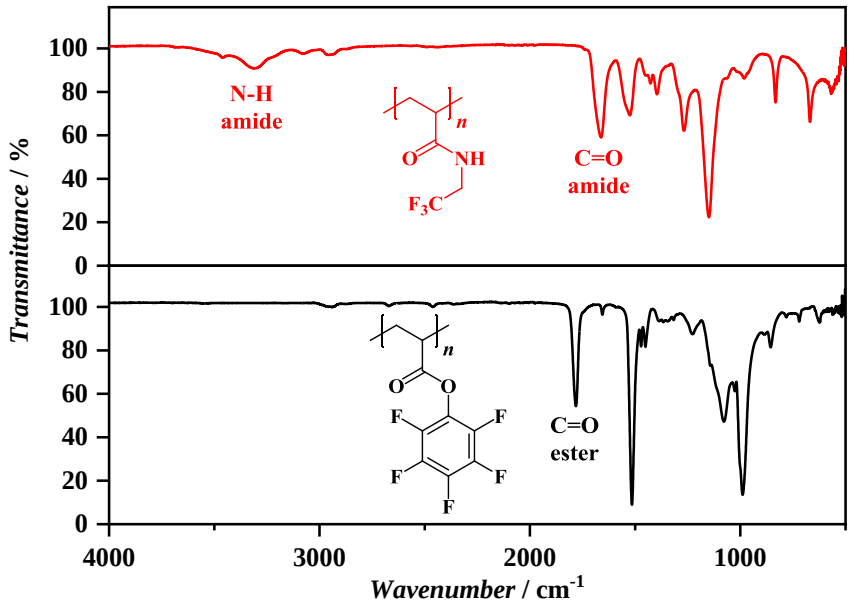

Figure 74. ATR-FT-IR spectroscopical comparison of PPFPA before (bottom, black line) and after PPM (top, red line).

Prior to this PPM procedure, experiments with the addition of triethylamine as auxiliary base were conducted, resulting in the formation of imide functionalities in considerable amounts:

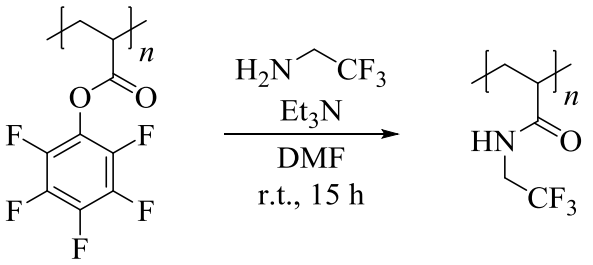

PPFPA (0.050 g, 0.210 mmol of repeating units, 1.00 eq.) was dissolved in anhydrous DMF (1 mL) and triethylamine (0.09 mL, 0.064 g, 0.630 mmol, 3.00 eq.) and 2,2,2-trifluoroethylamine (0.05 mL, 0.062 g, 0.630 mmol, 3.00 eq.) were added. The solution was stirred at room temperature for 15 hours and the solvent subsequently removed under reduced pressure. Afterwards, the residue was dissolved in acetone and precipitated in PE. The solids obtained by centrifugation were dissolved in acetone and precipitated a second time in PE. Finally, the solids were obtained by centrifugation and dried under vacuum.

^{19}F NMR (acetone-d_6): δ / ppm = -68.87 – -70.50 (3F, F_{imide}), -71.51 – -73.40 (3F, F_{amide}), -118.47 – -118.89 (1F, $F_{initiator}$).

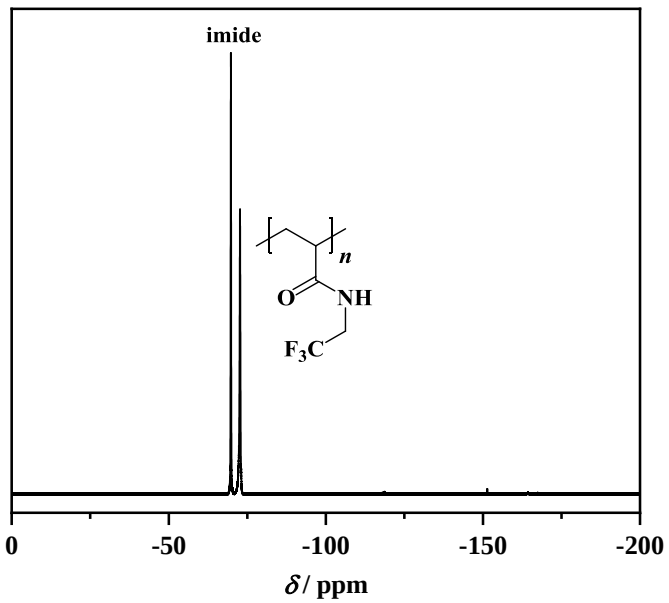

Figure 75. ^{19}F NMR spectrum of the product obtained by PPM with additional use of triethylamine as base; solvent: acetone-d_6.

6.4.3 DFPA as Reactive Monomer

6.4.3.1 Synthesis of DFPA

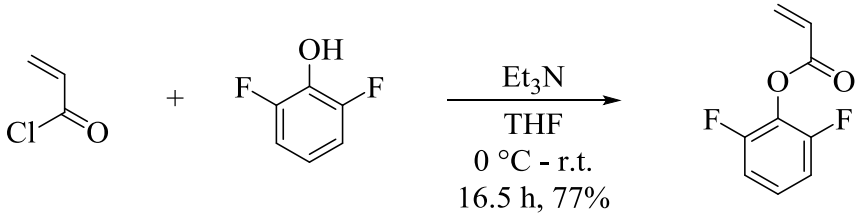

2,6-Difluorophenol (2.00 g, 15.4 mmol, 1.00 eq.) was dissolved in anhydrous THF (30 mL). The solution was cooled to 0 °C and triethylamine (2.57 mL, 1.87 g, 18.5 mmol, 1.20 eq.) was added. A solution of acryloyl chloride (1.50 mL, 1.67 g, 18.5 mmol, 1.20 eq.) in anhydrous THF (10 mL) was added slowly and the mixture was stirred at 0 °C for one hour and at room temperature for 15.5 hours. The solvent was removed under reduced pressure and diethyl ether (50 mL) was added. Afterwards, the organic phase was washed with water (3 × 50 mL) and with brine (1 × 50 mL). Subsequently, the organic phase was dried over magnesium sulfate and the solvent was removed under reduced pressure. Finally, the crude product was purified by column chromatography using a 20:1 mixture of cyclohexane (CH) / ethyl acetate (EA) as eluent giving a yellowish liquid (2.19 g, 11.88 mmol, 77%).

R_f (CH / EA 20:1) = 0.39

^{1}H NMR (acetone-d_6): δ / ppm = 7.34 – 7.43 (m, 1H, H_a), 7.15 – 7.23 (m, 2H, H_b), 6.68 (dd, J = 17.3, 1.2 Hz, 1H, H_c), 6.48 (dd, J = 17.3, 10.4 Hz, 1H, H_d), 6.24 (dd, J = 10.4, 1.2 Hz, 1H, H_c).

^{13}C NMR ($CDCl_3$): δ / ppm = 162.52, 155.35, 134.12, 127.13, 126.43, 126.28, 112.09.

^{19}F NMR (acetone-d_6): δ / ppm = -128.34 – -128.47 (m, 2F).

ATR-FT-IR: $\tilde{\nu}$ / cm^{-1} = 1755 (C=O), 1611, 1479, 1405, 1294, 1246, 1202, 1127, 1069, 1012, 981, 888, 775, 735, 697.

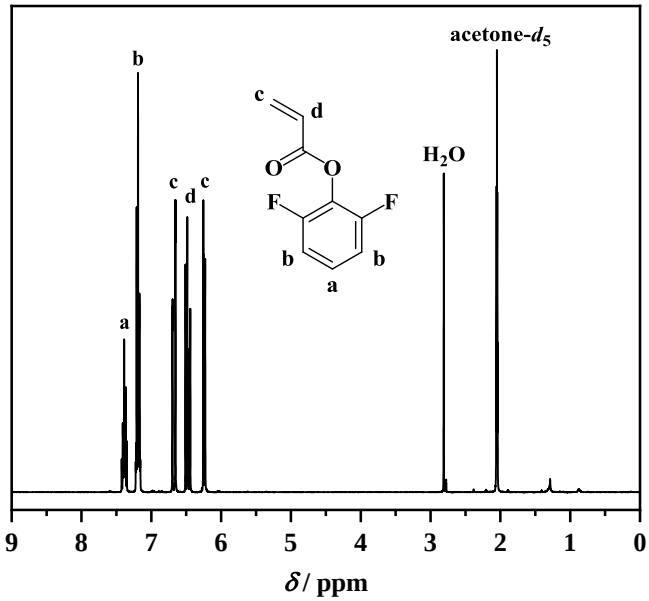

Figure 76. ^{1}H NMR spectrum of DFPA; solvent: acetone-d_6.

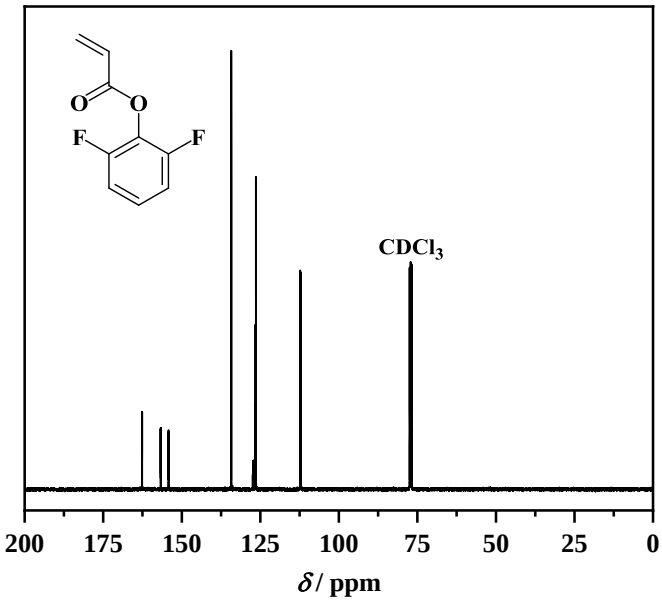

Figure 77. ^{13}C NMR spectrum of DFPA; solvent: $CDCl_3$.

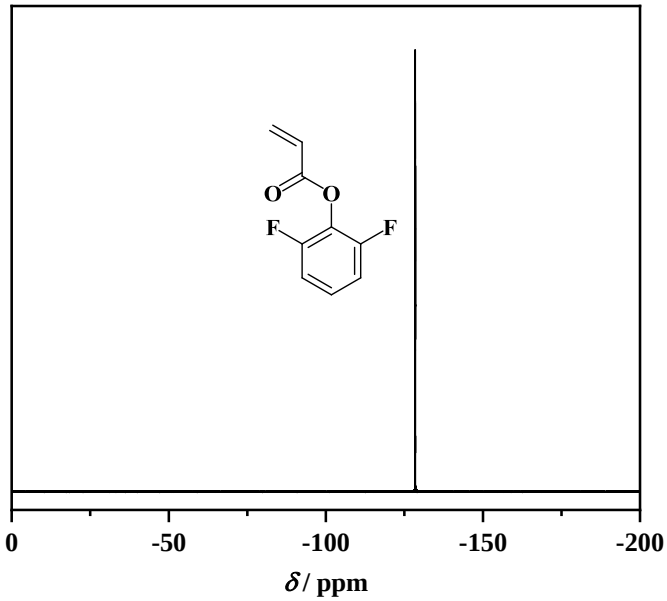

Figure 78. ^{19}F NMR spectrum of DFPA; solvent: acetone-d_6.

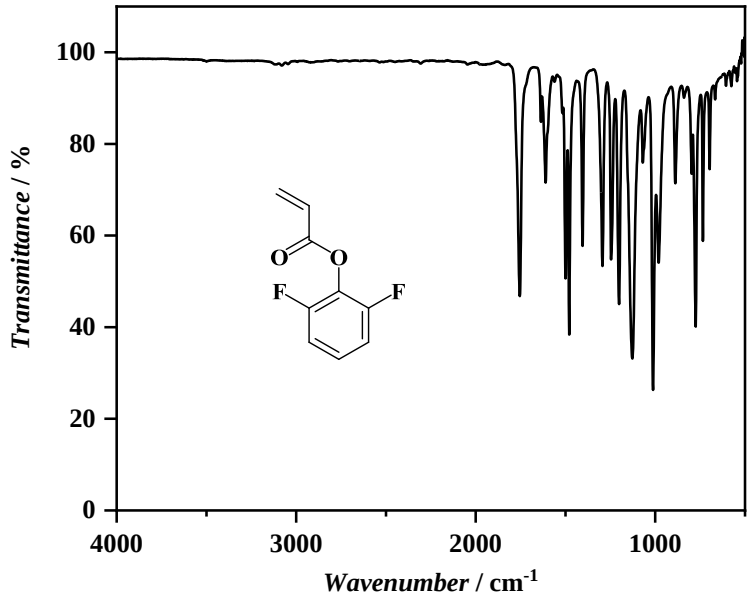

Figure 79. ATR-FT- IR spectrum of DFPA.

6.4.3.2 Electrochemically-Initiated Polymerization of DFPA

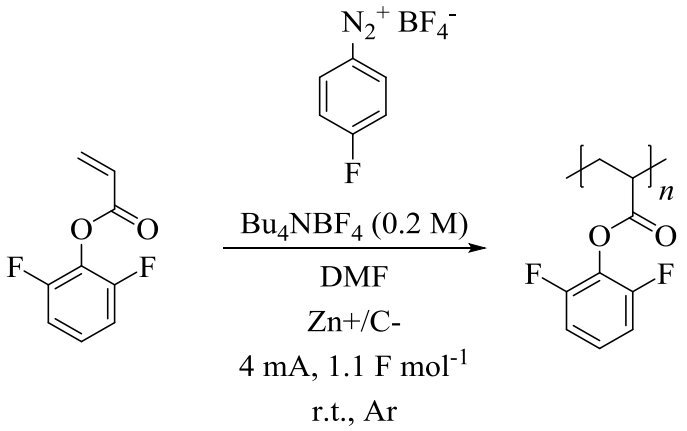

A dry ElectraSyn vial (5 mL) was charged with DFPA (see **Table 9** for equivalents), Bu_4NBF_4 (0.132 g, 0.400 mmol, 0.2 M), 4-fluorobenzenediazonium tetrafluoroborate (0.025 g, 0.120 mmol, 1.00 eq.), and anhydrous DMF (2 mL). The vial was closed with the respective IKA ElectraSyn cap bearing a sacrificial zinc anode and a graphite cathode and the solution was deoxygenated by argon purging for 15 minutes. A constant current of 4 mA was applied until 1.1 F mol^{-1} passed through the system. The electrodes were rinsed with THF and acetone. Afterwards, the mixture was precipitated in cold methanol, the solids obtained by centrifugation were dissolved in acetone and filtered (to remove graphite from the mixture) prior to a second precipitation in cold methanol. Finally, the solids were obtained by centrifugation and dried under vacuum giving a yellowish solid.

^{1}H NMR (acetone-d_6): δ / ppm = 7.15 – 7.38 (1H, H_a), 6.87 – 7.13 (2H, H_b), 3.22 – 3.42 (1H, H_c), 2.16 – 2.65 (2H, H_d).

^{19}F NMR (acetone-d_6): δ / ppm = -117.66 – -117.86 (1F, $F_{initiator}$), -125.08 – -128.10 (2F, F_{PDFPA}).

ATR-FT-IR: $\tilde{\nu}$ / cm^{-1} = 1770 (C=O), 1609, 1499, 1479, 1450, 1293, 1246, 1200, 1118, 1012, 772, 722, 695.

Table 9. Details and results of the electrochemically-initiated polymerization of DFPA (4 mA, 1.1 F mol^{-1}) as reactive monomer.

Entry	Eq.	M_n[a] g mol^{-1}	M_n[b] g mol^{-1}	M_n[c] g mol^{-1}	$Đ$[c]	M_n[d] g mol^{-1}	$Đ$[d]
1	10.00	-	35250	16800[e]	1.83[e]	14600[e]	2.49[e]
				15300[f]	1.75[f]	17300[f]	2.23[f]
2	5.00	-	21330	11300[e]	1.58[e]	8900[e]	2.13[e]
				10500[f]	1.50[f]	11000[f]	1.89[f]

[a] Determined by ^{1}H NMR spectroscopy; [b] determined by ^{19}F NMR spectroscopy; [c] determined by SEC using THF as eluent; [d] determined by SEC using DMAc as eluent; [e] PMMA calibration; [f] PS calibration.

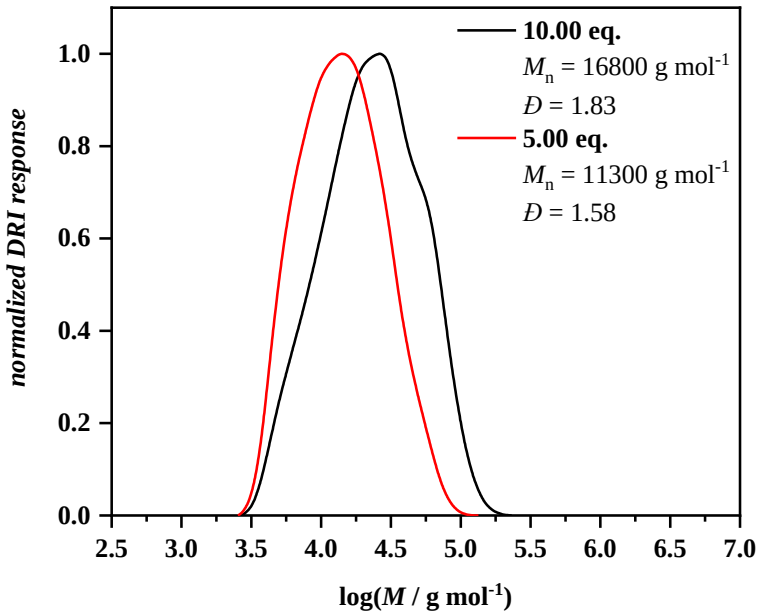

Figure 80. Comparison of SEC traces using THF as eluent (PMMA calibration) of the polymers obtained by the electrochemically-initiated polymerization of DFPA.

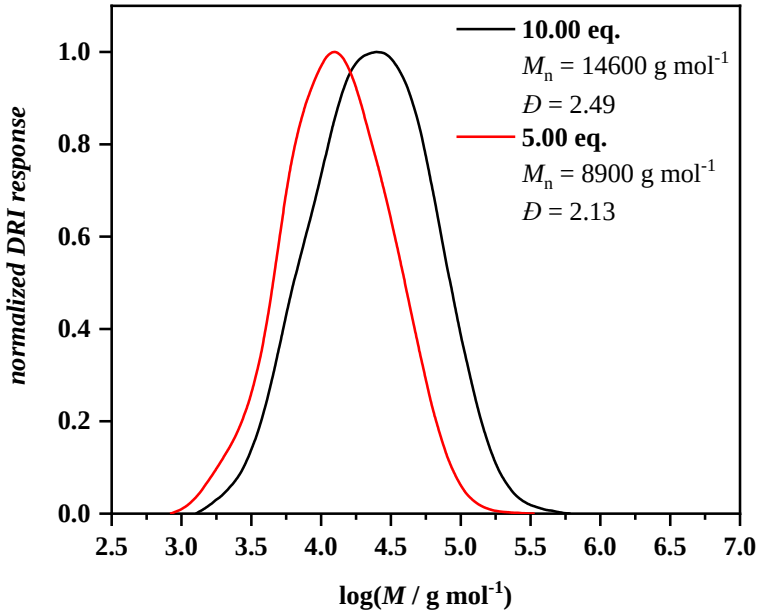

Figure 81. Comparison of SEC traces using DMAc as eluent (PMMA calibration) of the polymers obtained by the electrochemically-initiated polymerization of DFPA.

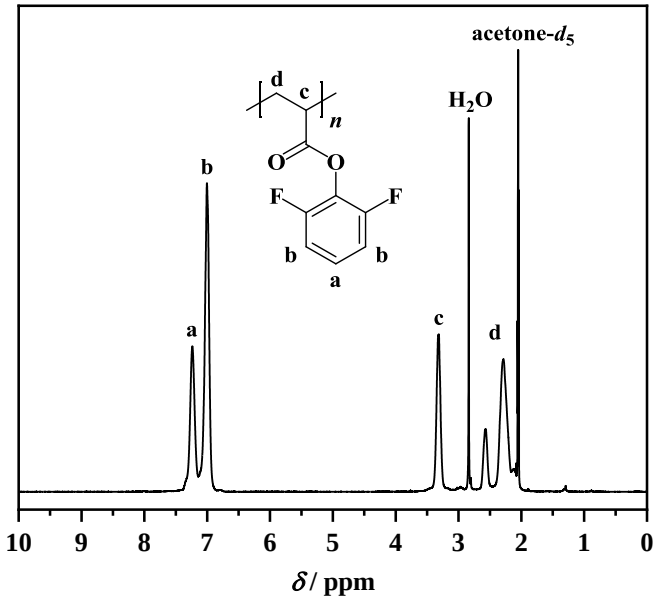

Figure 82. Exemplary ^{1}H NMR spectrum of PDFPA obtained by the electrochemically-initiated polymerization of DFPA (in this case: 10.00 eq. with respect to the initiator); solvent: acetone-d_6.

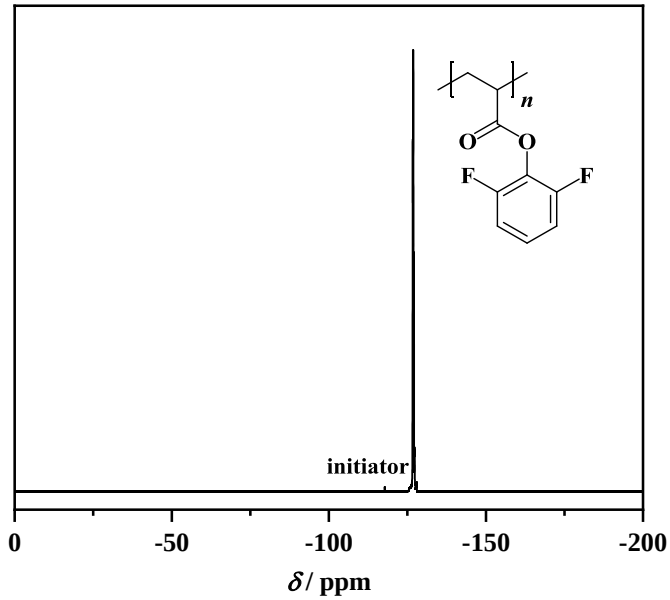

Figure 83. Exemplary ^{19}F NMR spectrum of PDFPA obtained by the electrochemically-initiated polymerization of DFPA (in this case: 10.00 eq. with respect to the initiator); solvent: acetone-d_6.

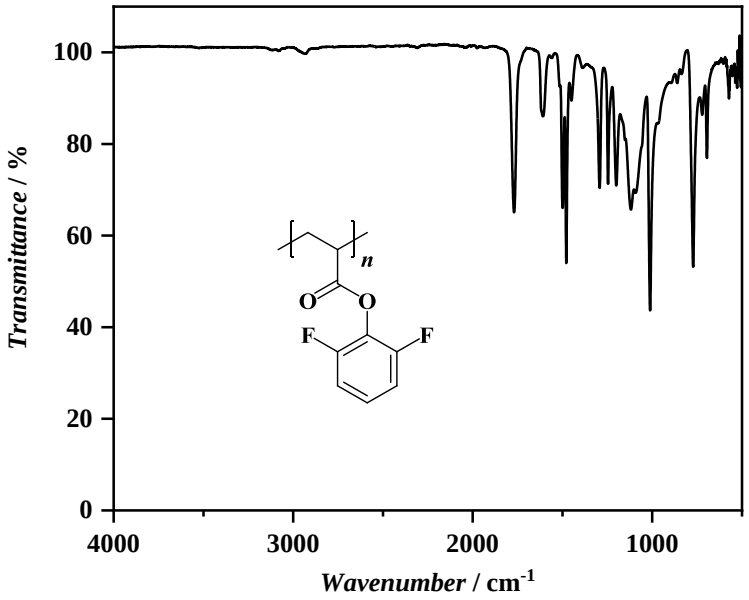

Figure 84. Exemplary ATR-FT-IR spectrum of PPFPA obtained by the electrochemically-initiated polymerization of DFPA (in this case: 10.00 eq. with respect to the initiator).

6.4.3.3 Post-Polymerization Modification (PPM) of PDFPA

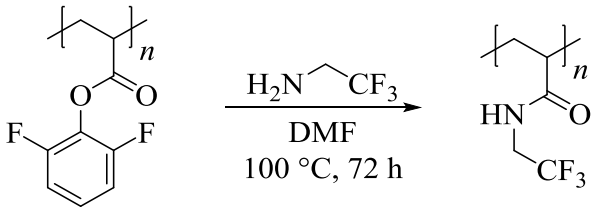

PDPFA (0.040 g, 0.217 mmol of repeating units, 1.00 eq.) was dissolved in anhydrous DMF (0.4 mL) and 2,2,2-trifluoroethylamine (0.43 mL, 0.538 g, 5.43 mmol, 25.0 eq.) was added. The solution was stirred at 100 °C for 72 hours and the solvent was removed under reduced pressure. Afterwards, the residue was dissolved in acetone and precipitated in PE. The solids obtained by centrifugation were dissolved in acetone and filtered prior to a second precipitation in PE. Finally, the solids were obtained by centrifugation and dried under vacuum.

^{1}H NMR (acetone-d_6): δ / ppm = 6.80 – 7.70, 4.29 – 4.60, 3.83 – 4.17, 2.50 – 3.35, 1.25 – 1.90.
^{19}F NMR (acetone-d_6): δ / ppm = -68.56 – -70.45 (3F, F_{imide}), -71.20 – -73.38 (3F, F_{amide}), -117.90 – -118.98 (1F, $F_{initiator}$).
ATR-FT-IR: $\tilde{\nu}$ / cm^{-1} = 3334 (N-H), 2939 (C-H), 1689 (C=O), 1626, 1398, 1341, 1261, 1153, 1116, 834, 668.

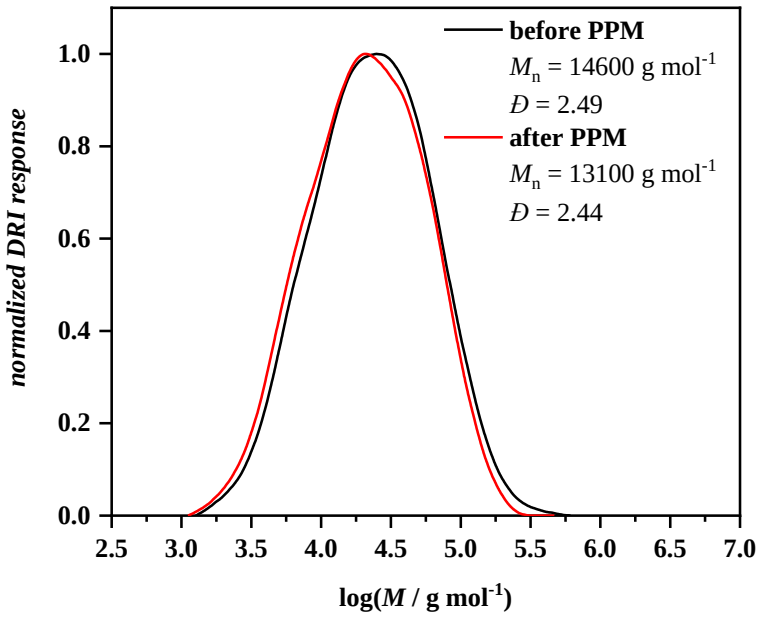

Figure 85. Comparison of SEC traces using DMAc as eluent (PMMA calibration) of PDFPA before (black line) and after PPM (red line).

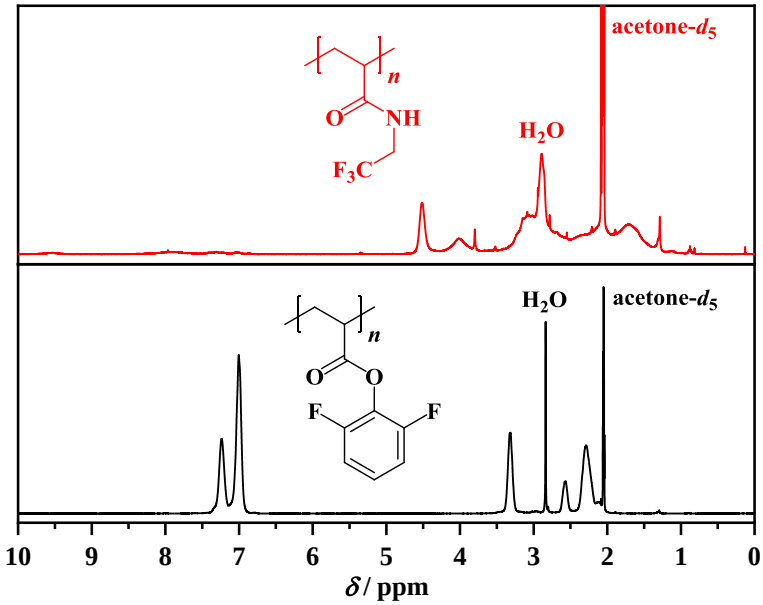

Figure 86. ^{1}H NMR spectroscopical comparison of PDFPA before (bottom, black line) and after PPM (top, red line); solvent: acetone-d_6.

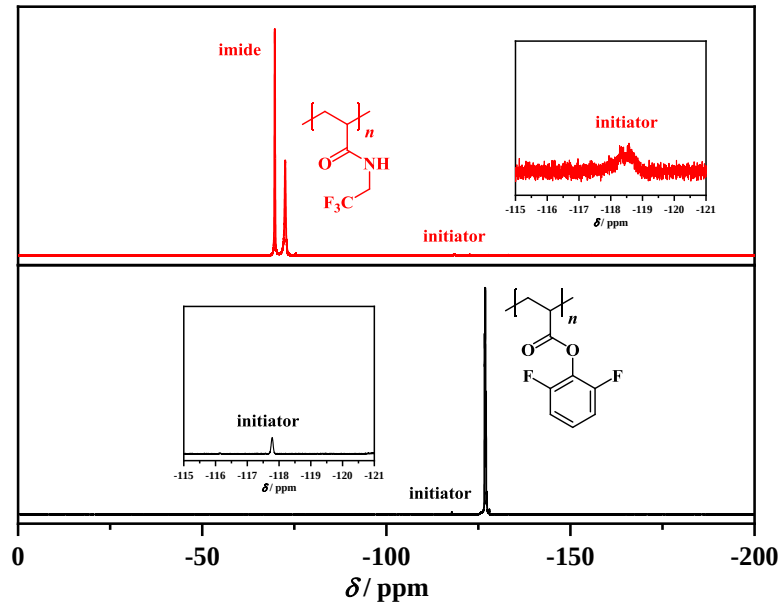

Figure 87. ^{19}F NMR spectroscopical comparison of PDFPA before (bottom, black line) and after PPM (top, red line); solvent: acetone-d_6.

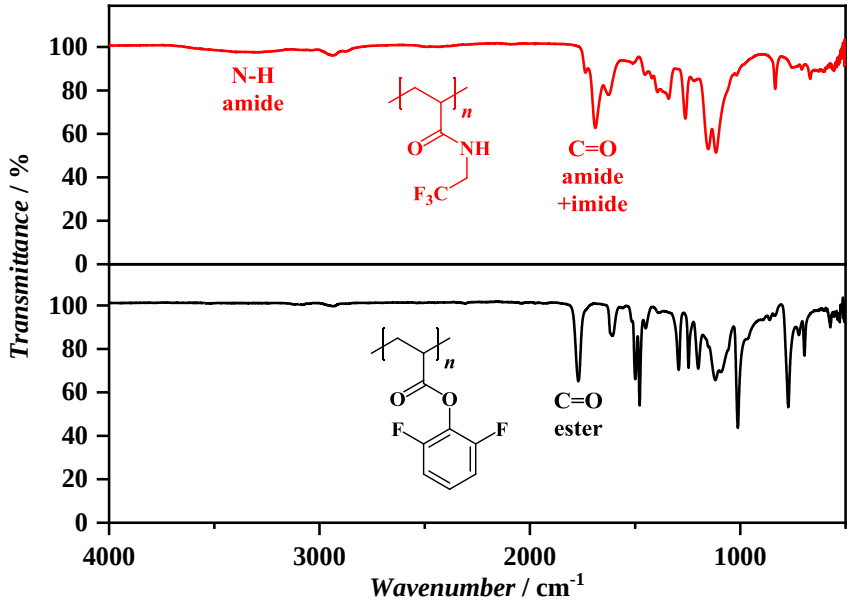

Figure 88. ATR-FT-IR spectroscopical comparison of PDFPA before (bottom, black line) and after PPM (top, red line).

6.4.4 GMA as Reactive Monomer

6.4.4.1 Electrochemically-Initiated Polymerization of PGMA

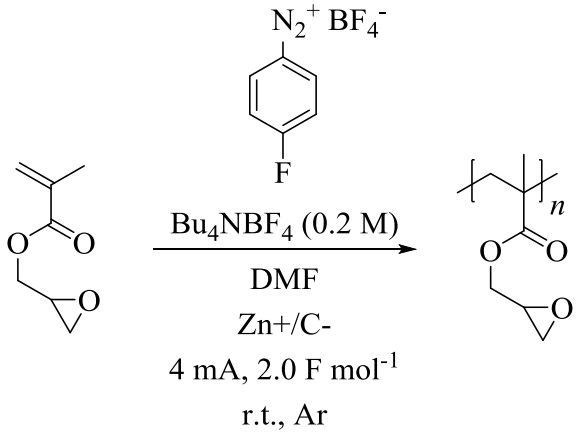

A dry ElectraSyn vial (5 mL) was charged with GMA (see **Table 10** for equivalents), Bu_4NBF_4 (0.132 g, 0.400 mmol, 0.2 M), 4-fluorobenzenediazonium tetrafluoroborate (0.025 g, 0.12 mmol, 1.00 eq.), and anhydrous DMF (2 mL). The vial was closed with the respective IKA ElectraSyn cap bearing a sacrificial zinc anode and a graphite cathode and the solution was deoxygenated by argon purging for 15 minutes. A constant current of 4 mA was applied until 2.0 F mol^{-1} passed through the system. The electrodes were rinsed with THF and acetone. Afterwards, the mixture was precipitated in cold methanol, the solids obtained by centrifugation were dissolved in acetone and filtered (to remove graphite from the mixture) prior to a second precipitation in cold methanol. Finally, the solids were obtained by centrifugation and dried under vacuum giving an off-white solid.

^{1}H NMR (DCM-d_2): δ / ppm = 6.90 – 7.36 (4H, $H_{initiator}$), 4.22 – 4.40 (1H, H_a), 3.69 – 3.85 (1H, H_a), 3.17 – 3.26 (1H, H_b), 2.75 – 2.87 (1H, H_c), 2.58 – 2.67 (1H, H_c), 1.63 – 2.10 (2H, H_d), 0.62 – 1.26 (3H, H_e).

^{19}F NMR (DCM-d_2): δ / ppm = -116.85 – -117.05 (1F, $F_{initiator}$).

^{1}H NMR (acetone-d_6): δ / ppm = 6.88 – 7.50 (4H, $H_{initiator}$), 4.27 – 4.71 (1H, H_a), 3.69 – 4.13 (1H, H_a), 3.15 – 3.54 (1H, H_b), 2.76 – 3.02 (1H, H_c), 2.56 – 2.75 (1H, H_c), 1.55 – 2.19 (2H, H_d), 0.72 – 1.41 (3H, H_e).

^{19}F NMR (acetone-d_6): δ / ppm = -117.60 – -118.09 (1F, $F_{initiator}$).

ATR-FT-IR: $\tilde{\nu}$ / cm^{-1} = 2999 (C-H), 1724 (C=O), 1483, 1448, 1387, 1340, 1254, 1147, 992, 906 (epoxide), 844, 759.

Table 10. Details and results of the electrochemically-initiated polymerization of GMA (4 mA, 2.0 F mol^{-1}) as reactive monomer.

Entry	Eq.	M_n[a] g mol^{-1}	M_n[b] g mol^{-1}	M_n[c] g mol^{-1}	$Đ$[c]	M_n[d] g mol^{-1}	$Đ$[d]
1	40.0	14500	-	15700[e]	2.40[e]	12600[e]	3.10[e]
				14700[f]	2.24[f]	15400[f]	2.68[f]
2	20.0	10350	-	8200[e]	1.85[e]	6200[e]	2.40[e]
				7900[f]	1.71[f]	8000[f]	2.06[f]
3	10.0	6970	-	6800[e]	1.60[e]	5200[e]	2.00[e]
				6500[f]	1.50[f]	6700[f]	1.76[f]

[a] Determined by ^{1}H NMR spectroscopy; [b] determined by ^{19}F NMR spectroscopy; [c] determined by SEC using THF as eluent; [d] determined by SEC using DMAc as eluent; [e] PMMA calibration; [f] PS calibration.

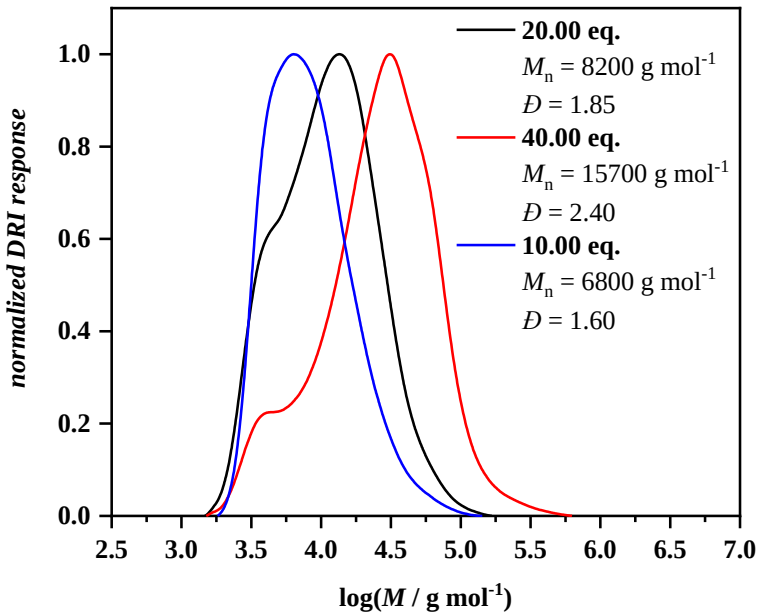

Figure 89. Comparison of SEC traces using THF as eluent (PMMA calibration) of the polymers obtained by the electrochemically-initiated polymerization of GMA.

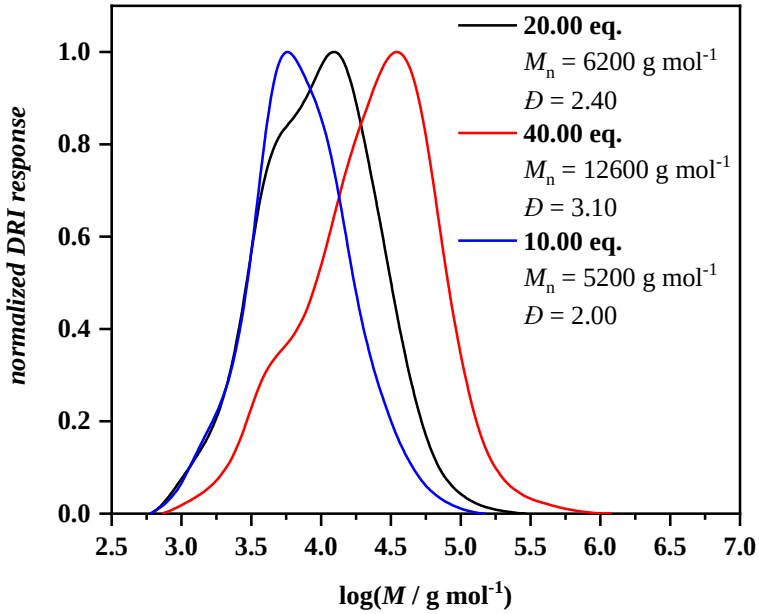

Figure 90. Comparison of SEC traces using DMAc as eluent (PMMA calibration) of the polymers obtained by the electrochemically-initiated polymerization of GMA.

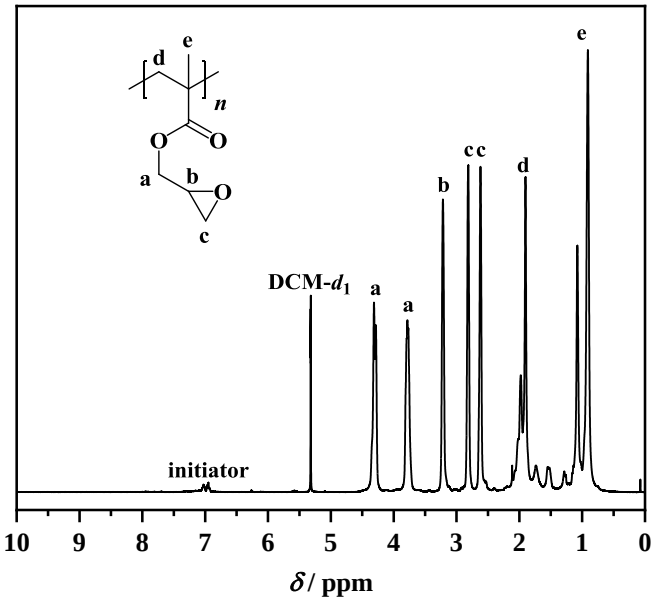

Figure 91. Exemplary ^{1}H NMR spectrum of PGMA obtained by the electrochemically-initiated polymerization of GMA (in this case: 20.00 eq. with respect to the initiator); solvent: DCM-d_2.

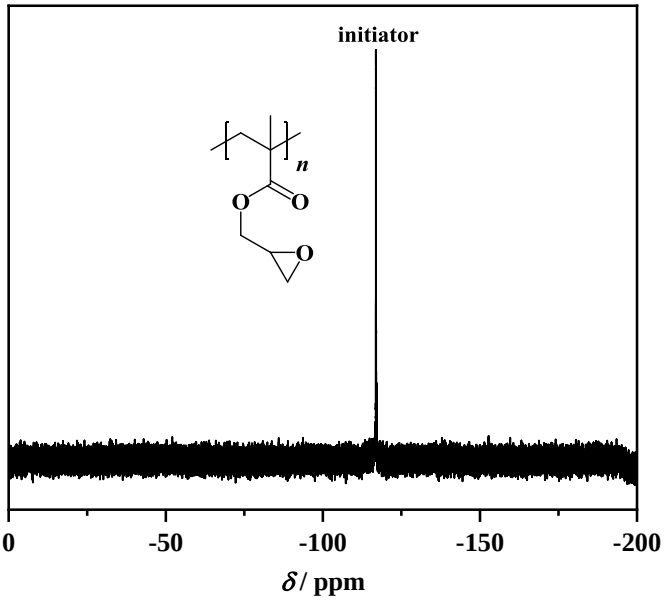

Figure 92. Exemplary ^{19}F NMR spectrum of PGMA obtained by the electrochemically-initiated polymerization of GMA (in this case: 20.00 eq. with respect to the initiator); solvent: DCM-d_2.

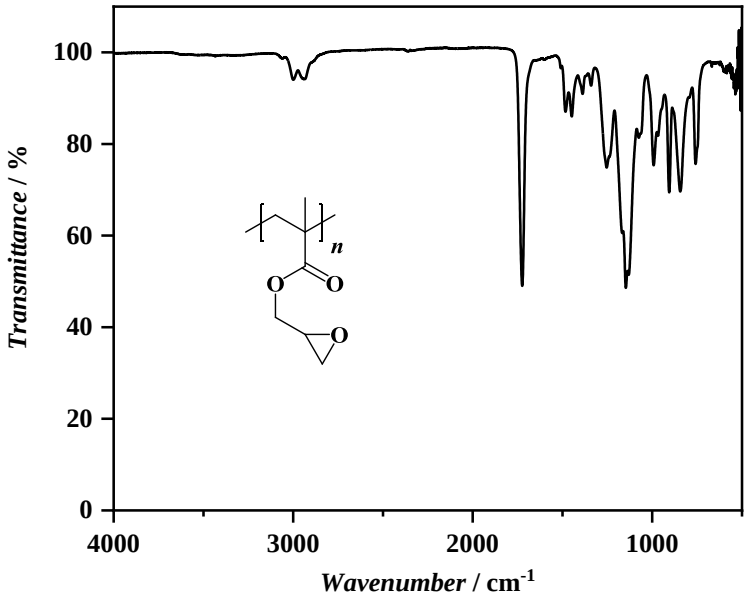

Figure 93. Exemplary ATR-FT-IR spectrum of PGMA obtained by the electrochemically-initiated polymerization of GMA (in this case: 20.00 eq. with respect to the initiator).

6.4.4.2 Post-Polymerization Modification (PPM) of PGMA

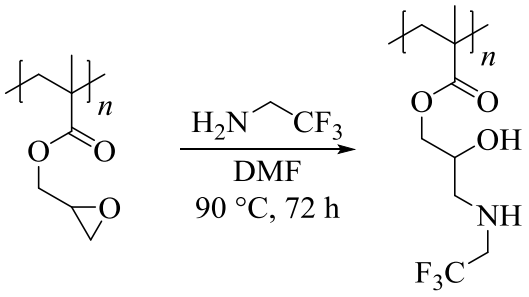

PGMA (0.040 g, 0.281 mmol of repeating units, 1.00 eq.) was dissolved in anhydrous DMF (0.6 mL) and 2,2,2-trifluoroethylamine (0.55 mL, 0.697 g, 7.04 mmol, 25.0 eq.) was added. The solution was stirred at 90 °C for 72 hours and the mixture was precipitated in cold diethyl ether. Afterwards, the solids obtained by centrifugation were dissolved in acetone and precipitated a second time in cold diethyl ether. Finally, the solids were obtained by centrifugation and dried under vacuum.

^{1}H NMR (acetone-d_6): δ / ppm = 6.97 – 8.08 (4H, $H_{initiator}$), 4.28 – 4.60 (1H, H_a), 3.89 – 4.17 (2H, H_b), 3.20 – 3.48 (2H, H_c), 2.74 – 2.99 (2H, H_d), 1.76 – 2.08 (2H, H_e), 0.72 – 1.45 (3H, H_f).

^{19}F NMR (acetone-d_6): δ / ppm = -71.10 – -71.76 (3F, $F_{poly(\beta\text{-amino alcohol})}$), -71.85 – -72.75 (3F, $F_{poly(\beta\text{-amino alcohol})}$), -117.80 – -118.01 (1F, $F_{initiator}$).

ATR-FT-IR: $\tilde{\nu}$ / cm^{-1} = 3365 (N-H, O-H), 2944, 1724 (C=O), 1455, 1393, 1266, 1139, 837, 748, 668.

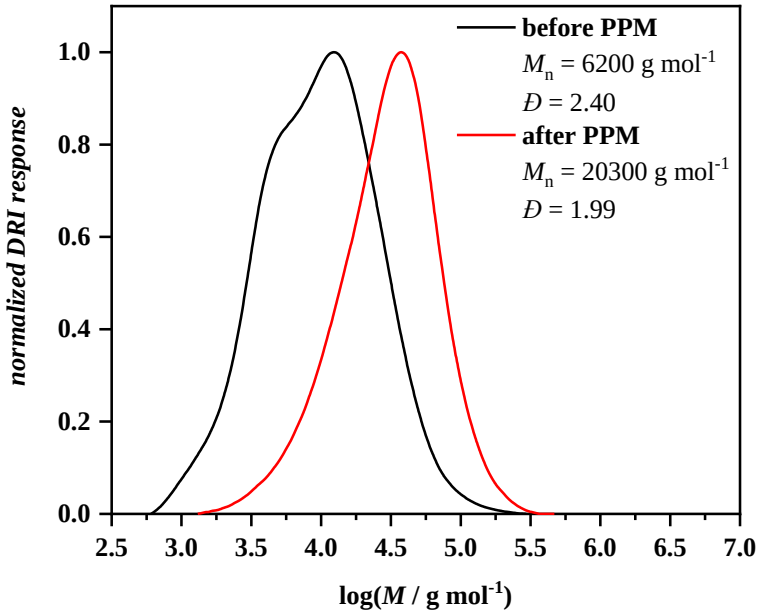

Figure 94. Comparison of SEC traces using DMAc as eluent (PMMA calibration) of PGMA before (black line) and after PPM (red line).

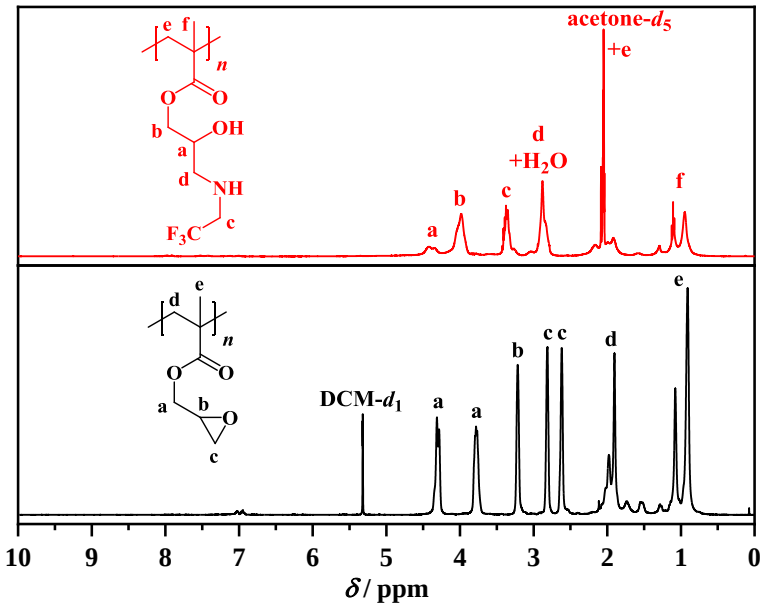

Figure 95. ^{1}H NMR spectroscopical comparison of PGMA before (bottom, black line) and after PPM (top, red line); solvent: DCM-d_2 (bottom, black line) and acetone-d_6 (top, red line).

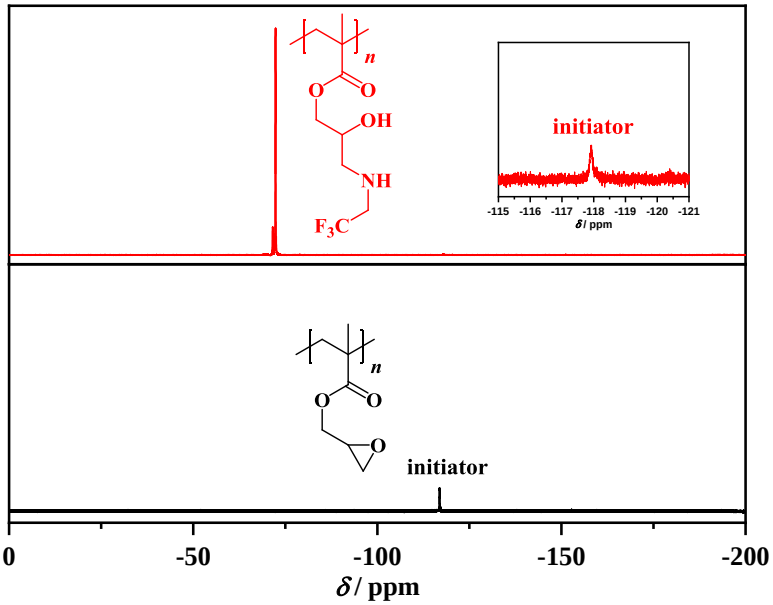

Figure 96. ^{19}F NMR spectroscopical comparison of PGMA before (bottom, black line) and after PPM (top, red line); solvent: DCM-d_2 (bottom, black line) and acetone-d_6 (top, red line).

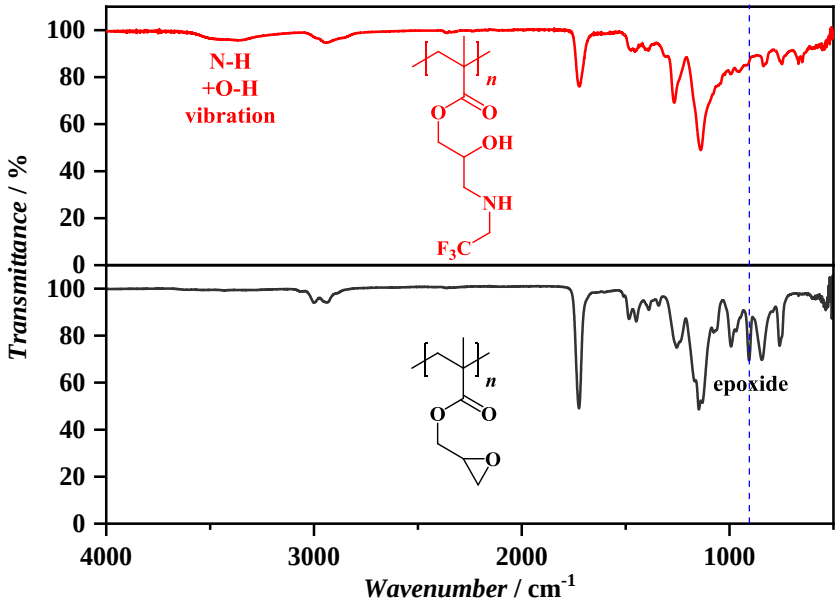

Figure 97. ATR-FT-IR spectroscopical comparison of PGMA before (bottom, black line) and after PPM (top, red line).

6.4.5 Synthesis and Polymerization of *N*-(2,2,2-Trifluoroethyl)acrylamide

6.4.5.1 Synthesis of *N*-(2,2,2-Trifluoroethyl)acrylamide*

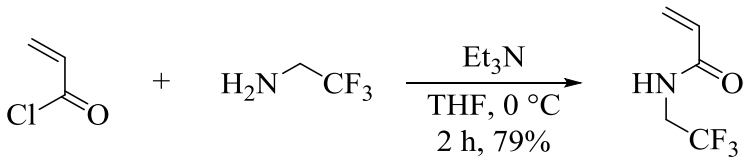

2,2,2-Trifluoroethylamine (1.00 mL, 1.26 g, 12.7 mmol, 1.00 eq.) was dissolved in anhydrous THF (5 mL). The solution was cooled to 0 °C and triethylamine (2.15 mL, 1.54 g, 15.3 mmol, 1.20 eq.) was added. A solution of acryloyl chloride (1.24 mL, 1.26 g, 12.7 mmol, 1.20 eq.) in anhydrous THF (3 mL) was added slowly and the mixture was stirred at 0 °C for two hours. Subsequently, the solvent was removed under reduced pressure and the crude product was purified by column chromatography using a 3:2 mixture of CH / EA giving a slightly yellowish solid (1.40 g, 10.05 mmol, 79%).

R_f (CH / EA 3:2) = 0.33

^{1}H NMR (acetone-d_6): δ / ppm = 7.90 (bs, 1H, H_a), 6.24 – 6.40 (m, 2H, H_b+H_c), 5.69 (dd, J = 9.6, 2.6 Hz, 1H, H_c), 4.06 (qd, J = 9.5, 6.5 Hz, 2H, H_d).

^{13}C NMR (acetone-d_6): δ / ppm = 166.05 (s), 131.45 (s), 129.91 (s), 127.38 (s), 127.15 (s), 124.38 (s), 40.77 (q, J = 34.2 Hz).

^{19}F NMR (acetone-d_6): δ / ppm = -72.99 (t, J = 9.5 Hz, 3F).

ATR-FT-IR: $\tilde{\nu}$ / cm^{-1} = 3306 (N-H), 3088, 2972, 1661 (C=O), 1631, 1553, 1432, 1410, 1386, 1288, 1265, 1232, 1145, 980, 968, 864, 832, 806, 690, 670.

* The synthesis was carried out by Tilman Grüger in the frame of his Bachelor Thesis "Electrochemically-initiated Polymerization of Fluorine-containing Monomers" under the laboratory supervision of Edgar Molle.

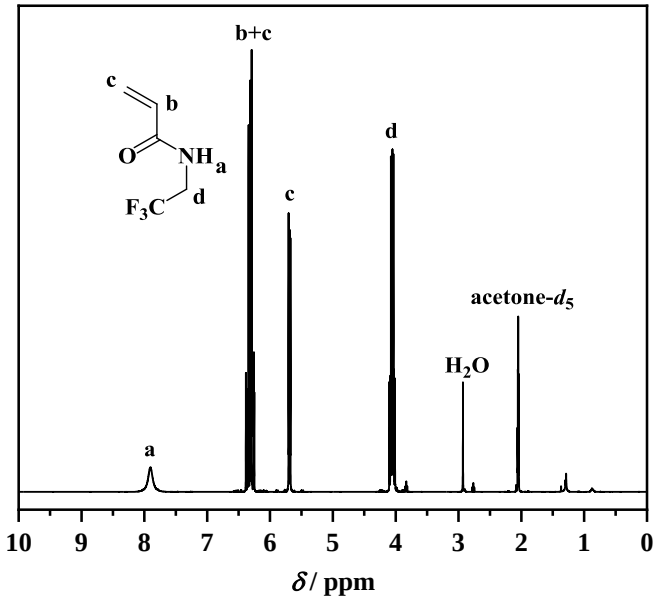

Figure 98. ^{1}H NMR spectrum of *N*-(2,2,2-trifluoroethyl)acrylamide; solvent: acetone-d_6.

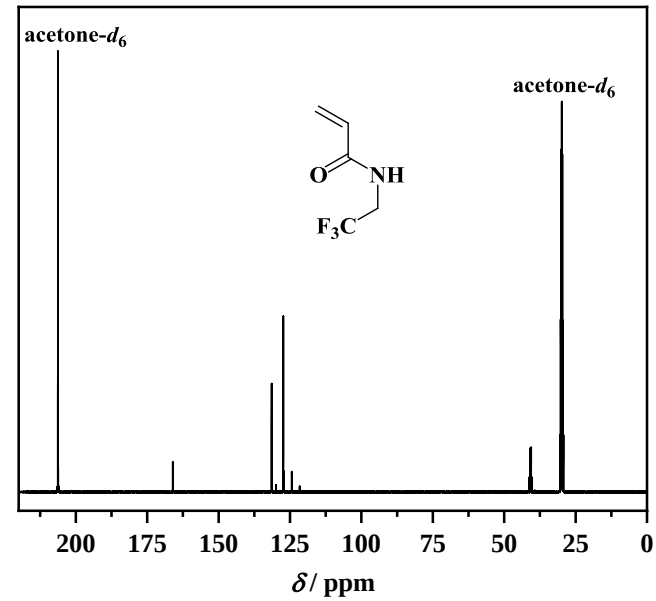

Figure 99. ^{13}C NMR spectrum of *N*-(2,2,2-trifluoroethyl)acrylamide; solvent: acetone-d_6.

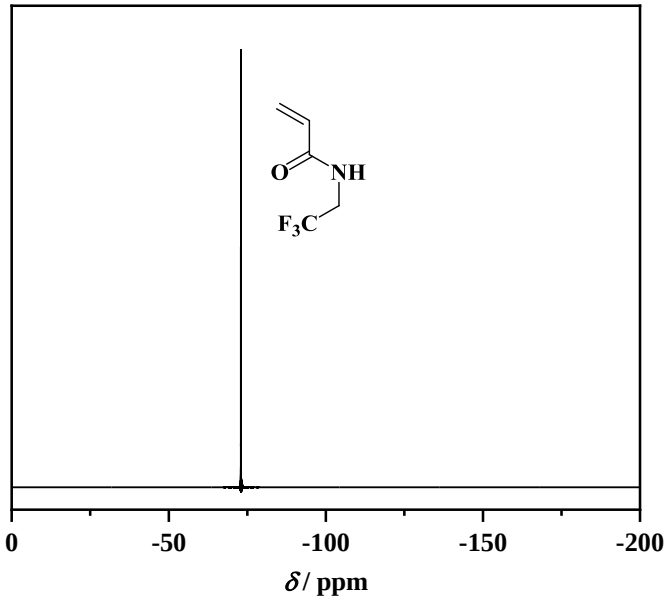

Figure 100. ^{19}F NMR spectrum of *N*-(2,2,2-trifluoroethyl)acrylamide; solvent: acetone-d_6.

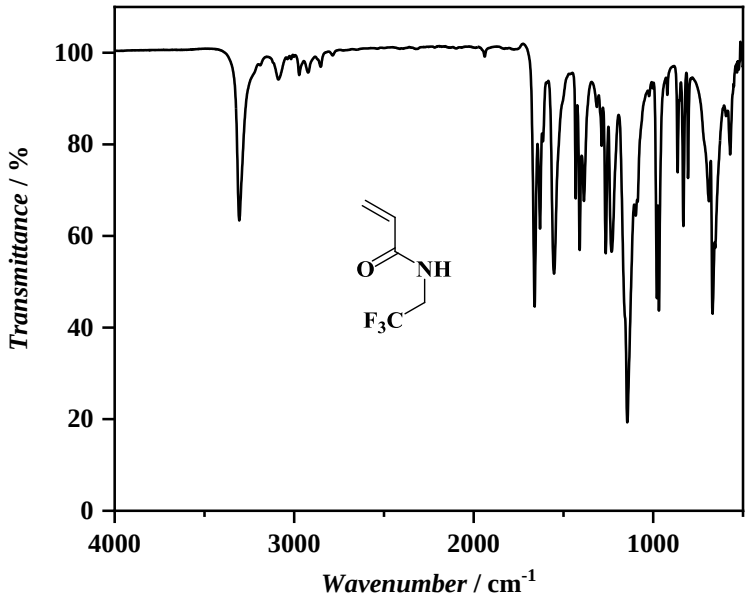

Figure 101. ATR-FT-IR spectrum of *N*-(2,2,2-trifluoroethyl)acrylamide.

6.4.5.2 Polymerization of *N*-(2,2,2-Trifluoroethyl)acrylamide

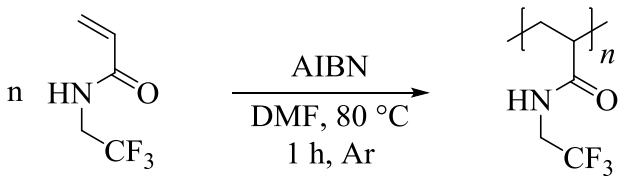

N-(2,2,2-Trifluoroethyl)acrylamide (0.200 g, 1.31 mmol, 20.0 eq.) and AIBN (0.011 g, 0.065 mmol, 1.00 eq.) were dissolved in anhydrous DMF (1.5 mL). The solution was deoxygenated by argon purging for 15 minutes. The flask was placed in a preheated oil bath at 80 °C for one hour. Afterwards, the mixture was precipitated in cold diethyl ether, the solids obtained by centrifugation were dissolved in acetone and precipitated a second time in cold diethyl ether. Finally, the solids were obtained by centrifugation and dried under vacuum.

^{1}H NMR (acetone-d_6): δ / ppm = 7.44 – 8.27 (1H, H_a), 3.65 – 4.35 (2H, H_b), 2.12 – 2.72 (1H, H_c), 1.38 – 1.97 (2H, H_d).

^{19}F NMR (acetone-d_6): δ / ppm = -71.47 – -73.96 (3F).

ATR-FT-IR: $\tilde{\nu}$ / cm^{-1} = 3309 (N-H), 1663 (C=O), 1522, 1427, 1395, 1271, 1148, 980, 833, 669.

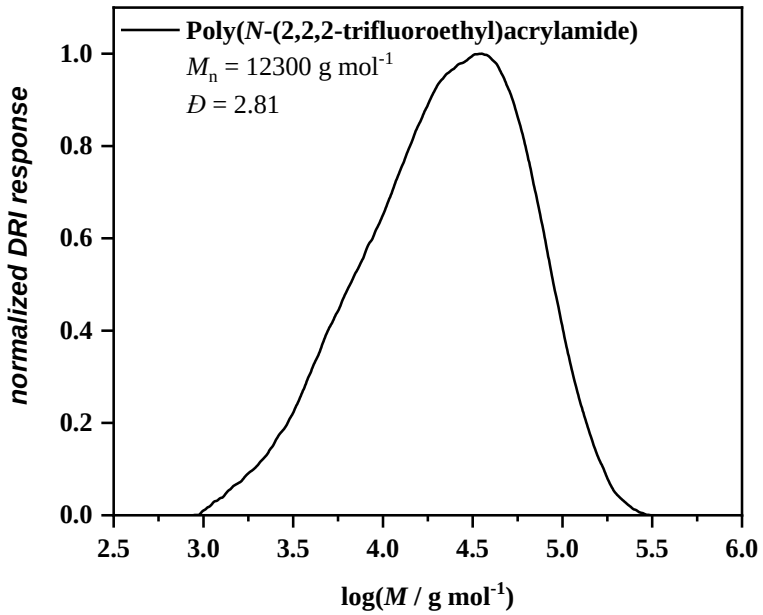

Figure 102. Size-exclusion chromatogram using DMAc as eluent (PMMA calibration) of poly(*N*-(2,2,2-trifluoroethyl)acrylamide).

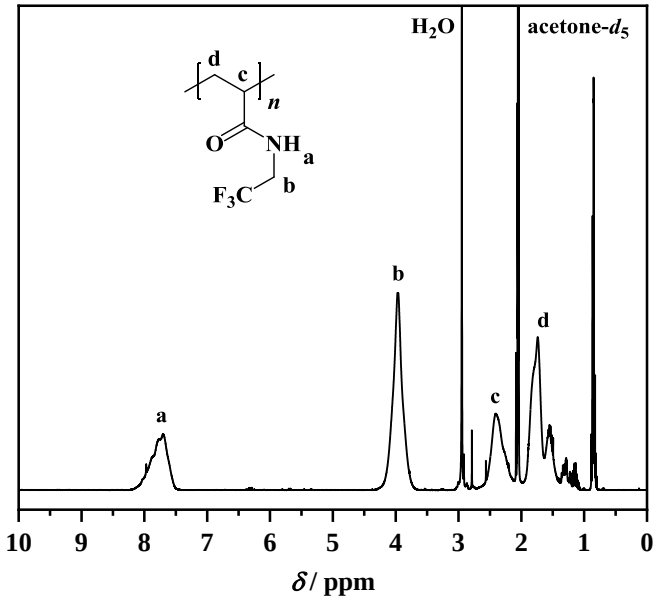

Figure 103. ^{1}H NMR spectrum of poly(*N*-(2,2,2-trifluoroethyl)acrylamide); solvent: acetone-d_6.

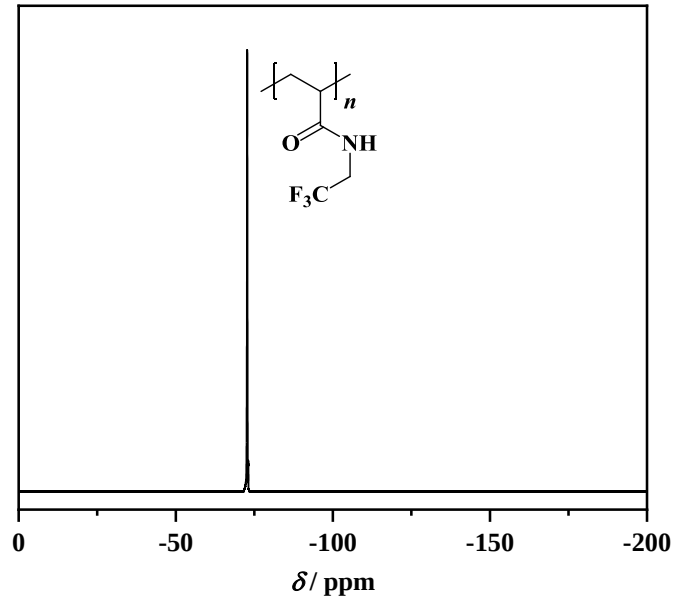

Figure 104. ^{19}F NMR spectrum of poly(*N*-(2,2,2-trifluoroethyl)acrylamide); solvent: acetone-d_6.

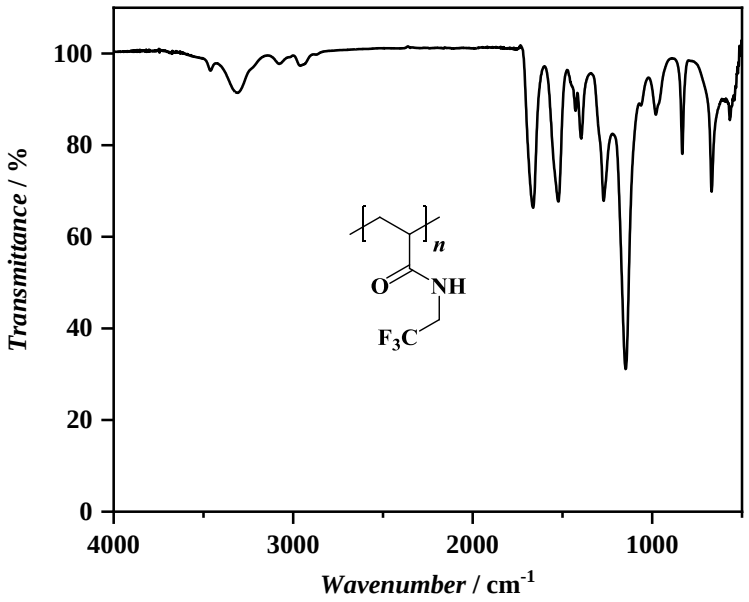

Figure 105. ATR-FT-IR spectrum of poly(*N*-(2,2,2-trifluoroethyl)acrylamide).

6.5 Procedures for the Electrochemically-Initiated Nickel-Catalyzed ω-Functionalization

6.5.1 Non-Polymeric Aryl Bromides for the Electrochemically-Mediated Nickel-Catalyzed ω-Functionalization

6.5.1.1 Screening of Different Aryl Bromides for the Electrochemically-Mediated Nickel-Catalyzed ω-Functionalization

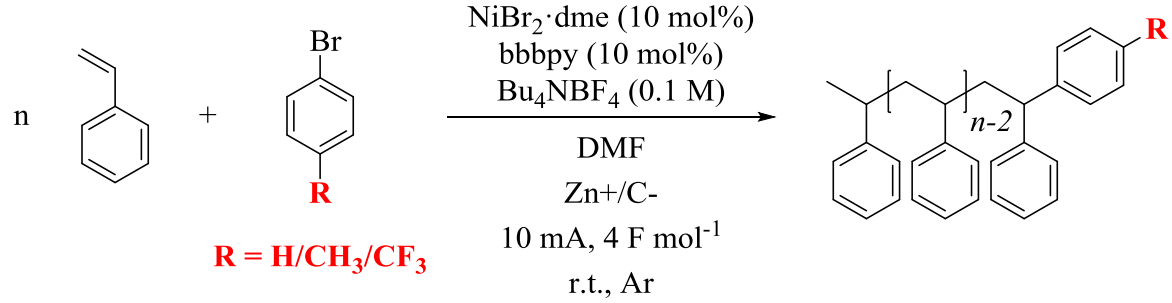

A dry ElectraSyn vial (5 mL) was charged with the respective aryl bromide (**Table 11**) (0.191 mmol, 1.00 eq.), Bu_4NBF_4 (0.066 g, 0.200 mmol), bbbpy (0.005 g, 0.019 mmol, 0.10 eq.), and $NiBr_2$·dme (0.006 g, 0.019 mmol, 0.10 eq.). The compounds were immediately after addition of the nickel complex dissolved in anhydrous DMF (2 mL). Deinhibited styrene (1.65 mL, 1.49 g, 14.3 mmol, 75.0 eq.) was added. The vial was closed with the respective IKA ElectraSyn cap bearing a sacrificial zinc anode and a graphite cathode and the solution was deoxygenated by argon purging for 15 minutes. A constant current of 10 mA was applied until 4 F mol^{-1} passed through the system. Afterwards, the electrodes were rinsed with EA and the mixture was precipitated in cold methanol. Finally, the precipitate obtained by centrifugation was dissolved in THF and reprecipitated in cold methanol.

Table 11. Results of the screening of different aryl bromides for the electrochemically-mediated nickel-catalyzed ω-functionalization using styrene as monomer.

Entry	Aryl bromide	M_n[a] g mol^{-1}	$Đ$[a]
1	Bromobenzene	4800	1.37
2	4-Bromotoluene	5800	1.49
3	4-Bromobenzotrifluoride[b]	10300	1.66

[a] Determined by SEC using THF as eluent (PS calibration); [b] low yields after reaction.

Bromobenzene as aryl bromide:

^{1}H NMR (DCM-d_2): δ / ppm = 6.34 – 7.33 (10H, $H_{aromatic}$), 0.77 – 3.14 (3H, $H_{backbone}$).

4-Bromotoluene as aryl bromide:

^{1}H NMR (DCM-d_2): δ / ppm = 6.33 – 7.36 (9H, $H_{aromatic}$), 0.77 – 3.27 (6H, H_{methyl}+$H_{backbone}$).

4-Bromobenzotrifluoride as aryl bromide:

^{1}H NMR (DCM-d_2): δ / ppm = 6.31 – 7.53 (9H, $H_{aromatic}$), 0.75 – 3.13 (3H, $H_{backbone}$).

^{19}F NMR (DCM-d_2): δ / ppm = -62.69 – -62.49 (3F).

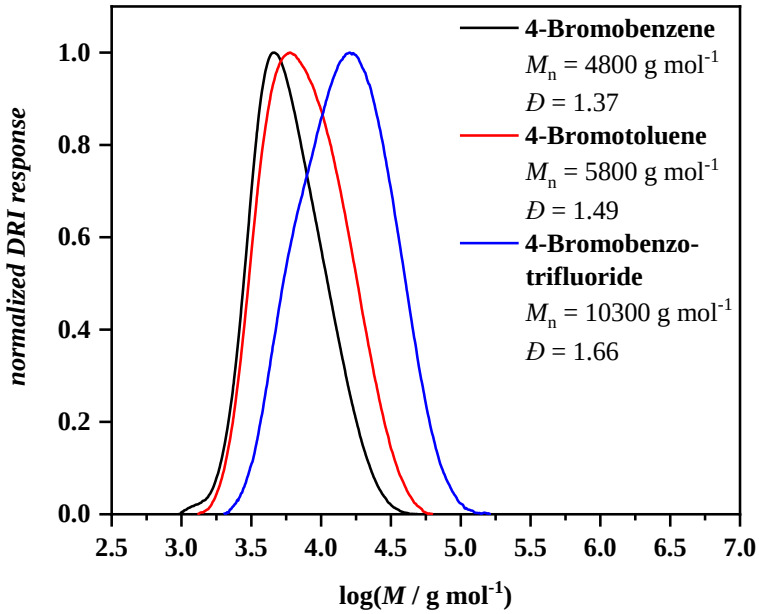

Figure 106. Comparison of SEC traces with THF as eluent (PS calibration) of different aryl bromides used in the electrochemically-mediated nickel-catalyzed ω-functionalization using styrene as monomer.

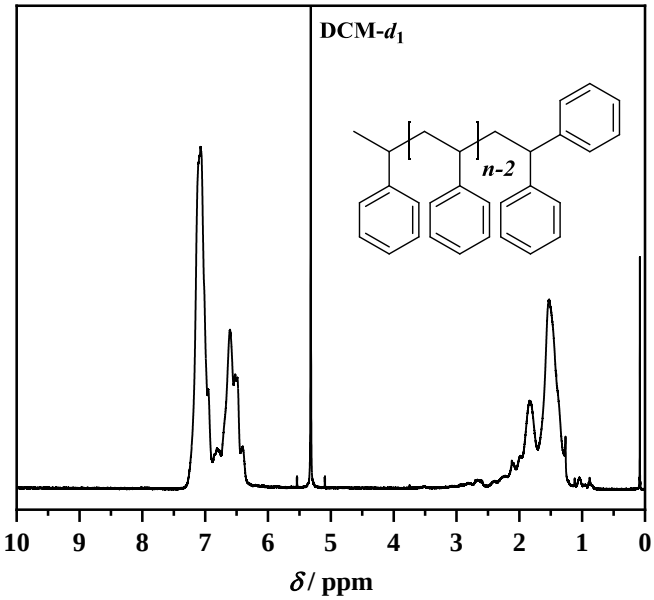

Figure 107. ^{1}H NMR spectrum of the electrochemically-mediated nickel-catalyzed ω-functionalization using bromobenzene as aryl bromide and styrene as monomer; solvent: DCM-d_2.

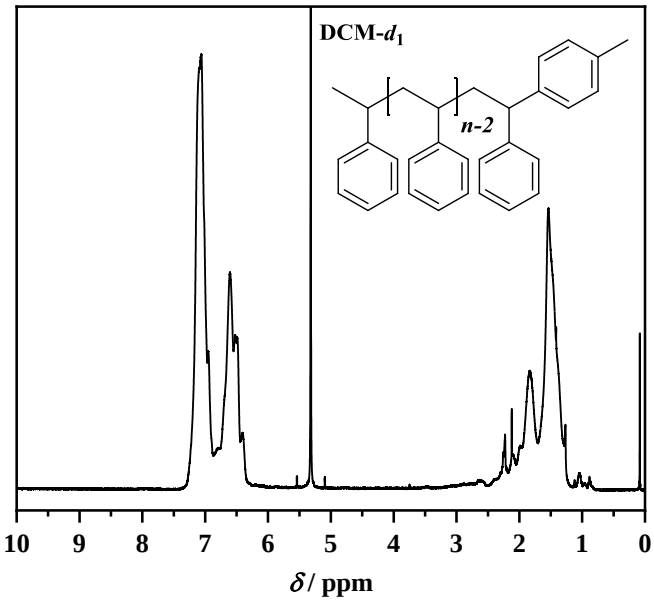

Figure 108. ^{1}H NMR spectrum of the electrochemically-mediated nickel-catalyzed ω-functionalization using 4-bromotoluene as aryl bromide and styrene as monomer; solvent: DCM-d_2.

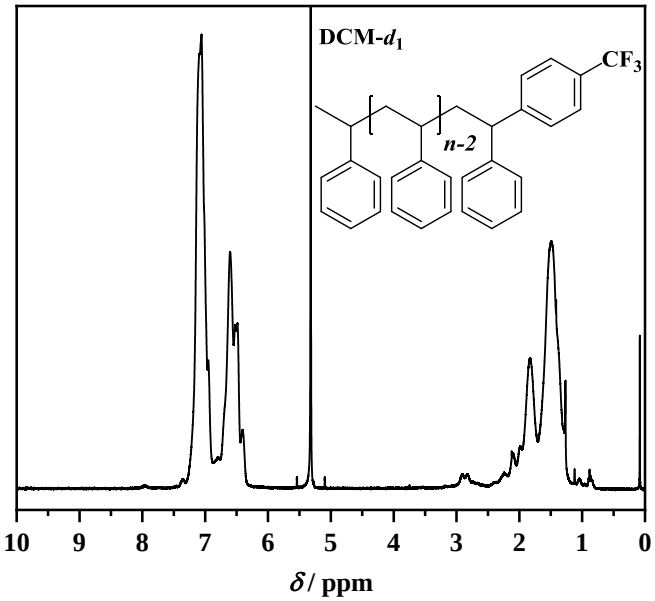

Figure 109. ^{1}H NMR spectrum of the electrochemically-mediated nickel-catalyzed ω-functionalization using 4-bromobenzotrifluoride as aryl bromide and styrene as monomer; solvent: DCM-d_2.

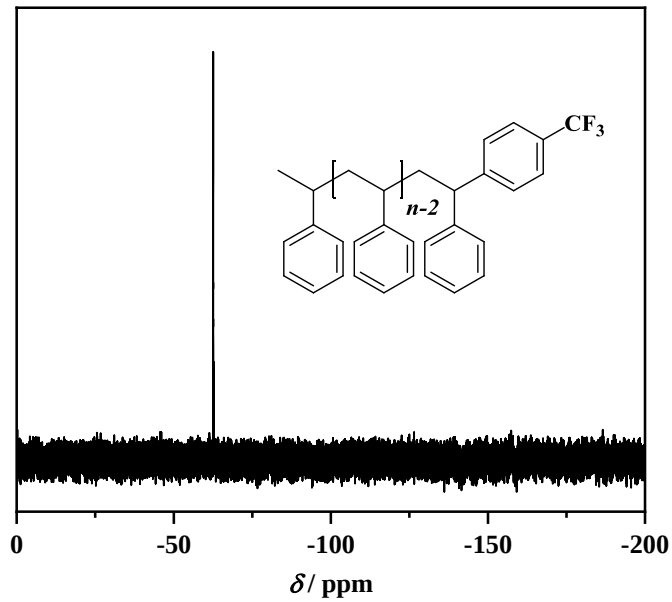

Figure 110. ^{19}F NMR spectrum of the electrochemically-mediated nickel-catalyzed ω-functionalization using 4-bromobenzotrifluoride as aryl bromide and styrene as monomer; solvent: DCM-d_2.

6.5.1.2 Influence of the Reaction Duration on the Electrochemically-Mediated Nickel-Catalyzed ω-Functionalization

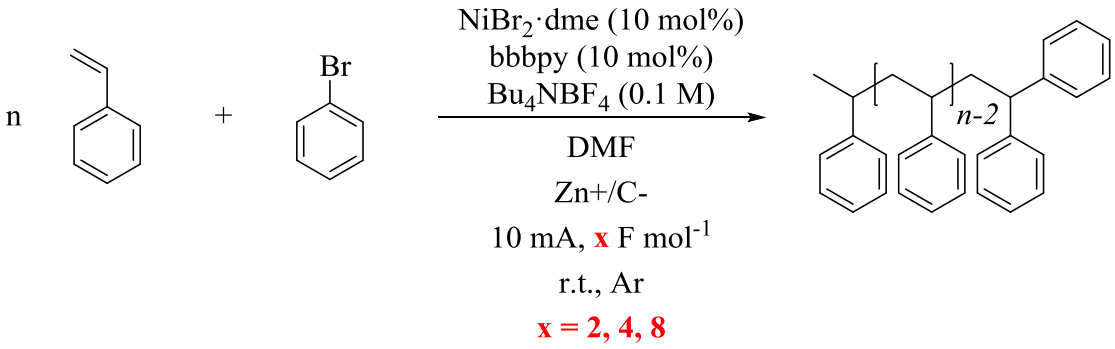

A dry ElectraSyn vial (5 mL) was charged with bromobenzene (0.030 g, 0.191 mmol, 1.00 eq.), Bu_4NBF_4 (0.066 g, 0.200 mmol), bbbpy (0.005 g, 0.019 mmol, 0.10 eq.), and $NiBr_2$·dme (0.006 g, 0.019 mmol, 0.10 eq.). The compounds were immediately after addition of the nickel complex dissolved in anhydrous DMF (2 mL). Deinhibited styrene (1.65 mL, 1.49 g, 14.3 mmol, 75.0 eq.) was added. The vial was closed with the respective IKA ElectraSyn cap bearing a sacrificial zinc anode and a graphite cathode and the solution was deoxygenated by argon purging for 15 minutes. A constant current of 10 mA was applied for different reaction times (**Table 12**). Afterwards, the electrodes were rinsed with EA and the mixture was precipitated in cold methanol. Finally, the precipitate obtained by centrifugation was dissolved in THF and reprecipitated in cold methanol.

Table 12. Results of the screening of different duration times for the electrochemically-mediated nickel-catalyzed ω-functionalization using styrene as monomer.

Entry	Duration time	M_n[a] g mol^{-1}	$Đ$[a]
1	2 F mol^{-1}	4500	1.23
2	4 F mol^{-1}	4800	1.37
3	8 F mol^{-1}	5400	1.74

[a] Determined by SEC using THF as eluent (PS calibration).

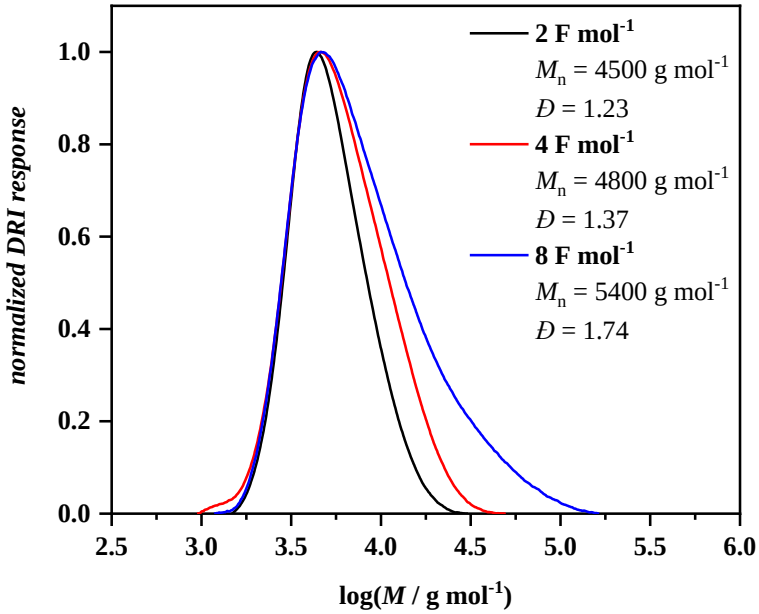

Figure 111. Comparison of SEC traces with THF as eluent (PS calibration) of the electrochemically-mediated nickel-catalyzed ω-functionalization using styrene as monomer and bromobenzene as aryl bromide with different duration times.

6.5.1.3 Influence of the Presence / Absence of an Aryl Bromide on the Electrochemically-Mediated Nickel-Catalyzed ω-Functionalization

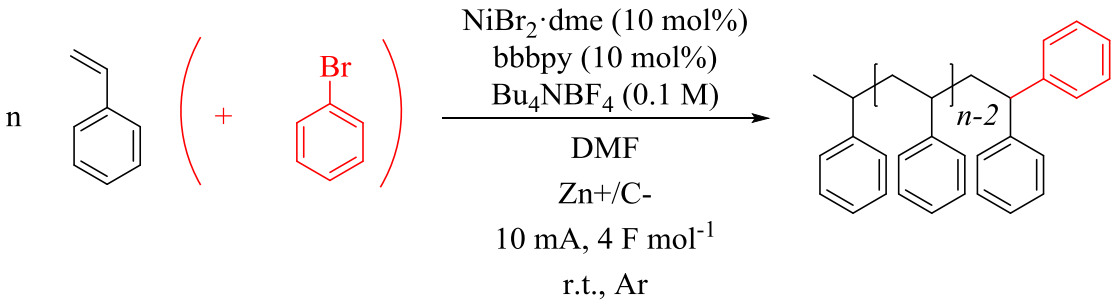

A dry ElectraSyn vial (5 mL) was charged with bromobenzene (the reaction was conducted in the absence of bromobenzene in the control experiment) (0.030 g, 0.191 mmol, 1.00 eq.), Bu_4NBF_4 (0.066 g, 0.200 mmol), bbbpy (0.005 g, 0.019 mmol, 0.10 eq.), and $NiBr_2$·dme (0.006 g, 0.019 mmol, 0.10 eq.). The compounds were immediately after addition of the nickel complex dissolved in anhydrous DMF (2 mL). Deinhibited styrene (1.1 mL, 0.995 g, 9.55 mmol, 50.0 eq.) was added. The vial was closed with the respective IKA ElectraSyn cap bearing a sacrificial zinc anode and a graphite cathode and the solution was deoxygenated by argon purging for 15 minutes. A constant current of 10 mA was applied until 4 F mol^{-1} passed through the system. Afterwards, the electrodes were rinsed with EA and the mixture was precipitated in cold methanol. Finally, the precipitate obtained by centrifugation was dissolved in THF and reprecipitated in cold methanol.

Table 13. Results of the influence of the presence / absence of bromobenzene as aryl bromide on the electrochemically-mediated nickel-catalyzed ω-functionalization using styrene as monomer.

Entry	Aryl Bromide	M_n[a] g mol^{-1}	$Đ$[a]
1	Bromobenzene	9800	2.05
2	-	6000	2.54

[a] Determined by SEC using THF as eluent (PS calibration).

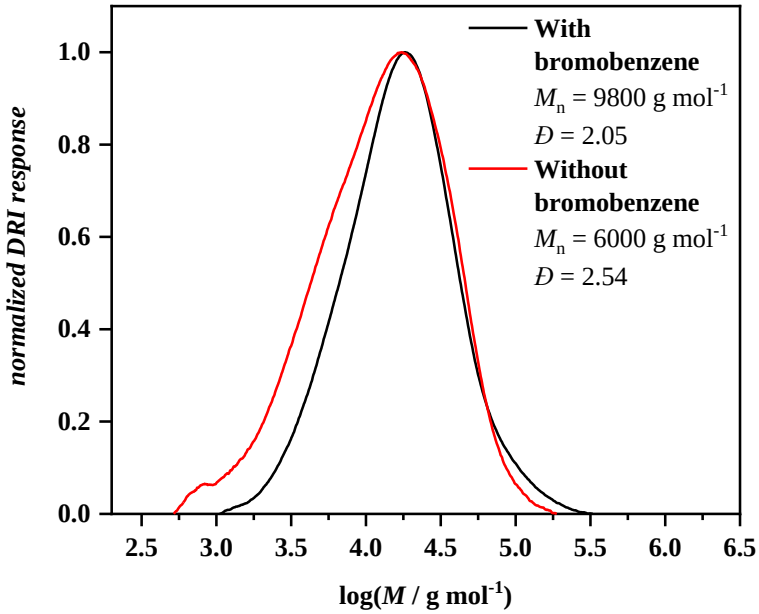

Figure 112. Comparison of SEC traces with THF as eluent (PS calibration) of the electrochemically-mediated nickel-catalyzed ω-functionalization using styrene as monomer in the presence (black line) and the absence (red line) of bromobenzene as aryl bromide.

6.5.1.4 Variation of Monomers for the Electrochemically-Mediated Nickel-Catalyzed ω-Functionalization with Bromobenzene as Aryl Bromide

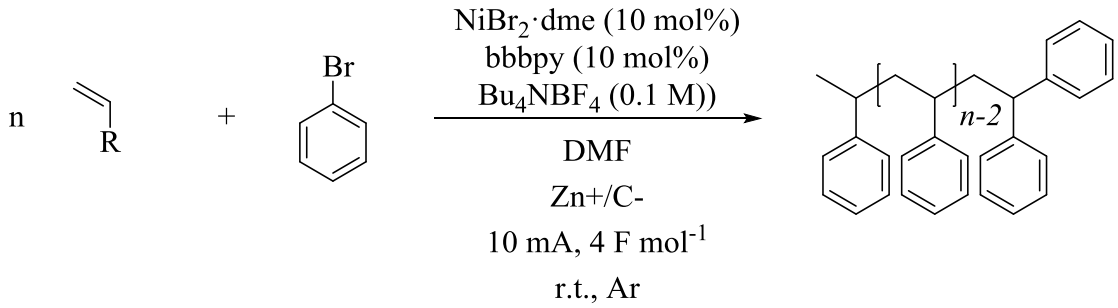

A dry ElectraSyn vial (5 mL) was charged with bromobenzene (0.030 g, 0.191 mmol, 1.00 eq.), Bu_4NBF_4 (0.066 g, 0.200 mmol), bbbpy (0.005 g, 0.019 mmol, 0.10 eq.), and $NiBr_2$·dme (0.006 g, 0.019 mmol, 0.10 eq.). The compounds were immediately after addition of the nickel complex dissolved in anhydrous DMF (2 mL). Deinhibited monomer (**Table 14**) (9.55 mmol, 50.0 eq.) was added. The vial was closed with the respective IKA ElectraSyn cap bearing a sacrificial zinc anode and a graphite cathode and the solution was deoxygenated by argon purging for 15 minutes. A constant current of 10 mA was applied until 4 F mol^{-1} passed through the system. Afterwards, the electrodes were rinsed with EA and the mixture was precipitated in cold methanol. Finally, the precipitate obtained by centrifugation was dissolved in THF and reprecipitated in cold methanol.

Table 14. Results of the screening of different monomers for the electrochemically-mediated nickel-catalyzed ω-functionalization using bromobenzene as aryl bromide.

Entry	Monomer	M_n[a] g mol^{-1}	$Đ$[a]
1	4-Fluorostyrene	16600[b]	1.47[b]
2	Acrylonitrile	4500[c]	2.74[c]
3	Butyl acrylate	-[d]	-[d]
4	Methyl methacrylate	-[d]	-[d]

[a] Determined by SEC (PS calibration); [b] THF as eluent; [c] DMAc as eluent; [d] hardly soluble material.

4 Fluorostyrene as monomer:

^{1}H NMR (DCM-d_2): δ / ppm = 6.24 – 7.26 (9H, $H_{aromatic}$), 0.75 – 2.40 (3H, $H_{backbone}$).

^{19}F NMR (DCM-d_2): δ / ppm = -118.34 – -117.51 (1F).

Acrylonitrile as monomer:

^{1}H NMR (DMSO-d_6): δ / ppm = 6.09 – 7.80 (5H, $H_{aromatic}$), 1.12 – 3.27 (3H, $H_{backbone}$).

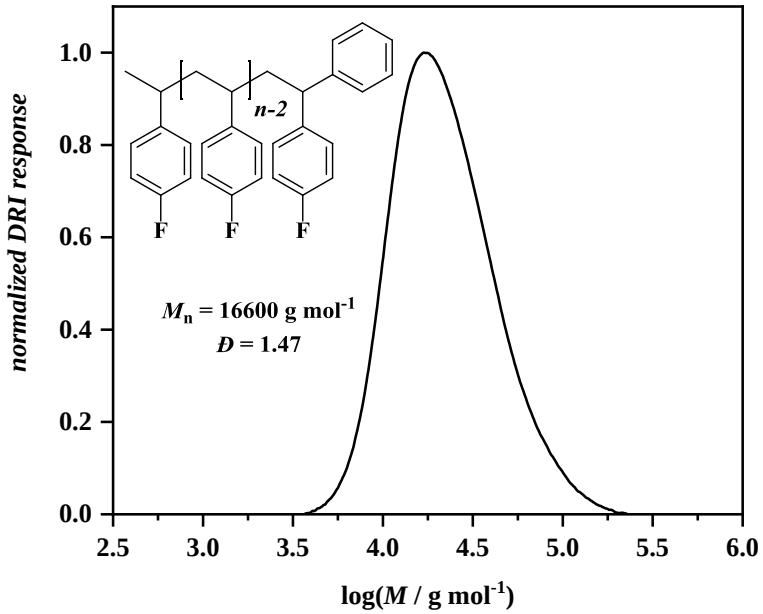

Figure 113. Size-exclusion chromatogram with THF as eluent (PS calibration) of the electrochemically-mediated nickel-catalyzed ω-functionalization using bromobenzene as aryl bromide and 4-fluorostyrene as monomer.

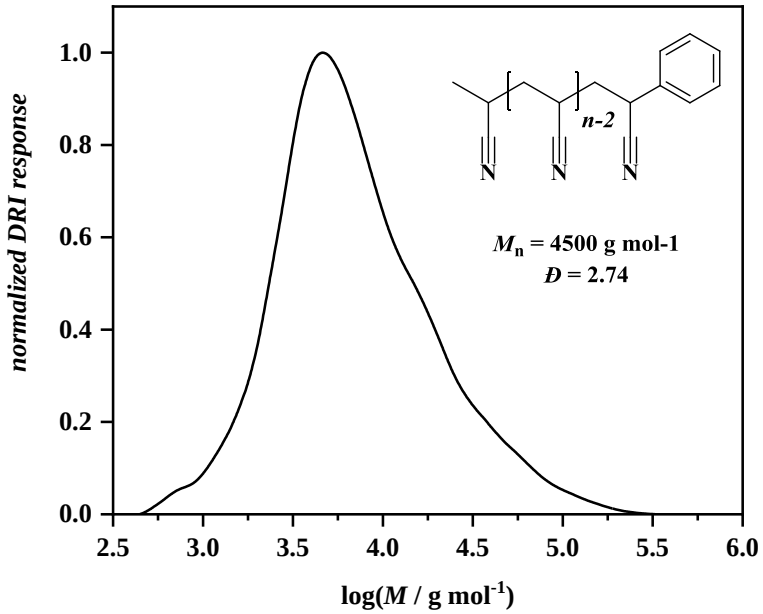

Figure 114. Size-exclusion chromatogram with DMAc as eluent (PS calibration) of the electrochemically-mediated nickel-catalyzed ω-functionalization using bromobenzene as aryl bromide and acrylonitrile as monomer.

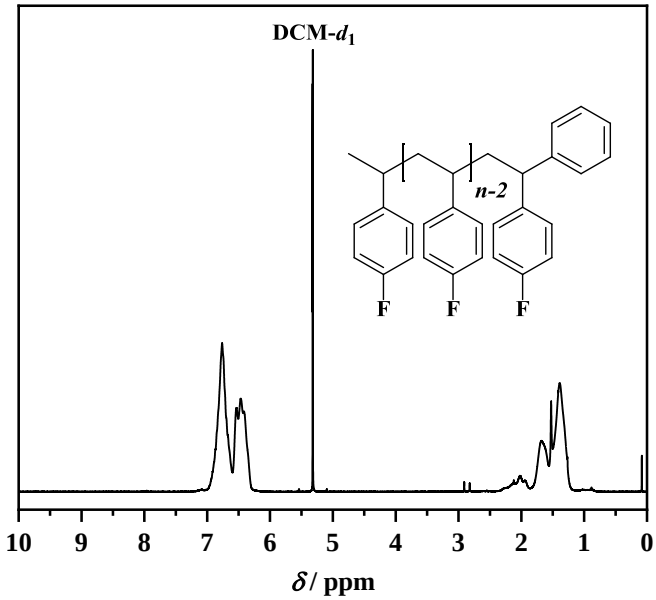

Figure 115. ^{1}H NMR spectrum of the polymer obtained after the electrochemically-mediated nickel-catalyzed ω-functionalization using bromobenzene as aryl bromide and 4-fluorostyrene as monomer; solvent: DCM-d_2.

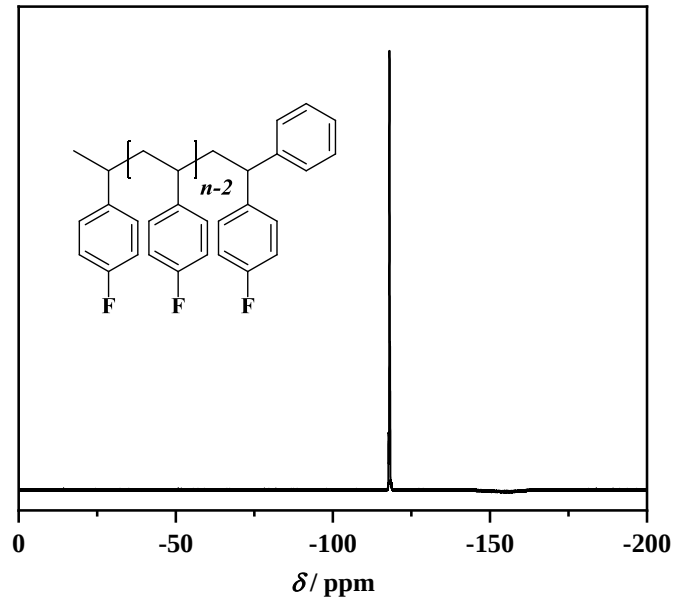

Figure 116. ^{19}F NMR spectrum of the polymer obtained after the electrochemically-mediated nickel-catalyzed ω-functionalization using bromobenzene as aryl bromide and 4-fluorostyrene as monomer; solvent: DCM-d_2.

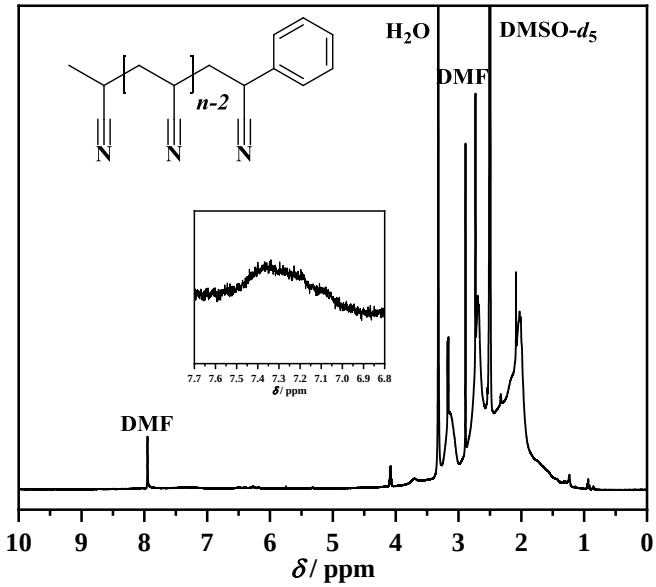

Figure 117. ^{1}H NMR spectrum of the polymer obtained after the electrochemically-mediated nickel-catalyzed ω-functionalization using bromobenzene as aryl bromide and acrylonitrile as monomer; solvent: DMSO-d_6.

6.5.1.5 Electrochemically-Mediated Nickel-Catalyzed ω-Functionalization with 4-Bromobenzotrifluoride as Aryl Bromide and 4-Fluorostyrene as Monomer

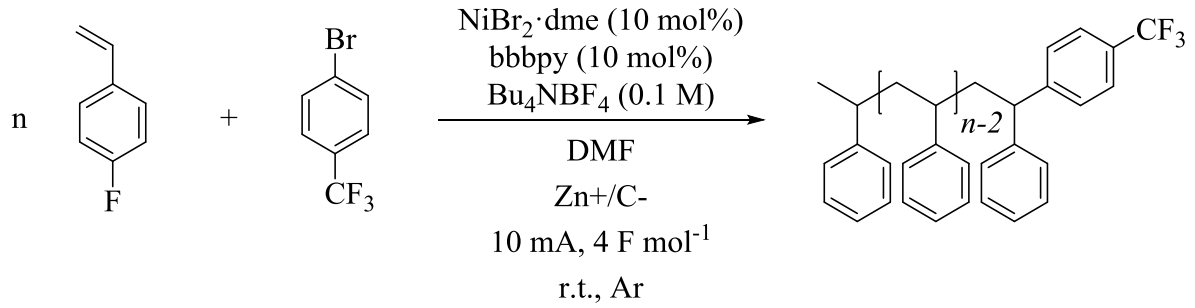

A dry ElectraSyn vial (5 mL) was charged with 4-bromobenzotrifluoride (0.043 g, 0.191 mmol, 1.00 eq.), Bu_4NBF_4 (0.066 g, 0.200 mmol), bbbpy (0.005 g, 0.019 mmol, 0.10 eq.), and $NiBr_2$·dme (0.006 g, 0.019 mmol, 0.10 eq.). The compounds were immediately after addition of the nickel complex dissolved in anhydrous DMF (2 mL). Deinhibited 4-fluorostyrene (1.1 mL, 1.17 g, 9.55 mmol, 50.0 eq.) was added. The vial was closed with the respective IKA ElectraSyn cap bearing a sacrificial zinc anode and a graphite cathode and the solution was deoxygenated by argon purging for 15 minutes. A constant current of 10 mA was applied until 4 F mol^{-1} passed through the system. Afterwards, the electrodes were rinsed with EA and the mixture was precipitated in cold methanol. Finally, the precipitate obtained by centrifugation was dissolved in THF and reprecipitated in cold methanol.

Table 15. Results of the electrochemically-mediated nickel-catalyzed ω-functionalization using 4-bromobenzotrifluoride as aryl bromide and 4-fluorostyrene as monomer.

Entry	M_n[a] g mol^{-1}	M_n[b] g mol^{-1}	$Đ$[b]
1	31100	18000	1.31

[a] Determined by ^{19}F NMR spectroscopy; [b] determined by SEC (PS calibration).

^1H NMR (THF-d_8): δ / ppm = 6.37 – 7.04 (8H, $H_{aromatic}$), 0.81 – 2.25 (3H, $H_{backbone}$).

^{19}F NMR (THF-d_8): δ / ppm = -64.96 – -64.86 (3F), -120.49 – -119.77 (1F).

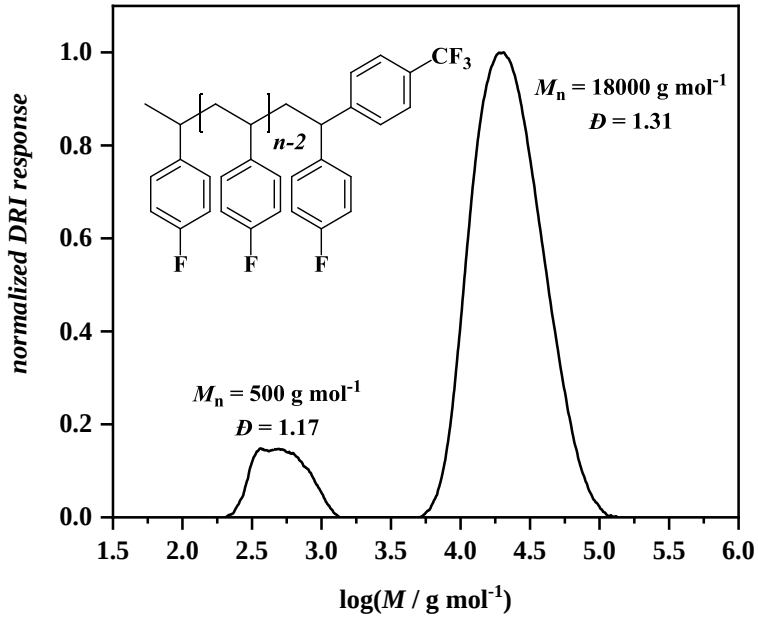

Figure 118. Size-exclusion chromatogram with THF as eluent (PS calibration) of the electrochemically-mediated nickel-catalyzed ω-functionalization using 4-bromobenzotrifluoride as aryl bromide and 4-fluorostyrene as monomer.

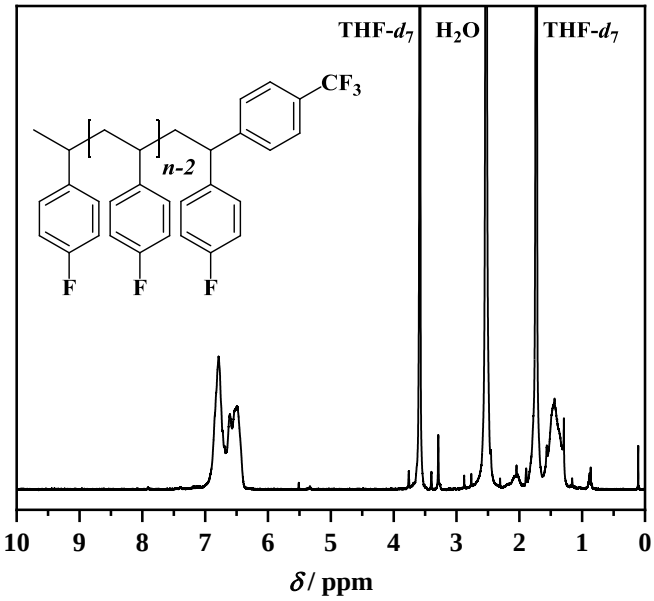

Figure 119. ^{1}H NMR spectrum of the polymer obtained after the electrochemically-mediated nickel-catalyzed ω-functionalization using 4-bromobenzotrifluoride as aryl bromide and 4-fluorostyrene as monomer; solvent: THF-d_8.

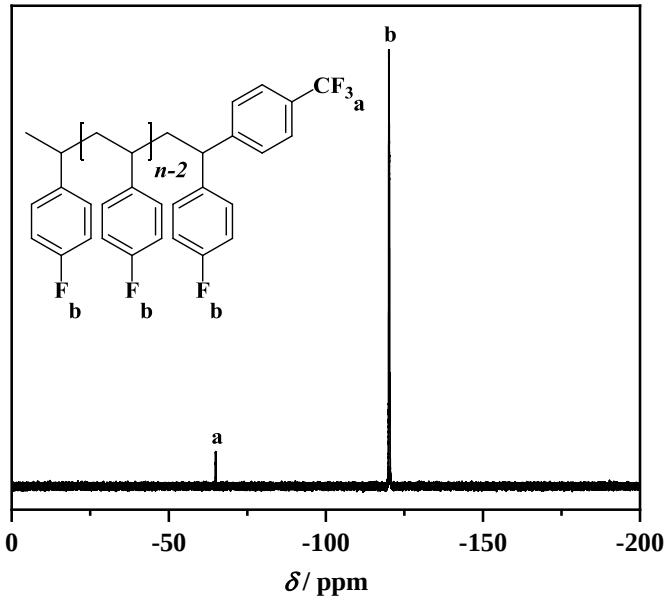

Figure 120. ^{19}F NMR spectrum of the polymer obtained after the electrochemically-mediated nickel-catalyzed ω-functionalization using 4-bromobenzotrifluoride as aryl bromide and 4-fluorostyrene as monomer; solvent: THF-d_8.

6.5.2 Polymeric Aryl Bromides for the Electrochemically-Mediated Nickel-Catalyzed ω-Functionalization

6.5.2.1 Synthesis of Poly(4-bromostyrene-*ran*-4-methylstyrene)

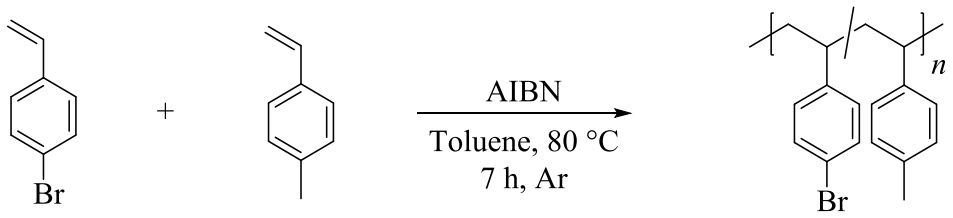

Deinhibited 4-bromostyrene (0.100 g, 0.546 mmol, 1.00 eq.), deinhibited 4-methylstyrene (0.194 g, 1.64 mmol, 3.00 eq.), and AIBN (0.036 g, 0.219 mmol, 0.40 eq.) were dissolved in anhydrous toluene (1.5 mL). The solution was deoxygenated at 0 °C by argon purging for 15 minutes. The flask was placed in a preheated oil bath at 80 °C for 7 hours. Afterwards, the polymer was precipitated in cold methanol and the precipitate obtained by centrifugation was dissolved and reprecipitated in cold methanol.

^{1}H NMR (acetone-d_6): δ / ppm = 6.17 – 7.59 (8H, $H_{aromatic}$), 2.13 – 2.47 (3H, H_{methyl}), 0.69 – 1.99 (6H, $H_{backbone}$).

ATR-FT-IR: $\tilde{\nu}$ / cm^{-1} = 3019 (C-H), 2921 (C-H), 1895, 1513, 1486, 1448, 1409, 1369, 1183, 1113, 1073, 1020, 1010, 813, 722, 643.

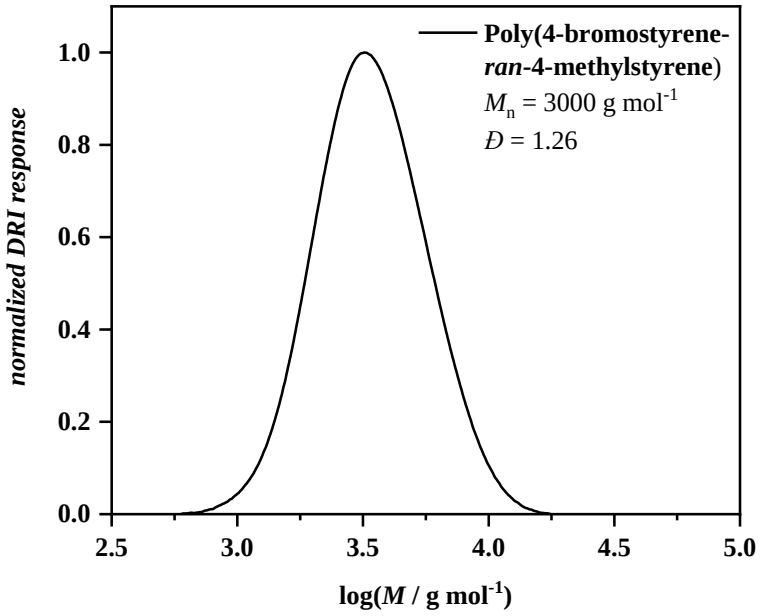

Figure 121. Size-exclusion chromatogram of poly(4-bromostyrene-*ran*-4-methylstyrene) using THF as eluent (PS calibration).

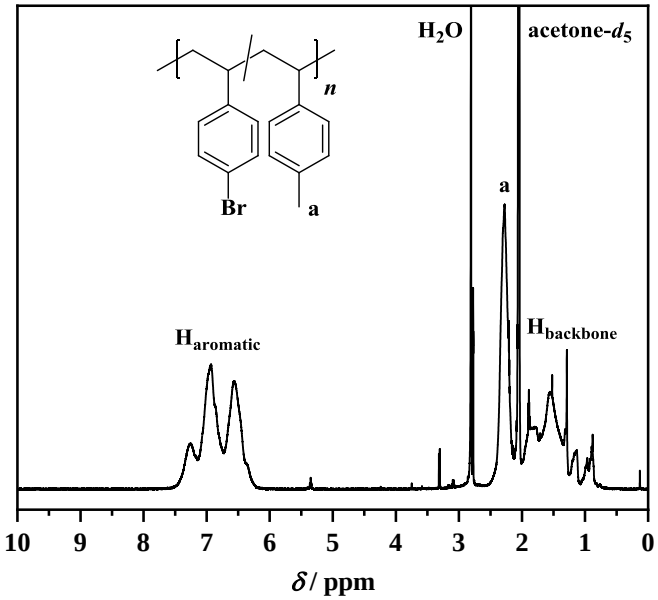

Figure 122. ^{1}H NMR spectrum of poly(4-bromostyrene-*ran*-4-methylstyrene); solvent: acetone-d_6.

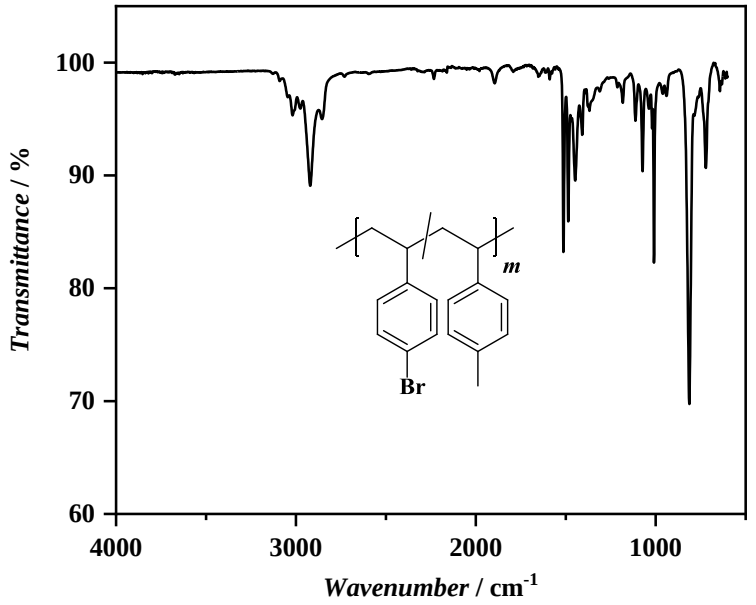

Figure 123. ATR-FT-IR spectrum of poly(4-bromostyrene-*ran*-4-methylstyrene).

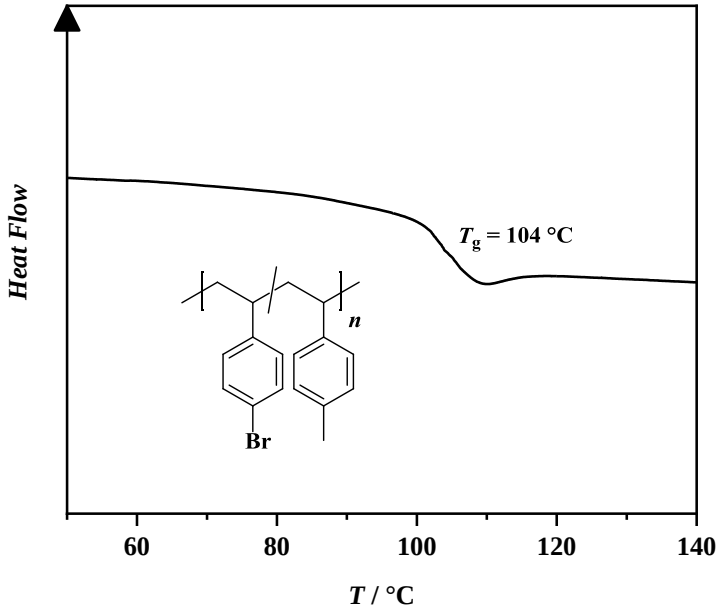

Figure 124. DSC data of poly(4-bromostyrene-*ran*-4-methylstyrene).

6.5.2.2 Poly(4-bromostyrene-*ran*-4-methylstyrene) as Aryl Bromide for the Electrochemically-Mediated Nickel-Catalyzed ω-Functionalization using 4-*Tert*-Butylstyrene as Monomer

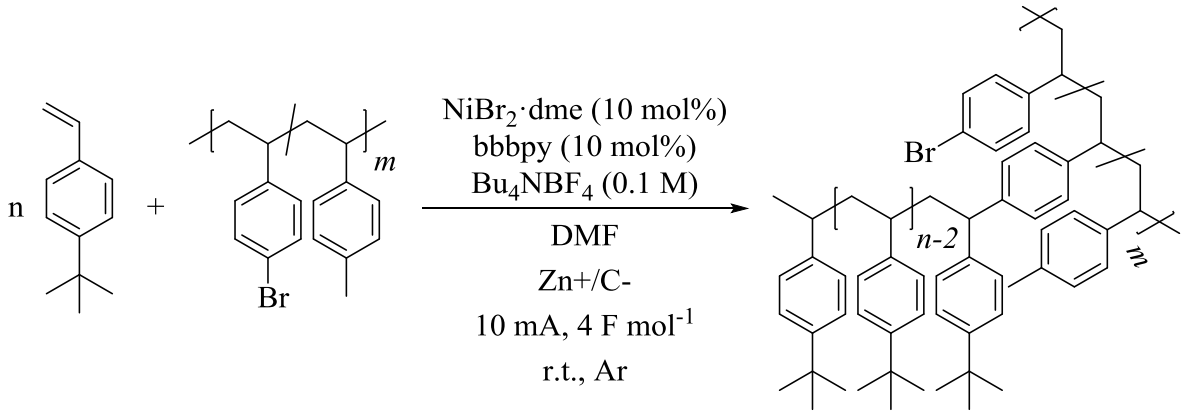

A dry ElectraSyn vial (5 mL) was charged with poly(4-bromostyrene-*ran*-4-methylstyrene) (0.035 g), Bu_4NBF_4 (0.066 g, 0.200 mmol), bbbpy (0.005 g, 0.019 mmol), and $NiBr_2$·dme (0.006 g, 0.019 mmol). The compounds were immediately after addition of the nickel complex dissolved in anhydrous DMF (2 mL). Deinhibited 4-*tert*-butylstyrene (1.75 mL, 1.53 g, 9.55 mmol) was added. The vial was closed with the respective IKA ElectraSyn cap bearing a sacrificial zinc anode and a graphite cathode and the solution was deoxygenated by argon purging for 15 minutes. A constant current of 10 mA was applied until 4 F mol^{-1} passed through the system. Afterwards, the electrodes were rinsed with EA and the mixture was precipitated in cold methanol. Finally, the precipitate obtained by centrifugation was dissolved in THF and reprecipitated in cold methanol.

^{1}H NMR (acetone-d_6): δ / ppm = 6.15 – 7.44 (12H, $H_{aromatic}$), 2.14 – 2.48 (3H, H_{methyl}), 0.77 – 1.79 (18H, $H_{backbone}$+$H_{tert\text{-}butyl}$).

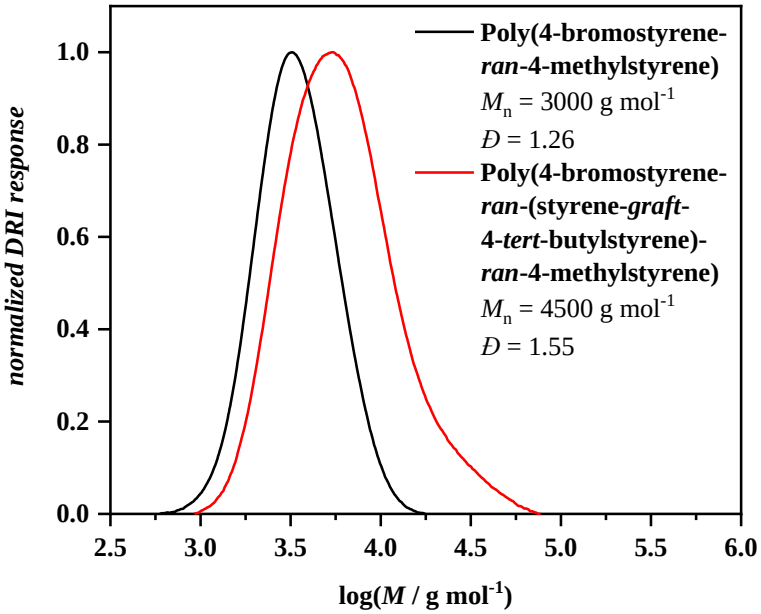

Figure 125. Comparison of the size-exclusion chromatograms (THF as eluent, PS calibration) of poly(4-bromostyrene-*ran*-4-methylstyrene) (black line) employed in the electrochemically-mediated nickel-catalyzed ω-functionalization using 4-*tert*-butylstyrene as monomer (red line).

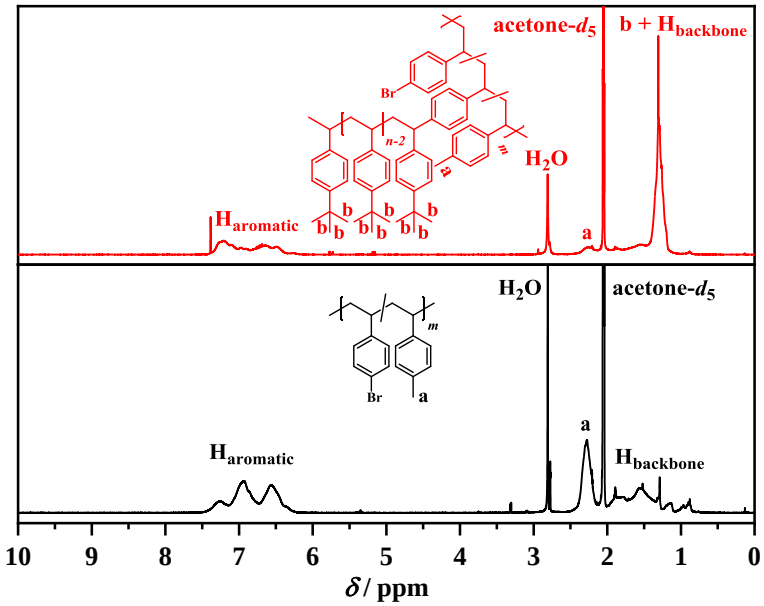

Figure 126. Comparison of the ^{1}H NMR spectra of poly(4-bromostyrene-*ran*-4-methylstyrene) (bottom, black line) employed in the electrochemically-mediated nickel-catalyzed ω-functionalization using 4-*tert*-butylstyrene as monomer (top, red line); solvent: acetone-d_6.

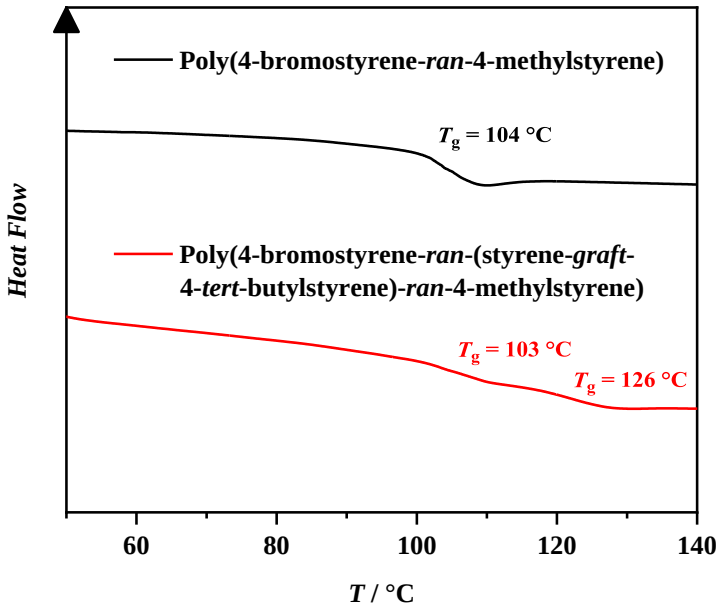

Figure 127. Comparison of the DSC results of poly(4-bromostyrene-*ran*-4-methylstyrene) (black line) employed in the electrochemically-mediated nickel-catalyzed ω-functionalization using 4-*tert*-butylstyrene as monomer (red line).

After this reaction, a control reaction in absence of 4-*tert*-butylstyrene as monomer was conducted:

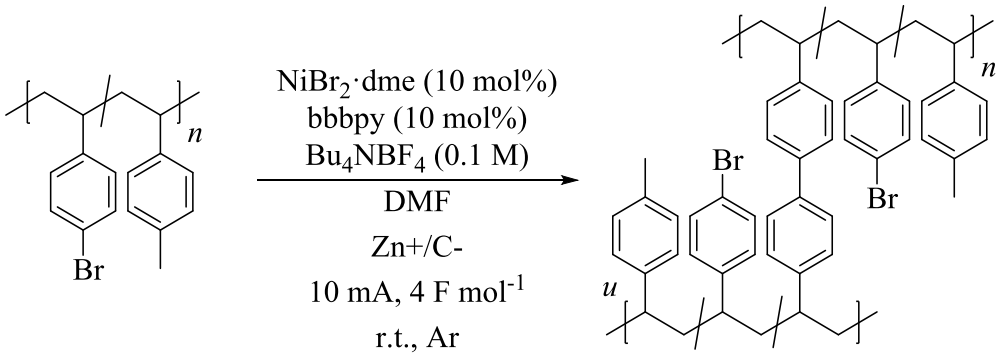

A dry ElectraSyn vial (5 mL) was charged with poly(4-bromostyrene-*ran*-4-methylstyrene) (0.035 g), Bu_4NBF_4 (0.066 g, 0.200 mmol), bbbpy (0.005 g, 0.019 mmol), and $NiBr_2$·dme (0.006 g, 0.019 mmol). The compounds were immediately after addition of the nickel complex dissolved in anhydrous DMF (2 mL). The vial was closed with the respective IKA ElectraSyn cap bearing a sacrificial zinc anode and a graphite cathode and the solution was deoxygenated by argon purging for 15 minutes. A constant current of 10 mA was applied until 4 F mol^{-1} passed through the system. Afterwards, the electrodes were rinsed with EA and the mixture was

precipitated in cold methanol. Finally, the precipitate obtained by centrifugation was reprecipitated in cold methanol, resulting in hardly soluble material.

^{1}H NMR (acetone-d_6): δ / ppm = 6.09 – 7.53 (12H, $H_{aromatic}$), 2.11 – 2.44 (3H, H_{methyl}), 0.52 – 1.74 (9H, $H_{backbone}$).

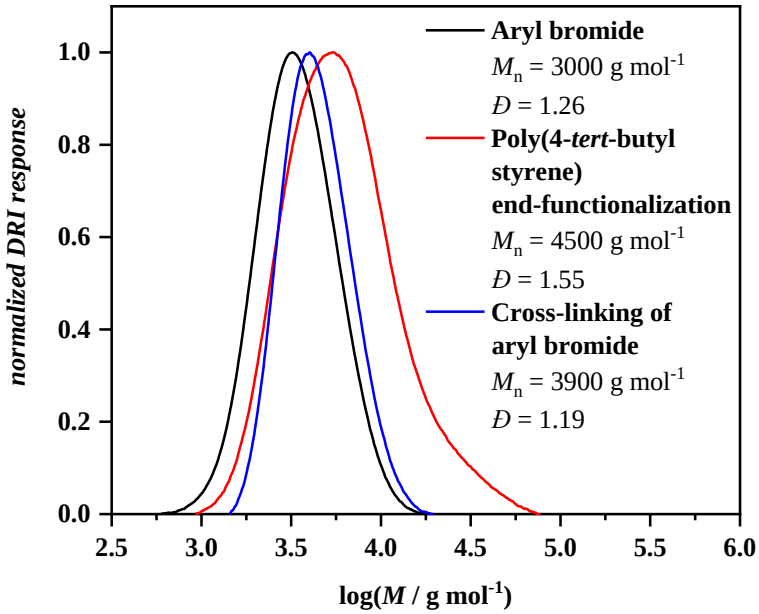

Figure 128. Comparison of the SEC traces (THF as eluent, PS calibration) of the polymeric aryl bromide (black line), the ω-functionalization of poly(4-*tert*-butylstyrene) using the latter (red line), and the control experiment in absence of a monomer (blue line).

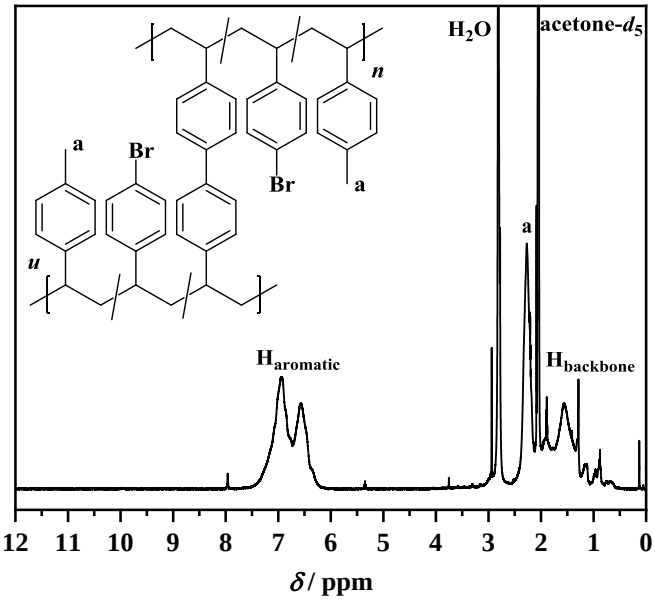

Figure 129. ^{1}H NMR spectrum of the soluble fraction obtained after the electrochemically-mediated nickel-catalyzed biaryl coupling of poly(4-bromostyrene-*ran*-4-methylstyrene) as control experiment in absence of 4-*tert*-butylstyrene as monomer; solvent: acetone-d_6.

6.5.2.3 Poly(4-bromostyrene-*ran*-4-methylstyrene) as Aryl Bromide for the Electrochemically-Mediated Nickel-Catalyzed ω-Functionalization using Acrylonitrile as Monomer

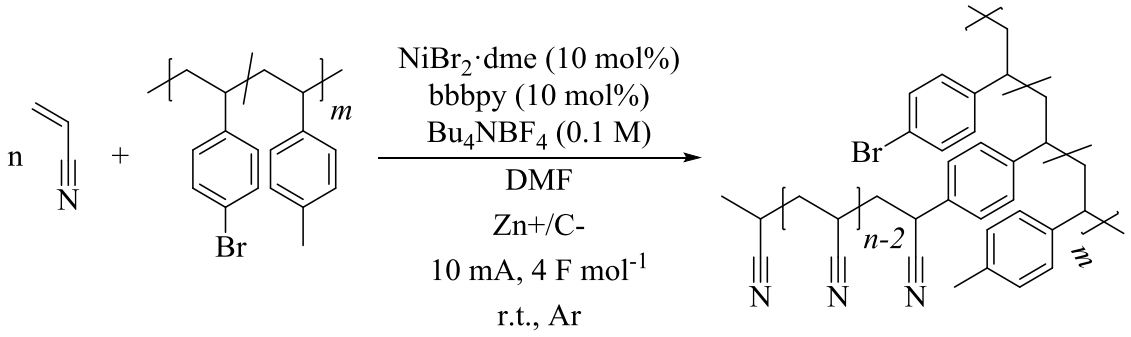

A dry ElectraSyn vial (5 mL) was charged with poly(4-bromostyrene-*ran*-4-methylstyrene) (0.035 g), Bu_4NBF_4 (0.066 g, 0.200 mmol), bbbpy (0.005 g, 0.019 mmol), and $NiBr_2$·dme (0.006 g, 0.019 mmol). The compounds were immediately after addition of the nickel complex dissolved in anhydrous DMF (2 mL). Deinhibited acrylonitrile (0.63 mL, 0.51 g, 9.55 mmol) was added. The vial was closed with the respective IKA ElectraSyn cap bearing a sacrificial zinc anode and a graphite cathode and the solution was deoxygenated by argon purging for 15 minutes. A constant current of 10 mA was applied until 4 F mol^{-1} passed through the system. Afterwards, the electrodes were rinsed with EA and the mixture was precipitated in cold methanol. Finally, the precipitate obtained by centrifugation was reprecipitated in cold methanol.

^{1}H NMR (acetone-d_6): δ / ppm = 6.29 – 7.58 (12H, $H_{aromatic}$), 0.79 – 3.42 (15H, $H_{backbone}$+H_{methyl}).

^{1}H NMR (DMSO-d_6): δ / ppm = 6.14 – 7.55 (12H, $H_{aromatic}$), 0.82 – 3.88 (15H, $H_{backbone}$+H_{methyl}).

ATR-FT-IR: $\tilde{\nu}$ / cm^{-1} = 2921 (C-H), 2244 (C≡N), 1661 (DMF), 1512, 1486, 1447, 1182, 1073, 1010, 813, 722, 659.

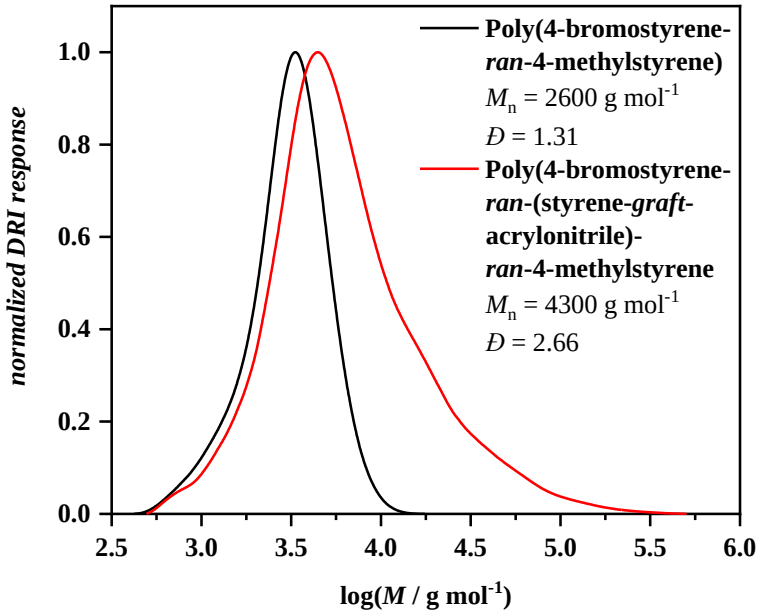

Figure 130. Comparison of the size-exclusion chromatograms (DMAc as eluent, PS calibration) of poly(4-bromostyrene-*ran*-4-methylstyrene) (black line) employed in the electrochemically-mediated nickel-catalyzed ω-functionalization using acrylonitrile as monomer (red line).

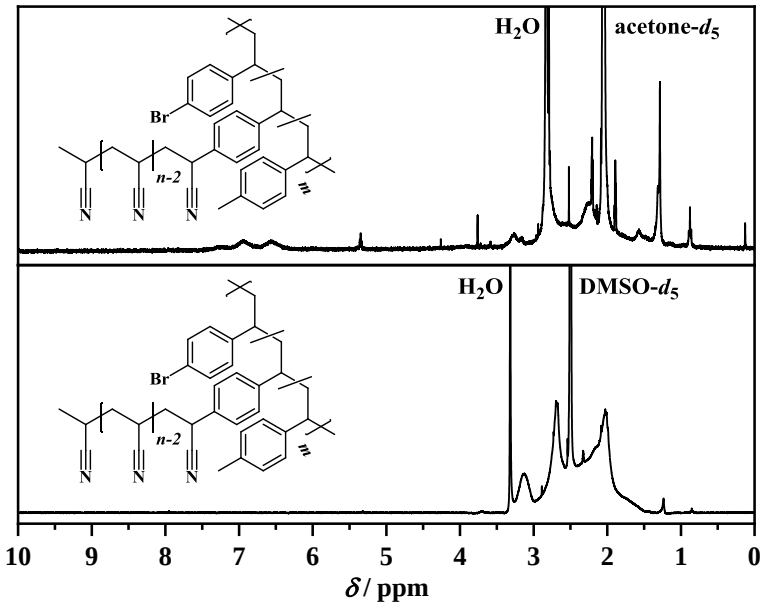

Figure 131. Comparison of the ^{1}H NMR spectra of the polymer obtained after the electrochemically-mediated nickel-catalyzed ω-functionalization using acrylonitrile as monomer and poly(4-bromostyrene-*ran*-4-methylstyrene); solvents: DMSO-d_6 (bottom); acetone-d_6 (top).

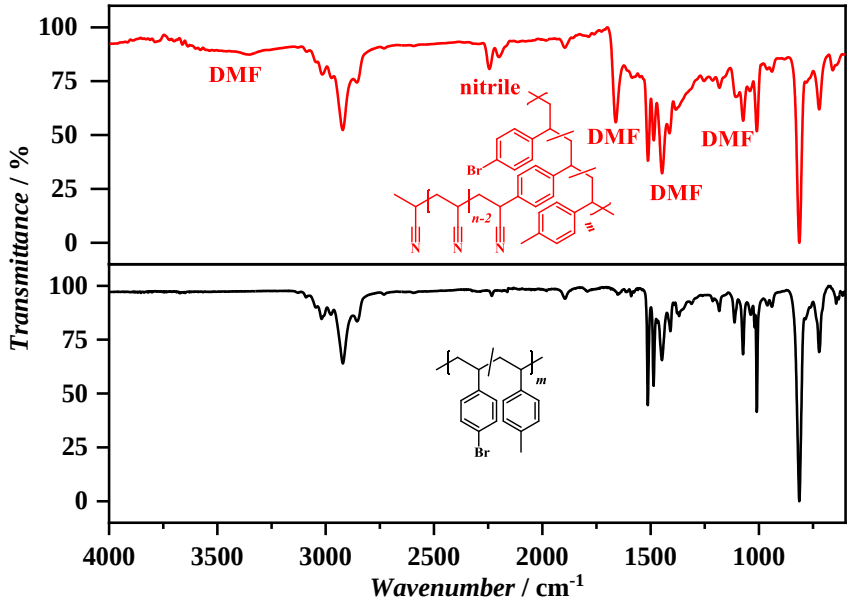

Figure 132. Comparison of the IR spectra of poly(4-bromostyrene-*ran*-4-methylstyrene) (bottom, black line) employed in the electrochemically-mediated nickel-catalyzed ω-functionalization using acrylonitrile as monomer (top, red line).

6.6 Procedures for the Synthesis and Post-Polymerization Modification of Poly(*N*-(4-vinylphenyl)sulfonamide)s

6.6.1 Synthesis Procedures of Aromatic Sulfonamide Monomers M1-M4

6.6.1.1 Synthesis of *N*-(4-Vinylphenyl)benzenesulfonamide (M1)

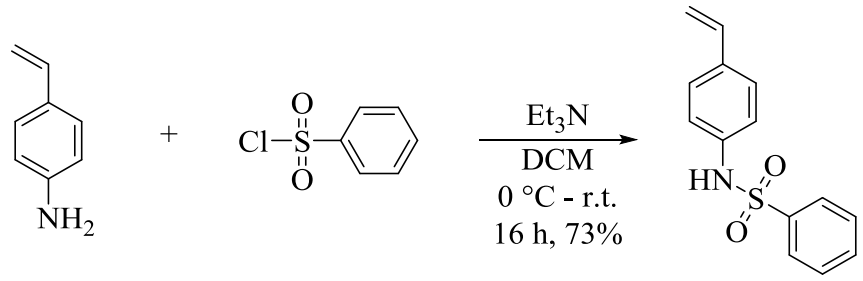

4-Vinylaniline (0.98 mL, 1.00 g, 8.39 mmol, 1.00 eq.) was dissolved in anhydrous DCM (20 mL) and the solution was cooled to 0 °C. Triethylamine (1.28 mL, 0.93 g, 9.23 mmol, 1.10 eq.) and benzenesulfonyl chloride (1.18 mL, 1.63 g, 9.23 mmol, 1.10 eq.) were added and the mixture was stirred at 0 °C for 1 hour and at room temperature for 15 hours. DCM (30 mL) was added and the organic phase was washed with 1 M HCl solution (50 mL) and with water (3 × 50 mL). Subsequently, the organic phase was dried over magnesium sulfate and the solvent was removed under reduced pressure. Finally, the crude product was purified by column chromatography using a 6:1 mixture of CH / EA giving a yellowish solid (1.58 g, 6.10 mmol, 73%).

R_f (CH / EA 6:1) = 0.21

^{1}H NMR (acetone-d_6): δ / ppm = 9.04 (s, 1H, H_e), 7.78 – 7.84 (m, 2H, H_f), 7.57 – 7.63 (m, 1H, H_h), 7.49 – 7.56 (m, 2H, H_g), 7.32 – 7.38 (m, 2H, H_c), 7.16 – 7.021 (m, 2H, H_d), 6.66 (dd, J = 17.6, 10.9 Hz, 1H, H_b), 5.70 (dd, J = 17.6, 1.0 Hz, 1H, H_a), 5.15 (dd, J = 10.9, 1.0 Hz, 1H, H_a).

^{13}C NMR ($CDCl_3$): δ / ppm = 139.08, 135.90, 135.03, 133.21, 129.21, 127.35, 127.27, 121.83, 113.95.

ATR-FT-IR: $\tilde{\nu}$ / cm^{-1} = 3235 (N-H), 2927 (C-H), 2859, 1631 (N-H), 1607, 1509 (N-H), 1464, 1446, 1420, 1397, 1326 (S=O), 1293, 1229, 1184, 1153 (S=O), 1124, 1089, 994, 910 (S-N), 851, 834, 746, 718, 680, 637, 602, 593, 573, 546.

ESI-MS: *m/z*: $[M + Na]^+$ calculated for $[C_{14}H_{13}NNaO_2S]^+$, 282.0559; found: 282.0558.

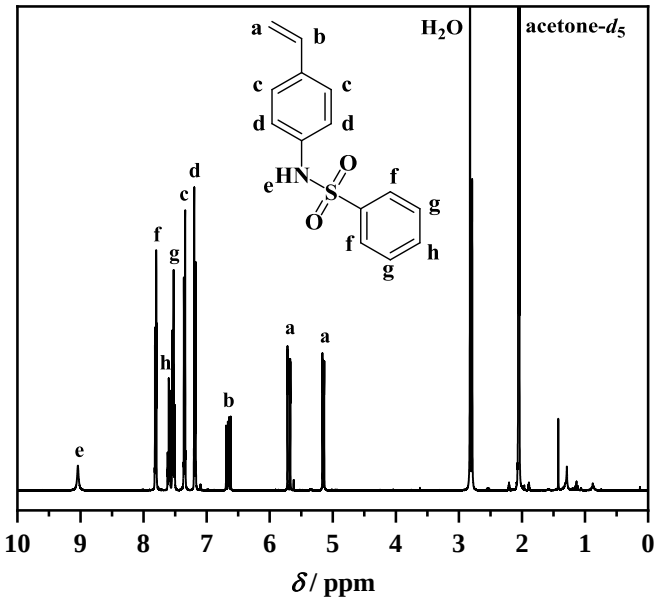

Figure 133. ^{1}H NMR spectrum of *N*-(4-vinylphenyl)benzenesulfonamide (M1); solvent: acetone-d_6.

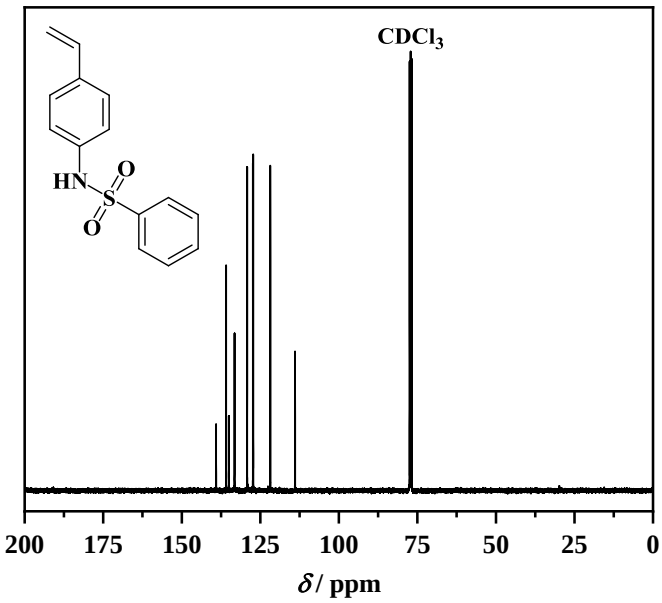

Figure 134. ^{13}C NMR spectrum of *N*-(4-vinylphenyl)benzenesulfonamide (M1); solvent: $CDCl_3$.

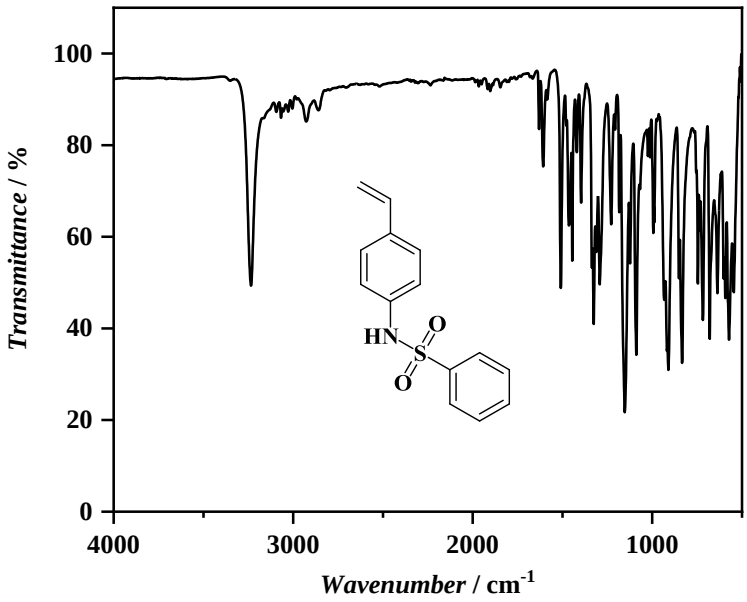

Figure 135. ATR-FT-IR spectrum of *N*-(4-vinylphenyl)benzenesulfonamide (M1).

6.6.1.2 Synthesis of 4-Methyl-*N*-(4-vinylphenyl)benzenesulfonamide (M2)

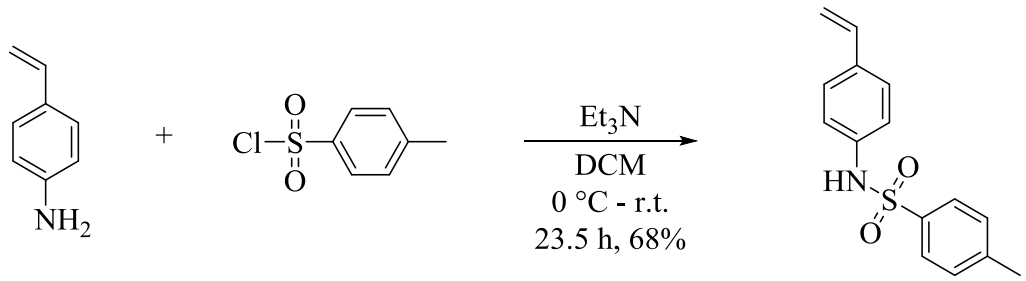

4-Methylbenzenesulfonyl chloride (1.68 g, 8.81 mmol, 1.05 eq.) was taken up in anhydrous DCM (20 mL). The mixture was cooled by an ice bath to 0 °C and triethylamine (1.22 mL, 0.89 g, 8.81 mmol, 1.05 eq.) and 4-vinylaniline (0.98 mL, 1.00 g, 8.39 mmol, 1.00 eq.) were added to the stirred solution. Then, the mixture was stirred at 0 °C for 1 hour and at room temperature for 22.5 hours. Afterwards, the reaction mixture was diluted with DCM (30 mL) and the organic phase was washed with 1 M HCl (50 mL) and with water (2 × 50 mL). Subsequently, the organic phase was dried over magnesium sulfate and the solvent was evaporated under reduced pressure. Finally, the crude product was purified by column chromatography using CH and EA in a ratio of 4:1 giving a yellowish solid (1.56 g, 5.70 mmol, 68%).

R_f (CH / EA 4:1) = 0.26

^{1}H NMR ($CDCl_3$): δ / ppm = 7.63 – 7.68 (m, 2H, H_f), 7.19 – 7.30 (m, 4H, H_g+H_c), 7.00 – 7.04 (m, 2H, H_d), 6.56 – 6.76 (b, 1H H_e), 6.62 (dd, *J* = 17.6, 10.9 Hz, 1H, H_b), 5.64 (d, *J* = 17.7 Hz, 1H, H_a), 5.20 (d, *J* = 10.9 Hz, 1H, H_a), 2.37 (s, 3H, H_h).

^{13}C NMR ($CDCl_3$): δ / ppm = 144.08, 136.12, 135.95, 134.80, 129.82, 127.41, 127.41, 121.58, 113.79, 21.67.

ATR-FT-IR: $\tilde{\nu}$ / cm^{-1} = 3275 (N-H), 2923 (C-H), 2853, 1598, 1506 (N-H), 1442, 1416, 1391, 1332 (S=O), 1291, 1272, 1222, 1183, 1157 (S=O), 1112, 1090, 1020, 993, 903 (S-N), 859, 813, 765, 737, 704, 675, 616, 575, 555, 539.

ESI-MS: *m/z*: $[M + Na]^+$ calculated for $[C_{15}H_{15}NNaO_2S]^+$, 296.0716; found: 296.0715.

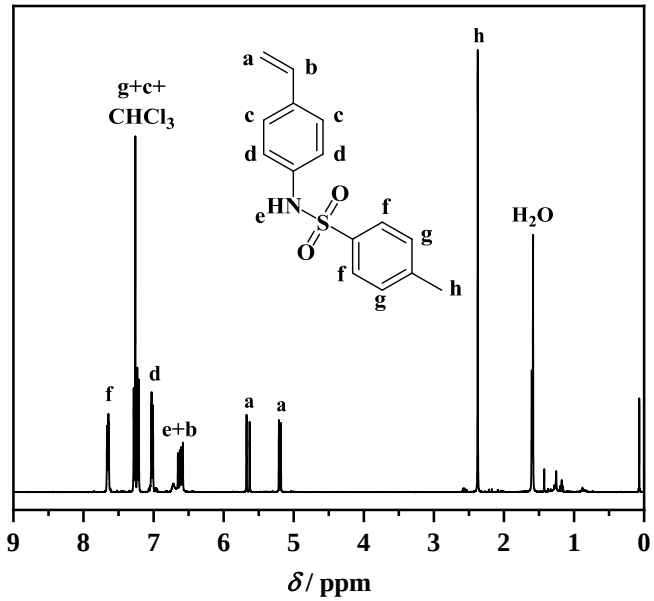

Figure 136. ^{1}H NMR spectrum of 4-methyl-*N*-(4-vinylphenyl)benzenesulfonamide (M2); solvent: $CDCl_3$.

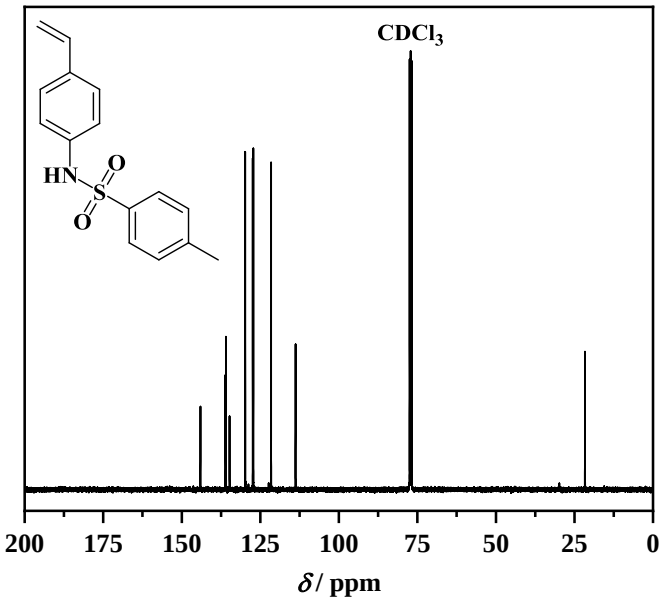

Figure 137. ^{13}C NMR spectrum of 4-methyl-*N*-(4-vinylphenyl)benzenesulfonamide (M2); solvent: $CDCl_3$.

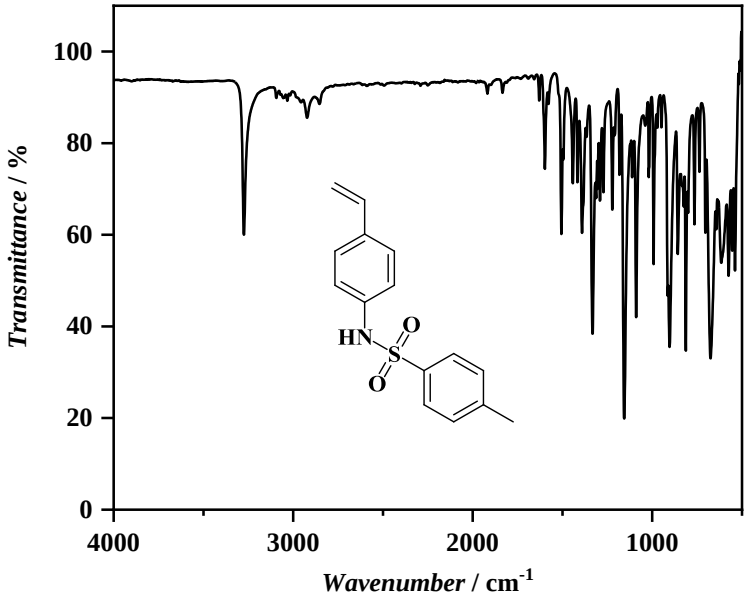

Figure 138. ATR-FT-IR spectrum of 4-methyl-*N*-(4-vinylphenyl)benzenesulfonamide (M2).

6.6.1.3 Synthesis of 4-Fluoro-*N*-(4-vinylphenyl)benzenesulfonamide (M3)

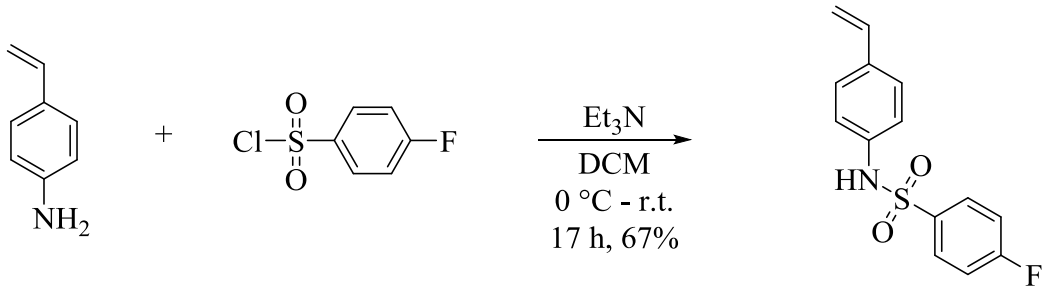

4-Fluorobenzenesulfonyl chloride (1.80 g, 9.23 mmol, 1.10 eq.) was taken up in anhydrous DCM (20 mL). The mixture was cooled by an ice bath to 0 °C and triethylamine (1.28 mL, 0.93 g, 9.23 mmol, 1.10 eq.) and 4-vinylaniline (0.98 mL, 1.00 g, 8.39 mmol, 1.00 eq.) were added to the stirred solution. Then, the mixture was stirred at 0 °C for 1 hour and at room temperature for 16 hours. Afterwards, the reaction mixture was diluted with DCM (30 mL) and the organic phase was washed with 1 M HCl (50 mL) and with water (3 × 50 mL). Subsequently, the organic phase was dried over magnesium sulfate and the solvent was evaporated under reduced pressure. Finally, the crude product was purified by column chromatography using PE and EA in a ratio of 6:1 to 4:1 giving a yellowish solid (1.56 g, 5.64 mmol, 67%).

R_f (PE / EA 6:1) = 0.17

^{1}H NMR (acetone-d_6): δ / ppm = 9.06 (bs, 1H, H_e), 7.80 – 7.90 (m, 2H, H_f), 7.34 – 7.39 (m, 2H, H_c), 7.25 – 7.33 (m, 2H, H_g), 7.16 – 7.21 (m, 2H, H_d), 6.66 (d, J = 17.17, 10.9 Hz, 1H, H_b), 5.71 (d, J = 17.6, 0.9 Hz, 1H, H_a), 5.16 (d, J = 10.9, 0.9 Hz, 1H, H_a).

^{13}C NMR ($CDCl_3$): δ / ppm = 166.68, 164.14, 135.82, 135.63, 135.30, 135.04, 135.00, 130.19, 130.10, 127.35, 122.03, 116.62, 116.39, 114.17.

^{19}F NMR (acetone-d_6): δ / ppm = -107.48 (m).

ATR-FT-IR: $\tilde{\nu}$ / cm^{-1} = 3235 (N-H), 2922 (C-H), 2855, 1629 (N-H), 1591, 1509 (N-H), 1493, 1455, 1421, 1394, 1335 (S=O), 1313, 1292, 1278, 1236, 1167, 1153 (S=O), 1122, 1089, 1015, 999, 911 (S-N), 856, 832, 767, 743, 709, 690, 628, 589, 551, 539.

ESI-MS: *m/z*: $[M + Na]^+$ calculated for $[C_{14}H_{11}FNNaO_2S]^+$, 300.0465; found: 300.0466.

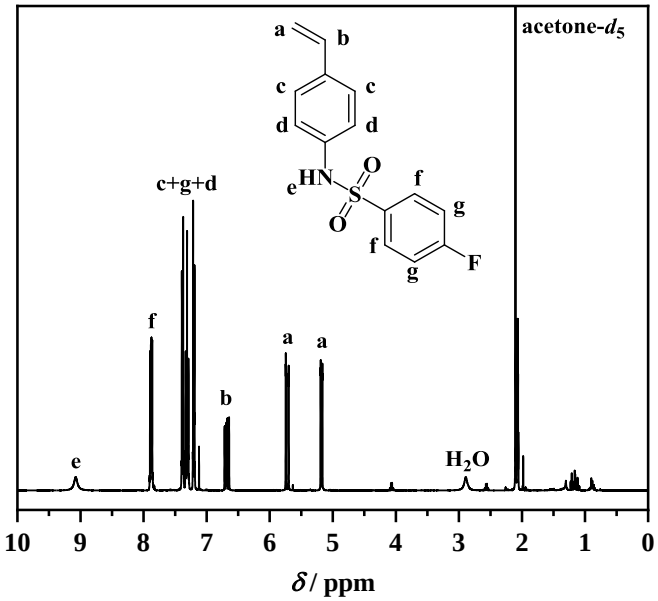

Figure 139. ^{1}H NMR spectrum of 4-fluoro-*N*-(4-vinylphenyl)benzenesulfonamide (M3); solvent: acetone-d_6.

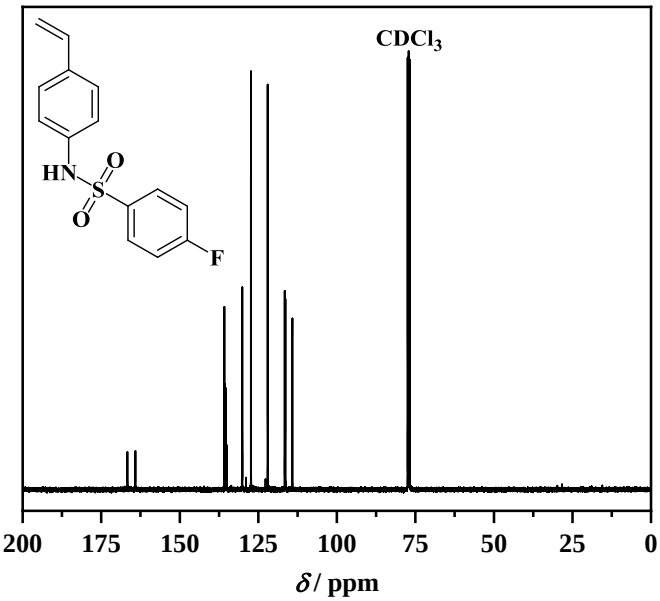

Figure 140. ^{13}C NMR spectrum of 4-fluoro-*N*-(4-vinylphenyl)benzenesulfonamide (M3); solvent: $CDCl_3$.

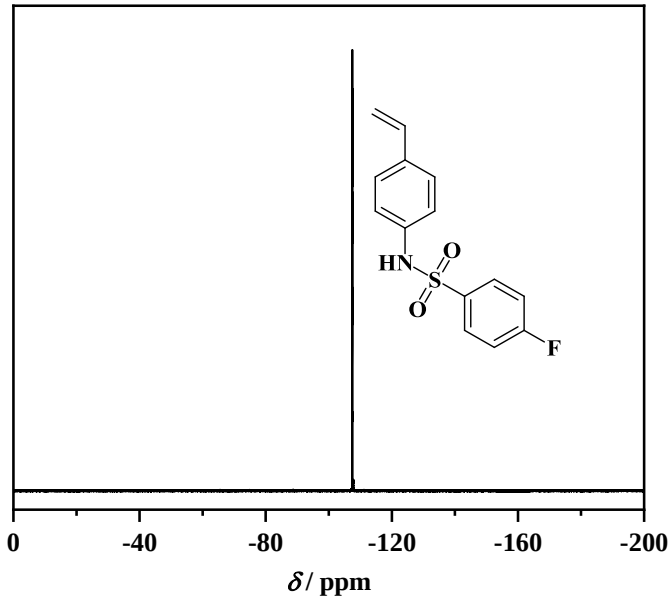

Figure 141. ^{19}F NMR spectrum of 4-fluoro-*N*-(4-vinylphenyl)benzenesulfonamide (M3); solvent: acetone-d_6.

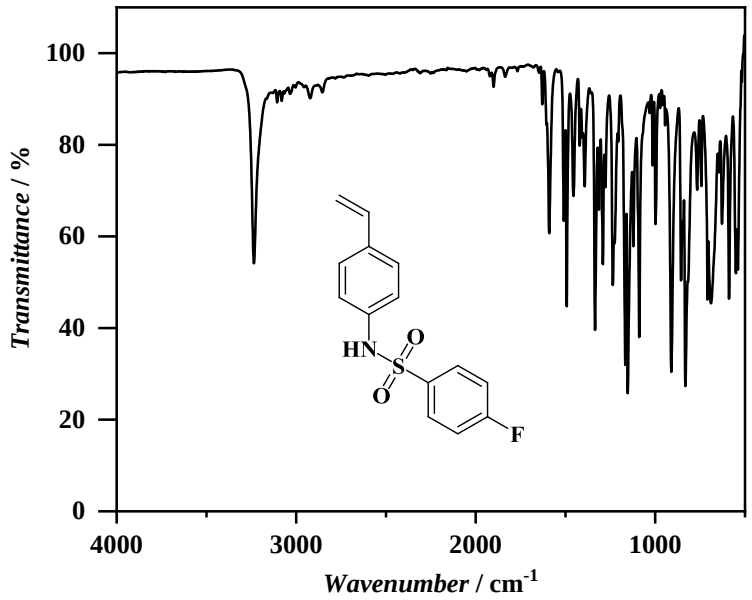

Figure 142. ATR-FT-IR spectrum of 4-fluoro-*N*-(4-vinylphenyl)benzenesulfonamide (M3).

6.6.1.4 Synthesis of 4-Nitro-*N*-(4-vinylphenyl)benzenesulfonamide (M4)

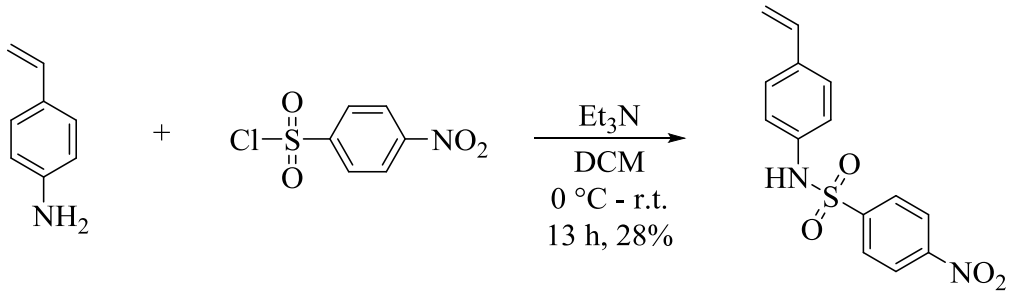

4-Nitrobenzenesulfonyl chloride (2.05 g, 9.23 mmol, 1.10 eq.) was taken up in anhydrous DCM (20 mL). The mixture was cooled by an ice bath to 0 °C and triethylamine (1.28 mL, 0.93 g, 9.23 mmol, 1.10 eq.) and 4-vinylaniline (0.98 mL, 1.00 g, 8.39 mmol, 1.00 eq.) were added to the stirred solution. Then, the mixture was stirred at 0 °C for 1 hour and at room temperature for 12 hours. Afterwards, the reaction mixture was diluted with DCM (30 mL) and the organic phase was washed with HCl conc. (0.5 mL) in water (50 mL) and three times with water (50 mL). Subsequently, the organic phase was dried over magnesium sulfate and the solvent was evaporated under reduced pressure. Finally, the crude product was purified by column chromatography using a 5:1 mixture of CH / EA giving a brownish solid (0.72 g, 2.36 mmol, 28 %).

R_f (CH / EA 5:1) = 0.17

^{1}H NMR (acetone-d_6): δ / ppm = 9.33 (bs, 1H, H_e), 8.36 – 8.41 (m, 2H, H_g), 8.02 – 8.09 (m, 2H, H_f), 7.36 – 7.42 (m, 2H, H_c), 7.18 – 7.23 (m, 2H, H_d), 6.67 (dd, J = 17.6, 11.0 Hz, 1H, H_b), 5.72 (dd, J = 17.6, 0.9 Hz, 1H, H_a), 5.18 (dd, J = 11.0, 0.1 Hz, 1H, H_a).

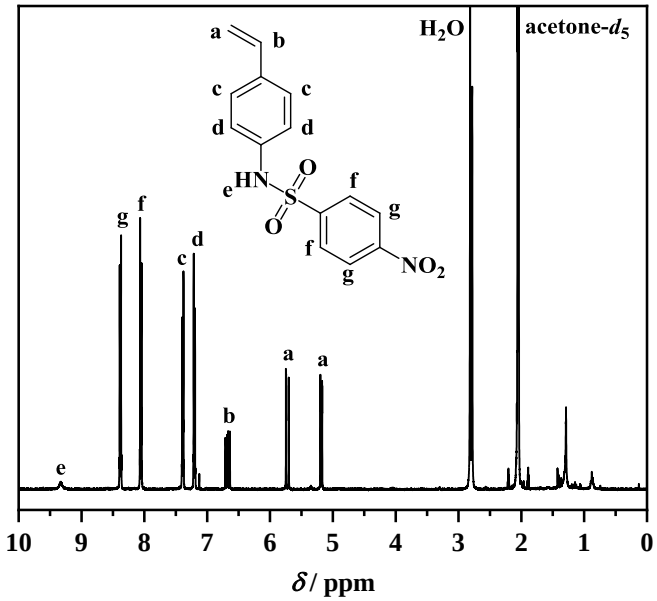

Figure 143. ^{1}H NMR spectrum of 4-nitro-*N*-(4-vinylphenyl)benzenesulfonamide (M4); solvent: acetone-d_6.

6.6.2 Synthesis Procedure of Methacrylate-Based Sulfonamide Monomer (M5)

6.6.2.1 Synthesis of *N*-(3-Hydroxypropyl)-4-methylbenzenesulfonamide

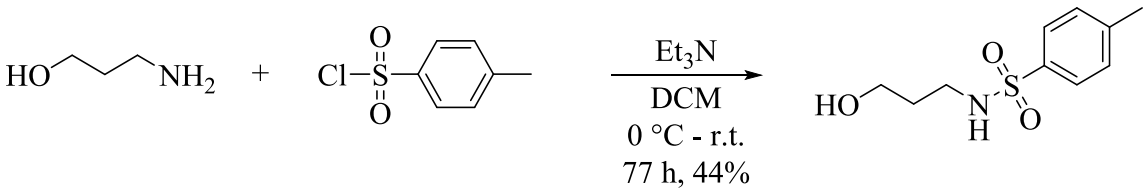

4-Methylbenzenesulfonyl chloride (6.98 g, 36.6 mmol, 1.10 eq.) was given into a dry roundbottom flask and taken up with anhydrous DCM (75 mL). The mixture was cooled by an ice bath to 0 °C and 3-aminopropanol (2.55 mL, 2.50 g, 33.3 mmol, 1.00 eq.) was added. Triethylamine (5.08 mL, 3.70 g, 36.6 mmol, 1.10 eq.) was added to the stirred solution. Then, the mixture was stirred at 0 °C for 1 hour and at room temperature for 76 hours. Afterwards, the reaction mixture was washed once with water (200 mL). The aqueous phase was extracted with EA (3 x 150 mL). Subsequently, the combined organic phases were dried over magnesium sulfate and the solvent was evaporated under reduced pressure. Finally, the crude product was purified by column chromatography using a 3:2 to 1:1 mixture of CH and EA yielding a white solid (3.36 g, 14.67 mmol, 44%).

R_f (CH / EA 3:2) = 0.09

^{1}H NMR ($CDCl_3$): δ / ppm = 7.68 – 7.76 (m, 2H, H_e), 7.26 – 7.31 (m, 2H, H_f), 5.49 (bs, 1H, H_d), 3.67 (t, J = 5.8 Hz, 2H, H_a), 3.04 (t, J = 6.3 Hz, 2H, H_c), 2.40 (s, 3H, H_g), 1.67 (p, J = 6.5 Hz, 3H, H_b).

^{13}C NMR ($CDCl_3$): δ / ppm = 143.49, 136.83, 129.82, 127.12, 60.38, 40.91, 31.59, 21.57.

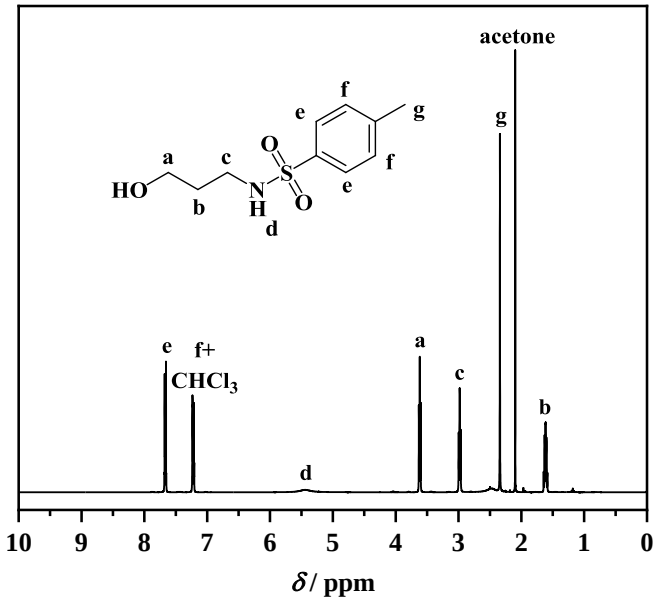

Figure 144. ^{1}H NMR spectrum of *N*-(3-hydroxypropyl)-4-methylbenzenesulfonamide; solvent: $CDCl_3$.

6.6.2.2 Synthesis of 3-((4-Methylphenyl)sulfonamide)propyl Methacrylate (M5)

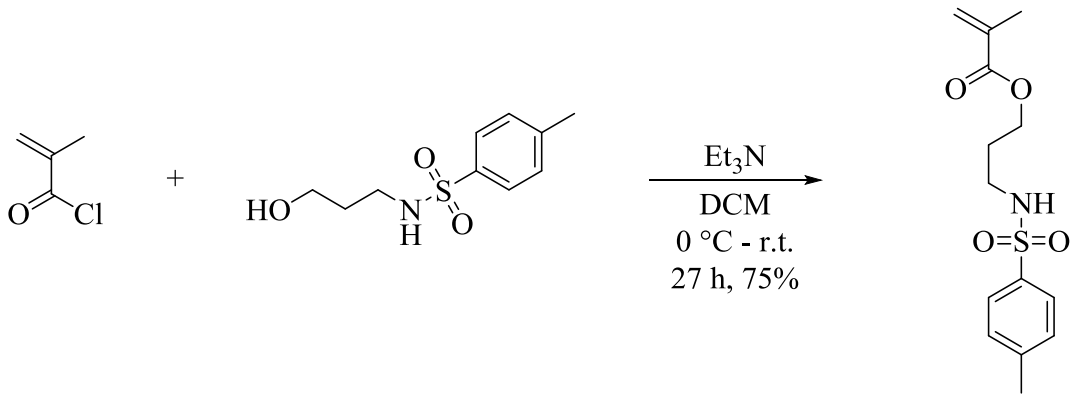

To a cold mixture of *N*-(3-hydroxypropyl)-4-methylbenzenesulfonamide (1.50 g, 6.54 mmol, 1.00 eq.) in anhydrous DCM (10 mL) in a dry roundbottom flask, triethylamine (2.63 mL, 1.92 g, 19.0 mmol, 2.90 eq.) was added and the mixture was deoxygenated by argon purging for 15 minutes. Methacryloyl chloride (0.77 mL, 0.82 g, 7.85 mmol, 1.20 eq.) in anhydrous DCM (10 mL) was added over 15 minutes. The mixture was stirred at 0 °C for 1 hour and afterwards at room temperature for 26 hours. DCM (100 mL) and water (100 mL) were added and the mixture was acidified by the addition of concentrated hydrochloric acid (2 mL). The aqueous phase was extracted with DCM (100 mL) three times. Subsequently, the combined organic phases were dried over magnesium sulfate and the solvent was evaporated under reduced pressure. Finally, the crude product was purified by column chromatography starting from a 3:1 mixture of CH / EA going to a 2:1 mixture yielding a yellowish oil (1.46 g, 4.92 mmol, 75%).

R_f (CH / EA 3:1) = 0.2

^{1}H NMR ($CDCl_3$): δ / ppm = 7.71 – 7.76 (m, 2H, H_g), 7.27 – 7.31 (m, 2H, H_h), 6.02 – 6.05 (m, 1H, H_a), 5.53 – 5.56 (m, 1H, H_a), 4.95 – 5.02 (m, 1H, H_f), 4.16 (t, J = 6.0 Hz, 2H, H_c), 3.02 (q, J = 6.6 Hz, 2H, H_e), 2.41 (s, 3H, H_i), 1.88 – 1.90 (m, 3H, H_b), 1.84 (q, J = 6.5 Hz, 2H, H_d).
^{13}C NMR ($CDCl_3$): δ / ppm = 167.50, 143.59, 136.96, 136.10, 129.85, 127.19, 126.00, 61.74, 40.14, 29.07, 21.62, 18.37.

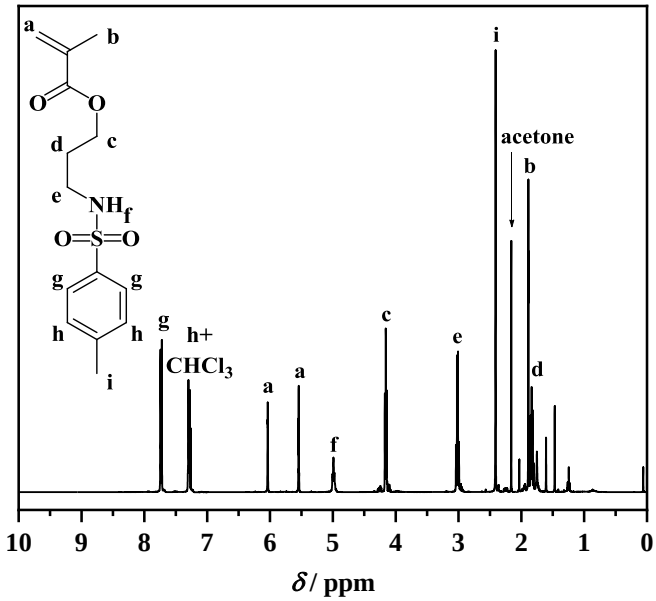

Figure 145. ^{1}H NMR spectrum of 3-((4-methylphenyl)sulfonamide)propyl methacrylate (M5); solvent: $CDCl_3$.

6.6.3 Free Radical Polymerization Procedures of Aromatic Sulfonamide Monomers M1-M4

6.6.3.1 Free Radical Polymerization of *N*-(4-Vinylphenyl)benzenesulfonamide (M1)

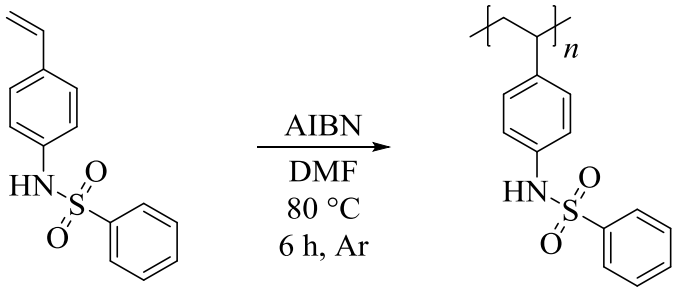

M1 **P1**

N-(4-Vinylphenyl)benzenesulfonamide (M1) (0.200 g, 0.771 mmol, 1.00 eq.) and AIBN (0.025 g, 0.154 mmol, 0.20 eq.) were dissolved in anhydrous DMF (1 mL). The solution was deoxygenated by argon purging for 15 minutes. The flask was placed in a preheated oil bath at 80 °C for 6 hours. Afterwards, polymer P1 was precipitated in cold diethyl ether, redissolved and precipitated again in cold diethyl ether giving a colorless solid (0.10 g).

^{1}H NMR (acetone-d_6): δ / ppm = 8.63 – 9.05 (1H, H_a), 7.62 – 7.88 (2H, H_b), 7.17 – 7.61 (4H, H_c+H_d), 6.74 – 7.15 (2H, H_e), 6.03 – 6.72 (2H, H_f), 0.70 – 1.81 (3H, H_g+H_h).
ATR-FT-IR: $\tilde{\nu}$ / cm^{-1} = 3258 (N-H), 2924 (C-H), 2848, 1657, 1612, 1510 (N-H), 1448, 1396, 1327 (S=O), 1292, 1223, 1157 (S=O), 1091, 918 (S-N), 833, 754, 723, 688, 640, 580, 554.

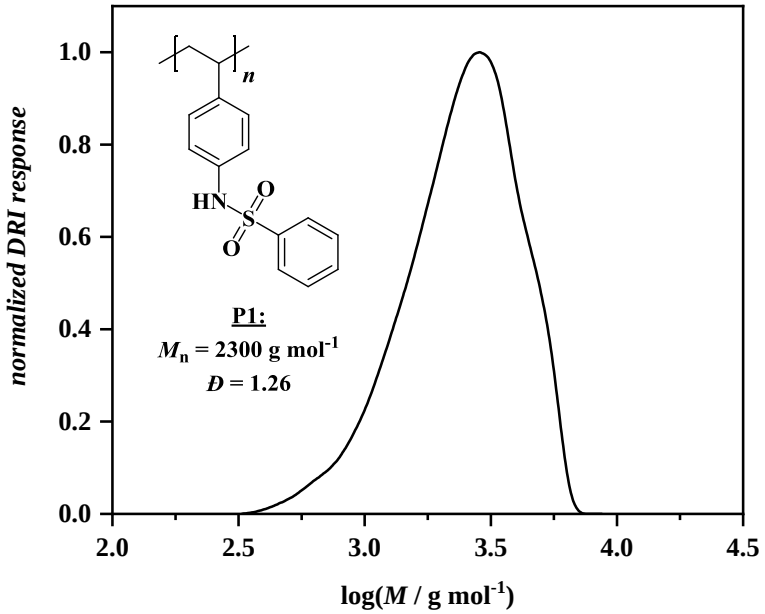

Figure 146. Size-exclusion chromatogram of poly(*N*-(4-vinylphenyl)benzenesulfonamide) (P1) using THF as eluent (PS calibration).

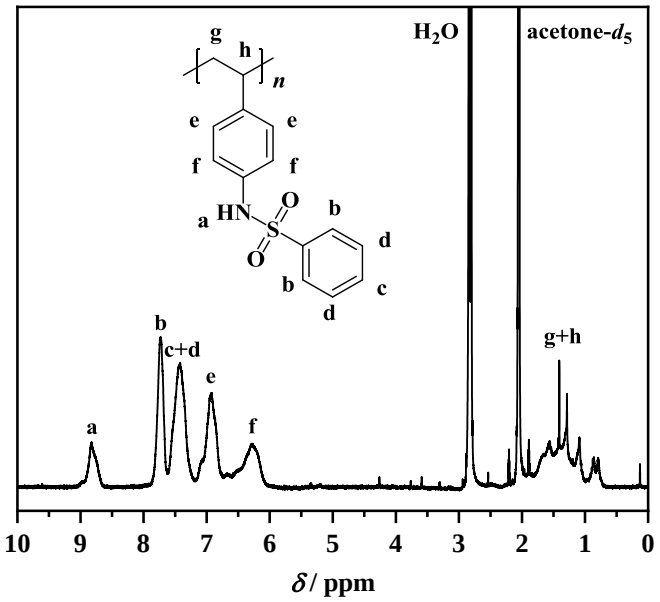

Figure 147. ^{1}H NMR spectrum of poly(*N*-(4-vinylphenyl)benzenesulfonamide) (P1); solvent: acetone-d_6.

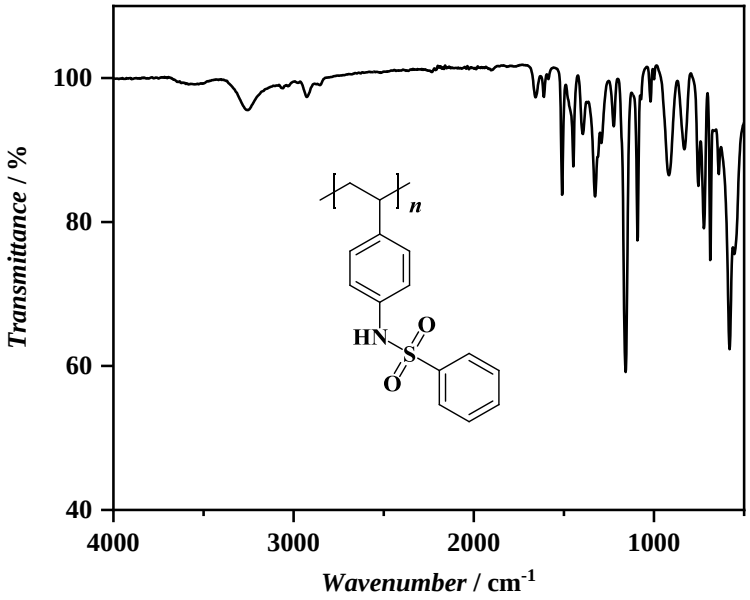

Figure 148. ATR-FT-IR spectrum of poly(*N*-(4-vinylphenyl)benzenesulfonamide) (P1).

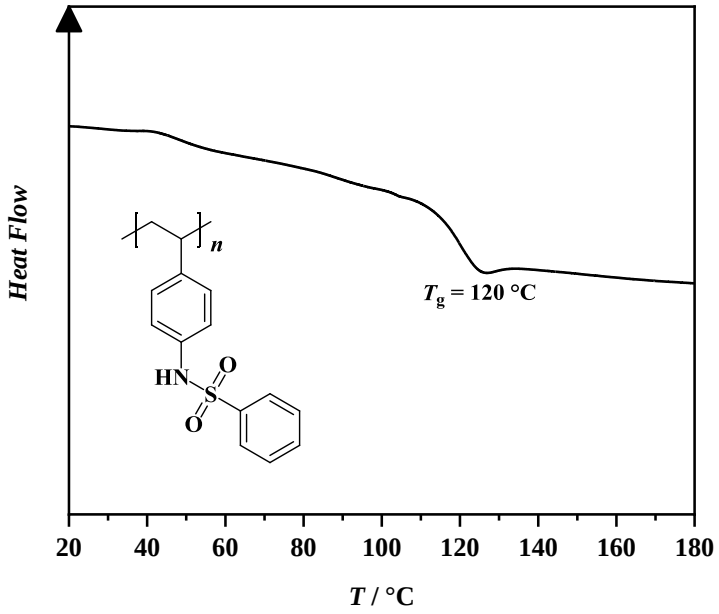

Figure 149. DSC results for poly(*N*-(4-vinylphenyl)benzenesulfonamide) (P1).

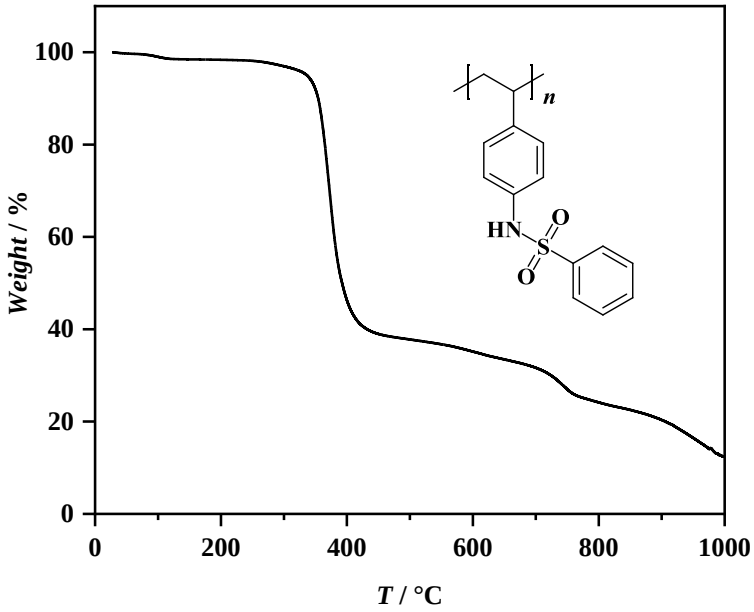

Figure 150. TGA results for poly(*N*-(4-vinylphenyl)benzenesulfonamide) (P1).

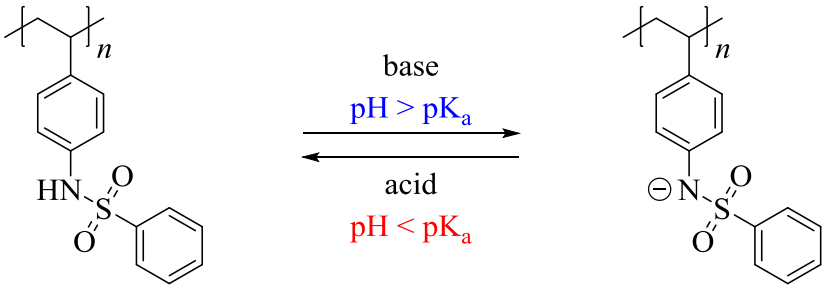

water-insoluble *water-soluble*

A vial was charged with P1 (6 mg) and distilled water (1 mL). The mixture was basified by addition of 1 M $NaOH_{aq.}$ and thereafter acidified by addition of 1 M $HCl_{aq.}$ resulting in clear solutions in the case of pH > pK_a, whereas the polymer precipitated when pH < pK_a.

6.6.3.2 Free Radical Polymerization of 4-Methyl-*N*-(4-vinylphenyl)benzenesulfonamide (M2)

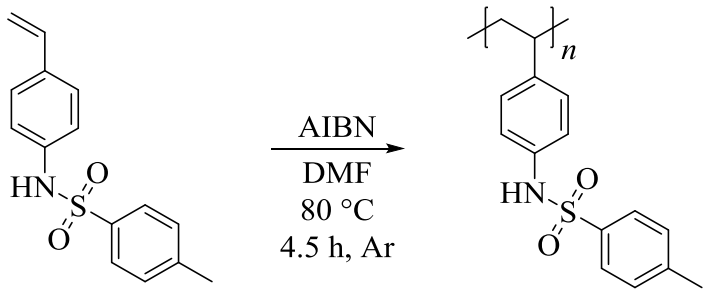

M2 **P2**

4-Methyl-*N*-(4-vinylphenyl)benzenesulfonamide (M2) (0.200 g, 0.732 mmol, 1.00 eq.) and AIBN (0.024 g, 0.146 mmol, 0.20 eq.) were dissolved in anhydrous DMF (1 mL). The solution was deoxygenated by argon purging for 15 minutes. The flask was placed in a preheated oil bath at 80 °C for 4.5 hours. Afterwards, polymer P2 was precipitated in cold diethyl ether, redissolved and precipitated again in cold diethyl ether giving a colorless solid (0.10 g).

^{1}H NMR (acetone-d_6): δ / ppm = 8.35 – 9.00 (1H, H_a), 7.40 – 7.74 (2H, H_b), 6.73 – 7.37 (4H, H_c+H_d), 6.02 – 6.49 (2H, H_e), 2.11 – 2.39 (3H, H_f), 0.72 – 1.86 (3H, H_g+H_h).
ATR-FT-IR: $\tilde{\nu}$ / cm^{-1} = 3258 (N-H), 2924 (C-H), 2854, 1659, 1612, 1598, 1510 (N-H), 1453, 1398, 1327 (S=O), 1305, 1290, 1225, 1185, 1158 (S=O), 1091, 1019, 916 (S-N), 813, 705, 664, 544.

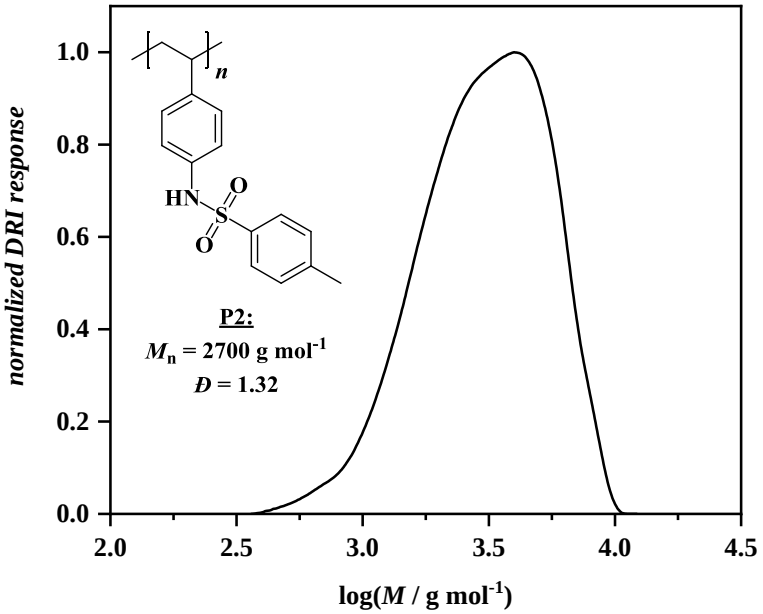

Figure 151. Size-exclusion chromatogram of poly(4-methyl-*N*-(4-vinylphenyl) benzenesulfonamide) (P2) using THF as eluent (PS calibration).

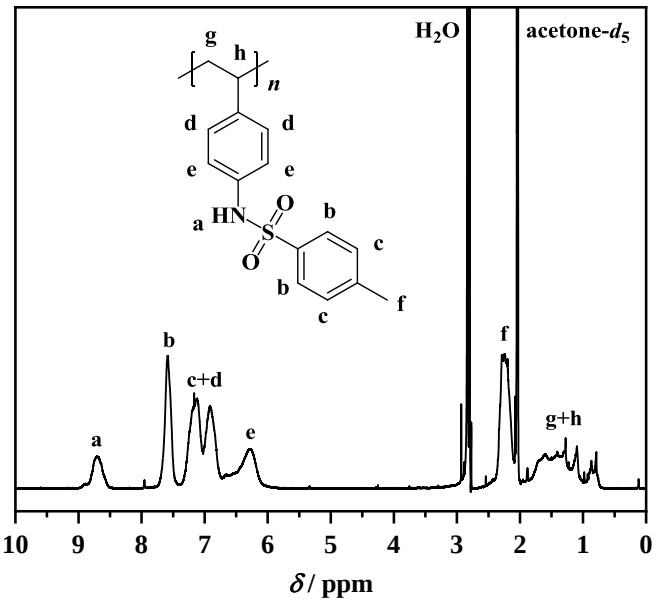

Figure 152. ^{1}H NMR spectrum of poly(4-methyl-*N*-(4-vinylphenyl)benzenesulfonamide) (P2); solvent: acetone-d_6.

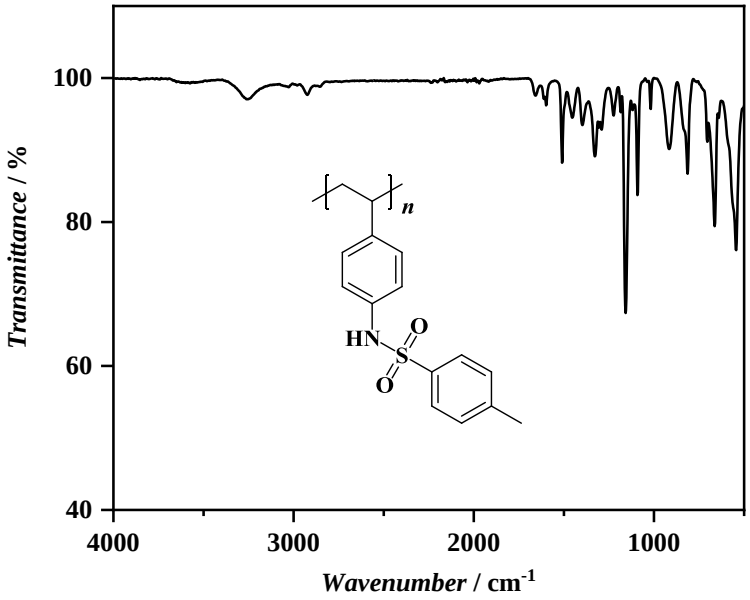

Figure 153. ATR-FT-IR spectrum of poly(4-methyl-*N*-(4-vinylphenyl)benzenesulfonamide) (P2).

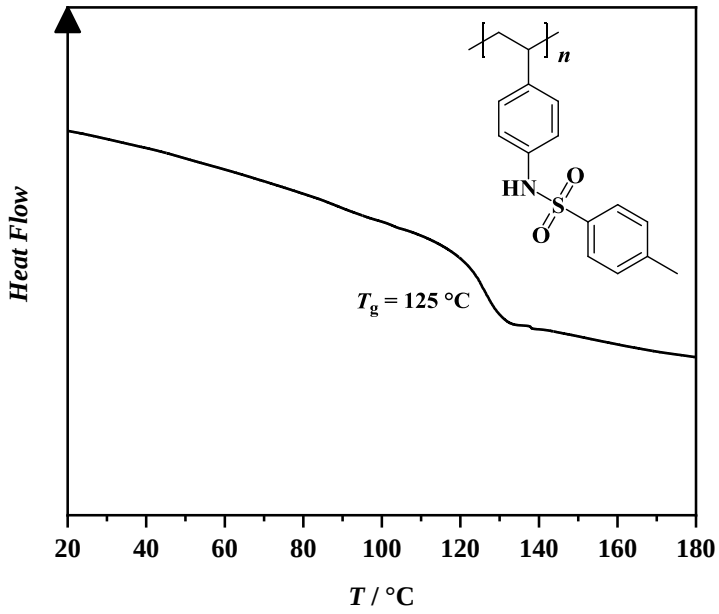

Figure 154. DSC results for poly(4-methyl-*N*-(4-vinylphenyl)benzenesulfonamide) (P2).

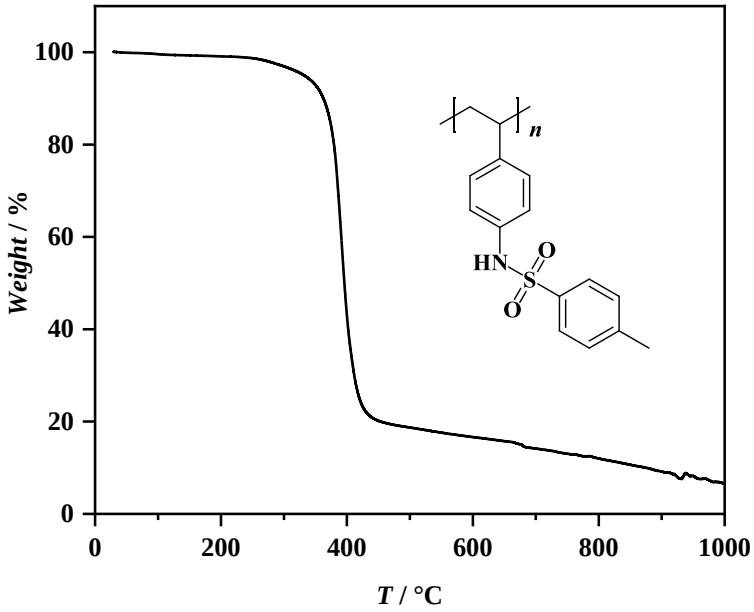

Figure 155. TGA results for poly(4-methyl-*N*-(4-vinylphenyl)benzenesulfonamide) (P2).

6.6.3.3 Free Radical Polymerization of 4-Fluoro-*N*-(4-vinylphenyl)benzenesulfonamide (M3)

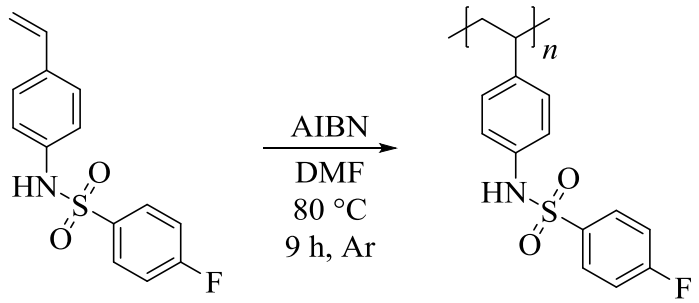

M3 **P3**

4-Fluoro-*N*-(4-vinylphenyl)benzenesulfonamide (M3) (0.200 g, 0.721 mmol, 1.00 eq.) and AIBN (0.012 g, 0.072 mmol, 0.10 eq.) were dissolved in anhydrous DMF (1 mL). The solution was deoxygenated by argon purging for 15 minutes. The flask was placed in a preheated oil bath at 80 °C for 9 hours. Afterwards, polymer P3 was precipitated in cold diethyl ether, redissolved and precipitated again in cold diethyl ether giving a colorless solid (0.11 g).

^{1}H NMR (acetone-d_6): δ / ppm = 8.58 – 9.18 (1H, H_a), 7.61 – 7.94 (2H, H_b), 6.76 – 7.35 (4H, H_c+H_d), 6.10 – 6.67 (2H, H_e), 0.70 – 1.87 (3H, H_f+H_g).

^{19}F NMR (acetone-d_6): δ / ppm = -107.82 – -106.20 (1F).

ATR-FT-IR: $\tilde{\nu}$ / cm^{-1} = 3252 (N-H), 2923 (C-H), 2852, 1590, 1510 (N-H), 1493, 1448, 1396, 1327 (S=O), 1291, 1224, 1152 (S=O), 1090, 1017, 914 (S-N), 834, 815, 666, 542.

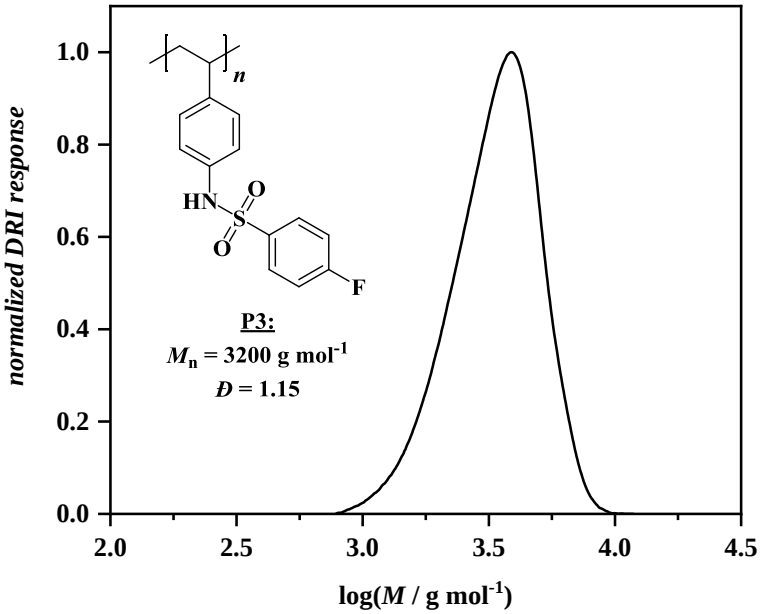

Figure 156. Size-exclusion chromatogram of poly(4-fluoro-*N*-(4-vinylphenyl) benzenesulfonamide) (P3) using THF as eluent (PS calibration).

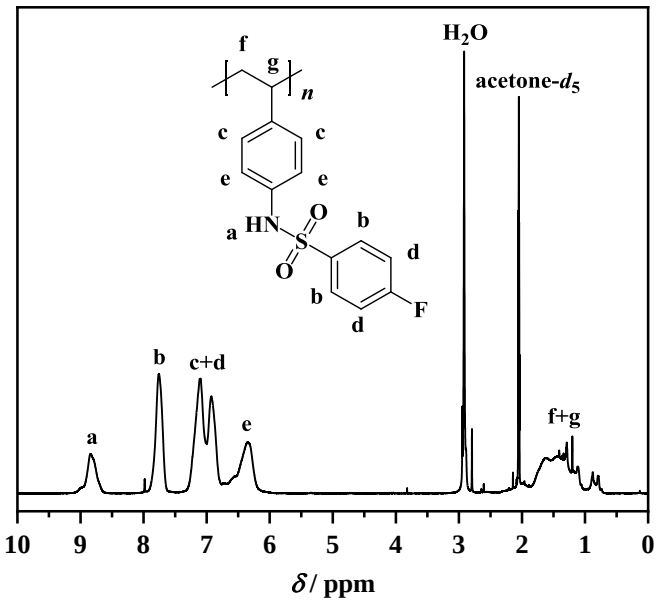

Figure 157. ^{1}H NMR spectrum of poly(4-fluoro-*N*-(4-vinylphenyl)benzenesulfonamide) (P3); solvent: acetone-d_6.

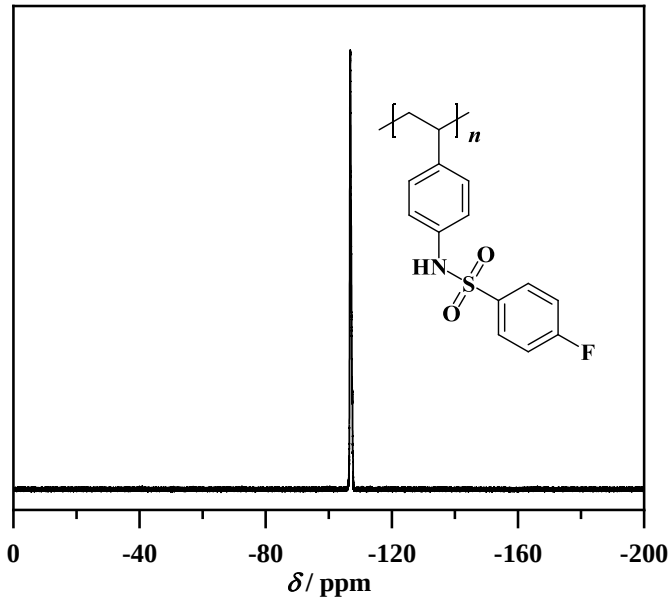

Figure 158. ^{19}F NMR spectrum of poly(4-fluoro-*N*-(4-vinylphenyl)benzenesulfonamide) (P3); solvent: acetone-d_6.

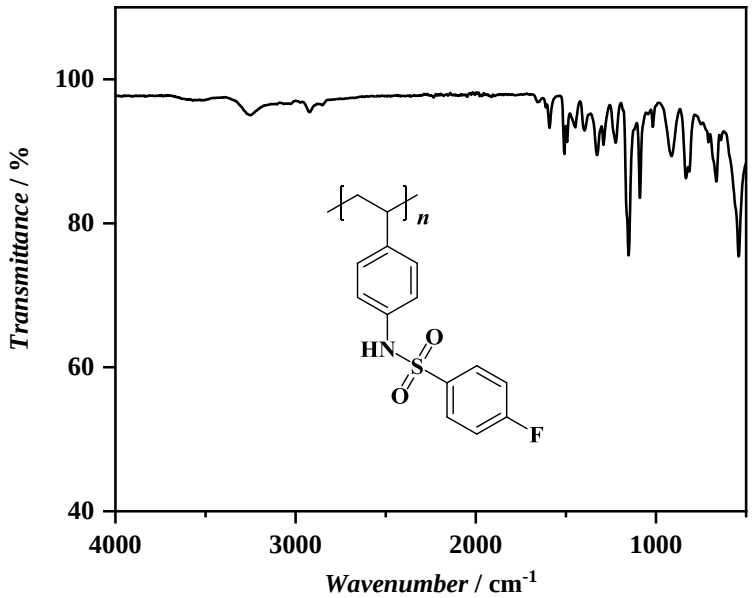

Figure 159. ATR-FT-IR spectrum of poly(4-fluoro-*N*-(4-vinylphenyl)benzenesulfonamide) (P3).

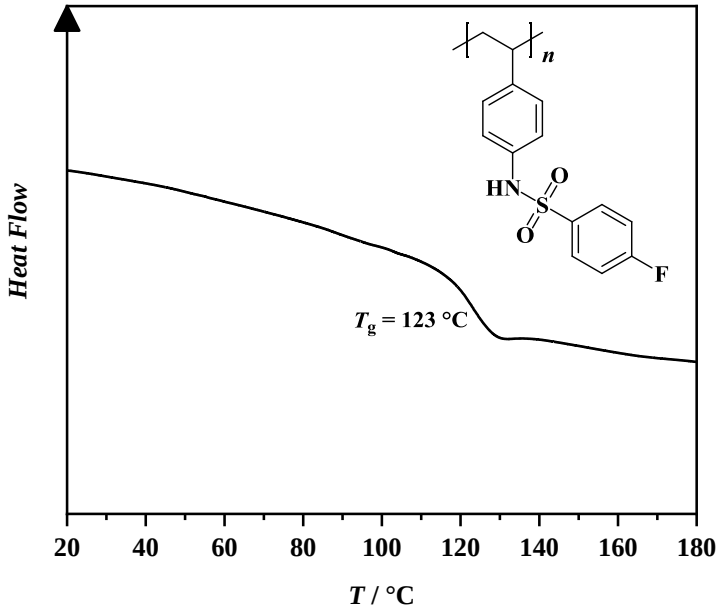

Figure 160. DSC results for poly(4-fluoro-*N*-(4-vinylphenyl)benzenesulfonamide) (P3).

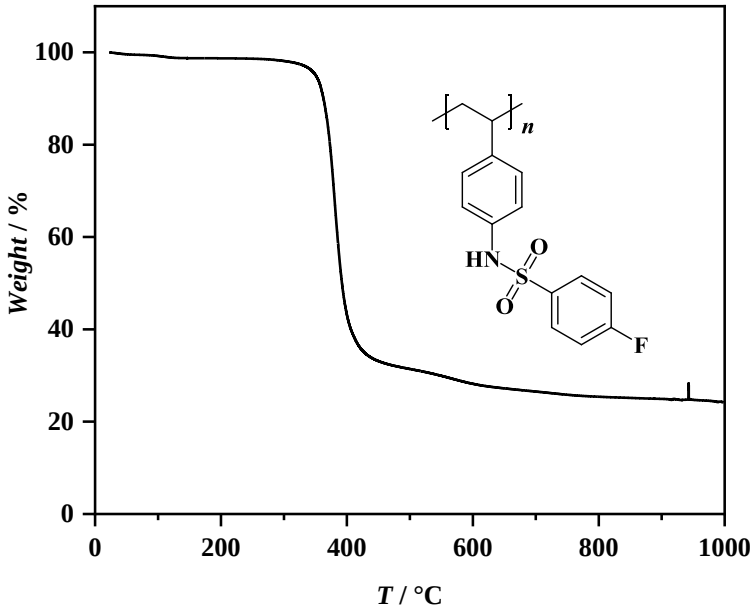

Figure 161. TGA results for poly(4-fluoro-*N*-(4-vinylphenyl)benzenesulfonamide) (P3).

6.6.3.4 Free Radical Polymerization of 4-Nitro-*N*-(4-vinylphenyl)benzenesulfonamide (M4)

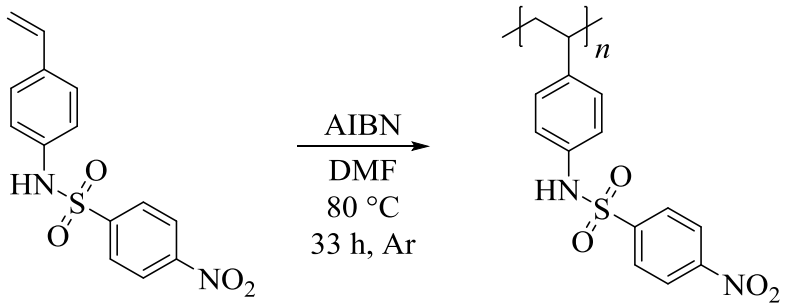

M4 **P4**

4-Nitro-*N*-(4-vinylphenyl)benzenesulfonamide (0.100 g, 0.329 mmol, 1.00 eq.) (M4) and AIBN (0.003 g, 0.016 mmol, 0.05 eq.) were dissolved in anhydrous DMF (0.75 mL). The solution was deoxygenated by argon purging for 15 minutes. The flask was placed in a preheated oil bath at 80 °C for 24.5 hours. Subsequently, the mixture was cooled to room temperature and AIBN (0.027 g, 0.164 mmol, 0.50 eq.) was added and the solution was deoxygenated by argon purging for 15 minutes. Then, the flask was placed in a preheated oil bath at 80 °C for 8.5 hours. Afterwards, polymer P4 was precipitated in cold diethyl ether, was redissolved in THF and precipitated in cold diethyl ether again giving a slightly yellowish solid.

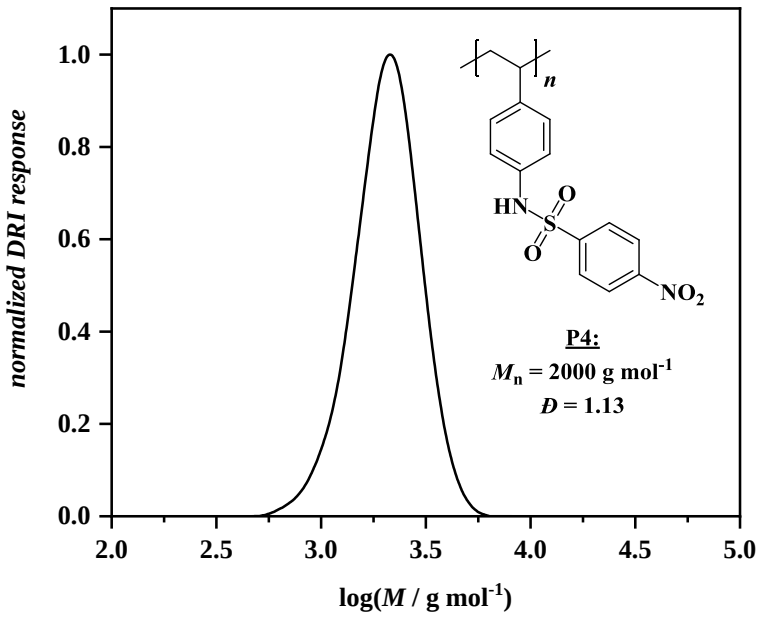

Figure 162. Size-exclusion chromatogram of poly(4-nitro-*N*-(4-vinylphenyl) benzenesulfonamide) (P4) using THF as eluent (PS calibration).

6.6.4 Post-Polymerization Modification Procedures of Aromatic Sulfonamide Polymers P1-P4

6.6.4.1 Post-Polymerization Modification of P1

6.6.4.1.1 Aza-Michael Addition of P1 with Butyl Acrylate

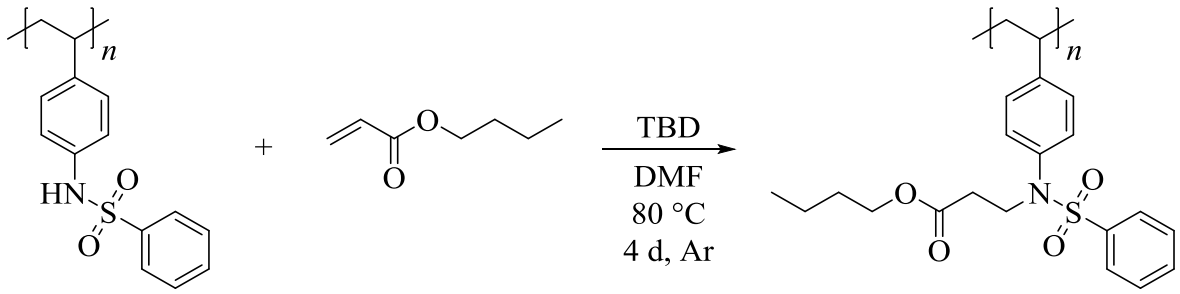

P1

Poly(*N*-(4-vinylphenyl)benzenesulfonamide) (P1) (0.040 g, 0.154 mmol of repeating units, 1.00 eq.) and TBD (0.011 g, 0.077 mmol, 0.50 eq. per repeating unit) were dissolved in anhydrous DMF (1 mL) in a dry vial. Deinhibited butyl acrylate (0.11 mL, 0.099 g, 0.771 mmol, 5.00 eq. per repeating unit) was added. The mixture was deoxygenated by argon purging for 15 minutes in an ice bath and the vial was placed in a preheated oil bath at 80 °C for 4 days. Afterwards, the polymer was precipitated in cold diethyl ether, redissolved and precipitated again in cold diethyl ether. Subsequently, the solid residue was dissolved in DCM (25 mL) and the organic phase was washed with water (3 × 25 mL). Finally, the organic phase was dried over magnesium sulfate and the solvent was removed under reduced pressure.

^{1}H NMR (DCM-d_2): δ / ppm = 5.72 – 8.05 (9H, H_a+H_b+H_c+H_d+H_e), 3.91 – 4.17 (2H, H_f), 3.47 – 3.90 (2H, H_g), 2.27 – 2.62 (2H, H_h), 0.76 – 1.67 (12H, H_i+H_j+H_k+H_l+H_m).
ATR-FT-IR: $\tilde{\nu}$ / cm^{-1} = 2955, 2926, 2872, 1728 (C=O), 1508, 1447, 1394, 1329 (S=O), 1291, 1225, 1156, 1091, 1018, 919, 835, 755, 722, 689, 663, 640, 578.

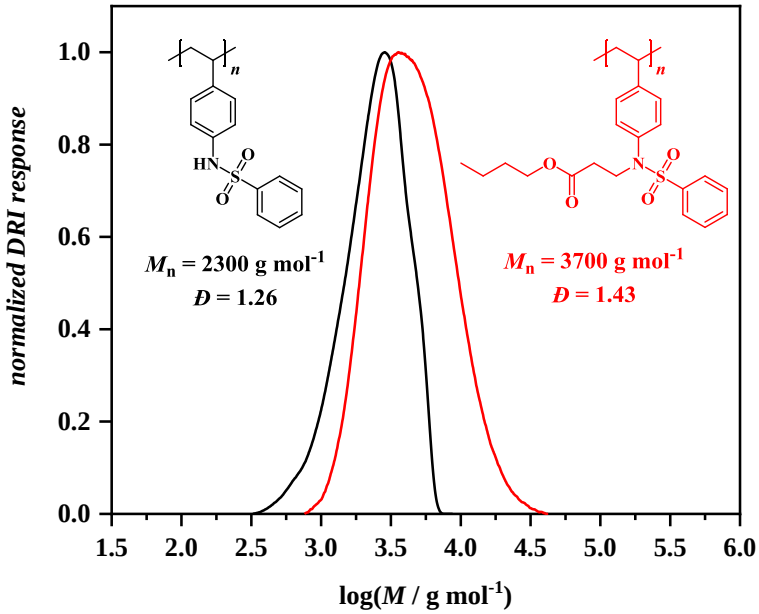

Figure 163. Comparison of size-exclusion chromatograms using THF as eluent (PS calibration) before (black line) and after (red line) PPM by aza-Michael addition of P1 with butyl acrylate.

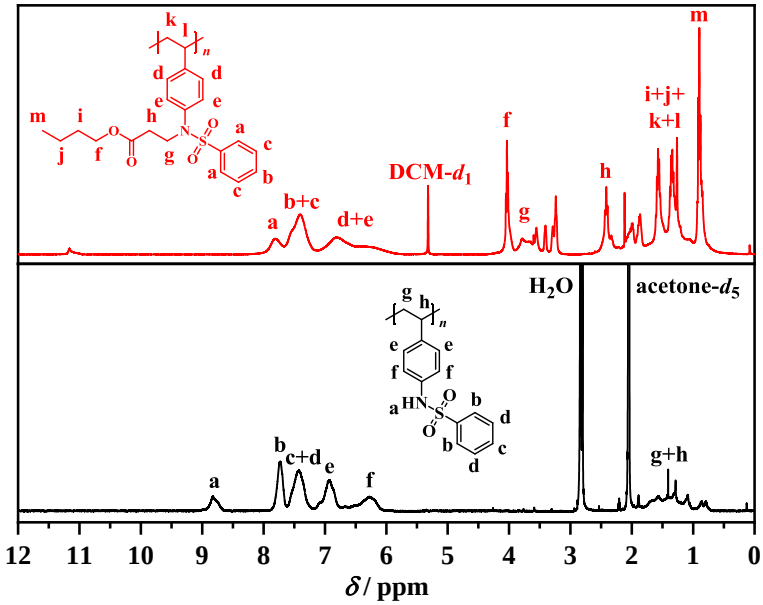

Figure 164. Comparison of ^{1}H NMR spectra before (bottom, black line; solvent: acetone-d_6) and after (top, red line; solvent: DCM-d_2) PPM by aza-Michael addition of P1 with butyl acrylate.

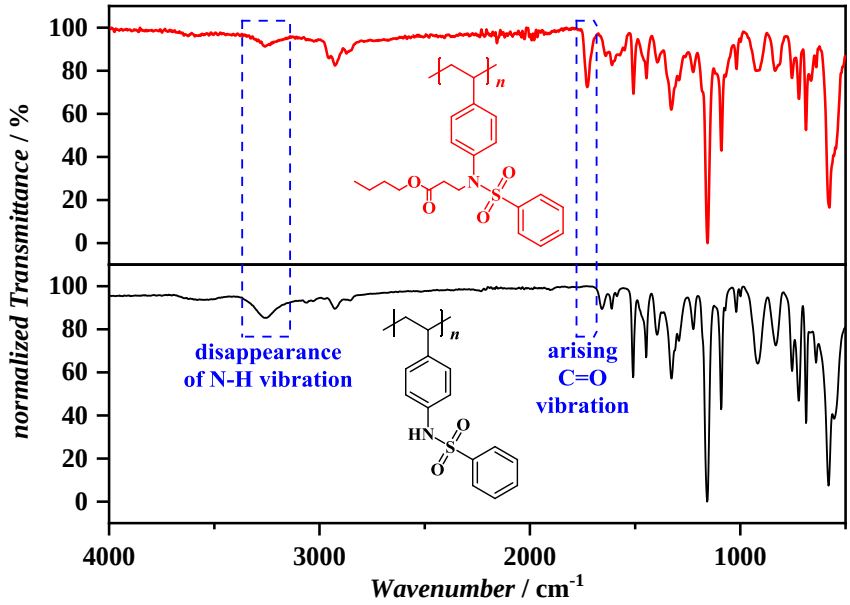

Figure 165. Comparison of ATR-FT-IR spectra before (bottom, black line) and after (top, red line) PPM by aza-Michael addition of P1 with butyl acrylate.

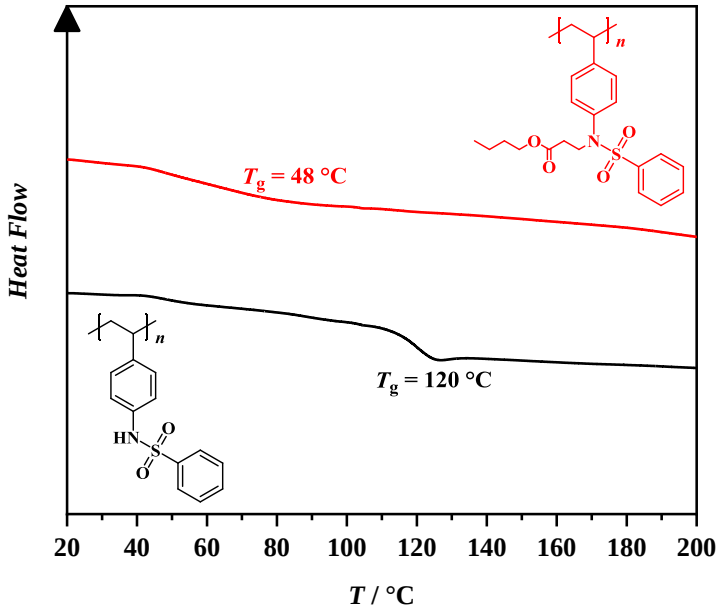

Figure 166. Comparison of DSC results before (black line) and after (red line) PPM by aza-Michael addition of P1 with butyl acrylate.

6.6.4.1.2 Aza-Michael Addition of P1 with Dodecyl Acrylate

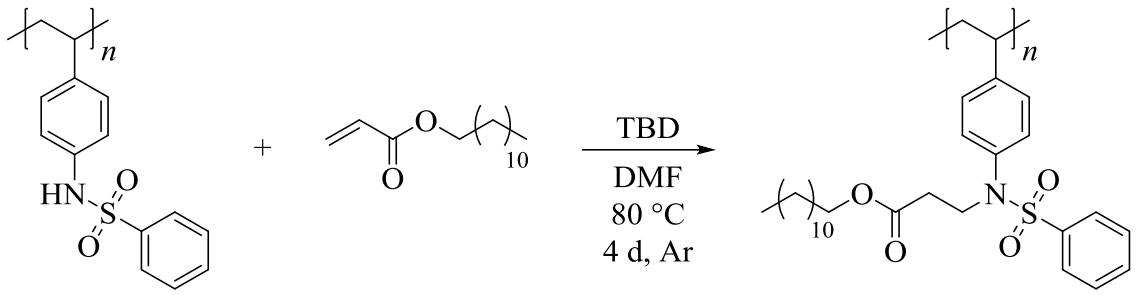

P1

Poly(*N*-(4-vinylphenyl)benzenesulfonamide) (**P1**) (0.040 g, 0.154 mmol of repeating units, 1.00 eq.) and TBD (0.011 g, 0.077 mmol, 0.50 eq. per repeating unit) were dissolved in anhydrous DMF (1 mL) in a dry vial. Deinhibited dodecyl acrylate (0.21 mL, 0.185 g, 0.771 mmol, 5.00 eq. per repeating unit) was added. The mixture was deoxygenated by argon purging for 15 minutes in an ice bath and the vial was placed in a preheated oil bath at 80 °C for 4 days. Afterwards, the polymer was precipitated in cold methanol, redissolved and precipitated again in cold methanol. Subsequently, the solid residue was dissolved in DCM (25 mL) and the organic phase was washed with water/brine (3 × 25 mL). Finally, the organic phase was dried over magnesium sulfate and the solvent was removed under reduced pressure.

^{1}H NMR (DCM-d_2): δ / ppm = 5.90 – 7.89 (9H, $H_{aromatic}$), 3.91 – 4.15 (2H, H_a), 3.49 – 3.89 (2H, H_b), 2.25 – 2.62 (2H, H_c), 0.57 – 1.85 (26H, $H_{backbone}$+H_d+H_e+H_f).
ATR-FT-IR: $\tilde{\nu}$ / cm^{-1} = 2922 (C-H), 2853, 1731 (C=O), 1507, 1464, 1447, 1351, 1331 (S=O), 1311, 1290, 1262, 1225, 1158 (S=O), 1092, 1052, 1018, 910, 832, 754, 721, 688, 640.

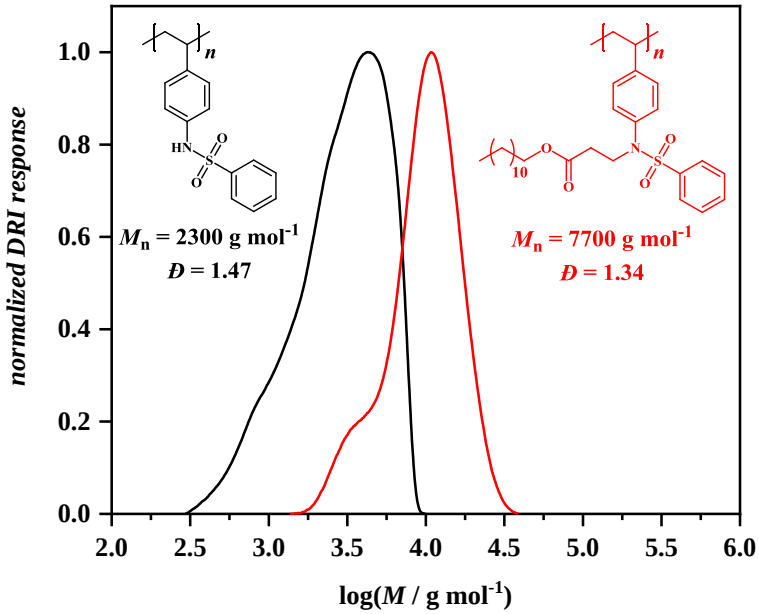

Figure 167. Comparison of size-exclusion chromatograms using THF as eluent (PS calibration) before (black line) and after (red line) PPM by aza-Michael addition of P1 with dodecyl acrylate.

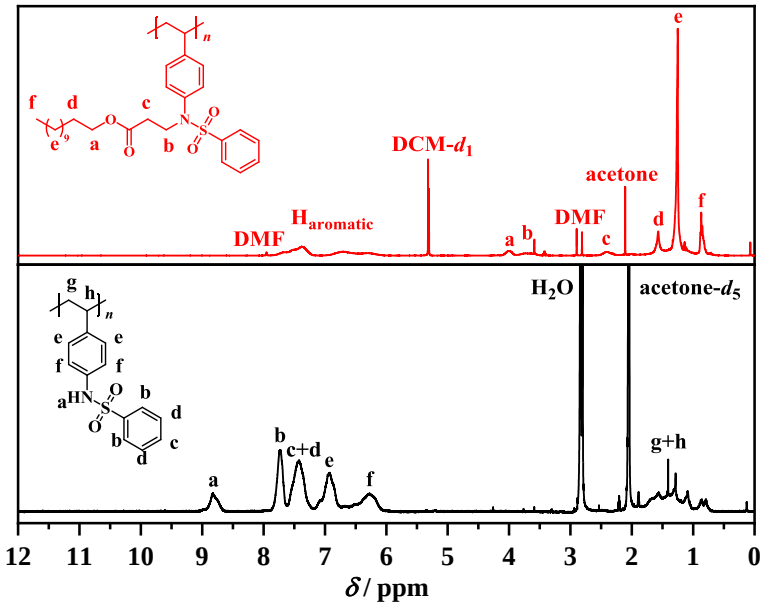

Figure 168. Comparison of ^{1}H NMR spectra before (bottom, black line; solvent: acetone-d_6) and after (top, red line; solvent: DCM-d_2) PPM by aza-Michael addition of P1 with dodecyl acrylate.

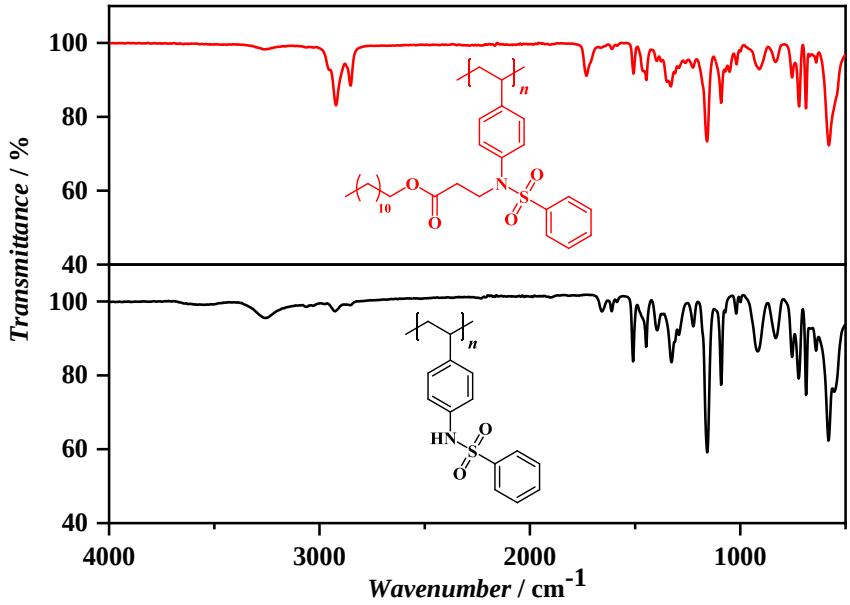

Figure 169. Comparison of ATR-FT-IR spectra before (bottom, black line) and after (top, red line) PPM by aza-Michael addition of P1 with dodecyl acrylate.

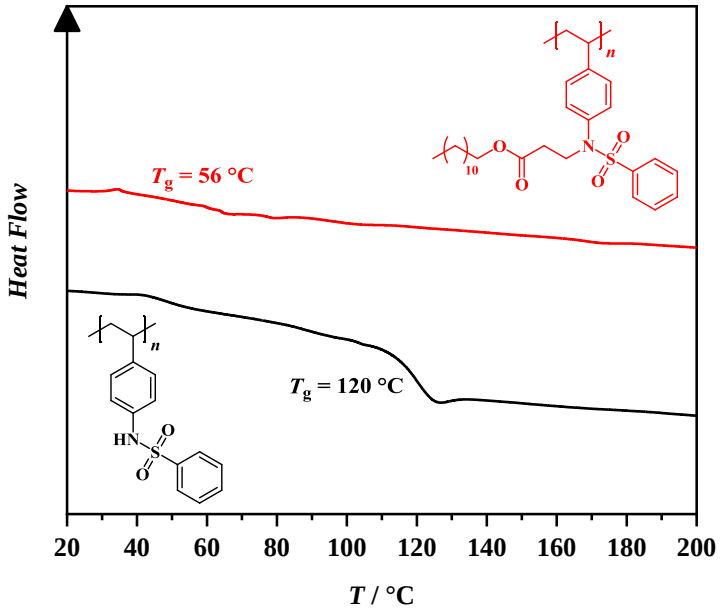

Figure 170. Comparison of DSC results before (black line) and after (red line) PPM by aza-Michael addition of P1 with dodecyl acrylate.

6.6.4.1.3 Aza-Michael Addition of P1 with Pentafluorophenyl Acrylate

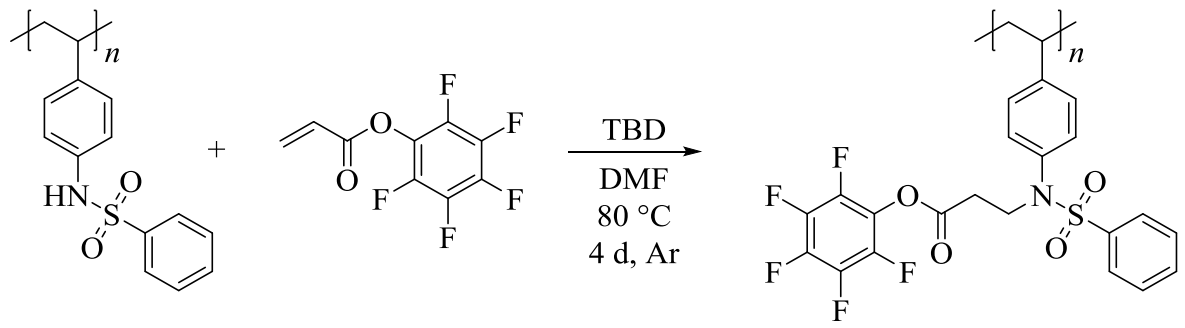

P1

Poly(*N*-(4-vinylphenyl)benzenesulfonamide) (P1) (0.040 g, 0.154 mmol of repeating units, 1.00 eq.) and TBD (0.011 g, 0.077 mmol, 0.50 eq. per repeating unit) were dissolved in anhydrous DMF (1 mL) in a dry vial. Pentafluorophenyl acrylate (0.13 mL, 0.184 g, 0.771 mmol, 5.00 eq. per repeating unit) was added. The mixture was deoxygenated by argon purging for 15 minutes in an ice bath and the vial was placed in a preheated oil bath at 80 °C for 4 days. Afterwards, the polymer was precipitated in cold diethyl ether, redissolved and precipitated twice in cold diethyl ether. Subsequently, the solid residue was dissolved in DCM (25 mL) and the organic phase was washed with brine (3 × 25 mL). Finally, the organic phase was dried over magnesium sulfate and the solvent was removed under reduced pressure.

^{1}H NMR (DCM-d_2): δ / ppm = 7.83 – 8.26, 7.22 – 7.79, 5.92 – 7.16, 3.12 – 4.45, 2.54 – 3.10, 0.51 – 2.34.

^{19}F NMR (DCM-d_2): δ / ppm = -151.10 – -154.15, -156.39 – -157.24, -157.93 – -159.39, -160.88 – -164.01.

ATR-FT-IR: $\tilde{\nu}$ / cm^{-1} = 2924, 2852, 1781, 1705, 1643, 1551, 1518, 1448, 1351, 1160, 1088, 995, 754, 723, 688, 582.

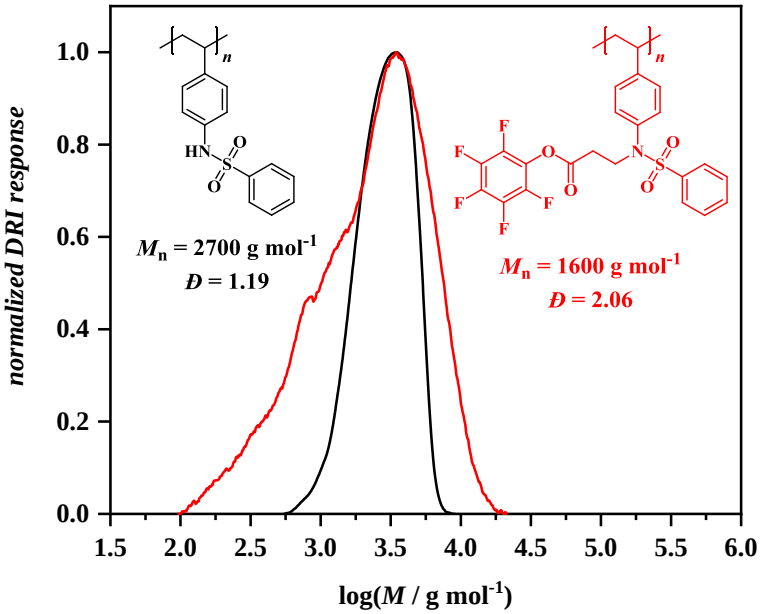

Figure 171. Comparison of size-exclusion chromatograms using THF as eluent (PS calibration) before (black line) and after (red line) PPM by aza-Michael addition of P1 with pentafluorophenyl acrylate.

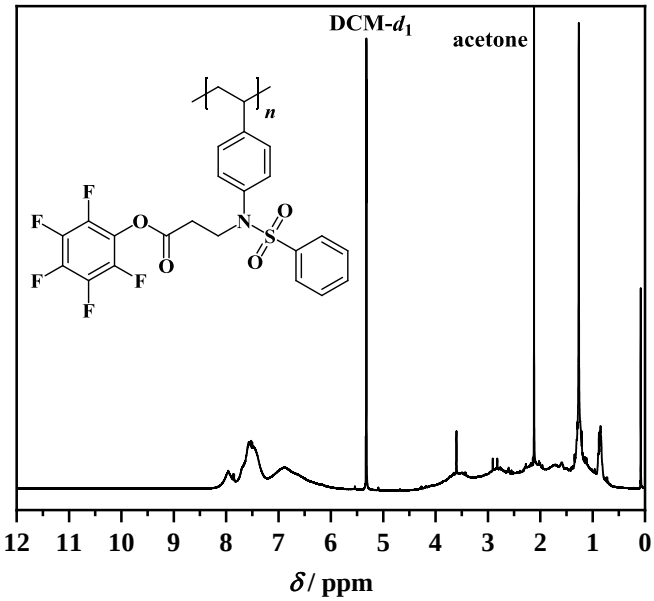

Figure 172. ^{1}H NMR spectrum after PPM by aza-Michael addition of P1 with pentafluorophenyl acrylate; solvent: DCM-d_2.

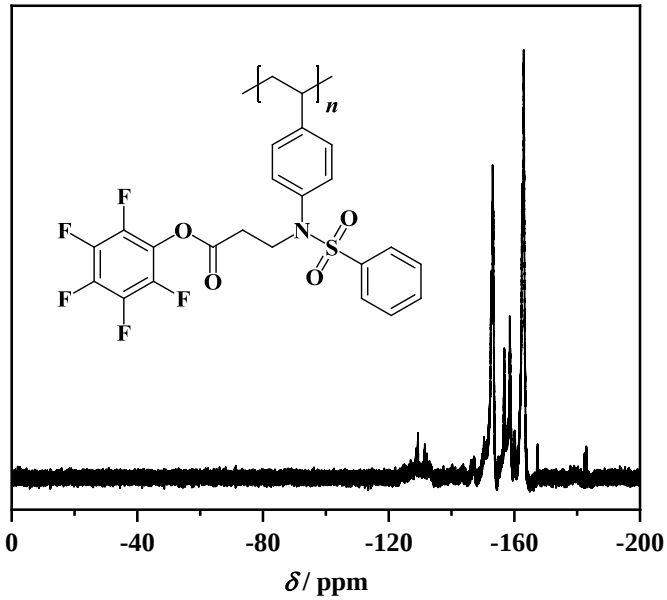

Figure 173. ^{19}F NMR spectrum after PPM by aza-Michael addition of P1 with pentafluorophenyl acrylate; solvent: DCM-d_2.

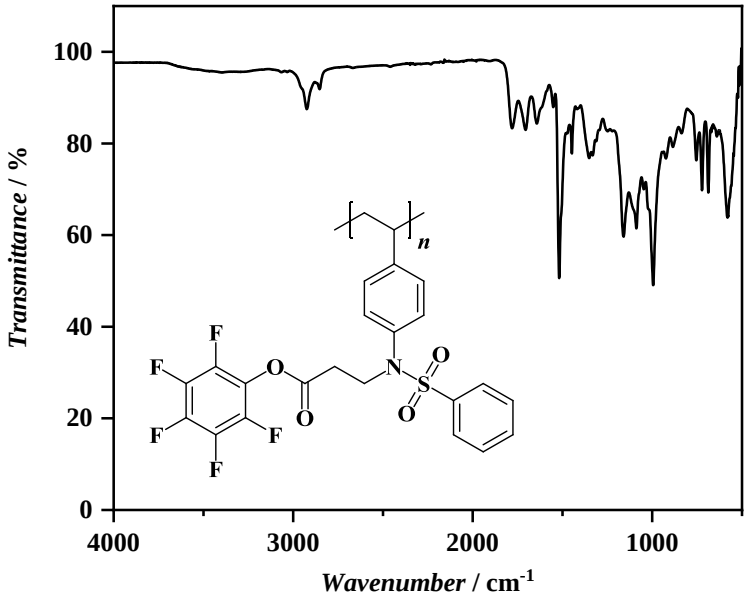

Figure 174. ATR-FT-IR spectum after PPM by aza-Michael addition of P1 with pentafluorophenyl acrylate.

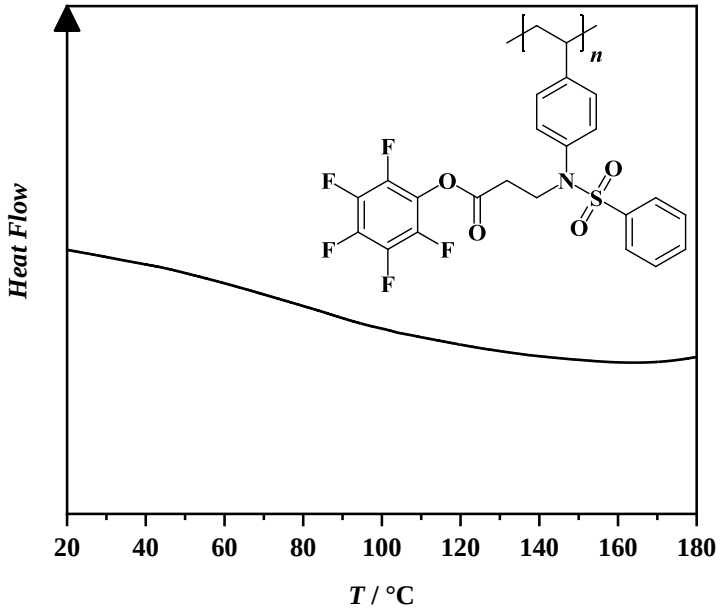

Figure 175. DSC results after PPM by aza-Michael addition of P1 with pentafluorophenyl acrylate.

6.6.4.2 Post-Polymerization Modification of P2

6.6.4.2.1 Aza-Michael Addition of P2 with Butyl Acrylate

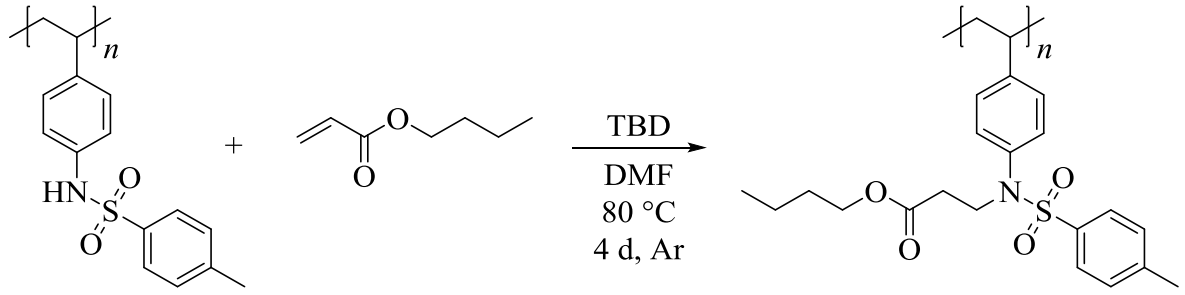

P2

Poly(4-methyl-*N*-(4-vinylphenyl)benzenesulfonamide) (P2) (0.040 g, 0.146 mmol of repeating units, 1.00 eq.) and TBD (0.010 g, 0.073 mmol, 0.50 eq. per repeating unit) were dissolved in anhydrous DMF (1 mL) in a dry vial. Deinhibited butyl acrylate (0.10 mL, 0.094 g, 0.732 mmol, 5.00 eq. per repeating unit) was added. The mixture was deoxygenated by argon purging for 15 minutes in an ice bath and the vial was placed in a preheated oil bath at 80 °C for 4 days. Afterwards, the polymer was precipitated in cold diethyl ether, redissolved and precipitated in cold diethyl ether. Subsequently, the solid residue was dissolved in DCM (25 mL) and the organic phase was washed with water (3 × 25 mL). Finally, the organic phase was dried over magnesium sulfate and the solvent was removed under reduced pressure.

^{1}H NMR (DCM-d_2): δ / ppm = 5.74 – 8.05 (8H, $H_{aromatic}$), 3.91 – 4.13 (2H, H_a), 3.48 – 3.89 (2H, H_b), 2.15 – 2.57 (5H, H_c+H_d), 0.58 – 1.78 (10H, $H_{backbone}$+H_e+H_f+H_g).
ATR-FT-IR: $\tilde{\nu}$ / cm^{-1} = 2958 (C-H), 2925, 2872, 1728 (C=O), 1642, 1596, 1550, 1508, 1453, 1392, 1328 (S=O), 1292, 1226, 1183, 1155 (S=O), 1090, 1018, 925, 837, 814, 707, 680, 660, 582, 544.

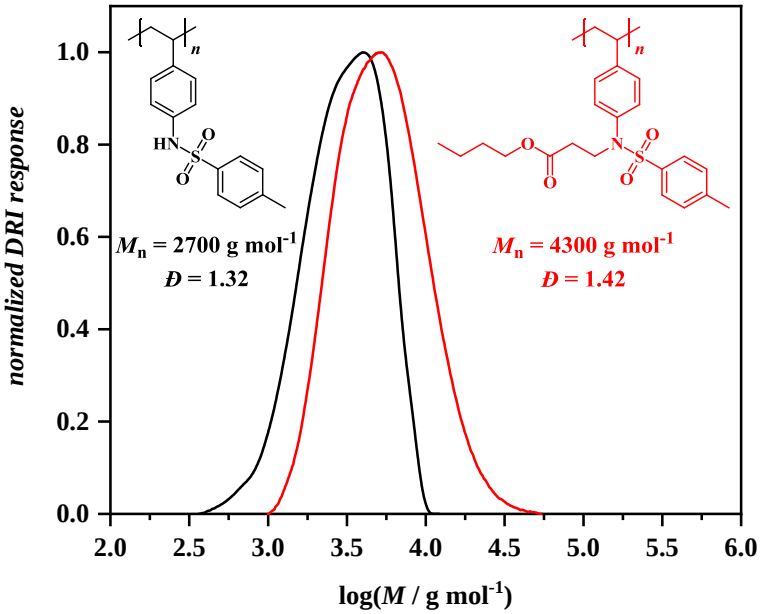

Figure 176. Comparison of size-exclusion chromatograms using THF as eluent (PS calibration) before (black line) and after (red line) PPM by aza-Michael addition of P2 with butyl acrylate.

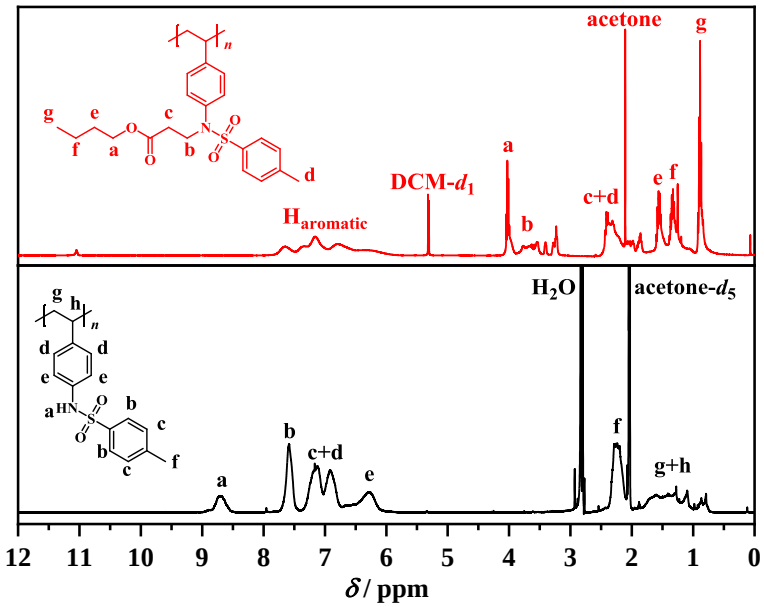

Figure 177. Comparison of ^{1}H NMR spectra before (bottom, black line; solvent: acetone-d_6) and after (top, red line; solvent: DCM-d_2) PPM by aza-Michael addition of P2 with butyl acrylate.

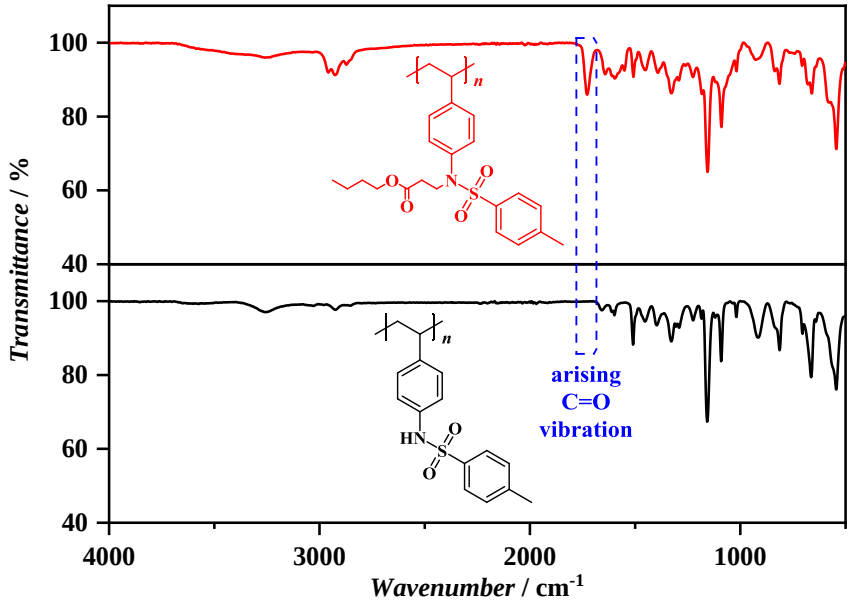

Figure 178. Comparison of ATR-FT-IR spectra before (bottom, black line) and after (top, red line) PPM by aza-Michael addition of P2 with butyl acrylate.

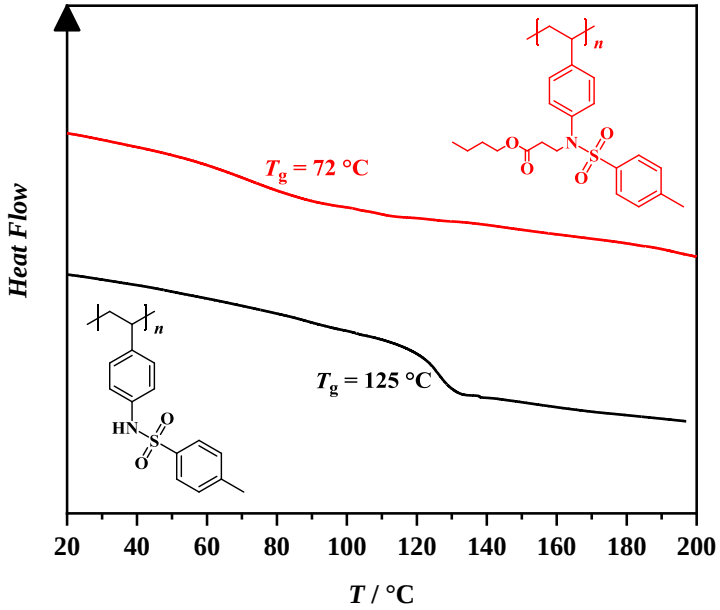

Figure 179. Comparison of DSC results before (black line) and after (red line) PPM by aza-Michael addition of P2 with butyl acrylate.

6.6.4.2.2 Aza-Michael Addition of P2 with Methyl Acrylate

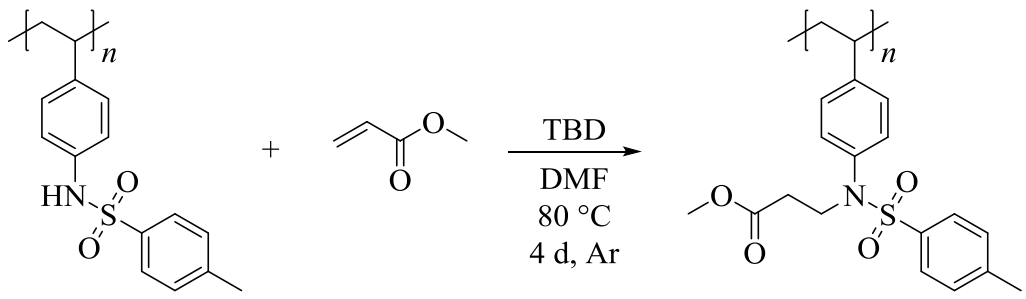

P2

Poly(4-methyl-*N*-(4-vinylphenyl)benzenesulfonamide) (P2) (0.040 g, 0.146 mmol of repeating units, 1.00 eq.) and TBD (0.010 g, 0.073 mmol, 0.50 eq. per repeating unit) were dissolved in anhydrous DMF (1 mL) in a dry vial. Deinhibited methyl acrylate (0.07 mL, 0.063 g, 0.732 mmol, 5.00 eq. per repeating unit) was added. The mixture was deoxygenated by argon purging for 15 minutes in an ice bath and the vial was placed in a preheated oil bath at 80 °C for 4 days. Afterwards, the polymer was precipitated in cold diethyl ether, redissolved and precipitated again in cold diethyl ether. Subsequently, the solid residue was dissolved in DCM (25 mL) and the organic phase was washed with water (3 × 25 mL). Finally, the organic phase was dried over magnesium sulfate and the solvent was removed under reduced pressure.

^{1}H NMR (DCM-d_2): δ / ppm = 5.99 – 7.88 (8H, $H_{aromatic}$), 3.45 – 3.96 (5H, H_a+H_b), 2.19 – 2.67 (5H, H_c+H_d), 0.71 – 1.83 (3H, $H_{backbone}$).
ATR-FT-IR: $\tilde{\nu}$ / cm^{-1} = 3253 (N-H), 2922 (C-H), 2853, 1735 (C=O), 1598, 1508, 1448, 1397, 1329 (S=O), 1306, 1289, 1225, 1185, 1156 (S=O), 1090, 1049, 1017, 913, 834, 813, 706, 662, 577.

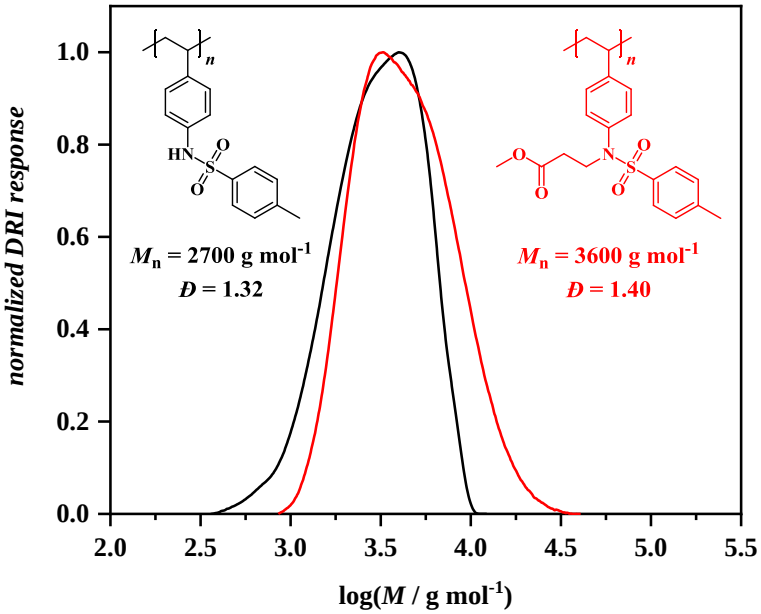

Figure 180. Comparison of size-exclusion chromatograms using THF as eluent (PS calibration) before (black line) and after (red line) PPM by aza-Michael addition of P2 with methyl acrylate.

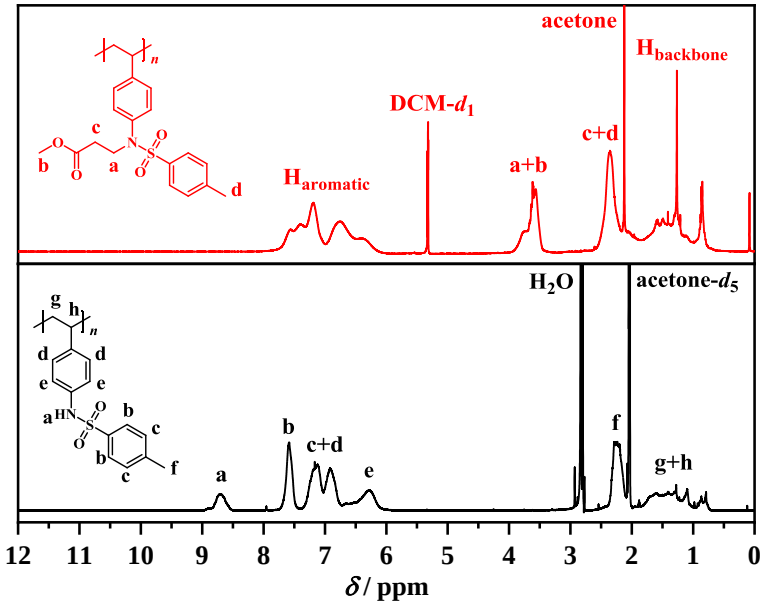

Figure 181. Comparison of ^{1}H NMR spectra before (bottom, black line; solvent: acetone-d_6) and after (top, red line; solvent: DCM-d_2) PPM by aza-Michael addition of P2 with methyl acrylate.

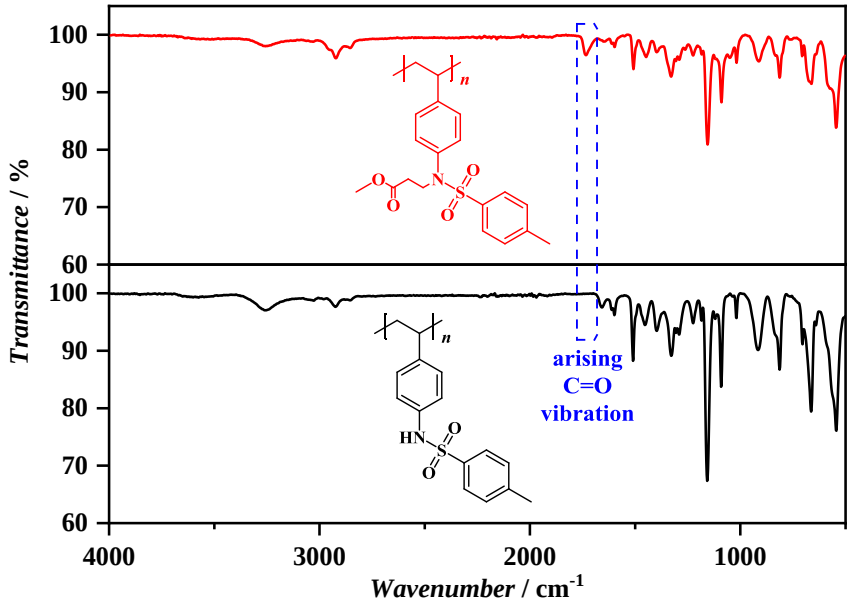

Figure 182. Comparison of ATR-FT-IR spectra before (bottom, black line) and after (top, red line) PPM by aza-Michael addition of P2 with methyl acrylate.

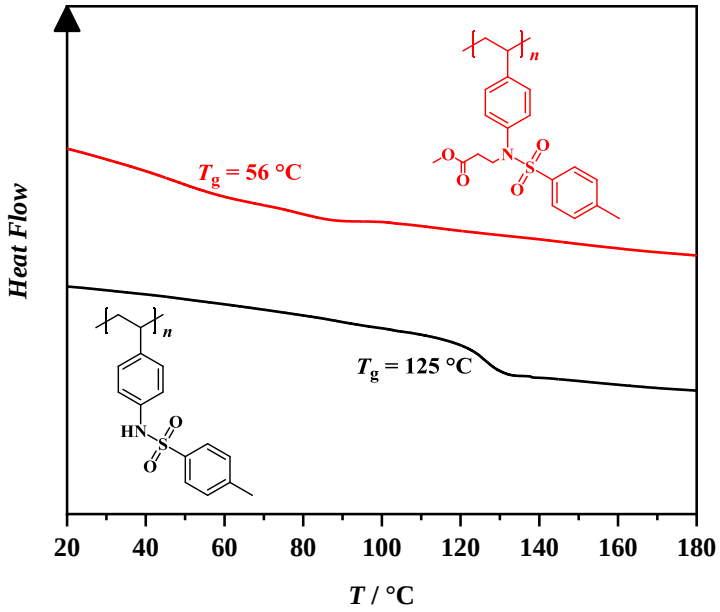

Figure 183. Comparison of DSC results before (black line) and after (red line) PPM by aza-Michael addition of P2 with methyl acrylate.

6.6.4.3 Post-Polymerization Modification of P3

6.6.4.3.1 Aza-Michael Addition of P3 with Butyl Acrylate

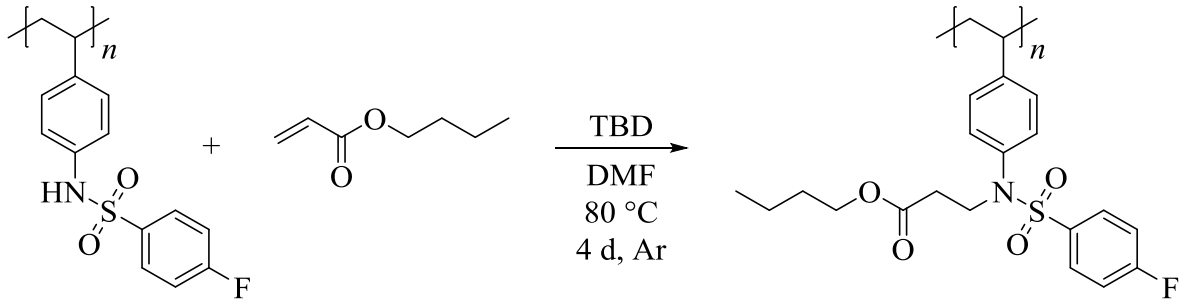

P3

Poly(4-fluoro-*N*-(4-vinylphenyl)benzenesulfonamide) (P3) (0.040 g, 0.144 mmol of repeating units, 1.00 eq.) and TBD (0.010 g, 0.072 mmol, 0.50 eq. per repeating unit) were dissolved in anhydrous DMF (1 mL) in a dry vial. Deinhibited butyl acrylate (0.10 mL, 0.092 g, 0.721 mmol, 5.00 eq. per repeating unit) was added. The mixture was deoxygenated by argon purging for 15 minutes in an ice bath and the vial was placed in a preheated oil bath at 80 °C for 4 days. Afterwards, the polymer was precipitated in cold diethyl ether, redissolved and precipitated again in cold diethyl ether. Subsequently, the solid residue was dissolved in DCM (25 mL) and the organic phase was washed with water (3 × 25 mL). Finally, the organic phase was dried over magnesium sulfate and the solvent was removed under reduced pressure.

^{1}H NMR (DCM-d_2): δ / ppm = 5.88 – 8.22 (8H, $H_{aromatic}$), 3.91 – 4.14 (2H, H_a), 3.49 – 3.90 (2H, H_b), 2.29 – 2.54 (2H, H_c), 0.58 – 1.79 (10H, $H_{aromatic}$+H_d+H_e+H_f).
ATR-FT-IR: $\tilde{\nu}$ / cm^{-1} = 2959 (C-H), 2926 (C-H), 2872, 1729 (C=O), 1642, 1612, 1590, 1552, 1508, 1494, 1452, 1397, 1331 (S=O), 1292, 1262, 1226, 1153 (S=O), 1090, 1018, 930, 836, 817, 711, 682, 663, 583, 544.

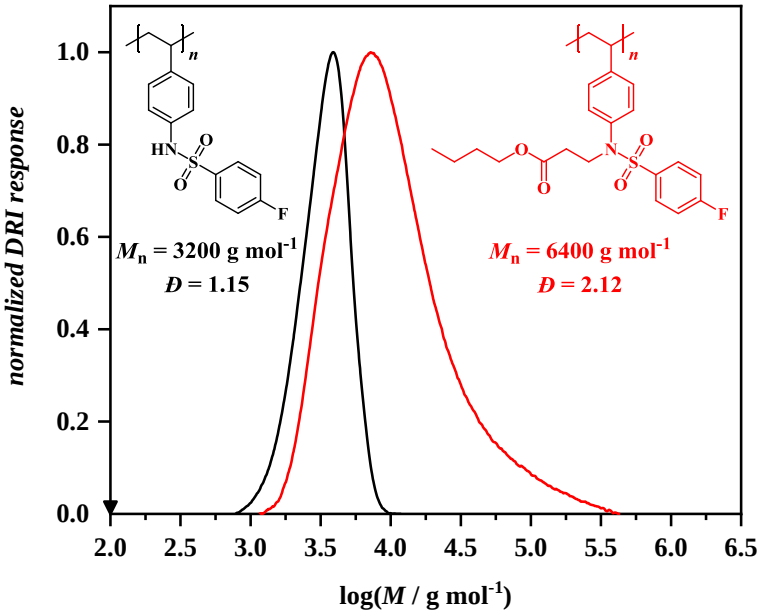

Figure 184. Comparison of size-exclusion chromatograms using THF as eluent (PS calibration) before (black line) and after (red line) PPM by aza-Michael addition of P3 with butyl acrylate.

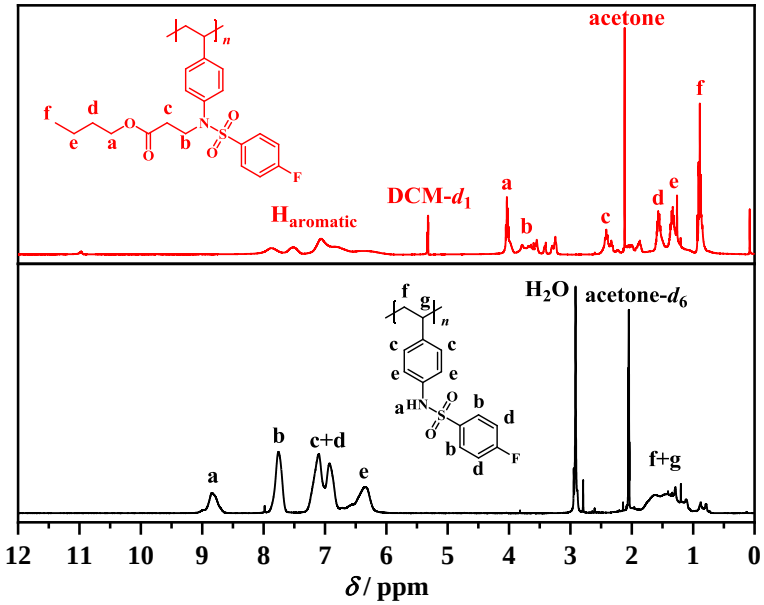

Figure 185. Comparison of ^{1}H NMR spectra before (bottom, black line; solvent: acetone-d_6) and after (top, red line; solvent: DCM-d_2) PPM by aza-Michael addition of P3 with butyl acrylate.

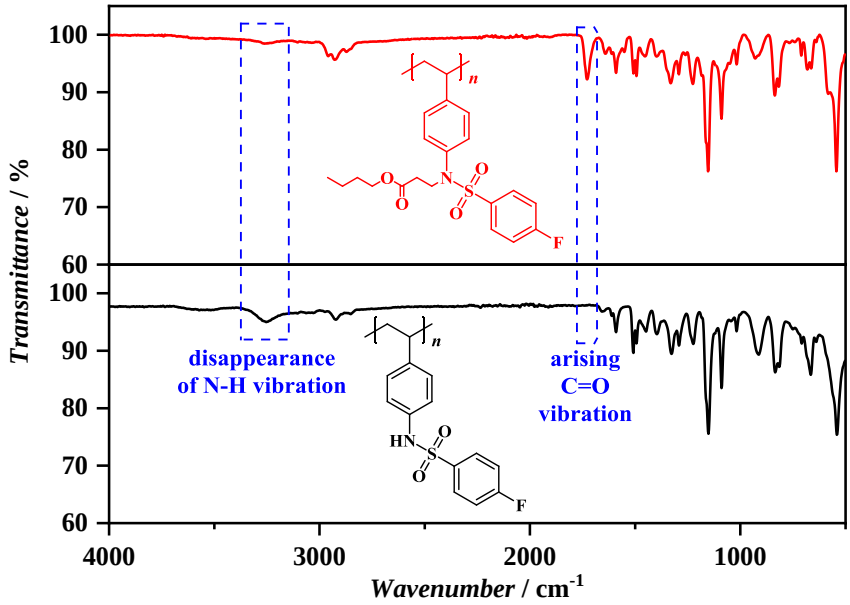

Figure 186. Comparison of ATR-FT-IR spectra before (bottom, black line) and after (top, red line) PPM by aza-Michael addition of P3 with butyl acrylate.

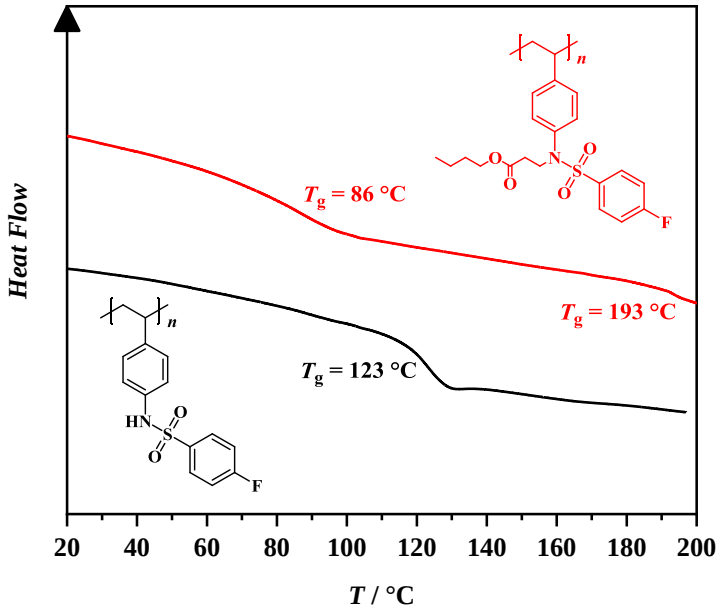

Figure 187. Comparison of DSC results before (black line) and after (red line) PPM by aza-Michael addition of P3 with butyl acrylate.

6.6.5 Synthesis and Aza-Michael Addition Procedures of *N*-Phenylbenzenesulfonamide

6.6.5.1 Synthesis of *N*-Phenylbenzenesulfonamide

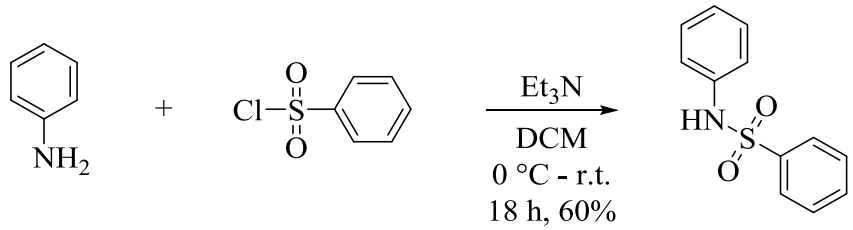

Aniline (0.30 g, 3.22 mmol, 1.00 eq.) was dissolved in anhydrous DCM (7 mL) and the solution was cooled to 0 °C. Triethylamine (0.49 mL, 0.36 g, 3.54 mmol, 1.10 eq.) and benzenesulfonyl chloride (0.45 mL, 0.63 g, 3.54 mmol, 1.10 eq.) were added and the mixture was stirred at 0 °C for 1 hour and at room temperature for 17 hours. DCM (20 mL) was added and the organic phase was washed with 1 M HCl solution (25 mL) and with water (3 × 25 mL). Subsequently, the organic phase was dried over magnesium sulfate and the solvent was removed under reduced pressure. Finally, the crude product was purified by column chromatography using a 8:1 mixture of CH / EA going to a 5:1 mixture giving a yellowish solid (0.45 g, 1.95 mmol, 60%).

R_f (8:1 CH/EA) = 0.14

^{1}H NMR (acetone-d_6): δ / ppm = 8.98 (s, 1H, H_a), 7.70 – 7.82 (m, 2H, H_b), 7.56 – 7.63 (m, 1H, H_c), 7.49 – 7.55 (m, 2H, H_d), 7.18 - 7.28 (m, 4H, H_{e+f}), 7.04 – 7.10 (m, 1H, H_g).
^{13}C NMR ($CDCl_3$): δ / ppm = 139.07, 136.51, 133.15, 129.45, 129.16, 127.36, 125.56, 121.79.
ATR-FT-IR: $\tilde{\nu}$ / cm^{-1} = 3203 (N-H), 2923 (C-H), 2877, 1597, 1495, 1474, 1447, 1413, 1329 (S=O), 1303, 1221, 1181, 1151 (S=O), 1093, 1029, 999, 927, 906 (S-N), 752, 723, 699, 685, 662, 622, 609, 579, 548.
ESI-MS: *m/z*: $[M + Na]^+$ calculated for $[C_{12}H_{11}NNaO_2S]^+$, 256.0403; found: 256.0399.

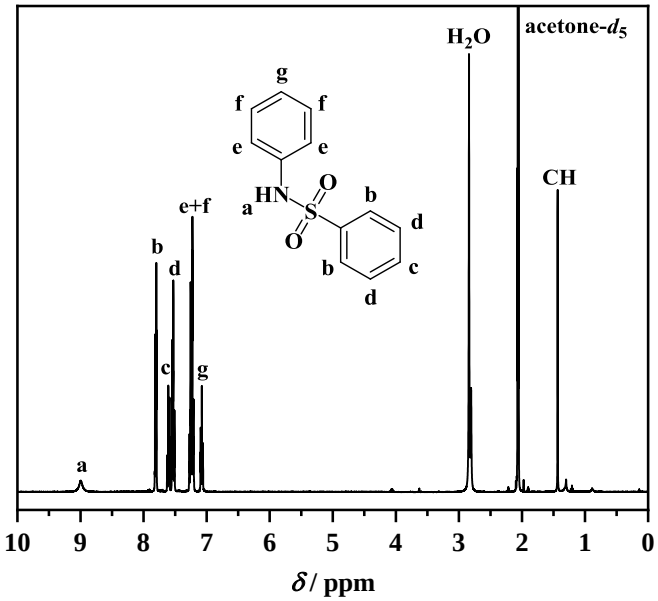

Figure 188. ^{1}H NMR spectrum of *N*-phenylbenzenesulfonamide; solvent: acetone-d_6.

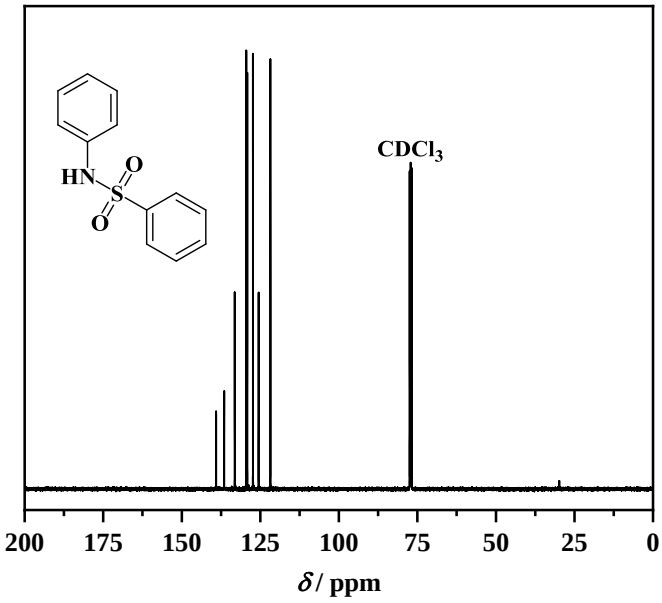

Figure 189. ^{13}C NMR spectrum of *N*-phenylbenzenesulfonamide; solvent: $CDCl_3$.

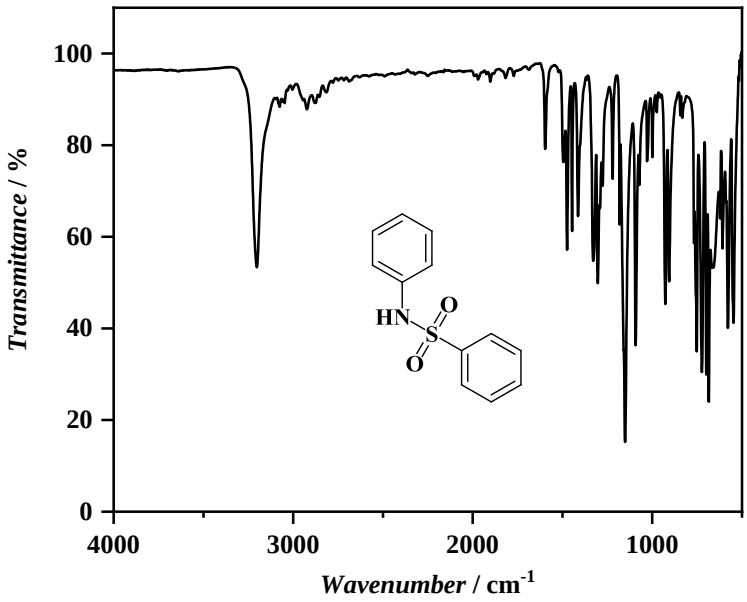

Figure 190. ATR-FT-IR spectrum of *N*-phenylbenzenesulfonamide.

6.6.5.2 Aza-Michael Addition of Butyl Acrylate to *N*-Phenylbenzenesulfonamide

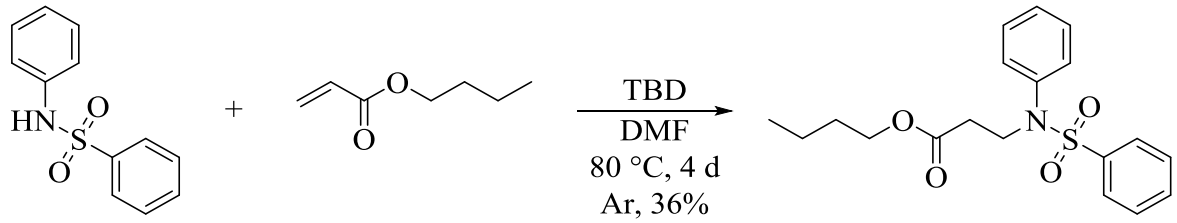

N-Phenylbenzenesulfonamide (0.036 g, 0.154 mmol, 1.00 eq.) and TBD (0.011 g, 0.077 mmol, 0.50 eq.) were dissolved in anhydrous DMF (1 mL). Deinhibited butyl acrylate (0.11 mL, 0.099 g, 0.771 mmol, 5.00 eq.) was added and the mixture was deoxygenated in an ice bath by argon purging for 15 minutes. The vial was placed in a preheated oil bath set to 80 °C for 4 days. The solvent was removed under reduced pressure and DCM (25 mL) was added. Afterwards, the organic phase was washed with water (3 × 25 mL) and was dried over magnesium sulfate. Subsequently, the solvent was removed under reduced pressure and the crude product was purified by column chromatography using a 4:1 mixture of CH / EA (0.02 g, 0.055 mmol, 36%).

R_f (4:1 CH/EA) = 0.44

^{1}H NMR (DCM-d_2): δ / ppm = 7.57 – 7.64 (m, 3H, H_{a+b}), 7.46 – 7.52 (m, 2H, H_c), 7.30 – 7.35 (m, 3H, H_{d+e}), 6.99 – 7.05 (m, 2H, H_f), 3.98 (t, J = 6.7 Hz, 2H, H_g), 3.84 (t, J = 7.3 Hz, 2H, H_h), 2.51 (t, J = 7.3 Hz, 2H, H_i), 1.49-1.58 (m, 2H, H_j), 1.29-1.38 (m, 2H, H_k), 0.91 (t, J = 7.4 Hz, 3H, H_l).

^{13}C NMR (DCM-d_2): δ / ppm = 171.35, 139.57, 138.68, 133.37, 129.64, 129.54, 129.47, 128.78, 128.18, 65.05, 47.53, 34.67, 31.10, 19.64, 14.02.

ATR-FT-IR: $\tilde{\nu}$ / cm^{-1} = 2958 (C-H), 2926, 1731 (C=O), 1595, 1493, 1447, 1351, 1163 (S=O), 1092, 1070, 1053, 1025, 946, 889, 759, 728, 691, 619, 588, 577, 562.

ESI-MS: *m/z*: $[M + Na]^+$ calculated for $[C_{19}H_{23}NNaO_4S]^+$, 384.1240; found: 384.1233.

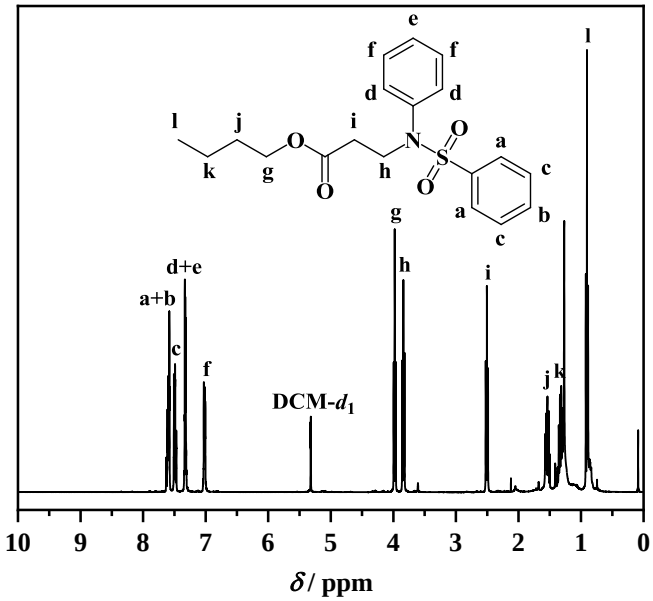

Figure 191. ^{1}H NMR spectrum of the model compound, i.e. butyl 3-(*N*-phenylphenylsulfonamido)propanoate, obtained after aza-Michael addition of *N*-phenylbenzenesulfonamide with butyl acrylate; solvent: DCM-d_2.

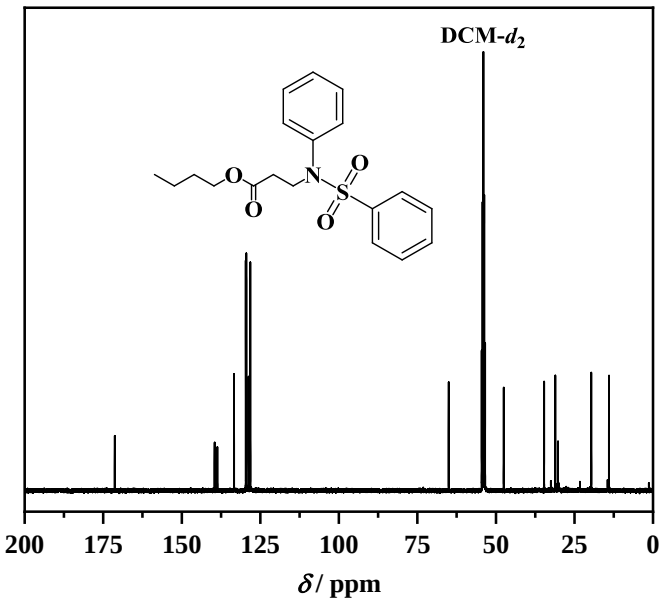

Figure 192. ^{13}C NMR spectrum of the model compound, i.e. butyl 3-(*N*-phenylphenylsulfonamido)propanoate, obtained after aza-Michael addition of *N*-phenylbenzenesulfonamide with butyl acrylate; solvent: DCM-d_2.

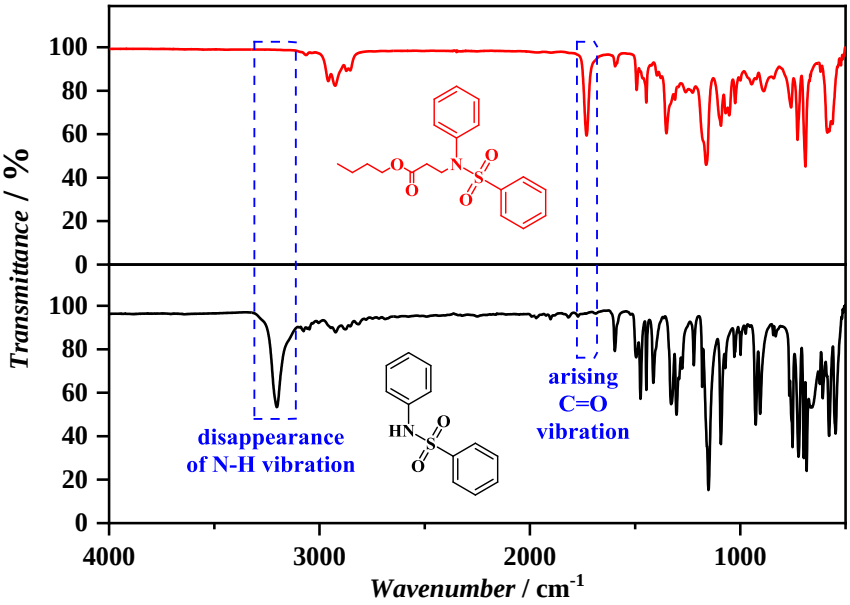

Figure 193. Comparison of the ATR-FT-IR spectra before (bottom, black line) and after (top, red line) the aza-Michael addition of *N*-phenylbenzenesulfonamide with butyl acrylate.

6.6.6 Electrolysis Procedures

6.6.6.1 Electrolysis of 4-Methyl-*N*-(4-vinylphenyl)benzenesulfonamide (M2)

6.6.6.1.1 Electrolysis Attempt using Bu_4NBF_4 as Electrolyte

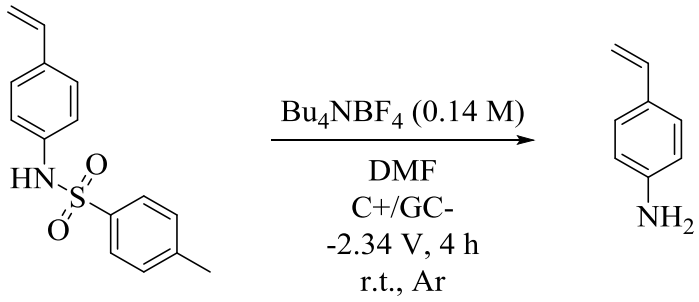

A dry ElectraSyn vial (10 mL) was charged with Bu_4NBF_4 (0.329 g, 1.00 mmol, 0.14 M) and 4-methyl-*N*-(4-vinylphenyl)benzenesulfonamide (M2) (0.048 g, 0.175 mmol). Subsequently, the solids were dissolved in anhydrous DMF (7 mL). The vial was closed with the respective IKA ElectraSyn cap bearing a graphite anode and a glassy carbon cathode and the solution was deoxygenated by argon purging for 15 minutes. A constant potential of -2.34 V was applied for 4 hours.

TLC exhibited that the majority of starting material remained intact during the experiment.

6.6.6.1.2 Electrolysis Attempt using Bu_4NHSO_4 as Electrolyte

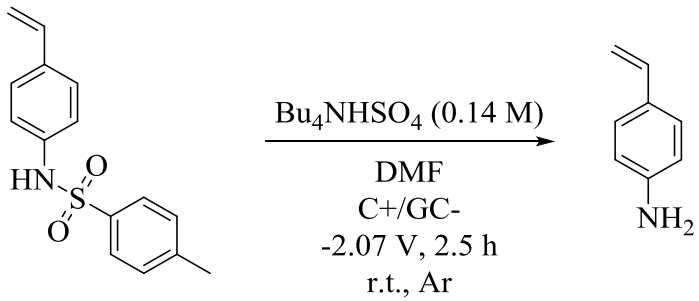

A dry ElectraSyn vial (10 mL) was charged with Bu_4NHSO_4 (0.340 g, 1.00 mmol, 0.14 M) and 4-methyl-*N*-(4-vinylphenyl)benzenesulfonamide (M2) (0.048 g, 0.175 mmol). Subsequently, the solids were dissolved in anhydrous DMF (7 mL). The vial was closed with the respective IKA ElectraSyn cap bearing a graphite anode and a glassy carbon cathode and the solution was deoxygenated by argon purging for 15 minutes. A constant potential of -2.07 V was applied for 2.5 hours.

TLC exhibited that the majority of starting material remained intact during the experiment.

6.6.6.1.3 Electrolysis Attempt using Naphthalene as Mediator

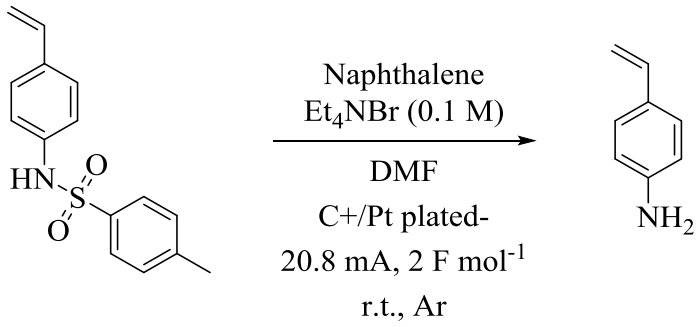

A dry ElectraSyn vial (10 mL) was charged with Et_4NBr (0.168 g, 0.800 mmol, 0.1 M), 4-methyl-*N*-(4-vinylphenyl)benzenesulfonamide (M2) (0.060 g, 0.220 mmol, 1.00 eq.), and naphthalene (0.014 g, 0.110 mmol, 0.50 eq.). Subsequently, the solids were dissolved in anhydrous DMF (8 mL). The vial was closed with the respective IKA ElectraSyn cap bearing a graphite anode and a platinum plated cathode and the solution was deoxygenated by argon purging for 15 minutes. A constant current of 20.8 mA was applied until 2 F mol^{-1} passed through the system. Saturated $Na_2S_2O_3$ solution (50 mL) and 1 M HCl (50 mL) were added and the aqueous phase was extracted with DCM (100 mL) three times. The combined organic phases were dried over magnesium sulfate. The solvent was removed under reduced pressure. TLC exhibited the formation of numerous products, this method is thus not applicable for the electrochemical deprotection on the polymer level.

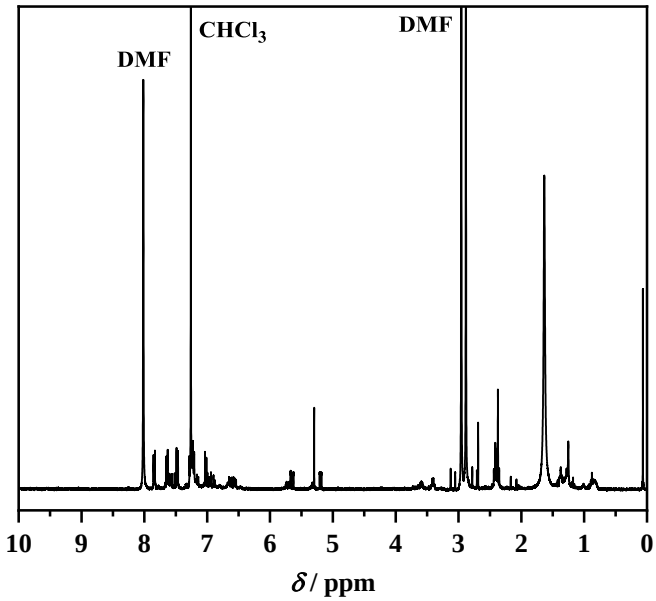

Figure 194. ^1H NMR spectrum of the crude product obtained after electrolysis with naphthalene as mediator; solvent: $CDCl_3$.

6.6.6.2 Electrolysis of Poly(4-methyl-*N*-(4-vinylphenyl)benzenesulfonamide) (P2)

6.6.6.2.1 Polymerization of 4-Methyl-*N*-(4-vinylphenyl)benzenesulfonamide) (M2)

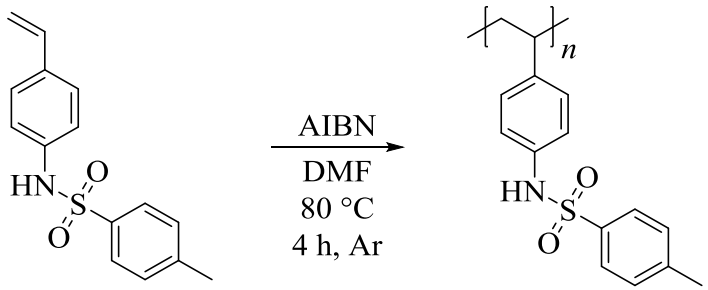

M2 **P2**

4-Methyl-*N*-(4-vinylphenyl)benzenesulfonamide (M2) (0.100 g, 0.366 mmol, 1.00 eq.) and AIBN (0.012 g, 0.073 mmol, 0.20 eq.) were dissolved in anhydrous DMF (0.5 mL). The solution was deoxygenated by argon purging for 15 minutes. The flask was placed in a preheated oil bath at 80 °C for 4 hours. Afterwards, polymer P2 was precipitated in cold diethyl ether, redissolved and precipitated again in cold diethyl ether giving a colorless solid (0.06 g).

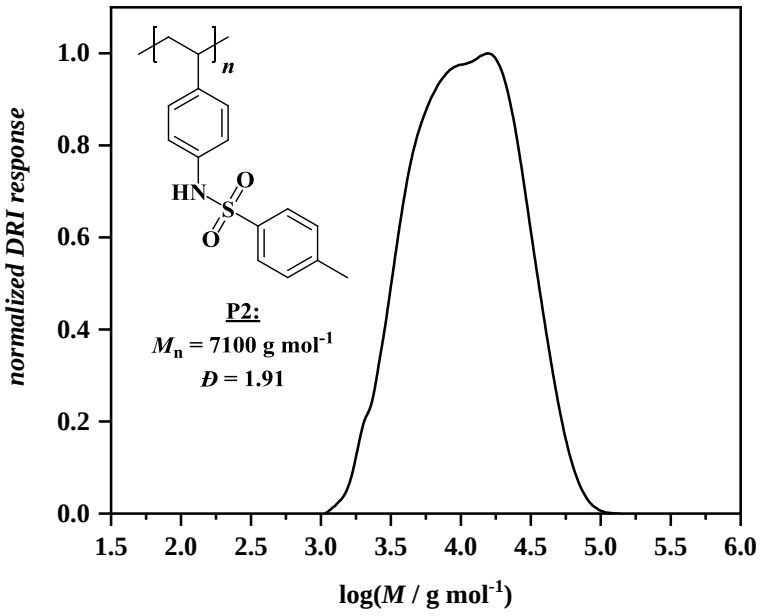

Figure 195. Size-exclusion chromatogram of poly(4-methyl-*N*-(4-vinylphenyl) benzenesulfonamide) (P2) using DMAc as eluent (PS calibration).

6.6.6.2.2 Electrolyis Attempt of Poly(4-methyl-*N*-(4-vinylphenyl)benzenesulfonamide) (P2)

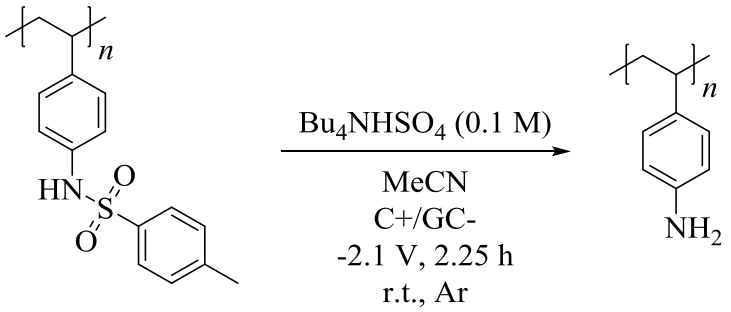

A dry ElectraSyn vial (10 mL) was charged with Bu_4NHSO_4 (0.238 g, 0.70 mmol, 0.1 M) and poly(4-methyl-*N*-(4-vinylphenyl)benzenesulfonamide) (P2) (0.067 g, 0.010 mmol). Subsequently, the solids were dissolved in anhydrous acetonitrile (7 mL). The vial was closed with the respective IKA ElectraSyn cap bearing a graphite anode and a glassy carbon cathode and the solution was deoxygenated by argon purging for 15 minutes. A constant potential of -2.10V was applied for 2.25 hours. The mixture was precipitated in water and the residue was obtained by centrifugation.

^{1}H NMR (DMSO-d_6): δ / ppm = 9.58 – 10.19 (1H, H_a), 7.39 – 7.66 (2H, H_b), 6.57 – 7.35 (4H, H_c+H_d), 5.71 – 6.42 (2H, H_e), 1.83 – 2.43 (3H, H_f), 0.58 – 1.71 (3H, H_g+H_h).

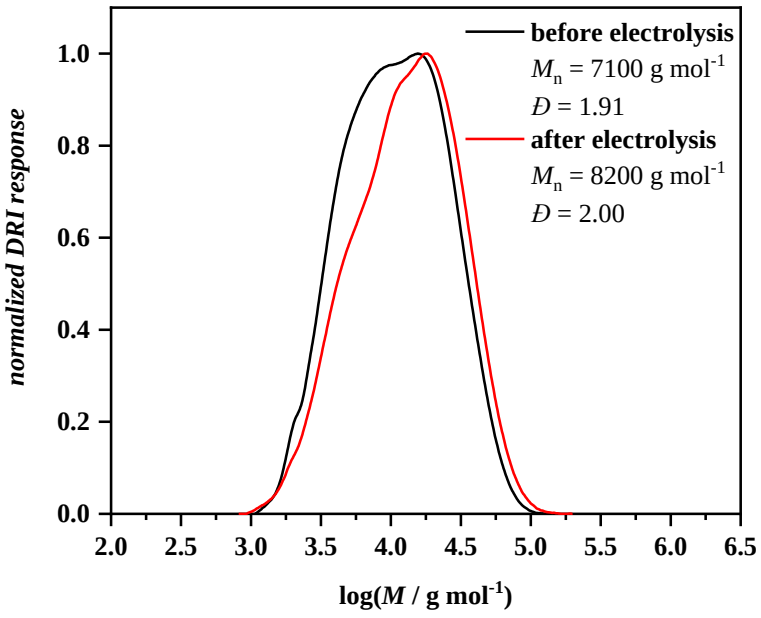

Figure 196. Comparison of size-exclusion chromatograms using DMAc as eluent (PS calibration) before (black line) and after (red line) electrolysis of P2.

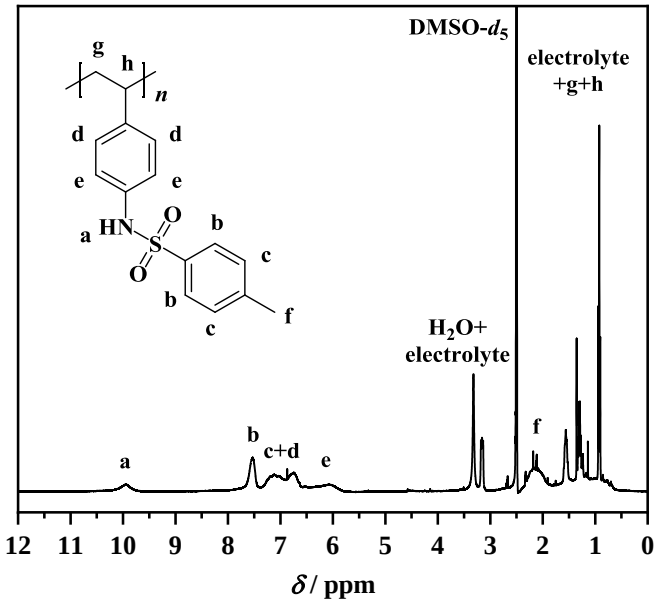

Figure 197. ^{1}H NMR spectrum after electrolysis of P2; solvent: DMSO-d_6.

7 Abbreviations

7.1 List of Abbreviations

%	Percentage
°C	Degree Celsius
α	Alpha
Ag/AgCl	Silver/silver chloride
AIBN	2,2′-Azobis(2-methylpropionitrile)
Aq.	Aqueous
Ar	Argon
ATR-FT-IR	Attenuated total reflection fourier-transform infrared spectroscopy
ATRP	Atom-transfer radical polymerization
BA	Butyl acrylate
Bbbpy	4,4′-Di-*tert*-butyl-2,2′-dipyridyl
Bu_4NBF_4	Tetrabutylammonium tetrafluoroborate
Bu_4NHSO_4	Tetrabutylammonium hydrogensulfate
Bu_4NPF_6	Tetrabutylammonium hexafluorophosphate
C+	Graphite anode
C-	Graphite cathode
CH	Cyclohexane
CO_2	Carbon dioxide
CPAD	4-Cyano-4-(phenylcarbonothioylthio)-2-methylpropionic acid
CSIRO	Commonwealth Scientific and Industrial Research Organisation
CTA	Chain-transfer agent
CuAAC	Copper-catalyzed alkyne-azide cycloaddition
CV	Cyclic voltammetry
DCM	Dichloromethane
Δ	Delta
δ	Chemical shift in NMR spectroscopy
d	Day
DFPA	2,6-Difluorophenyl acrylate
DLS	Dynamic light scattering
DMAc	*N*,*N*-Dimethylacetamide
DMF	*N*,*N*-Dimethylformamide

Abbreviations

DMSO	Dimethyl sulfoxide
DNA	Deoxyribonucleic acid
DP_n	Degree of polymerization
DSC	Differential scanning calorimetry
e.g.	exempli gratia
EA	Ethyl acetate
E_{app}	Applied voltage
eATRP	Electrochemically-mediated atom-transfer radical polymerization
Eq.	Equivalents
eRAFT	Electrochemically-mediated reversible addition-fragmentation chain-transfer
ESI-MS	Electrospray ionization mass spectrometry
et al.	Et alii
Et_3N	Triethylamine
Et_4NBr	Tetraethylammonium bromide
F	Faraday
F mol^{-1}	Faraday per mole
FRP	Free radical polymerization
GC-	Glassy carbon cathode
GMA	Glycidyl methacrylate
h	Hour
HBF_4	Tetrafluoroboric acid
HCl	Hydrochloric acid
i.e.	Id est
IR	Infrared
K	Kelvin
M	Molar
M1	*N*-(4-Vinylphenyl)benzenesulfonamide
M2	4-Methyl-*N*-(4-vinylphenyl)benzenesulfonamide
M3	4-Fluoro-*N*-(4-vinylphenyl)benzenesulfonamide
M4	4-Nitro-*N*-(4-vinylphenyl)benzenesulfonamide
M5	3-((4-Methylphenyl)sulfonamido)propyl methacrylate
M_n	Number-average molar mass
M_w	Weight-average molar mass

mA	Milliampere
Me_6TREN	Tris[2-(dimethylamino)ethyl]amine
MeCN	Acetonitrile
MeOH	Methanol
MHz	Megahertz
mL	Milliliter
mm	millimeter
mM	Millimolar
MMA	Methyl methacrylate
mmol	Millimole
mol	Mole
mol%	Mole percentage
N_2	Nitrogen
$NaNO_2$	Sodium nitrite
NaOH	Sodium hydroxide
$Na_2S_2O_3$	Sodium thiosulfate
NHS	*N*-Hydroxysuccinimide
$NiBr_2$·dme	Nickel(II) bromide ethylene glycol dimethyl ether complex
NMP	Nitroxide-mediated polymerization
NMR	Nuclear magnetic resonance
ω	Omega
p	Extent of reaction
P1	Poly(*N*-(4-vinylphenyl)benzenesulfonamide)
P2	Poly(4-methyl-*N*-(4-vinylphenyl)benzenesulfonamide)
P3	Poly(4-fluoro-*N*-(4-vinylphenyl)benzenesulfonamide)
P4	Poly(4-nitro-*N*-(4-vinylphenyl)benzenesulfonamide)
PBA	Poly(butyl acrylate)
PDFPA	Poly(2,6-difluorophenyl acrylate)
PE	Petroleum ether
PEO	Poly(ethylene oxide)
PFPA	Pentafluorophenyl acrylate
PFTR	*Para*-fluoro-thiol reactions
PGMA	Poly(glycidyl methacrylate)
PMA	Poly(methyl acrylate)

PMCCP	Pentakis(methoxycarbonyl)cyclopentadiene
PMMA	Poly(methyl methacrylate)
PPFPA	Poly(pentafluorophenyl acrylate)
PPM	Post-polymerization modification
ppm	Parts per million
PS	Polystyrene
Pt plated-	Platinum plated cathode
r.t.	Room temperature
RAFT	Reversible addition-fragmentation chain-transfer
RDRP	Reversible-deactivation radical polymerization
RI	Refractive index
ROP	Ring-opening polymerization
RVC	Reticulated vitreous carbon
Salen	2,2′-Ethylenebis(nitrilomethylidene)diphenol
sat.	Saturated
SCE	Saturated calomel electrode
SCNP	Single-chain nanoparticle
seATRP	Simplified electrochemically-mediated atom-transfer radical polymerization
SEC	Size-exclusion chromatography
T	Temperature
TBD	1,5,7-Triazabicyclo[4.4.0]dec-5-ene
TEMPO	2,2,6,6-Tetramethylpiperidinyl-1-oxy
T_g	Glass transition temperature
TGA	Thermogravimetric analysis
THF	Tetrahydrofuran
TLC	Thin-layer chromatography
Tosyl	Toluenesulfonyl
unsat.	Unsaturated
UV/Vis	Ultraviolet-visible
V	Voltage
vs.	Versus
$\tilde{\nu}$	Wavenumber
wt%	Weight percentage

Zn+	Zinc anode

8 List of Schemes, Figures, and Tables

8.1 List of Schemes

8.2 List of Figures

8.3 List of Tables

9 Danksagung

An dieser Stelle möchte ich allen Personen, die mich während meiner Promotion begleitet und unterstützt haben, meinen herzlichsten Dank aussprechen.

An erster Stelle möchte ich PROF. DR. PATRICK THÉATO danken. Ich bin Dir sehr dankbar dafür, dass Du mir ermöglicht hast, meine Doktorarbeit in Deiner Arbeitsgruppe anfertigen zu dürfen. Außerdem möchte ich Dir dafür danken, dass Du meinen Forschungsaufenthalt am Scripps Research ermöglicht hast und mich dahingehend auch unterstützt hast. Des Weiteren bedanke ich mich für die Korrektur der vorliegenden Arbeit und für die Evaluierung dieser Arbeit im Rahmen als 1. Referent.
Im Zuge dessen möchte ich mich auch herzlichst bei PROF. DR. MICHAEL MEIER für die bereitwillige Übernahme der Rolle des Korreferenten bedanken.
Außerdem möchte ich bei den Prüfern in der Promotionsprüfung, namentlich PROF. DR. MICHAEL MEIER, PROF. DR. ROLF SCHUSTER sowie PRIV.-DOZ. MANUEL TSOTSALAS bedanken. Darüber hinaus gilt mein Dank PROF. DR. PAVEL LEVKIN für die Übernahme des Prüfungsvorsitzes in selbiger.

Mein weiterer Dank gilt PROF. DR. PHIL BARAN, der mich im Rahmen meines Auslandsforschungsaufenthalts in seine Gruppe aufgenommen hat und mir diesen damit erst ermöglicht hat. Ich bin sehr dankbar, dass ich im "Baran Lab" arbeiten durfte und ich damit die Erfahrung machen durfte, knapp 3 Monate in San Diego zu leben. Dieser Aufenthalt hat mich persönlich, aber auch wissenschaftlich sehr bereichert.
Diesbezüglich möchte ich mich auch bei allen Mitgliedern des "Baran Lab" für die herzliche Aufnahme und die gute Arbeitsatmosphäre bedanken. Vor allem danken möchte ich "462", namentlich JULIEN, SAMER, KEVIN, CODY, EVA und JOHANNES "JOJO" TESKE. Letzterem gilt mein aufrichtiger Dank für die Unterstützung bei der Planung des Aufenthalts sowie Tipps rund um San Diego. Weiterhin danke ich YUSUKE, mit dem ich im "Baran Lab" an einem gemeinsamen Projekt arbeiten durfte. Ich habe mich immer gut aufgehoben gefühlt und habe dabei noch sehr viel gelernt, danke dafür.
An dieser Stelle möchte ich mich auch direkt beim KARLSRUHE HOUSE OF YOUNG SCIENTISTS (KHYS) für die Förderung meines Auslandsaufenthalts bedanken. Ich bin sehr dankbar für die Unterstützung, die den Auslandsaufenthalt erst möglich gemacht hat. Es war eine wertvolle Erfahrung und eine schöne Zeit, auf die ich positiv zurückblicken werde.

Danksagung

Ein großes Dankeschön möchte ich KATHARINA ELIES aussprechen. Danke für Deine frohe und lustige Art und dafür, dass Du die Gruppe am Laufen hältst. Ich hoffe, Dir widerfährt die Anerkennung für Deine Leistungen, die Dir gebührt.
Im Zuge dessen möchte ich mich bei EVELYN STÜHRING, VERA NOGA, BÄRBEL SEUFERT-DAUSMANN, MARTINA RITTER, BIRGIT HUBER und nicht zuletzt DR. DOMINIK VOLL für die bürokratische und organisatorische Unterstützung bedanken.
Außerdem gilt mein herzlicher Dank DR. HATICE MUTLU, dank ihr nahm das letzte Forschungsprojekt eine erfolgreiche Wende und ohne sie wären die Vorarbeiten umsonst gewesen. Vielen Dank für die herausragende Betreuung und die reibungslose Zusammenarbeit. Ich wünsche Dir für Deine berufliche, aber auch persönliche Zukunft nur das Beste.

Darüber hinaus möchte ich meinen Dank meinem Bachelorstudenten TILMAN GRÜGER aussprechen, es war mir eine Freude, mit Dir ein neues Themengebiet zu erschließen.

Natürlich möchte ich mich auch bei allen Mitgliedern der Forschungsgruppe von Prof. Théato für die angenehme Zusammenarbeit bedanken. Namentlich erwähnen möchte ich hier zuerst MARTIN, mit dem ich nicht nur zeitgleich im Januar 2018 und als erste Doktoranden von Prof. Théato am KIT anfangen durfte, sondern nun auch zusammen die Arbeit einreichen werde. Es war eine schöne und unterhaltsame Zeit zusammen und ich bin froh, in Dir einen guten Freund sowie „Leidensgenossen“ gefunden zu haben. Nicht unerwähnt lassen möchte ich außerdem SERGEJ, der kurz nach unserem Start unserem Labor beitrat und mit dem es mir eine Freude war, den Arbeitsalltag zu bewältigen. Danke für die gemeinsame Zeit über all die Jahre.
Mein besonderer Dank gilt hierbei ANDREAS und STEFAN, die ich mittlerweile zu meinen sehr guten Freunden zählen darf. Es war eine äußerst schöne und lustige Zeit zusammen und ich bin froh, dass wir uns kennengelernt haben. Ich bin mir sicher, dass der Kontakt auch weiterhin so lebhaft aufrecht erhalten bleibt und wünsche euch weiterhin viel Erfolg auf euren Wegen. Danke auch für die Korrektur dieser Arbeit.

Forthin möchte ich mich bei meinen Studienfreunden für die Begleitung auf meinem Weg und die dadurch entstandenen Freundschaften bedanken. Namentlich hier genannt werden sollen MAXIMILIANE, DAVID, SEBASTIAN, FELIX, DANIEL, FABIAN, MAREEN und KEVIN. Auch hier hoffe ich, dass wir weiterhin in engem Kontakt stehen werden. Diesbezüglich möchte ich ausdrücklich MAXIMILIANE und DAVID für gemeinsame Urlaube, Erlebnisse und Unterstützung

in jeglicher Hinsicht sowie für die Korrektur dieser Arbeit danken. Ich habe keine Zweifel, dass wir auch weiterhin schöne gemeinsame Erlebnisse teilen werden.
Auch meinen langjährigen Freunden, PASCAL D. und PASCAL G., KEVIN und SVEN, JANNIS, TINA, PIOTR und JULIAN möchte ich meinen ausdrücklichen Dank aussprechen.

Schlussendlich liegt mir nichts näher, als mich bei meiner Familie für die großartige und bedingungslose Unterstützung zu bedanken. Ihr habt mich durch schöne und nicht ganz so schöne Zeiten begleitet und ohne euch könnte ich diese Arbeit heute nicht im Ansatz einreichen. Es ist schwierig, meine unendliche Dankbarkeit in Worte auszudrücken und hoffe euch irgendwann all das zurückgeben zu können, was ihr mir gegeben habt. Aus diesen Gründen möchte ich euch hier an dieser Stelle dieser Arbeit verewigt wissen.

Danksagung

10 List of Publications

Publications Arising from this Thesis

[2] Electrochemically-Initiated Polymerization of Reactive Monomers via 4-Fluorobenzenediazonium Salts
E. Molle, S. Frech, T. Grüger, P. Theato, *Polym. Chem.* **2021**, under Revision.

[1] Synthesis and Post-Polymerization Modification of Poly(*N*-(4-Vinylphenyl) Sulfonamide)s
E. Molle, H. Mutlu, P. Theato, *Macromol. Rapid Commun.* **2021**, *30*, 2100063.

Other Publications

[4] Ethylene-free Synthesis of Polyethylene Copolymers and Block Copolymers
S. Frech, E. Molle, A. J. Butzelaar, P. Theato, *Macromolecules*, submitted.

[3] Synthesis and Post-Polymerization Modification of Defined Functional Poly(Vinyl ether)s
A. J. Butzelaar, S. Schneider, E. Molle, P. Theato, *Macromol. Rapid Commun.* **2021**, *42*, 2100133.

[2] Access to Photoreactive Core-Shell Nanomaterials by Photoinitiated Polymerization-Induced Self-Assembly
E. Molle, D. Le, T. N. Abbariki, M. S. Akdemir, M. Takamiya, E. Miceli, O. Kassel, G. Delaittre, *ChemPhotoChem* **2019**, *3*, 1084-1089.

[1] Star polymer synthesis *via* λ-orthogonal photochemistry
K. Hiltebrandt, M. Kaupp, E. Molle, J. P. Menzel, J. P. Blinco, C. Barner-Kowollik, *Chem. Commun.* **2016**, *52*, 9426-9429.

Conference Contributions

[1] pH-Switchable Water Solubility of Sulfonamide-based Polymers and their Post-Polymerization Modification
Poster at the “100 Years Macromolecular Chemistry” Conference, September 28th - 29th, 2020.

11 References

[1] X. Xu, L. He, B. Zhu, J. Li, J. Li, *Polym. Chem.* **2017**, *8*, 807–823.

[2] S. H. Dickens, J. W. Stansbury, K. M. Choi, C. J. E. Floyd, *Macromolecules* **2003**, *36*, 6043–6053.

[3] D. Rokaya, V. Srimaneepong, J. Sapkota, J. Qin, K. Siraleartmukul, V. Siriwongrungson, *J. Adv. Res.* **2018**, *14*, 25–34.

[4] A. Kowalska, J. Sokolowski, K. Bociong, *Polymers* **2021**, *13*, 470.

[5] B. Fu, J. Gao, *J. Phys. Conf. Ser.* **2020**, *1676*, 12044.

[6] N. Li, *Adv. Mater. Res.* **2014**, *1028*, 337–340.

[7] M. Yan, Y. Kawamata, P. S. Baran, *Chem. Rev.* **2017**, *117*, 13230–13319.

[8] A. Wiebe, T. Gieshoff, S. Möhle, E. Rodrigo, M. Zirbes, S. R. Waldvogel, *Angew. Chem. Int. Ed.* **2018**, *57*, 5594–5619.

[9] B. A. Frontana-Uribe, R. D. Little, J. G. Ibanez, A. Palma, R. Vasquez-Medrano, *Green Chem.* **2010**, *12*, 2099–2119.

[10] G. G. Botte, *Electrochem. Soc. Interface* **2014**, *23*, 49–55.

[11] R. J. Waltman, J. Bargon, *Can. J. Chem.* **1986**, *64*, 76–95.

[12] F. Garnier, G. Tourillon, M. Gazard, J. C. Dubois, *J. Electroanal. Chem.* **1983**, *148*, 299–303.

[13] S. Sadki, P. Schottland, N. Brodie, G. Sabouraud, *Chem. Soc. Rev.* **2000**, *29*, 283–293.

[14] A. F. Diaz, K. K. Kanazawa, G. P. Gardini, *J. Chem. Soc., Chem. Commun.* **1979**, 635–636.

[15] S. Kim, L. K. Jang, H. S. Park, J. Y. Lee, *Sci. Rep.* **2016**, *6*, 30475.

[16] B. K. Garg, R. A. V. Raff, R. V. Subramanian, *J. Appl. Polym. Sci.* **1978**, *22*, 65–87.

[17] P. Chmielarz, M. Fantin, S. Park, A. A. Isse, A. Gennaro, A. J. D. Magenau, A. Sobkowiak, K. Matyjaszewski, *Prog. Polym. Sci.* **2017**, *69*, 47–78.

[18] F. Lorandi, M. Fantin, A. A. Isse, A. Gennaro, *Curr. Opin. Electrochem.* **2018**, *8*, 1–7.

[19] Y. Wang, M. Fantin, S. Park, E. Gottlieb, L. Fu, K. Matyjaszewski, *Macromolecules* **2017**, *50*, 7872–7879.

[20] W. Sang, M. Xu, Q. Yan, *ACS Macro Lett.* **2017**, *6*, 1337–1341.

[21] F. Lorandi, M. Fantin, S. Shanmugam, Y. Wang, A. A. Isse, A. Gennaro, K. Matyjaszewski, *Macromolecules* **2019**, *52*, 1479–1488.

[22] C. Bray, G. Li, A. Postma, L. T. Strover, J. Wang, G. Moad, *Aust. J. Chem.* **2021**, *74*, 56–64.

[23] A. Sangroniz, J. B. Zhu, X. Tang, A. Etxeberria, E. Y. X. Chen, H. Sardon, *Nat. Commun.* **2019**, *10*, 3559.

[24] Z. O. G. Schyns, M. P. Shaver, *Macromol. Rapid Commun.* **2021**, *42*, 2000415.

[25] F. C. Cabrera, *Polym. Compos.* **2021**, 1–25.

[26] F. A. Cruz Sanchez, H. Boudaoud, M. Camargo, J. M. Pearce, *J. Clean. Prod.* **2020**, *264*, 121602.

[27] K. Kaiser, M. Schmid, M. Schlummer, *Recycling* **2018**, *3*, 1.

[28] J. Hopewell, R. Dvorak, E. Kosior, *Philos. Trans. R. Soc. B Biol. Sci.* **2009**, *364*, 2115–2126.

[29] J. D. Watson, F. H. C. Crick, *Nature* **1953**, *171*, 737–738.

[30] D. Feldman, *Des. Monomers Polym.* **2008**, *11*, 1–15.

[31] R. B. Seymour, *J. Chem. Educ.* **1988**, *65*, 327–334.

[32] R. E. Oesper, *J. Chem. Educ.* **1929**, *6*, 677–685.

[33] W. A. Cunningham, *J. Chem. Educ.* **1935**, *12*, 120–124.

[34] P. E. M. Berthelot, *C. R. Hebd. Seances Acad. Sci.* **1866**, *63*, 479.

[35] P. E. M. Berthelot, *C. R. Hebd. Seances Acad. Sci.* **1866**, *63*, 515.

[36] P. E. M. Berthelot, *Bull. Soc. Chim. Fr.* **1866**, *2*, 268.

[37] P. E. M. Berthelot, *Justus Liebigs Ann. Chem.* **1867**, *141*, 173.

[38] A. S. Abd-El-Aziz, M. Antonietti, C. Barner-Kowollik, W. H. Binder, A. Böker, C. Boyer, M. R. Buchmeiser, S. Z. D. Cheng, F. D'Agosto, G. Floudas, et al., *Macromol. Chem. Phys.* **2020**, *221*, 2000216.

[39] H. Staudinger, *Ber. Dtsch. Chem. Ges.* **1920**, *53*, 1073–1085.

[40] H. Frey, T. Johann, *Polym. Chem.* **2020**, *11*, 8–14.

[41] A. D. Jenkins, R. F. T. Stepto, P. Kratochvíl, U. W. Suter, *Pure Appl. Chem.* **1996**, *68*, 2287–2311.

[42] T. C. Ward, *J. Chem. Educ.* **1981**, *58*, 867–879.

[43] R. Whitfield, N. P. Truong, D. Messmer, K. Parkatzidis, M. Rolland, A. Anastasaki, *Chem. Sci.* **2019**, *10*, 8724–8734.

[44] D. Colombani, *Prog. Polym. Sci.* **1997**, *22*, 1649–1720.

[45] K. Marsh, B. Bugusu, *J. Food Sci.* **2007**, *72*, 39–55.

[46] N. H. Ramli Sulong, S. A. S. Mustapa, M. K. Abdul Rashid, *J. Appl. Polym. Sci.* **2019**, *136*, 47529.

[47] J. G. Pick, R. F. Knee, *J. Cell. Plast.* **1967**, *3*, 108–114.

[48] J. O. Akindoyo, M. D. H. Beg, S. Ghazali, M. R. Islam, N. Jeyaratnam, A. R. Yuvaraj,

RSC Adv. **2016**, *6*, 114453–114482.

[49] F. E. Golling, R. Pires, A. Hecking, J. Weikard, F. Richter, K. Danielmeier, D. Dijkstra, *Polym. Int.* **2019**, *68*, 848–855.

[50] G. T. Howard, *Int. Biodeterior. Biodegrad.* **2002**, *49*, 245–252.

[51] N. Hadjichristidis, M. Pitsikalis, S. Pispas, H. Iatrou, *Chem. Rev.* **2001**, *101*, 3747–3792.

[52] S. Aoshima, S. Kanaoka, *Chem. Rev.* **2009**, *109*, 5245–5287.

[53] E. Y. X. Chen, *Chem. Rev.* **2009**, *109*, 5157–5214.

[54] N. E. Kamber, W. Jeong, R. M. Waymouth, R. C. Pratt, B. G. G. Lohmeijer, J. L. Hedrick, *Chem. Rev.* **2007**, *107*, 5813–5840.

[55] P. Nesvadba, Radical Polymerization in Industry. In *Encyclopedia of Radicals in chemistry, Biology and Materials*; Wiley: New Jersey, **2012**.

[56] K. S. Khuong, W. H. Jones, W. A. Pryor, K. N. Houk, *J. Am. Chem. Soc.* **2005**, *127*, 1265–1277.

[57] W. Devonport, L. Michalak, E. Malmström, M. Mate, B. Kurdi, C. J. Hawker, G. G. Barclay, R. Sinta, *Macromolecules* **1997**, *30*, 1929–1934.

[58] Y. K. Chong, E. Rizzardo, D. H. Solomon, *J. Am. Chem. Soc.* **1983**, *105*, 7761–7762.

[59] Y. Kotsuchibashi, R. Narain, *Polym. Chem.* **2014**, *5*, 3061–3070.

[60] A. A. R. Hmayed, S. Norsic, V. Monteil, J. Raynaud, *Polym. Chem.* **2020**, *11*, 1001–1009.

[61] J. E. McGrath, *J. Chem. Educ.* **1981**, *58*, 844–861.

[62] H. Tobita, *Processes* **2018**, *6*, 14.

[63] T. Furuncuoğlu, I. Uğur, I. Degirmenci, V. Aviyente, *Macromolecules* **2010**, *43*, 1823–1835.

[64] K. Hong, H. Zhang, J. W. Mays, A. E. Visser, C. S. Brazel, J. D. Holbrey, W. M. Reichert, R. D. Rogers, *Chem. Commun.* **2002**, 1368–1369.

[65] A. D. Jenkins, R. G. Jones, G. Moad, *Pure Appl. Chem.* **2010**, *82*, 483–491.

[66] M. Szwarc, *Nature* **1956**, *178*, 1168–1169.

[67] H. Frey, T. Ishizone, *Macromol. Chem. Phys.* **2017**, *218*, 1700217.

[68] J. Chiefari, Y. K. B. Chong, F. Ercole, J. Krstina, J. Jeffery, T. P. T. Le, R. T. A. Mayadunne, G. F. Meijs, C. L. Moad, G. Moad, et al., *Macromolecules* **1998**, *31*, 5559–5562.

[69] T. P. Le, G. Moad, E. Rizzardo, S. H. Thang, *Polymerization with Living Characteristics*, **1998**, WO1998001478.

[70] P. Corpart, D. Charmot, T. Biadatti, S. Zard, D. Michelet, *Method for Block Polymer*

Synthesis by Controlled Radical Polymerisation, **1998**, WO1998058974.

[71] M. Kato, M. Kamigaito, M. Sawamoto, T. Higashimura, *Macromolecules* **1995**, *28*, 1721–1723.

[72] J.-S.- Wang, K. Matyjaszewski, *J. Am. Chem. Soc.* **1995**, *117*, 5614–5615.

[73] P. C. D. H. Solomon, E. Rizzardo, *Poymerization Process and Polymers Produced Thereby*, **1986**, US4581429.

[74] M. Najafi, H. Roghani-Mamaqani, V. Haddadi-Asl, M. Salami-Kalajahi, *Adv. Polym. Technol.* **2011**, *30*, 257–268.

[75] G. Moad, E. Rizzardo, S. H. Thang, *Polymer* **2008**, *49*, 1079–1131.

[76] S. Perrier, *Macromolecules* **2017**, *50*, 7433–7447.

[77] M. Destarac, *Polym. Chem.* **2018**, *9*, 4947–4967.

[78] T. Otsu, M. Yoshida, T. Tazaki, *Makromol. Chem., Rapid Commun.* **1982**, *3*, 133–140.

[79] J. Phommalysack-Lovan, Y. Chu, C. Boyer, J. Xu, *Chem. Commun.* **2018**, *54*, 6591–6606.

[80] C. Barner-Kowollik, M. Buback, B. Charleux, M. L. Coote, M. Drache, T. Fukuda, A. Goto, B. Klumperman, A. B. Lowe, J. B. Mcleary, et al., *J. Polym. Sci. Part A Polym. Chem.* **2006**, *44*, 5809–5831.

[81] X. Tian, J. Ding, B. Zhang, F. Qiu, X. Zhuang, Y. Chen, *Polymers* **2018**, *10*, 318.

[82] M. Benaglia, J. Chiefari, Y. K. Chong, G. Moad, E. Rizzardo, S. H. Thang, *J. Am. Chem. Soc.* **2009**, *131*, 6914–6915.

[83] G. Moad, D. Keddie, C. Guerrero-Sanchez, E. Rizzardo, S. H. Thang, *Macromol. Symp.* **2015**, *350*, 34–42.

[84] S. Sinnwell, A. J. Inglis, T. P. Davis, M. H. Stenzel, C. Barner-Kowollik, *Chem. Commun.* **2008**, 2052–2054.

[85] A. Beloqui, S. R. Mane, M. Langer, M. Glassner, D. M. Bauer, L. Fruk, C. Barner-Kowollik, G. Delaittre, *Angew. Chem. Int. Ed.* **2020**, *59*, 19951–19955.

[86] K. Matyjaszewski, M. Wei, J. Xia, N. E. McDermott, *Macromolecules* **1997**, *30*, 8161–8164.

[87] T. Ando, M. Kamigaito, M. Sawamoto, *Macromolecules* **1997**, *30*, 4507–4510.

[88] B. Wang, Y. Zhuang, X. Luo, S. Xu, X. Zhou, *Macromolecules* **2003**, *36*, 9684–9686.

[89] N. Ayres, *Polym. Rev.* **2011**, *51*, 138–162.

[90] W. Tang, K. Matyjaszewski, *Macromolecules* **2006**, *39*, 4953–4959.

[91] W. Tang, N. V. Tsarevsky, K. Matyjaszewski, *J. Am. Chem. Soc.* **2006**, *128*, 1598–1604.

[92] W. Tang, Y. Kwak, W. Braunecker, N. V. Tsarevsky, M. L. Coote, K. Matyjaszewski,

J. Am. Chem. Soc. **2008**, *130*, 10702–10713.

[93] W. Tang, K. Matyjaszewski, *Macromolecules* **2007**, *40*, 1858–1863.

[94] J. Lu, Y. Zheng, D. Wu, D. Sun, Q. Shan, S. Fan, *FEBS Lett.* **2006**, *580*, 6730–6740.

[95] P. Dusek, P. M. Roos, T. Litwin, S. A. Schneider, T. P. Flaten, J. Aaseth, *J. Trace Elem. Med. Biol.* **2015**, *31*, 193–203.

[96] N. V. Tsarevsky, B. S. Sumerlin, K. Matyjaszewski, *Macromolecules* **2005**, *38*, 3558–3561.

[97] J. F. Lutz, H. G. Börner, K. Weichenhan, *Macromolecules* **2006**, *39*, 6376–6383.

[98] A. P. Vogt, B. S. Sumerlin, *Macromolecules* **2006**, *39*, 5286–5292.

[99] J. F. Lutz, H. G. Börner, K. Weichenhan, *Macromol. Rapid Commun.* **2005**, *26*, 514–518.

[100] J. A. Opsteen, J. C. M. Van Hest, *Chem. Commun.* **2005**, 57–59.

[101] R. Huisgen, G. Szeimies, L. Möbius, *Chem. Ber.* **1967**, *100*, 2494–2507.

[102] D. H. Solomon, E. Rizzardo, P. Cacioli, *Free Radical Polymerization and the Produced Polymers*, **1985**, EP135280A2.

[103] C. J. Hawker, A. W. Bosman, E. Harth, *Chem. Rev.* **2001**, *101*, 3661–3688.

[104] M. K. Georges, R. P. N. Veregin, P. M. Kazmaier, G. K. Hamer, *Macromolecules* **1993**, *26*, 2987–2988.

[105] C. J. Hawker, *J. Am. Chem. Soc.* **1994**, *116*, 11185–11186.

[106] C. J. Hawker, G. G. Barclay, A. Orellana, J. Dao, W. Devonport, *Macromolecules* **1996**, *29*, 5245–5254.

[107] Y. Guillaneuf, P. E. Dufils, L. Autissier, M. Rollet, D. Gigmes, D. Bertin, *Macromolecules* **2010**, *43*, 91–100.

[108] E. Harth, C. J. Hawker, W. Fan, R. M. Waymouth, *Macromolecules* **2001**, *34*, 3856–3862.

[109] M. Szwarc, M. Levy, R. Milkovich, *J. Am. Chem. Soc.* **1956**, *78*, 2656–2657.

[110] J. K. Stille, *J. Chem. Educ.* **1981**, *58*, 862–866.

[111] P. J. Flory, *J. Am. Chem. Soc.* **1936**, *58*, 1877–1885.

[112] W. H. Carothers, *J. Am. Chem. Soc.* **1929**, *51*, 2548–2559.

[113] W. H. Carothers, *Trans. Faraday Soc.* **1936**, *32*, 39–49.

[114] S. Kéki, M. Zsuga, Á. Kuki, *J. Phys. Chem. B* **2013**, *117*, 4151–4155.

[115] K. Pang, R. Kotek, A. Tonelli, *Prog. Polym. Sci.* **2006**, *31*, 1009–1037.

[116] A. Kausar, *J. Plast. Film Sheeting* **2019**, *35*, 331–353.

[117] M. Winnacker, *Biomater. Sci.* **2017**, *5*, 1230–1235.

[118] P. Theato, H.-A. Klok, *Functional Polymers by Post-Polymerization Modification: Concepts, Guidelines, and Applications*, Wiley-VCH Verlag GmbH & Co. KGaA, Weinheim, **2013**.

[119] W. Xue, H. Mutlu, P. Theato, *Eur. Polym. J.* **2020**, *130*, 109660.

[120] V. V. Rostovtsev, L. G. Green, V. V. Fokin, K. B. Sharpless, *Angew. Chem. Int. Ed.* **2002**, *41*, 2596–2599.

[121] C. W. Tornøe, C. Christensen, M. Meldal, *J. Org. Chem.* **2002**, *67*, 3057–3064.

[122] T. Posner, *Ber. Dtsch. Chem. Ges.* **1905**, *38*, 646–657.

[123] A. B. Lowe, *Polym. Chem.* **2010**, *1*, 17–36.

[124] G. Delaittre, N. K. Guimard, C. Barner-Kowollik, *Acc. Chem. Res.* **2015**, *48*, 1296–1307.

[125] M. Eberhardt, R. Mruk, R. Zentel, P. Théato, *Eur. Polym. J.* **2005**, *41*, 1569–1575.

[126] A. Das, P. Theato, *Macromolecules* **2015**, *48*, 8695–8707.

[127] E. M. Muzammil, A. Khan, M. C. Stuparu, *RSC Adv.* **2017**, *7*, 55874–55884.

[128] P. Wu, A. K. Feldman, A. K. Nugent, C. J. Hawker, A. Scheel, B. Voit, J. Pyun, J. M. J. Fréchet, K. B. Sharpless, V. V. Fokin, *Angew. Chem. Int. Ed.* **2004**, *43*, 3928–3932.

[129] D. D. Díaz, S. Punna, P. Holzer, A. K. McPherson, K. B. Sharpless, V. V. Fokin, M. G. Finn, *J. Polym. Sci. Part A Polym. Chem.* **2004**, *42*, 4392–4403.

[130] H. Ben El Ayouchia, L. Bahsis, H. Anane, L. R. Domingo, S. E. Stiriba, *RSC Adv.* **2018**, *8*, 7670–7678.

[131] M. Gauthier-Jaques, P. Theato, *ACS Macro Lett.* **2020**, *9*, 700–705.

[132] A. J. Butzelaar, S. Schneider, E. Molle, P. Theato, *Macromol. Rapid Commun.* **2021**, 2100133.

[133] V. Kottisch, J. O'Leary, Q. Michaudel, E. E. Stache, T. H. Lambert, B. P. Fors, *J. Am. Chem. Soc.* **2019**, *141*, 10605–10609.

[134] P. Ferruti, A. Bettelli, A. Feré, *Polymer* **1972**, *13*, 462–464.

[135] H.-G. Batz, G. Franzmann, H. Ringsdorf, *Angew. Chem. Int. Ed.* **1972**, *11*, 1103–1104.

[136] A. Das, P. Theato, *Chem. Rev.* **2016**, *116*, 1434–1495.

[137] A. P. P. Kröger, J. W. D. Paats, R. J. E. A. Boonen, N. M. Hamelmann, J. M. J. Paulusse, *Polym. Chem.* **2020**, *11*, 6056–6065.

[138] R. K. Roy, J. F. Lutz, *J. Am. Chem. Soc.* **2014**, *136*, 12888–12891.

[139] M. Zamfir, P. Theato, J. F. Lutz, *Polym. Chem.* **2012**, *3*, 1796–1802.

[140] H. Son, J. Ku, Y. Kim, S. Li, K. Char, *Biomacromolecules* **2018**, *19*, 951–961.

[141] N. V. Tsarevsky, S. A. Bencherif, K. Matyjaszewski, *Macromolecules* **2007**, *40*, 4439–4445.

[142] F.-R. Minz, R. Schliebs, *Chemie unserer Zeit* **1978**, *5*, 135–145.

[143] J. L. Gustin, *Chem. Heal. Saf.* **2005**, *12*, 5–16.

[144] M. Faraday, *Ann. Phys.* **1834**, *109*, 433–451.

[145] H. Kolbe, *Justus Liebigs Ann. Chem.* **1849**, *69*, 257–294.

[146] A. K. Vijh, B. E. Conway, *Chem. Rev.* **1967**, *67*, 623–664.

[147] J. B. Sperr, D. L. Wright, *Chem. Soc. Rev.* **2006**, *35*, 605–621.

[148] C. Kingston, M. D. Palkowitz, Y. Takahira, J. C. Vantourout, B. K. Peters, Y. Kawamata, P. S. Baran, *Acc. Chem. Res.* **2020**, *53*, 72–83.

[149] G. Hilt, *ChemElectroChem* **2020**, *7*, 395–405.

[150] J. Chaussard, J. C. Folest, J. Y. Nedelec, J. Perichon, S. Sibille, M. Treupel, *Synth.* **1990**, *1990*, 369–381.

[151] D. Pletcher, R. A. Green, R. C. D. Brown, *Chem. Rev.* **2018**, *118*, 4573–4591.

[152] T. Noël, Y. Cao, G. Laudadio, *Acc. Chem. Res.* **2019**, *52*, 2858–2869.

[153] S. Dapperheld, E. Steckhan, K. G. Brinkhaus, T. Esch, *Chem. Ber.* **1991**, *124*, 2557–2567.

[154] M. Uchimiya, A. T. Stone, *Chemosphere* **2009**, *77*, 451–458.

[155] R. Francke, R. D. Little, *J. Am. Chem. Soc.* **2014**, *136*, 427–435.

[156] M. F. Semmelhack, C. S. Chou, D. A. Cortes, *J. Am. Chem. Soc.* **1983**, *105*, 4492–4494.

[157] B. Elsler, D. Schollmeyer, K. M. Dyballa, R. Franke, S. R. Waldvogel, *Angew. Chem. Int. Ed.* **2014**, *53*, 5210–5213.

[158] C. Li, Y. Kawamata, H. Nakamura, J. C. Vantourout, Z. Liu, Q. Hou, D. Bao, J. T. Starr, J. Chen, M. Yan, et al., *Angew. Chem. Int. Ed.* **2017**, *56*, 13088–13093.

[159] J. Cornella, J. T. Edwards, T. Qin, S. Kawamura, J. Wang, C. Pan, R. Gianatassio, M. Schmidt, M. D. Eastgate, P. S. Baran, *J. Am. Chem. Soc.* **2016**, *138*, 2174–2177.

[160] F. Lian, K. Xu, W. Meng, H. Zhang, Z. Tan, C. Zeng, *Chem. Commun.* **2019**, *55*, 14685–14688.

[161] R. J. Perkins, D. J. Pedro, E. C. Hansen, *Org. Lett.* **2017**, *19*, 3755–3758.

[162] T. Koyanagi, A. Herath, A. Chong, M. Ratnikov, A. Valiere, J. Chang, V. Molteni, J. Loren, *Org. Lett.* **2019**, *21*, 816–820.

[163] K.-J. Jiao, D. Liu, H.-X. Ma, H. Qiu, P. Fang, T.-S. Mei, *Angew. Chem. Int. Ed.* **2020**, *59*, 6520–6524.

[164] K. Tanaka, T. Shichiri, S. Wang, T. Yamabe, *Synth. Met.* **1988**, *24*, 203–215.

[165] S. Sadki, P. Schottland, N. Brodie, G. Sabouraud, *Chem. Soc. Rev.* **2000**, *29*, 283–293.

[166] M. Mertens, C. Calberg, L. Martinot, R. Jérôme, *Macromolecules* **1996**, *29*, 4910–4918.

[167] J. M. Ortega, S. Menolasina, O. P. de Márquez, J. Márquez, *Polymer (Guildf).* **1986**, *27*, 1304–1306.

[168] V. Bonometti, E. Labbé, O. Buriez, P. Mussini, C. Amatore, *J. Electroanal. Chem.* **2009**, *633*, 99–105.

[169] A. J. D. Magenau, N. C. Strandwitz, A. Gennaro, K. Matyjaszewski, *Science (80-.).* **2011**, *332*, 81–84.

[170] S. Park, P. Chmielarz, A. Gennaro, K. Matyjaszewski, *Angew. Chem. Int. Ed.* **2015**, *54*, 2388–2392.

[171] H. Mutlu, P. Theato, *Macromol. Rapid Commun.* **2020**, *41*, 2000181.

[172] J. M. Scheiger, C. Direksilp, P. Falkenstein, A. Welle, M. Koenig, S. Heissler, J. Matysik, P. A. Levkin, P. Theato, *Angew. Chem. Int. Ed.* **2020**, *59*, 18639–18645.

[173] F. P. Burt, *J. Chem. Soc., Trans.* **1910**, *97*, 1171–1174.

[174] A. G. MacDiarmid, C. M. Mikulski, P. J. Russo, M. S. Saran, A. F. Garito, A. J. Heeger, *J. Chem. Soc., Chem. Commun.* **1975**, 476–477.

[175] T. A. Graf, *Poly(Disulfidediamines) : New Biodegradable Polymers*, University of Iowa, **2012**.

[176] J. Yoo, *Synthesis of New Biodegradable Polysulfenamides for Applications in Medicine*, Iowa, **2011**.

[177] T. Tirri, M. Aubert, W. Pawelec, A. Holappa, C.-E. Wilén, *Polymers* **2016**, *8*, 360.

[178] J. Yoo, S. R. D'Mello, T. Graf, A. K. Salem, N. B. Bowden, *Macromolecules* **2012**, *45*, 688–697.

[179] Y. P. Losev, Y. M. Paushkin, V. N. Isakovich, *Polym. Sci. U.S.S.R.* **1974**, *16*, 2906–2911.

[180] T. A. Graf, J. Yoo, A. B. Brummett, R. Lin, M. Wohlgenannt, D. Quinn, N. B. Bowden, *Macromolecules* **2012**, *45*, 8193–8200.

[181] S. A. Sundet, W. A. Murphey, S. B. Speck, *J. Polym. Sci.* **1959**, *40*, 389–397.

[182] Y. Imai, H. Okunoyama, *J. Polym. Sci. Part A-1 Polym. Chem.* **1972**, *10*, 2257–2264.

[183] B. A. Abel, M. B. Sims, C. L. McCormick, *Macromolecules* **2015**, *48*, 5487–5495.

[184] S. Il Kang, Y. H. Bae, *J. Control. Release* **2002**, *80*, 145–155.

[185] S. Baek, D. Kim, S. L. Jeon, J. Seo, *React. Funct. Polym.* **2017**, *120*, 57–65.

[186] P. D. Pickett, C. R. Kasprzak, D. T. Siefker, B. A. Abel, M. A. Dearborn, C. L. McCormick, *Macromolecules* **2018**, *51*, 9052–9059.

[187] R. Kakuchi, P. Theato, *Polym. Chem.* **2014**, *5*, 2320–2325.

[188] S. Shaaban, A. Jolit, D. Petkova, N. Maulide, *Chem. Commun.* **2015**, *51*, 13902–13905.

[189] D. Prasad Hari, T. Hering, B. König, *Angew. Chem. Int. Ed.* **2014**, *53*, 725–728.

[190] S. P. Green, K. M. Wheelhouse, A. D. Payne, J. P. Hallett, P. W. Miller, J. A. Bull, *Org. Process Res. Dev.* **2020**, *24*, 67–84.

[191] J. M. Friedrich, C. Ponce-de-León, G. W. Reade, F. C. Walsh, *J. Electroanal. Chem.* **2004**, *561*, 203–217.

[192] T. Grüger, *Electrochemically-Initiatied Polymerization of Fluorine-Containing Monomers*, Karlsruhe, **2020**.

[193] C. Battistella, Y. Yang, J. Chen, H. A. Klok, *ACS Omega* **2018**, *3*, 9710–9721.

[194] K. A. Günay, N. Schüwer, H. A. Klok, *Polym. Chem.* **2012**, *3*, 2186–2192.

[195] H. Son, J. Ku, Y. Kim, S. Li, K. Char, *Biomacromolecules* **2018**, *19*, 951–961.

[196] G. Fantini, E. Dallerba, M. Massi, A. B. Lowe, *Macromol. Chem. Phys.* **2020**, *221*, 2000135.

[197] W. Graisuwan, H. Zhao, S. Kiatkamjornwong, P. Theato, V. P. Hoven, *J. Polym. Sci. Part A: Polym. Chem.* **2015**, *53*, 1103–1113.

[198] K. G. McCurdy, K. J. Laidler, *Can. J. Chem.* **1964**, *42*, 825–829.

[199] L. M. Meng, Y. C. Yuan, M. Z. Rong, M. Q. Zhang, *J. Mater. Chem.* **2010**, *20*, 6030–6038.

[200] M. Ma, F. Li, F. J. Chen, S. X. Cheng, R. X. Zhuo, *Macromol. Biosci.* **2010**, *10*, 183–191.

[201] S. Edmondson, W. T. S. Huck, *J. Mater. Chem.* **2004**, *14*, 730–734.

[202] F. J. Xu, Y. Zhu, M. Y. Chai, F. S. Liu, *Acta Biomater.* **2011**, *7*, 3131–3140.

[203] D. Varadharajan, G. Delaittre, *Polym. Chem.* **2016**, *7*, 7488–7499.

[204] J. Rieger, *J. Therm. Anal.* **1996**, *46*, 965–972.

[205] Y. Li, D. Lin, J. Xu, X. Zhou, B. Zuo, O. K. C. Tsui, W. Zhang, X. Wang, *J. Chem. Phys.* **2020**, *152*, 064904.

[206] S. L. Malhotra, P. Lessard, L. P. Blanchard, *J. Macromol. Sci.-Chem.* **1981**, *15*, 121–141.

[207] E. Molle, H. Mutlu, P. Theato, *Macromol. Rapid Commun.* **2021**, *30*, 2100063.

[208] A. Hess, B. V. K. J. Schmidt, H. Schlaad, *Polym. Chem.* **2020**, *11*, 7677–7684.

[209] H. Willcock, R. K. O'Reilly, *Polym. Chem.* **2010**, *1*, 149–157.

[210] G. Moad, E. Rizzardo, S. H. Thang, *Aust. J. Chem.* **2012**, *65*, 985–1076.

[211] G. B. Desmet, D. R. D'Hooge, M. K. Sabbe, M. F. Reyniers, G. B. Marin, *J. Org. Chem.* **2016**, *81*, 11626–11634.

[212] L. Horner, H. Neumann, *Chem. Ber.* **1965**, *98*, 3462–3469.

[213] L. Horner, H. Neumann, *Chem. Ber.* **1965**, *98*, 1715–1721.

[214] A. Lebouc, P. Martigny, R. Carlier, J. Simonet, *Tetrahedron* **1985**, *41*, 1251–1258.

[215] V. Coeffard, C. Thobie-Gautier, I. Beaudet, E. Le Grognec, J.-P. Quintard, *Eur. J. Org. Chem.* **2008**, *2008*, 383–391.

[216] E. R. Civitello, H. Rapoport, *J. Org. Chem.* **1992**, *57*, 834–840.

[217] T. Iwasaki, K. Matsumoto, M. Matsuoka, T. Takahashi, K. Okumura, *Bull. Chem. Soc. Jpn.* **1973**, *46*, 852–855.

[218] H. L. S. Maia, L. S. Monteiro, F. Degerbeck, L. Grehn, U. Ragnarsson, *J. Chem. Soc. Perkin Trans. 2* **1993**, 495–500.

[219] B. Nyasse, L. Grehn, U. Ragnarsson, H. L. S. Maia, L. S. Monteiro, I. Leito, I. Koppel, J. Koppel, *J. Chem. Soc. Perkin Trans. 1* **1995**, 2025–2031.

[220] R. A. Bernhoft, *J. Environ. Public Health* **2012**, *2012*, 460508.

[221] N. A. Wynberg, L. J. Leger, M. L. Conrad, C. M. Vogels, A. Decken, S. J. Duffy, S. A. Westcott, *Can. J. Chem.* **2005**, *83*, 661–667.

[222] H. Senboku, K. Nakahara, T. Fukuhara, S. Hara, *Tetrahedron Lett.* **2010**, *51*, 435–438.

[223] F. Tüdös, I. Kende, M. Azori, *J. Polym. Sci.* **1961**, *53*, 17–25.

[224] W. Heintz, N. Sokoloff, P. Latschinoff, *Ber. Dtsch. Chem. Ges.* **1874**, *7*, 1518–1520.

[225] P. R. Haeseler, *Org. Synth.* **1926**, *6*, 28–30.

[226] N. Sokoloff, P. Latschinoff, *Ber. Dtsch. Chem. Ges.* **1874**, *7*, 1384–1387.

[227] M. Ashfaq, R. Tabassum, M. M. Ahmad, N. A. Hassan, H. Oku, G. Rivera, *Med. Chem.* **2015**, *5*, 295–309.

[228] D. Seebach, A. K. Beck, D. J. Bierbaum, *Chem. Biodivers.* **2004**, *1*, 1111–1239.

[229] D. Enders, C. Wang, J. X. Liebich, *Chem. Eur. J.* **2009**, *15*, 11058–11076.